



GRADUATE SCHOOL  
EAST TENNESSEE STATE UNIVERSITY

East Tennessee State University  
Digital Commons @ East  
Tennessee State University

---

Electronic Theses and Dissertations

Student Works

---

5-2021

## Morphology and Paleoecology of *Nimravides galiani* (Felidae) and *Barbourofelis loveorum* (Barbourofelidae) from the Late Miocene of Florida

Christianne Ormsby  
*East Tennessee State University*

Follow this and additional works at: <https://dc.etsu.edu/etd>

 Part of the [Paleobiology Commons](#), and the [Paleontology Commons](#)

---

### Recommended Citation

Ormsby, Christianne, "Morphology and Paleoecology of *Nimravides galiani* (Felidae) and *Barbourofelis loveorum* (Barbourofelidae) from the Late Miocene of Florida" (2021). *Electronic Theses and Dissertations*. Paper 3902. <https://dc.etsu.edu/etd/3902>

This Thesis - embargo is brought to you for free and open access by the Student Works at Digital Commons @ East Tennessee State University. It has been accepted for inclusion in Electronic Theses and Dissertations by an authorized administrator of Digital Commons @ East Tennessee State University. For more information, please contact [digilib@etsu.edu](mailto:digilib@etsu.edu).

Morphology and Paleoecology of *Nimravides galiani* (Felidae) and *Barbourofelis loveorum*  
(Barbourofelidae) from the Late Miocene of Florida

---

A thesis  
presented to  
the faculty of the Department of Geosciences  
East Tennessee State University

In partial fulfillment  
of the requirements for the degree  
Master of Science in Geosciences

---

by  
Christianne Ormsby  
May 2021

---

Steven Wallace, PhD, Chair  
Blaine Schubert, PhD  
Joshua Samuels, PhD

Keywords: competition, ecomorphology, locomotion, Love Bone Bed, niche partitioning

## ABSTRACT

Morphology and Paleoecology of *Nimravides galiani* (Felidae) and *Barbourofelis loveorum* (Barbourofelidae) from the Late Miocene of Florida

by

Christianne Ormsby

Saber-toothed remains have been found worldwide throughout the Cenozoic, until the end of the Pleistocene. One site from Alachua County, Florida preserves a diverse Miocene fauna, including the machairodontine *Nimravides galiani* (Felidae) and the saber-toothed *Barbourofelis loveorum* (Barbourofelidae). Both taxa roamed what would become the Love Bone Bed site during the Late Miocene (Late Clarendonian NALMA), ~ 9.5 Mya. Previous descriptions focused on crania; yet the large sample of postcrania remained undescribed. Hence, this project includes a detailed postcranial description of both taxa. Results show that *N. galiani* resembles extant felids, whereas *B. loveorum* resembles *Smilodon fatalis*, as well as ursids. Additionally, locomotion and hunting behavior (prey capture) was examined quantitatively to assess ecologic overlap (niche partitioning vs direct competition). *N. galiani* probably displayed terrestrial locomotion in open habitats, whereas *B. loveorum* likely inhabited the deciduous forest as an ambulatory opportunistic/ambush predator. Results support niche partitioning, rather than direct competition.

## TABLE OF CONTENTS

ABSTRACT.....	2
LIST OF TABLES .....	7
LIST OF FIGURES .....	8
CHAPTER 1. INTRODUCTION .....	11
Geology and Ecology of the Love Bone Bed .....	13
Relationships among Felidae, Nimravidae, and Barbourofelidae .....	14
CHAPTER 2. MORPHOLOGICAL COMPARISONS OF <i>NIMRAVIDES GALIANI</i> AND <i>BARBOUROFELIS LOVEORUM</i> WITH COMMENTS ON PALEOECOLOGY .....	18
Materials and Methods.....	18
Descriptive Anatomy .....	21
Forelimb.....	21
Scapulae .....	21
Humeri .....	24
Radii.....	30
Ulnae .....	34
Carpals .....	40
Scapholunar.....	40
Pisiform.....	44
Unciform .....	47
Magnum .....	50
Trapezoid .....	54
Metacarpals .....	56

Metacarpal I .....	56
Metacarpal II.....	59
Metacarpal III.....	62
Metacarpal IV .....	65
Metacarpal V.....	68
Phalanx: MC I Proximal .....	71
Hindlimb .....	73
Innominate .....	73
Femora .....	77
Tibiae .....	81
Fibulae.....	86
Tarsals.....	89
Astragalus .....	89
Calcaneus .....	92
Cuboid.....	95
Navicular.....	99
Ectocuneiform.....	102
Metatarsals .....	105
Metatarsal II.....	105
Metatarsal III.....	108
Metatarsal IV .....	111
Metatarsal V.....	114
Vertebrae.....	117
Atlas .....	117
Axis .....	120

Cervical Vertebrae 3 .....	123
Cervical Vertebrae 4 .....	126
Cervical Vertebrae 5 .....	128
Cervical Vertebrae 6 .....	130
Cervical Vertebrae 7 .....	132
Sacra.....	134
Functional Morphology .....	139
Forelimb.....	139
Scapulae .....	139
Humeri .....	139
Radii.....	142
Ulnae .....	143
Carpals .....	145
Metacarpals .....	147
Hindlimb .....	148
Innominate .....	148
Femora .....	149
Tibiae .....	151
Fibulae.....	152
Tarsals .....	152
Metatarsals .....	157
Vertebrae.....	160
Cervical .....	160
Sacrum .....	162

CHAPTER 3. PREDICTING PALEOECOLOGICAL BEHAVIORS FOR NIMRAVIDES

GALIANI AND BARBOUROFELIS LOVEORUM.....	164
Traditional Locomotor Classifications .....	165
Traditional Hunting Behavior Classifications .....	168
Materials and Methods.....	170
Results.....	178
Locomotion.....	178
Hunting Behavior.....	183
Prediction Discussion .....	188
CHAPTER 4. DISCUSSION.....	191
Paleoecology .....	191
Conclusion .....	199
Future Work.....	200
REFERENCES .....	202
APPENDICES .....	215
Appendix A. Taxa used in the analyses and mean postcranial measurements.....	215
Appendix B: Assigned locomotor groups for extant felids from literature.....	217
Appendix C: Assigned predatory groups for extant felids from literature.....	218
VITA.....	219

LIST OF TABLES

Table 1. Morphological Indices and Definitions ..... 172

Table 2. Locomotor Descriptions Used in This Study..... 174

Table 3. Hunting Behavior Descriptions ..... 176

Table 4. Locomotor Prediction Discriminant Function Structure Matrix..... 179

Table 5. Prediction Probabilities for Extinct Taxa Locomotion. .... 179

Table 6. Hunting Behavior Prediction Discriminant Function Structure Matrix..... 184

Table 7. Prediction Probabilities for Extinct Taxa Hunting Behavior..... 184

## LIST OF FIGURES

Figure 1. Fossil localities dated to the Late Miocene .....	12
Figure 2. Scapula comparison views between both taxa .....	23
Figure 3. Humerus comparison views between both taxa .....	28
Figure 4. Radius comparison views between both taxa.....	33
Figure 5. Ulna comparison views between both taxa .....	38
Figure 6. Scapholunar comparison views between both taxa.....	43
Figure 7. Pisiform comparison views between both taxa .....	46
Figure 8. Unciform comparison views between both taxa .....	49
Figure 9. Magnum comparison views between both taxa.....	53
Figure 10. Trapezoid views for <i>Nimravides galiani</i> .....	55
Figure 11. Metacarpal I comparison views between both taxa.....	58
Figure 12. Metacarpal II comparison views between both taxa .....	61
Figure 13. Metacarpal III comparison views between both taxa .....	64
Figure 14. Metacarpal IV comparison views between both taxa.....	67
Figure 15. Metacarpal V comparison views between both taxa .....	70
Figure 16. Proximal Phalanx of MC I views for <i>Nimravides galiani</i> .....	72
Figure 17. Pelvis comparison views between both taxa .....	75
Figure 18. Femur comparison views between both taxa.....	79
Figure 19. Tibia comparison views between both taxa.....	84
Figure 20. Fibula comparison views between both taxa.....	88
Figure 21. Astragalus comparison views between both taxa.....	91

Figure 22. Calcaneus comparison views between both taxa.....	94
Figure 23. Cuboid comparison views between both taxa .....	98
Figure 24. Navicular comparison views between both taxa .....	101
Figure 25. Pisiform comparison views between both taxa .....	104
Figure 26. Metatarsal II comparison views between both taxa .....	107
Figure 27. Metatarsal III comparison views between both taxa .....	110
Figure 28. Metatarsal IV comparison views between both taxa.....	113
Figure 29. Metatarsal V comparison views between both taxa .....	116
Figure 30. Atlas comparison views between both taxa.....	119
Figure 31. Axis comparison views between both taxa .....	122
Figure 32. C3 comparison views between both taxa .....	125
Figure 33. C4 comparison views between both taxa .....	127
Figure 34. C5 comparison views between both taxa .....	129
Figure 35. C6 comparison views between both taxa .....	131
Figure 36. C7 comparison views between both taxa .....	133
Figure 37. Sacrum comparison views between both taxa.....	137
Figure 38. Measurements used for analyses in mm.....	173
Figure 39. Felid locomotion and phylogenetic tree .....	175
Figure 40. Felid hunting behavior and phylogenetic tree .....	177
Figure 41. Locomotion DFA Stepwise plot.....	180
Figure 42. Boxplots of the locomotor morphological indices .....	182
Figure 43. Hunting behavior DFA Stepwise plot .....	185

Figure 44. Boxplots of the hunting behavior morphological indices..... 187

## CHAPTER 1. INTRODUCTION

In 1974, the Love Bone Bed site of Alachua County, Florida was discovered by Ron Love on his farmland, and excavated by the Florida Museum of Natural History and students from the University of Florida until 1981 (Fig. 1) (Webb et al. 1981). Many fragmentary bones of Miocene fauna covered the ground surface, brought there by a paleo-channel, with many more fossils unearthed to a depth of approximately 3 meters (Webb et al. 1981). Amongst these specimens is a large sample of the machairodontine felid *Nimravides galiani* and the saber-toothed barbourofelid *Barbourofelis loveorum* (Baskin 1981). Both taxa were described as new species in a brief manuscript focused on the crania (Baskin 2005), but the large sample of postcranial elements recovered for each taxon remained undescribed. Later studies on *N. galiani* and *B. loveorum* mentioned some of the postcranial skeletal remains, but full descriptions were lacking (Baskin 2005). *Nimravides galiani* and *B. loveorum* were differentiated from other felid and barbourofelid species, respectively, through differences in the auditory bulla and basicranium (Baskin 1981; Bryant 1991; Morlo et al. 2004; Werdelin 2010). Presence of these two species in the Love Bone Bed indicates they likely coexisted, but whether they directly competed, or partitioned their respective niches remains unresolved. Consequently, this study seeks to not only describe the postcrania of these taxa in detail, but also interpret their functional morphology and behavior. Such insight into species competition or niche partitioning between morphologically similar species provides additional information on ecological relationships that can be used on coexisting extant carnivoran taxa undergoing the same ecological pressures (Di Bitetti et al. 2010; Meachen-Samuels 2012).

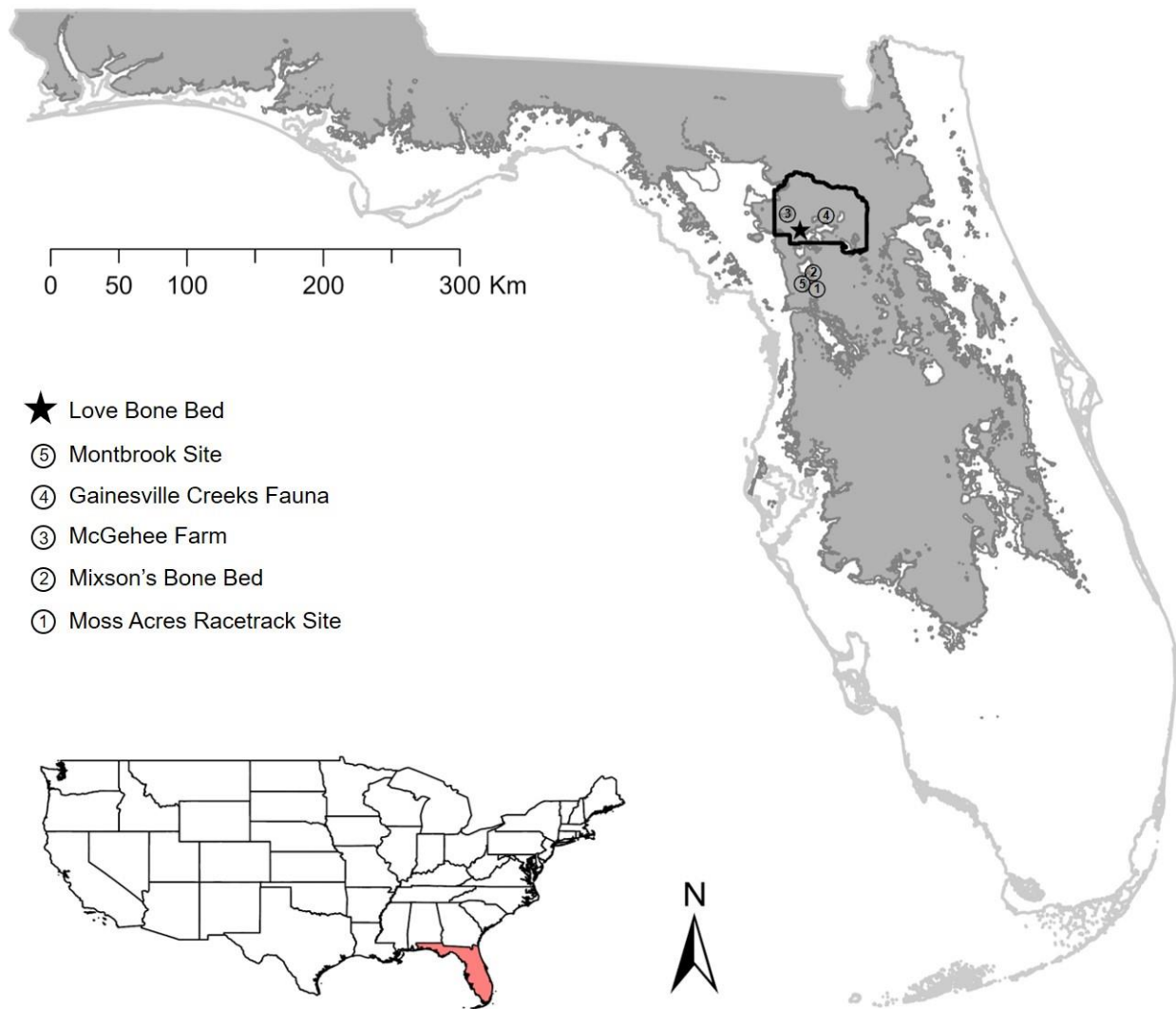


Figure 1. Fossil localities dated to the Late Miocene are shown clustered around the Love site. Alachua County, Florida is outlined. Sea level during the late Clarendonian was approximately 20 m higher than present in Florida (Webb et al. 1981), as indicated by the grey outlined and shaded-in region.

## *Geology and Ecology of the Love Bone Bed*

In the southwest region of Alachua County, Florida, the Love Bone Bed contains a rich concentration of terrestrial mammals preserved in fluvial deposits of the Alachua Formation (Webb et al. 1981). Underlying this paleo-channel is the karst Crystal River Formation, which formed in the late Eocene and was incised by many fluvial meandering streams during the late Miocene; the sands and gravels of which comprise the Alachua Formation (Williams et al. 1977; Webb et al. 1981). These fluvial sediments consist of non-marine blue-gray to tan-orange clay that were deposited in waters which generally flowed north to south (Webb et al. 1981). The paleo-channel that formed the Love site was variable in thickness and, at most, buried animals up to a depth of 3 meters (Webb et al. 1981). Within the paleo-channel, the Alachua Formation is divided into three successive layers: a basal unit of abundant bone breccia and limestone boulders, a middle unit comprising of fossiliferous sandy-clay sediments, and the top unit consists of an orange clayey sand that better-preserved bones (Webb et al. 1981). The continuous fining-upward depositional sequence of the three units has been suggested by Webb et al. (1981) to represent a single depositional cycle, due to the continuous fining upward sediment sequence, and implies the Love site accumulation occurred over a very short amount of geologic time. Just west of this paleo-channel is the Hawthorn Formation, which consists of marine fossiliferous beds, indicating that sea level was much higher in the Miocene than present (Williams et al. 1977; Webb et al. 1981).

Not surprising with the depositional environment interpreted for the site, most of the fossils recovered from the Love site are disarticulated due to fluvial transport. Of the more than 80 taxa recovered thus far, 43 are mammals (Webb et al. 1981; Baskin 2005). Dated to the Late

Miocene C13 (Late Clarendonian NALMA) (Tedford et al. 2004), at approximately 9.5 mya (Webb et al. 1981), the channel bed deposits preserve vertebrates from terrestrial and transitional environments (Webb et al. 1981). Three primary terrestrial habitats are preserved at the site: stream-bank, closed-deciduous forest, and open-grassland (Webb et al. 1981). Fossils have undergone taphonomic modification such as abrasion and differential weathering due to the flow of the river channel at that time (Webb et al. 1981). The Love site is very diverse, and includes canids, procyonids, mustelids, proboscideans, perissodactyls, rhinocerotids, equids, artiodactyls, camelids, ruminants, the felid *Nimravides galiani*, and the barbourofelid *Barbourofelis loveorum* (Webb et al. 1981; Baskin 2005). Most of these taxa co-occur with related fauna found on the West Coast and the Great Plains, thus the age of the fauna is inferred by a co-occurrence interval (Webb et al. 1981; Baskin 2005). The distinct lack of immigrant taxa, such as the neotropical giant ground sloths, Eurasian ursids, and Eurasian machairodonts, indicates a pre-Hemphillian NALMA (North American Land Mammal Age) (Webb et al. 1981). Similarly, the presence of rapidly evolving taxa, such as *Eucastor cf. planus*, identified by Webb et al. (1981), and the immigrant mustelid, *Beckia* sp. (Webb et al. 1981), provides the constrained age for the Love site to be latest Clarendonian (Webb et al. 1981; Tedford et al. 2004).

#### *Relationships among Felidae, Nimravidae, and Barbourofelidae*

There have been many issues regarding feliformia phylogeny, due to incomplete and fragmented fossil records, as well as high levels of convergence (Werdelin 2010). However, recent studies have begun to shed new light on the phylogenetic relationships among the North American extinct saber-toothed carnivorans (found within Felidae, Nimravidae, and

Barbourofelidae) (Bryant 1991; Morlo et al. 2004; Christiansen 2013; Barrett 2016; Paijmans et al. 2017; Piras et al. 2018; Wang et al. 2020). Part of this confusion stems from the early group of ‘cat-like’ saber-toothed mammals, known as nimravids, which originated during the late Eocene in North America and became increasingly abundant (Bryant 1991; Antón 2013; Barrett 2016). Some of the best-known taxa include *Dinictis*, *Hoplophoneus*, and *Nimravus*; all of whom were large, dominant predators in the quickly drying climate of North America (Bryant 1991; Antón 2013). Nimravids were successful for millions of years, but by the end of the Oligocene, approximately 24 mya, they had all gone extinct (Bryant 1991; Antón 2013).

Barbourofelids first appeared in Eurasia during the early Miocene and dispersed throughout the Old World; later (approximately 12 mya) immigrating into North America (Antón 2013). Well-known barbourofelids include *Prosansanosmilus*, *Sansanosmilus*, and *Barbourofelis* (E.g. Bryant 1991; Morlo et al. 2004; Antón 2013; Barrett 2016). Unfortunately, barbourofelids were short-lived, going extinct by the late Miocene-early Pliocene (Antón 2013; Piras et al. 2018).

Coincidental with the barbourofelid extinction, felids were able to radiate and fill the vacated niches (Antón 2013). Similar to barbourofelids, felids first appeared in Eurasia, beginning with *Proailurus* approximately 30 mya (Rothwell 2003), and subsequently dispersed into North America during the early Miocene, approximately 18.5 mya (Rothwell 2003; Johnson et al. 2006; Antón 2013). Felidae currently contains two subfamilies Machairodontinae (extinct saber-toothed felids), and Felinae (conical-toothed felids). Well known machairodonts include *Nimravides*, *Smilodon*, *Homotherium*, and many others, whereas Felinae currently consists of all extant felids that began their radiation approximately 10.8 mya (Johnson 2006; O’Brian and Johnson 2007; Antón 2013). As such, *N. galiani* is classified within Felidae, and in the subfamily

Machairodontinae (Baskin 1981; Baskin 2005; Anton et al. 2013). Lack of fossil material in North America from nimravids, barbourofelids, or felids between the time nimravids went extinct and the first occurrence of felids has been informally referred to as the ‘cat-gap’: an extended period of geologic time where it is assumed felids and cat-like carnivorans were not present in North America (Van Valkenburgh 1999; Rothwell 2003; Wesley-Hunt 2005; Antón 2013). North America’s 5 mya ‘cat-gap’ ended with the first occurrence of *Pseudaelurus* (Rothwell 2003).

Previous workers placed barbourofelids within Nimravidae (Martin 1980; Baskin 1981; Bryant 1991; Wang et al. 2020); however, others have recognized the distinct family Barbourofelidae (Morlo et al. 2004; Meachen-Samuels 2012; Barrett 2016; Piras et al. 2018); justifying the separation with shared synapomorphies within the clade. Originally considered a second radiation of nimravids during the Miocene (after the ‘cat-gap’), barbourofelids are now considered to be phylogenetically closer to felids; with Nimravidae considered a sister-group to both Barbourofelidae and Felidae (Morlo et al. 2004; Meachen-Samuels 2012).

Specifically, Nimravidae were cat-like carnivoran that greatly differed in the basicranial anatomy to that of Felidae and/or Barbourofelidae (Bryant 1991). The auditory bullae of nimravids lack a bilaminar septum and the entotympanic is not completely ossified (Bryant 1991). Barbourofelidae are morphologically distinct from Nimravidae by having a completely ossified bulla overrunning the mastoid, an absence of the postglenoid foramen, a thin wall of the caudal entotympanic (as opposed to three layers in Nimravidae), a parastyle on P4, and a shortened palate (Morlo et al. 2004). Differences between Barbourofelidae and Felidae are more subtle. The later barbourofelids, *Barbourofelis* and *Sansanosmilus*, are distinguished by their

dental anatomy, whereas earlier barbourfelids, *Prosansanosmilus* and *Afrosmilus*, are similar to felids in dental morphology (Morlo et al. 2004).

CHAPTER 2. MORPHOLOGICAL COMPARISONS OF *NIMRAVIDES GALIANI* AND  
*BARBOUROFELIS LOVEORUM* WITH COMMENTS ON PALEOECOLOGY

*Materials and Methods*

**Institutional Abbreviations**— **AMNH**, American Museum of Natural History; **ETVP**, East Tennessee Vertebrate Paleontology; **LACM** and **LACMHC**, Natural History Museum of Los Angeles County; **NAU QSP**, Northern Arizona University, Quaternary Sciences Program; **UCLA**, University of California, Los Angeles; **UF**, Florida Museum of Natural History, University of Florida, Gainesville, Florida; **USNM**, Smithsonian National Museum of Natural History.

**Morphological Abbreviations**—**C**, Cervical Vertebra; **MC**, Metacarpal; **MT**, Metatarsal

**Terminology**—Morphological descriptions and nomenclature of the Love Bone Bed taxa follow Flower (1885), Reighard and Jennings (1901), McFadyean (1908), Barone (1999), Julik et al. (2012), Salesa et al. (2008), and Salesa et al. (2019).

Please note that the specimens of *Nimravides galiani* and *Barbourofelis loveorum* from the Love Bone Bed described here are composites. To date, no articulated skeletons of either taxa have been recovered from this site. All remains are housed in the Florida Museum of Natural History at the University of Florida and have been identified to species level by Webb et al. (1981) and Baskin (1981). Postcranial material is well preserved, and most was available for description. Additionally, the postcranial remains described here have been compared to similar descriptions made from past research (Webb et al. 1981; Baskin 1981; Baskin 2005), as well as

to extant felids (Appendix A). Unfortunately, postcrania not described includes most of the axial skeleton (thoracic, lumbar, and caudal vertebrae and the ribs) and some of the appendicular skeleton (cuneiform, trapezium, mesocuneiform, endocuneiform, patella, and nearly all the phalanges as most phalanges have not been identified to their corresponding digits) due to either a lack of preservation for these bones, no identification made from previous researchers, or a lack certainty in bone identification on the species level. Measurements for each postcranial element are listed in Appendix A, along with similar measurements on extant and extinct felids and extinct nimravids.

Referred specimens of *N. galiani* described here—Scapula: one partial right, UF 490610; Humerus: one right, UF 37031; Radius: two left, UF 25625, UF 25624; Ulna: one right, UF 25622; Scapholunar: three right, UF 25142, UF 464300, UF 464301, one left, UF 25139; Pisiform: one left, UF 464290; Unciform: one right, UF 26159, two left, UF 26158, UF 26157; Magnum: one right, UF 26155, two left, UF 26154, UF 26156; Trapezoid: one left, UF 37116; MC I: one right, UF 25327; MC II: one right, UF 25334; MC III: one right, UF 25348, one left, UF 25352; MC IV: one left, UF 25354; MC V: two right: UF 25360, UF 25361; Proximal Phalanx for MC I: one left, UF 37144; Innominate: three partial right: UF 37158, UF 25680, UF 37154, one left, UF 37154; Femur: one right, UF 37064, two partial left, UF 25483, UF 25490; Tibia: two right, UF 37079, UF 25553, one left, UF 25552; Fibula: two partial left: UF 490608, UF 490607; Astragalus: one right, UF 25197, two left, UF 37098, UF 37097; Calcaneus: one right, UF 37089, two left, UF 25136, UF 25167; Cuboid: one right, UF 25661, one left, UF 25664; Navicular: one left, UF 69825; Ectocuneiform: one right, UF 25672; MT II: one right, UF 25371, one left, UF 25368; MT III: two right, UF 25372, UF 25352; MT IV: two left, UF 37112, UF 25354; MT V: two right, UF 25397, UF 25361; Atlas Vertebra: UF 25593; Axis Vertebra:

UF 490611; Third Cervical Vertebra: UF 490612; Fourth Cervical Vertebra: UF 490613; Fifth Cervical Vertebra: UF 490615; Sixth Cervical Vertebra: UF 490617; Seventh Cervical Vertebra: UF 490619; Sacrum: UF 26137, UF 21138, UF 37156, UF 37157.

Referred specimens of *B. loveorum* described here—Scapula: one partial left, UF 29892; Humerus: three partial left: UF 25101, UF 36883, UF 25081; Radius: three right, UF 25446, UF 25441, UF 25444, two left, UF 25438, UF 36928; Ulna: two right, UF 36893, UF 27253, two left, UF 25103, UF 25104; Scapholunar: two left, UF 25149, UF 25156; Pisiform: one left, UF 490627; Unciform: one right, UF 26148; Magnum: one right, UF 26139; MC I: one right, UF 25326; MC II: two right, UF 37848, UF 25249; MC III: two left, UF 25269, UF 25267; MC IV: one right, UF 25274, one left, UF 25283; MC V: two left, UF 25285, UF 25294; Innominate: two partial, one right, UF 25689, one left, UF 36998; Femur: one right, UF 27259, one left, UF 27258; Tibia: one right, UF 25526, two left, UF 36974, UF 25521; Fibula: one partial right: UF 466164; Astragalus: three left, UF 466158, UF 25228, UF 25226; Calcaneus: three right, UF 25194, UF 25189, UF 466155, two left, UF 466151, UF 466152; Cuboid: one right, UF 25668; Navicular: one right, UF 90310; Ectocuneiform: one left, UF 25670; MT II: one right, UF 25302, one left, UF 25313; MT III: two right, UF 25320, UF 25319; MT IV: one right, UF 275518, one left, UF 25321; MT V: one left, UF 25325; Atlas Vertebra: UF 36990; Axis Vertebra: UF 36485; Third Cervical Vertebra: UF 466169; Fourth Cervical Vertebra: UF 466173; Fifth Cervical Vertebra: UF 490621; Sixth Cervical Vertebra: UF 490622; Seventh Cervical Vertebra: UF 490623; Sacrum: UF 25605, UF 466166.

## *Descriptive Anatomy*

### *Forelimb*

*Scapulae. Nimravides galiani: one partial right, UF 490610.*

The one scapula available of *N. galiani* (Fig. 2) is mostly incomplete, of which only the distal end is present, from the broken acromion process to the gleno-humeral articular region. In ventral view the glenoid fossa is elliptical, slightly compressed mediolaterally and elongated anteroposteriorly. On the glenoid border, the anterolateral margin is distally projected to a point. A round, pronounced supraglenoid tubercle on the anterior surface is projected anteromedially, forming a deep medial notch. On the medial side of the supraglenoid tubercle is a long and thin posteromedially projected coracoid process with a deep groove on the medial side of the coracoid border. On the coracoid border, proximal to the coracoid process, is a round and wide suprascapular notch. In lateral view, the glenoid angle is wide and proximally inset, distal to the spine. Between the glenoid angle and the distal end of the acromion is a wide and medial-oriented great scapular notch.

*Barbourofelis loveorum: one partial left, UF 29892.*

The one scapula available of *B. loveorum* (Fig. 2) is largely incomplete, lacking the majority of the infraspinous fossa poster proximally and the supraspinous fossa anter proximally in lateral view, and most of the subscapular fossa in medial view. Additionally, the acromion, as well as the proximal and distal ends of the spine are broken off and there's a noticeable hole in the center of the spine protrusion. In ventral view the glenoid fossa is oval, elongated anteroposteriorly. On the glenoid border, the anterolateral margin is distally projected to a smooth point. An elliptical supraglenoid tubercle is present on the anterior side of the

glenoid border, projecting anteromedially, forming a deep medial groove. There is no coracoid process present. Proximal to the supraglenoid tubercle is a deep and sharp-angled suprascapular notch. In lateral view, the glenoid angle is narrow and deeply proximally inset, distal to the spine. Between the glenoid angle, and the distal end of the acromion, is a deep and narrow, distally-positioned great scapular notch.

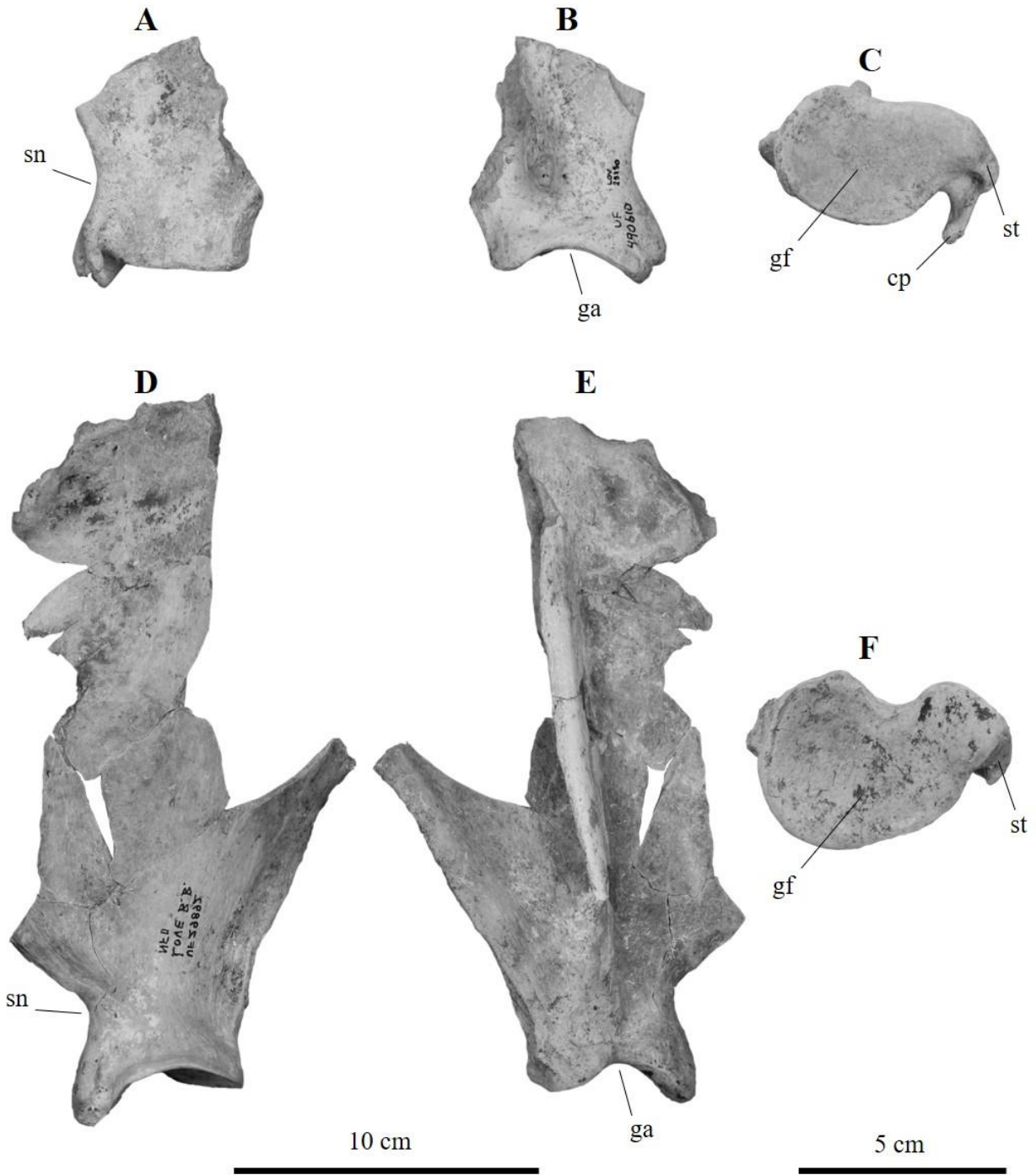


Figure 2. Scapula comparison views between both taxa. A-C *Nimravides galiani* UF 490610, right: medial (A), lateral (B), ventral (C) views. D-F *Barbouroufelis loveorum* UF 29892, left side inverted to right side: medial (D), lateral (E), ventral (F) views. Small bar for C, F views. Abbreviations: cp, coracoid process; gf, glenoid fossa; ga, glenoid angle; sn, suprascapular notch; st, supraglenoid tubercle.

Remarks— Scapulae from *N. galiani* and *B. loveorum* are incomplete with intact distal ends. In ventral view, *B. loveorum* has a rounder glenoid fossa and, in lateral view, has a sharper glenoid angle than in *N. galiani*. On the anterodistal tip of the glenoid fossa, *N. galiani* has a rounder supraglenoid tubercle, projecting further from the glenoid cavity proximally. Additionally, *N. galiani* has a well-formed coracoid process anteromedially on the supraglenoid tubercle which is absent in *B. loveorum*. The suprascapular notch and the great scapular notch in *B. loveorum* are both deeper and narrower than in *N. galiani*, with the great scapular notch being distally-oriented in the former, as opposed to medially-oriented (as seen in the latter).

*Humeri. N. galiani*: one right, UF 37031.

The humerus of *N. galiani* (Fig. 3) has a nearly straight diaphysis in anterior and posterior views, whereas the lateral and medial views have a slight, anterior-oriented, curve. Along the medial surface the diaphysis is nearly flattened anteroposteriorly. On the proximal epiphysis, in dorsal view, the articular head is elliptical in shape, compressed mediolaterally, and has a posteriorly projected distal notch. Bordering the anterolateral margin, the greater tubercle is proximally projected further than the articular head, and the lateral surface has an oval attachment scar depression. The greater tubercle crest protrudes anteromedially and is elongated distally along the anterior surface of the diaphysis, joining with the distal end of the deltoid tuberosity. Along the anteromedial margin of the articular head is a medially projected lesser tubercle. Between the greater and lesser tubercle, in medial view, lies a deep and narrow intertubercular groove, compressed anteroposteriorly. Below the articular head is a long and pronounced neck with a shallow lateral facet (muscle scar), posterodistal from the infraspinatus groove of the greater tubercle. Margins of the facet are not strongly pronounced. From this lateral facet extends a shallow anterodistal deltoid crest on the lateral surface, joining the

pectoral ridge in the middle of the diaphysis. On the medial surface of the proximal diaphysis is an elliptically elongated and rough facet, located anteriorly and close to the pectoral ridge.

On the distal epiphysis, the medial epicondyle is medially extended and larger than the lateral epicondyle. Lateral to the medial epicondyle is the trochlea (medial condyle), which is the distal most part of the humerus in anterior view. The lateral epicondyle is not well developed, but slightly protrudes laterally. Medial to the lateral epicondyle is the capitulum (lateral condyle). Between the trochlea and capitulum is a convex curve separating the two structures, where the capitulum is wider than the trochlea in anterior view. There is a large and well-developed supracondylar foramen (entepicondylar foramen), with a wide supracondylar ridge, on the proximal end of the medial epicondyle. On the medial epicondyle, at the distal end of the supracondylar ridge, is a round projection. On the posterior surface of the distal epiphysis is a deep and mediolaterally compressed olecranon fossa, with a straight lateral border. In the lateral epicondyle there is a shallow groove on the posterior side. The lateral supracondylar crest slightly protrudes laterally and is proximally projected into the middle of the diaphysis on the posterior surface.

*B. loveorum*: three partial left: UF 25081, UF 25101, UF 36883.

The humerus of *B. loveorum* (Fig. 3) has a nearly straight diaphysis with a gentle proximo-medial curve in anterior and posterior views, whereas the lateral and medial views have a slight, anterior-oriented, curve. Overall, the humerus is very robust. Along the medial surface, the diaphysis is flattened anteroposteriorly. On the proximal epiphysis, in dorsal view, the articular head is round, slightly compressed mediolaterally, and has a weak posteriorly projected distal notch. Bordering the anterolateral margin, the greater tubercle is greatly projected proximally past the articular head, and the lateral surface has an oval facet depression. The

greater tubercle crest protrudes anteromedially and is elongated distally along the anterior surface of the diaphysis, joining with the distal end of the deltoid tuberosity. Along the anteromedial margin of the articular head is the lesser tubercle, which has a reduced medial projection, a well-formed anterior crest, and is elongated distally. A long, smooth crest is projected distally from the distal end of the lesser tubercle to the diaphysis, minimizing the size of the neck medially. Between the greater and lesser tubercle, in medial view, lies a deep and wide intertubercular groove. Below the articular head is a short neck with a deep lateral facet, posterodistal from the infraspinatus groove of the greater tubercle. Margins of the facet are pronounced. From this lateral facet, extends a deep anterodistal deltoid crest on the lateral surface, joining the pectoral ridge in the middle of the diaphysis. On the medial surface of the proximal diaphysis is an elliptically elongated and rough scar, located posteriorly and close to the distal crest of the lesser tubercle.

On the distal epiphysis, the medial epicondyle is mediolaterally extended and larger than the lateral epicondyle. Lateral to the medial epicondyle is the trochlea (medial condyle), which is nearly level, yet more distal, to the medial epicondyle in anterior view. The lateral epicondyle is well developed, and greatly expanded laterally. Medial to the lateral epicondyle is the capitulum (lateral condyle). Between the trochlea and capitulum is a convex curve separating the two structures, where the capitulum and the trochlea are similar in width in anterior view. There is a small supracondylar foramen, with a narrow supracondylar ridge, on the proximal end of the medial epicondyle. On the medial epicondyle, at the distal end of the supracondylar ridge is an elliptical and deeply grooved scar. On the posterior surface of the distal epiphysis is a deep and wide olecranon fossa, with a straight lateral border. In the lateral epicondyle there is a deep groove on the posterior side. A groove continues distally, then proximally as it wraps around the

lateral epicondylar. The lateral supracondylar crest greatly protrudes laterally, and is proximally projected into the middle of the diaphysis on the posterior surface.

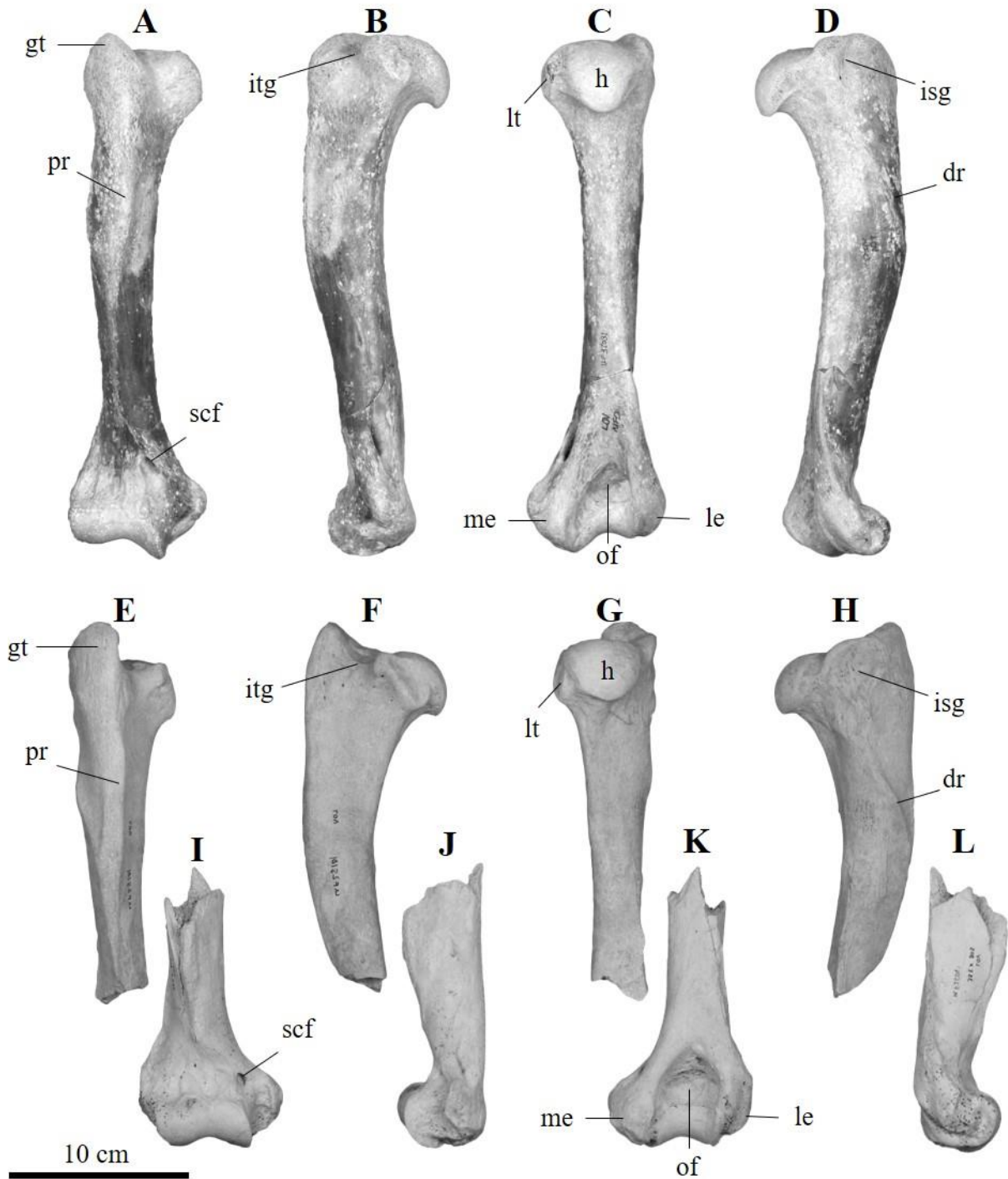


Figure 3. Humerus comparison views between both taxa. A-D *Nimravides galiani* UF 37031 right: anterior (A), medial (B), posterior (C), lateral (D) views. E-H *Barbourofelis loveorum* proximal UF 25101, I-L distal UF 25081, left sides inverted to right sides: anterior (E, I), medial (F, J), posterior (G, K), lateral (H, L) views. Abbreviations: dr, deltoid ridge; gt, greater tubercle; h, head; isg, infraspinatus groove; itg, intertubercular groove; le, lateral epicondyle; me, medial epicondyle; of, olecranon fossa; pr, pectoral ridge; scf, supracondylar foramen.

Remarks— The humeri diaphyses of *N. galiani* and *B. loveorum* are both nearly straight anteroposteriorly; with an anterior-oriented curve, mediolaterally. In medial view, the diaphysis is flattened more prominently in *B. loveorum* than *N. galiani*, which has a nearly flattened proximal end, and medially curved distal end. On the proximal epiphysis, the articular head is elliptical and mediolaterally compressed; with a noticeable posterior notch in *N. galiani*, whereas the head in *B. loveorum* is round with a reduced posterior notch. In dorsal view, the greater tubercle of *B. loveorum* is approximately the same width as the head anteroposteriorly, and noticeably larger than *N. galiani* in the anteromedial projection. The lesser tubercle is more medially projected and has a shorter and less defined anterior crest in *N. galiani*. In medial view, *B. loveorum* has a wider intertubercular groove, which is not compressed by the greater and lesser tubercles. Distal to the head, the neck is longer in *N. galiani*, with a less pronounced muscle scar. Along the anterior and lateral surfaces, the deltoid crest is higher ridged in *B. loveorum*, and the pectoral ridge is more robust and straighter than that of *N. galiani*. On the distal epiphysis, the medial epicondyle is slightly more medially projected in *N. galiani*, whereas *B. loveorum* has more pronounced and deeper ridges. Additionally, *B. loveorum* has visible small, round projections distally on the medial epicondyle. The trochlea is more distally extended in *N. galiani* and is approximately half the width and height of the capitulum. In *B. loveorum* the trochlea is approximately the same width and is near level proximally with the capitulum. On the lateral side, *B. loveorum* has a further projected lateral epicondyle, with more developed ridges and a deeper posterior groove. A larger supracondylar foramen with a thicker bar is present in several *N. galiani* specimens. Posteriorly, *B. loveorum* has a wider and larger olecranon fossa, whereas in *N. galiani*, the olecranon fossa is mediolaterally compressed and proximodistally shortened.

*Radii. N. galiani*: two left, UF 25625, UF 25624.

The radius of *N. galiani* (Fig. 4) has an anteroposteriorly compressed diaphysis which is posteriorly concave and anteriorly convex. In anterior and posterior views, the diaphysis has the same relative thickness proximodistally. On the proximal epiphysis, in posterior view, the bicipital tuberosity is elliptical and elongated proximodistally. Proximal to the bicipital tuberosity is a deep pit. Just proximal to this pit is a contracted neck followed by a medially inclined head. In dorsal view, the humeral articular fovea is elliptical and concave with a distinct proximally projected capitular eminence point on the anterior border. The medial border of the head is mediodistally projected and the neck is concave distally to the medial side of the head. Surrounding the head is the ulnar articular circumference which is narrow on the posterolateral side and wide anteromedially. Distal to the bicipital tuberosity, on the lateral surface, is a rough scar ridge elongated proximodistally towards the midsection of the diaphysis.

The distal epiphysis is mediolaterally expanded with the anterior surface a continuation of the diaphysis, whereas the posterior surface is separated from the diaphysis by a mediolateral ridge. On the medial surface, the styloid process is distally projected to a point. Along the medial border, proximal to the styloid process, is a large, well-developed, medially-protruding ridge. In lateral view, the distal ulnar facet is round and located anterodistally on the lateral surface, and projects laterally. On the anterior surface, a series of proximodistally oriented ridges are present: a larger elliptical ridge in the center, and two smaller ridges on the lateral and medial margins, respectively. Between these ridges are shallow grooves; one lateral to the central ridge, and another medial to the central ridge. In distal view, the scapholunate facet is mediolaterally elliptical and concave, with the lateral side anteroposteriorly wider than the medial side.

*B. loveorum*: three right, UF 25446, UF 25441, UF 25444, two left, UF 25438, UF 36928.

The radius of *B. loveorum* (Fig. 4) is robust and has an anteroposteriorly compressed diaphysis which is posteriorly concave and anteriorly convex. In anterior and posterior views, the diaphysis is mediolaterally wider on the distal end and is thinner on the proximal end. On the proximal epiphysis, in posterior view, the bicipital tuberosity is round and slightly elongated mediolaterally, with a deep groove on its distal surface. Lateral to the bicipital tuberosity is a smaller, well-developed, and round tuberosity. Proximal to the bicipital tuberosity is a contracted neck, followed by a medially inclined head. In dorsal view, the humeral articular fovea is elliptical and concave with a prominent proximally projected capitular eminence point on the anterior border. The medial border of the head is mediodistally projected, and the neck is concave distally to the medial side (of the head). Surrounding the head is the ulnar articular circumference which is narrow on the posterolateral side and wide anteromedially. Distal to the bicipital tuberosity, on the lateral surface, is a rough scar ridge which is elongated proximodistally towards the midsection of the diaphysis.

The distal epiphysis is mediolaterally expanded with the anterior surface being a continuation of the diaphysis, whereas the posterior surface is separated from the diaphysis by a mediolateral ridge. On the medial surface, the styloid process is distally projected to a point. Along the medial border, proximal to the styloid process, is a small, well-developed, anteromedially-protruding ridge. In lateral view, the distal ulnar facet is elliptical and located anterodistally on the lateral surface. On the anterior surface, a series of well-developed, proximodistally oriented ridges are present: a larger elliptical ridge in the center, and two smaller ridges on the lateral and medial margins. Between these ridges are deep grooves, one lateral to

the central ridge, and the other medial to the central ridge. In distal view, the scapholunate facet is mediolaterally elliptical and concave, with the lateral side being wider than the medial side.

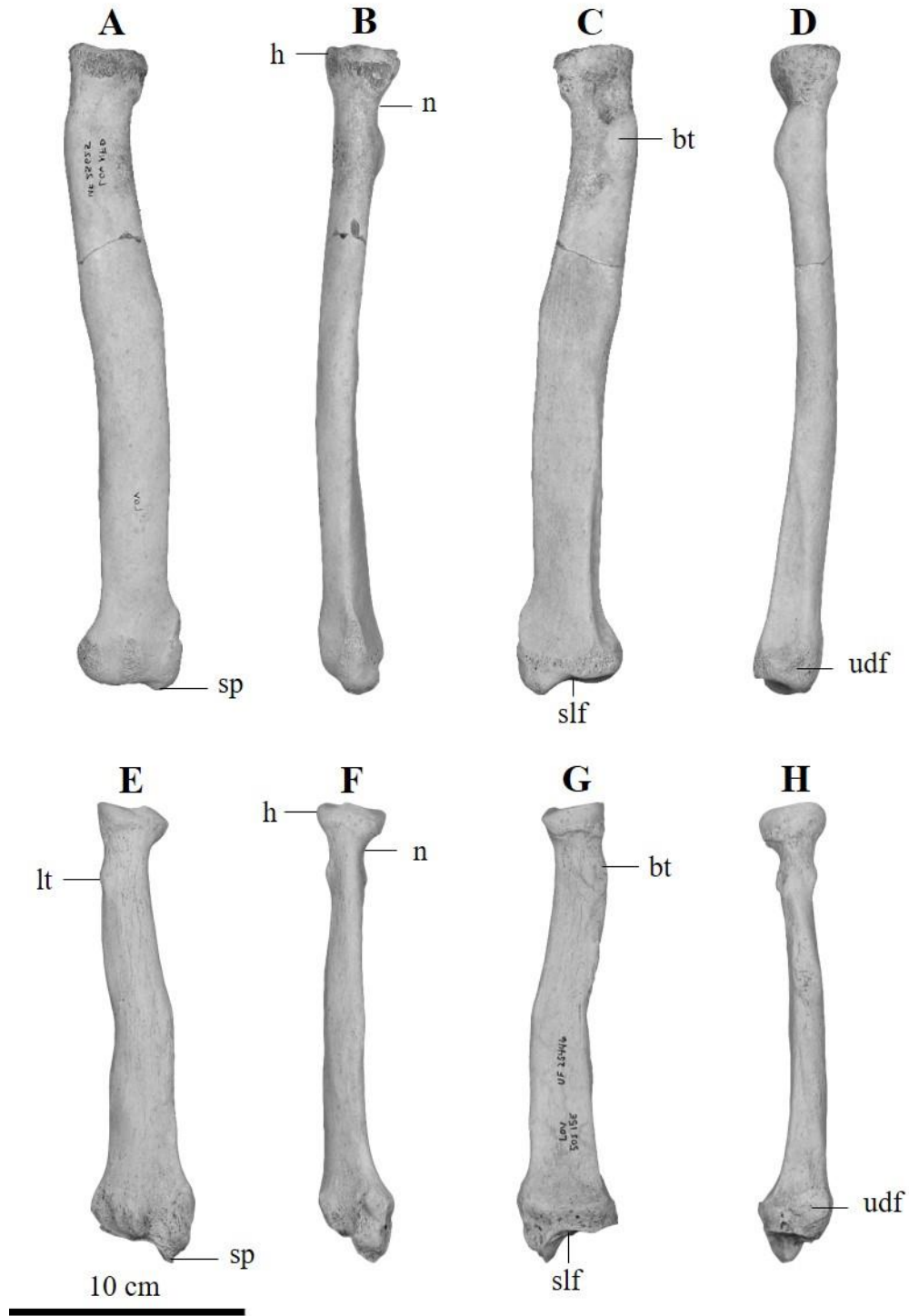


Figure 4. Radius comparison views between both taxa. A-D *Nimravides galiani* UF 25625 left side inverted to right side: anterior (A), medial (B), posterior (C), lateral (D) views. E-H *Barbourofelis loveorum* UF 25446 right: anterior (E), medial (F), posterior (G), lateral (H) views. Abbreviations: bt, bicipital tuberosity; h, head; lt, lateral tuberosity; n, neck; slp, scapholunar facet; sp, styloid process; udf, ulnar distal facet.

Remarks— The diaphysis is similar in shape and curvature between *N. galiani* and *B. loveorum*, however *B. loveorum* has a mediolaterally wider distal shaft which becomes thinner towards the proximal end. In anterior and posterior views, the diaphysis is nearly straight in the distal half, then sharply bends laterally and has a slight convex lateral curve in the proximal half of *B. loveorum*, whereas in *N. galiani* the kink is slightly more proximally oriented. In posterior view, the bicipital tuberosity is much larger and more proximodistally elliptical in *N. galiani*. In contrast, the tuberosity lateral to the bicipital tuberosity is much more pronounced and developed in *B. loveorum*. On the proximal epiphysis, the neck of *N. galiani* is proximodistally longer than in *B. loveorum*, and there is a deep, round groove proximal to the bicipital tuberosity in posterior view. On the distal epiphysis, the medial surface is ridged and more medially projected in *N. galiani*, and the medial border of the styloid process is laterally inset, whereas in *B. loveorum*, the bulbous medial border is continuous with the medial side of the styloid process. In lateral view, the ulnar facet is more elliptical in *B. loveorum*, but projects laterally in *N. galiani*. On the anterior surface, *B. loveorum* has a larger developed proximodistal central ridge, deeper medial and lateral grooves on either side of the ridge, and more pronounced medial and lateral ridges. In distal view, the scapholunate facet takes up the majority of the distal end in *N. galiani*, whereas in *B. loveorum* the anterior ridges protrude anteriorly past the articular ridge.

*Ulnae. N. galiani*: one right, UF 25622.

The ulna of *N. galiani* (Fig. 5) is slender and proximodistally elongate, tapering distally. In lateral and medial views, the diaphysis is mediolaterally flattened and nearly straight, whereas in anterior and posterior views there is a lateral-oriented curve. At the midsection on the diaphysis, on the lateral surface, is a proximodistally elongated scar, mediolaterally wider at the proximal end and thinning towards the distal epiphysis. On the proximal epiphysis is a wide and

well-developed, semilunar trochlear notch, distal to the olecranon. In lateral view, distal to the trochlear notch, is an anterolaterally elongated radial notch with a medially-oriented concave curve. A shallow groove between the radial notch and the lateral surface of the shaft extends just distal to the radial notch. The medial side of the radial notch extends anteriorly, forming the medially projected coronoid process, and is proximodistally thinner than the lateral process, and continues onto the medial surface. In medial view, the coronoid process extends anterodistally, past the anterior width of the diaphysis. Distal to the coronoid process is a small, proximodistal elliptical scar. Proximal to the radial notch and coronoid process is a mediolaterally narrow trochlear notch; a posteriorly-oriented, concave humeral facet. On the proximoposterior border of the trochlear notch is an elliptical groove. Along the proximal border of the trochlear notch is the anterolaterally projected anconeal process. Proximal to the anconeal process is the well-developed and proximally elongated olecranon. The olecranon is slightly posteriorly inclined on the posterior border, in lateral and medial views, and is greatly curved medially in anterior and posterior views. A pair of tubercles is present on the anteroproximal surface of the olecranon, laterally and medially, separated by a groove. Of these two, the medial tubercle is more proximally and distally extended, whereas the lateral tubercle is smaller and more anteriorly set. In medial view, the olecranon's proximal border is deeply ridged; however, in lateral view, the proximal border is smooth.

The distal epiphysis is anteroposteriorly constricted proximally and anteroposteriorly widened distally in medial and lateral views. In anterior and posterior views, the proximal region is mediolaterally widened on the medial surface by a round and medially projected ridge originating from the diaphysis. Distal to the medial projection, on the anterior surface, is an anterodistally elongated and oval ulnar head. On the medial surface, medial to the head, is a deep

proximoposterior groove. In lateral view, a proximoposterior-oriented groove originates from the distal head and leads to the medially curved, and posterodistally elongated, styloid process. The facet on the styloid process is on the medial surface and is elliptical.

*B. loveorum*: two right, UF 36893, UF 27253

The ulna of *B. loveorum* (Fig. 5) is robust and proximodistally short, tapering distally. There is an obvious lack of curvature on the diaphysis, which has approximately the same thickness mediolaterally as it does anteroposteriorly. At the midsection on the diaphysis, on the lateral surface, is a long proximodistal scar, mediolaterally wider at the proximal end and thinning towards the distal epiphysis. On the proximal epiphysis is a round and well-developed, semilunar trochlear notch, distal to the olecranon. A deep groove is between the radial notch and the lateral surface of the shaft, extending to the lateral diaphysis muscle scar. The medial side of the radial notch greatly extends anteriorly, forming the medially projected coronoid process on the medial surface, and has approximately the same proximodistal thickness as the lateral process. In medial view, the coronoid process extends nearly anteroproximally, past the anterior width of the diaphysis. Distal to the coronoid process is a small, proximodistal elliptical scar. Proximal to the radial notch and coronoid process is a mediolaterally wide trochlear notch; a posteriorly-oriented, concave humeral facet. On the proximoposterior border of the trochlear notch is an elliptical groove. Along the proximal border of the trochlear notch is the anterolaterally projected anconeal process. Proximal to the anconeal process is the well-developed, and proximally elongated, olecranon. The olecranon is nearly straight on the posterior border, in lateral and medial views, and is curved medially in anterior and posterior views. A pair of tubercles is located on the anteroproximal surface of the olecranon, laterally and medially, not separated by a groove. Of these two, the lateral tubercle is more proximally and anteriorly

extended, whereas the medial tubercle is smaller and more posteriorly set. In medial view, the olecranon's proximal border is deeply ridged. However, in lateral view, the proximal border is smooth, and the posterior border is ridged.

The distal epiphysis is slightly anteroposteriorly constricted proximally and anteroposteriorly widened distally in medial and lateral views. In anterior and posterior views, the proximal region is mediolaterally widened on the medial surface by an elongated and medially projected ridge originating from the diaphysis. Distal to this projection, on the anterior surface, is an anterodistally elongated and oval ulnar head. On the medial surface, medial to the head, is a deep proximoposterior groove. In lateral view, a proximoposterior-oriented curve originates from the distal head and leads to the medially curved and posterodistally elongated styloid process. The facet on the styloid process is on the medial surface and is elliptical.

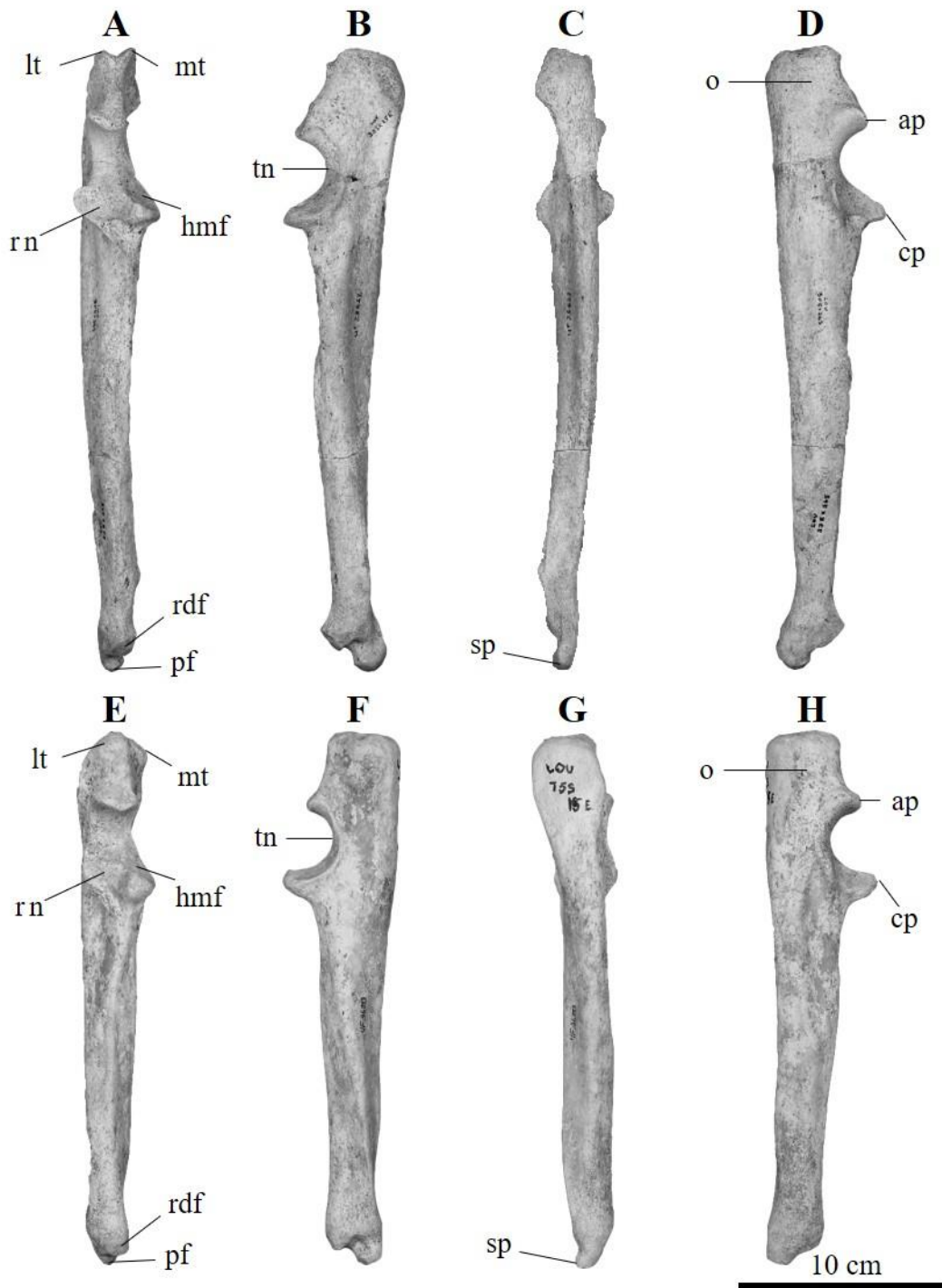


Figure 5. Ulna comparison views between both taxa. A-D *Nimravides galiani* UF 25622 right: anterior (A), medial (B), posterior (C), lateral (D) views. E-H *Barbourofelis loveorum* UF 36893 right: anterior (E), medial (F), posterior (G), lateral (H) views. Abbreviations: ap, anconeal process; cp, coronoid process; hmf, humeral medial distal facet; lt, lateral tubercle; mt, medial tubercle; o, olecranon; pf, pisiform facet; rdf, radial distal facet; rn, radial notch; sp, styloid process; tn, trochlear notch.

Remarks— The ulna of *N. galiani* is long and mediolaterally flattened with a lateral-oriented curve in anterior and posterior views, whereas *B. loveorum* has a short and stout ulna that is nearly straight in all views and has a uniform thickness. A large, proximodistally elongated scar on the lateral surface of the diaphysis is present on both taxa, but is more pronounced in the *N. galiani* specimens observed. On the proximal epiphysis, *B. loveorum* has a mediolaterally wider trochlear notch. Distal to the trochlear notch is the radial notch, which is similar in length mediolaterally on both species. However, *N. galiani* has a wider lateral process proximodistally. Additionally, there is a mediolateral groove directly distal to the radial notch in *N. galiani*, but is mostly absent in *B. loveorum*. Lateral to the radial notch, *B. loveorum* has a deeper and proximodistally longer groove. Medial to the radial notch is the coronoid process, expanding anterolaterally in *N. galiani* and slightly anterop proximally in *B. loveorum* in medial view. On the proximal border of the trochlear notch, the anconeal process is mediolaterally wider in *B. loveorum*. Proximal to the trochlear notch is the olecranon which is mediolaterally wider and nearly straight on the posterior border of *B. loveorum*, whereas the posterior border in *N. galiani* is posteriorly bent. On the olecranon, the lateral tubercle of *B. loveorum* is more enlarged than the medial tubercle and is more anterior oriented, whereas the lateral tubercle of *N. galiani* is less developed than the enlarged medial tubercle. Between the olecranon tubercles there is a deep anteroposterior groove in *N. galiani* and no clear separation in *B. loveorum*. The distal epiphysis of *B. loveorum* is robust with a medially elongated proximodistal ridge, only present in *N. galiani* as a round projection. On the lateral surface, *B. loveorum* has a laterally thicker distal epiphysis than in *N. galiani*. Distal to the medial ridge, in anterior view, both taxa have similar ulnar heads and proximoposterior grooves. However, *N. galiani* has a larger styloid process, projecting further posteriorly, and cuneiform articular surface.

## *Carpals*

*Scapholunar. N. galiani*: three right, UF 25142, UF 464300, UF 464301, one left, UF 25139.

The scapholunar of *N. galiani* (Fig. 6) is the largest carpal and roughly quadrangular in shape. On the proximal surface, the radial facet is rectangular and mediolaterally convex. Along the mediolateral region, the articular surface is proximally extended, whereas the lateropalmar border is curved distally. Continuing mediolaterally, an elongated palmar tubercle is mediopalmarly orientated and compressed mediolaterally. Located on the medial surface of the palmar tubercle is a small and oval facet for the radial sesamoid. In distal view, there are a series of clearly separated grooves and facets, mostly running dorsolaterally to palmar-medially. On the lateral surface of the distal face, the facet for the unciform is mediolaterally thin and flattened, elongated palmar-dorsally. In distomedial view, the proximal end of the unciform facet is proximally concave, continuing palmarly into a distally convex face. Medial to the unciform facet is a deeply gouged groove for the magnum. Separating the unciform and magnum articulations is a sharp dorsopalmar ridge. The dorsal region of the groove for the magnum is dorsodistally elongated. On the center of the medial border, the magnum groove is slightly mediolaterally constricted, yet still wider than the unciform facet. Medial to the magnum facet is a less pronounced trapezoid facet, clearly separated from the magnum facet by a distally elongated ridge. Nearly triangular in shape, the trapezoid facet borders the dorsomedial edge of the distal surface and the medial edge of the magnum facet. On the dorsomedial region, the articular surface is round and flat. Through the center of the facet, mediolaterally, there is a sharp and distally elongated convex curve. In dorsal view, the trapezoid facet is proximally concave, as the dorsolateral region is distally elongated along with the dorsomedial surface of the magnum

facet. Palmar to the trapezoid facet, and medial to the magnum facet, is a smooth articular surface for the trapezium. The separation between the trapezoid and trapezium articular surfaces is not clear. Similar to the trapezoid facet, the trapezium articular surface is slightly triangular shaped. There are two primary smooth articular surfaces: a smooth, round area medio-palmar to the trapezoid facet, and a mediolaterally elliptical, and proximally concave, groove medial to the magnum facet. In the center of the trapezium is a continuation of the mediolateral ridge from the trapezoid facet.

*B. loveorum*: two left, UF 25149, UF 25156.

The scapholunar of *B. loveorum* (Fig. 6) is the largest carpal and roughly quadrangular in shape. On the proximal surface, the radial facet is rectangular and mediolaterally convex. Along the mediolateral region, the articular surface is proximally extended, whereas the lateropalmar border is curved distally. Continuing mediolaterally, an elongated and thick palmar tubercle is mediopalmarly orientated, curving proximopalmarly. Located on the medial surface of the palmar tubercle is a small and oval facet for the radial sesamoid. In distal view, there are a series of separated grooves and facets, mostly running dorsolaterally to palmar-medially. On the lateral surface of the distal face, the groove for the unciform articulation is mediolaterally thin and elongated palmar-dorsally. In distomedial view, the unciform facet is proximally concave and deep. The palmar border of the groove sharply curves palmar-proximally, forming a distal-oriented convex angle. Medial to the unciform facet is an inset magnum articular groove. Separating the unciform and magnum articulations is a smooth dorsopalmar ridge. The dorsal region of the magnum groove is greatly dorsodistally elongated, with the dorsomedial border curving dorsally. On the center of the medial border, the magnum facet is mediolaterally constricted and is approximately the same width as the unciform facet. Medial to the magnum

facet is a pronounced trapezoid facet, clearly separated by the magnum facet by an elongated ridge, dorsally, and a ridge, palmarly. Nearly triangular in shape, the trapezoid facet borders the dorsomedial edge of the distal surface and the mediodorsal edge of the magnum facet. On the dorsomedial region, the articular surface is slightly proximally concave. Through the center of the facet, mediolaterally, there is a shallow groove, whereas the palmar border is distally ridged. In dorsal view, the trapezoid facet is proximally concave, as the dorsolateral region is greatly distally elongated along with the dorsomedial surface of the magnum facet. Palmar to the trapezoid facet, and medial to the magnum facet, is a smooth articular surface for the trapezium. The separation between the trapezoid and trapezium articular surfaces is very noticeable. Unlike the trapezoid facet, the trapezium facet is mediolaterally elliptical. In distal view, the facet is dorsopalmarly flattened and elongated onto the distal side of the palmar tubercle.

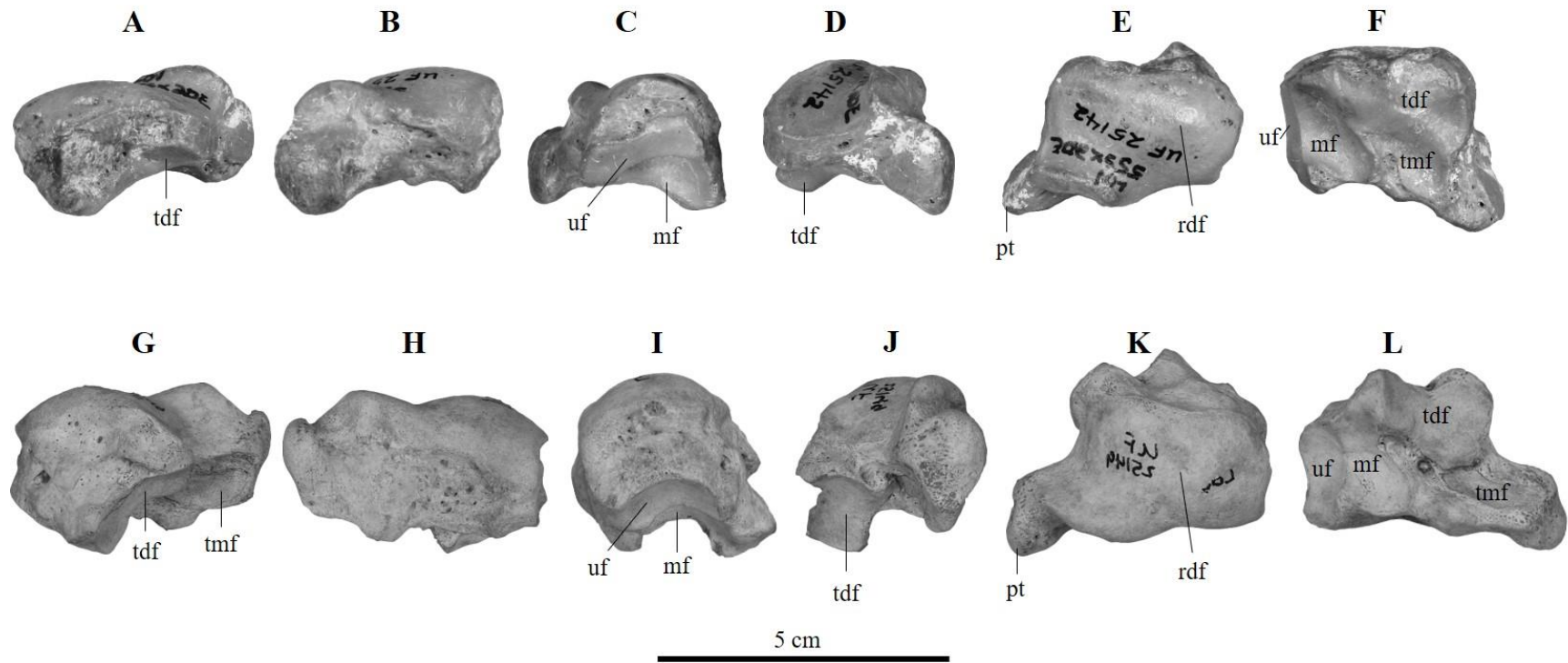


Figure 6. Scapholunar comparison views between both taxa. A-F *Nimravides galiani* UF 25142 right: dorsal (A), palmar (B), medial (C), lateral (D), proximal (E), distal (F) views. G-L *Barbourofelis loveorum* UF 25149 left side inverted to right side: dorsal (G), palmar (H), medial (I), lateral (J), proximal (K), distal (L) views. Abbreviations: mf, magnum facet; pt, palmar tubercle; rdf, radial distal facet; tdf, trapezoid facet; tmf, trapezium facet; uf, unciform facet.

Remarks—The scapholunar of *B. loveorum* is more robust, and larger relative to body size, than that of *N. galiani*. On the mediolateral border, *B. loveorum* has a thicker palmar tubercle that is prominently curved lateropalmarly, compared to the mediopalmarly straightened tubercle on *N. galiani*. In distal view, *N. galiani* has a mediolaterally thin and flattened unciform facet, whereas *B. loveorum* has a thicker facet, which is deeply concave. Both taxa have an inset magnum facet, however, in *N. galiani* the facet is proximally deeper. Additionally, the magnum facet in *N. galiani* is mediolaterally wider than the unciform facet. In dorsal view, *B. loveorum* has a more distally projected trapezoid facet and, in distal view, a clear separation between the articulations for the magnum and the trapezium. In *N. galiani*, the trapezoid facet has a mediolateral convex curve through the center. The trapezium facet in *B. loveorum* is less triangular and more elliptical than in *N. galiani*.

*Pisiform. N. galiani*: one left, UF 464290.

The pisiform of *N. galiani* (Fig. 7) is dorsopalmarly elongated with a mediolaterally widened palmar tubercle. On the dorsal end, the pisiform is elongated proximodistally, with the proximal side greatly protruding out dorsoproximally. Located on the dorsal surface are two smooth facets separated by a sharp, convex angular ridge as both facets slant in opposite directions. In medial view, the cuneiform articular surface is proximodistally elliptical and flattened, widened in the distal border, and dips palmar-medially. Palmar to the cuneiform facet is an enlarged, rounded ridge wrapping around the facet, and connecting to the protruding proximal border. On the lateral surface the ulnar facet is triangular, stretching lateropalmarly, and is slightly concave. The palmar border of the ulnar facet protrudes distally, forming a ridge and groove along the lateral border. Palmardistally to the ulna facet is a narrow dorsopalmar groove followed by a parallel ridge connecting at the dorsodistal end to the lateral region of the

palmar tubercle. On the palmar tubercle, there is a defined ridge outlining the tubercle from the rest of the pisiform, proximodistally, on the medial surface. In palmar view, the palmar tubercle is elongated mediolaterally and rounded, with a groove roughly mediolaterally-oriented on the lateral side. Lateral to the groove, the tubercle is laterally projected.

*B. loveorum*: one left, UF 490627.

The pisiform of *B. loveorum* (Fig. 7) is dorsopalmarly elongated with a mediolaterally widened palmer tubercle. On the dorsal end, the pisiform is elongated proximodistally, with the proximal side greatly protruding out dorsoproximally. Located on the dorsal surface are two smooth facets separated by a sharp, convex angular ridge as both facets slant in opposite directions. In medial view, the cuneiform articular surface is proximodistally elliptical and flattened, widened in the proximal border, and dips palmar-medially. Palmar to the cuneiform facet is a small and round, grooved ridge. On the lateral surface the ulnar facet is triangular, stretching lateropalmarly, and is greatly proximodistally concave. The palmar border of the ulnar facet protrudes distally, forming a shallow groove along the lateral border. Palmardistally to the ulna facet, the pisiform shaft is constricted and thin mediolaterally, followed by a sharp, and proximodistally thin, lateral ridge approximately at the midsection of the pisiform. On the palmar tubercle, there is a slight ridge outlining the tubercle from the rest of the pisiform, proximodistally, on the medial surface. In palmar view, the palmar tubercle is elongated mediolaterally and rounded, with a very shallow groove roughly mediolaterally-oriented on the lateral side. Lateral to the groove, the tubercle is laterodistally projected.

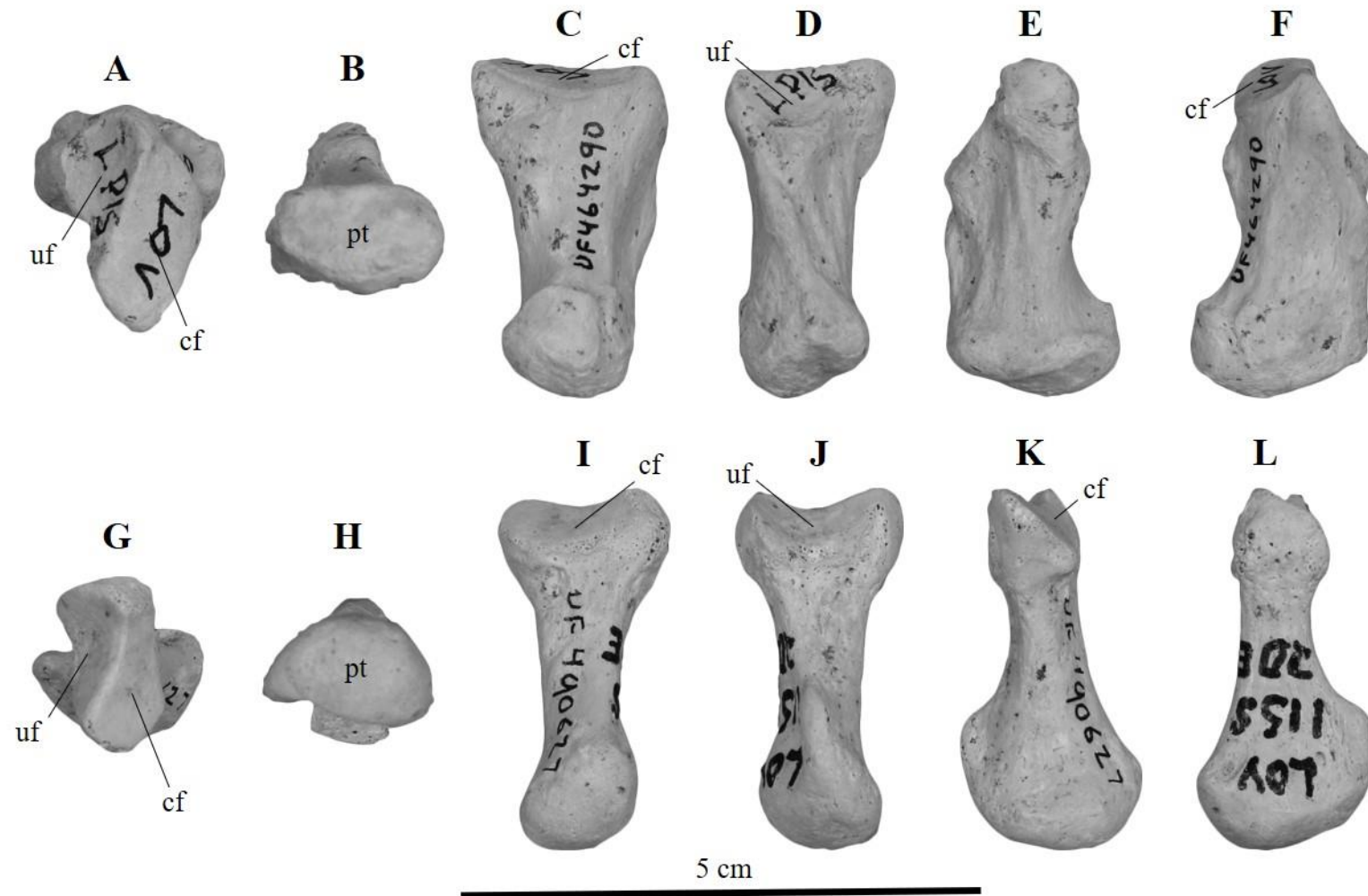


Figure 7. Pisiform comparison views between both taxa. A-F *Nimravides galiani* UF 464290 left: dorsal (A), palmar (B), medial (C), lateral (D), proximal (E), distal (F) views. G-L *Barbourofelis loveorum* UF 490627 left side inverted to right side: dorsal (G), palmar (H), medial (I), lateral (J), proximal (K), distal (L) views. Abbreviations: cf, cuneiform facet; pt, palmar tubercle; uf, ulnar facet.

Remarks— Both taxa have similarly pisiforms, dorsopalmarly. However, the pisiform of *B. loveorum* is much more proximodistally constricted than that of *N. galiani*. On the medial surface, the cuneiform facet points lateropalmarly in *B. loveorum*, and mediopalmarly in *N. galiani*. Palmar to the cuneiform facet, a large ridge is found in *B. loveorum*, whereas in *N. galiani* only a small groove is seen. On the lateral surface, the ulnar facet is more concave in *B. loveorum*. Palmar to the ulnar facet, *N. galiani* has a large, laterally protruding ridge running from the dorsal surface to the palmar tubercle, whereas in *B. loveorum*, the dorsal half of this ridge is not present on this specimen. On the palmar tubercle, *N. galiani* has a strong ridge, and clear separation, along the tubercle border, and there is a deep lateral groove on the tubercle's palmar surface, differing from the weak separation of shallow tubercle groove in *B. loveorum*.

*Unciform. N. galiani*: one right, UF 26159, two left, UF 26158, UF 26157.

The unciform of *N. galiani* (Fig. 8) is mostly cubed and mediolaterally wider towards the dorsal surface. In dorsal view, the surface is rough and slightly concave. From the proximal to distal border, the dorsal surface widens mediolaterally. On the unciform's proximal surface there is a smoothed and mediolaterally thin scapholunar facet, proximally convex, dorsally, and distally concave, palmarly. In lateral view, a smooth, oval cuneiform facet is present dorsoproximally, slightly projecting laterally. Palmar to the cuneiform facet is a deep proximodistal groove and is the thinnest part of the unciform, mediolaterally. Distal to the cuneiform facet, the dorsal surface extends laterally. On the medial surface, in the dorsal region, is a proximodistally elongated magnum facet, dorsopalmarly wider in the distal region. The palmar border of the magnum facet is dorsopalmarly constricted at the center, more so palmarly. Palmar to the magnum facet is a deep and round groove, centered in the same region as the groove from the lateral side. On the distal surface is the largest facet for the fourth and fifth

metacarpals on the medial and lateral sides, respectively. The MC IV and V facet is proximally concave and nearly triangular with a thin, smooth ridge dorsopalmarly through the center, marking the articular separation of the metacarpals. Along the lateral border, the center of the MC V facet is mediolaterally constricted.

*B. loveorum*: one right, UF 26148.

The unciform of *B. loveorum* (Fig. 8) is slightly cubed and mediolaterally wider towards the dorsal surface. In dorsal view, the surface is rough and slightly convex. From the proximal to distal border, the dorsal surface widens mediolaterally. On the unciform's proximal surface there is a smoothed and mediolaterally thin scapholunar facet, strongly proximally convex, dorsally, and greatly distally concave, palmarly. In lateral view, a smooth, oval cuneiform facet is present dorsoproximally, slightly projecting laterally. Palmar to the cuneiform facet is a deep circular groove and is the thinnest part of the unciform, mediolaterally. Distal to the cuneiform facet, the dorsal surface extends laterally. On the medial surface, in the dorsal region, is a proximodistally elongated magnum facet, dorsopalmarly wider in the distal region. The palmar border of the magnum facet is dorsopalmarly constricted at the center, more so palmarly. Palmar to the magnum facet is a deep and round groove, centered in the same region as the groove from the lateral side. Palmardistally to the groove is an elongated ridge. On the distal surface is the largest facet for the fourth and fifth metacarpals on the medial and lateral sides, respectively. The MC IV and V facet is proximally concave and nearly triangular with a thin, smooth ridge dorsopalmarly through the center, marking the articular separation of the metacarpals.

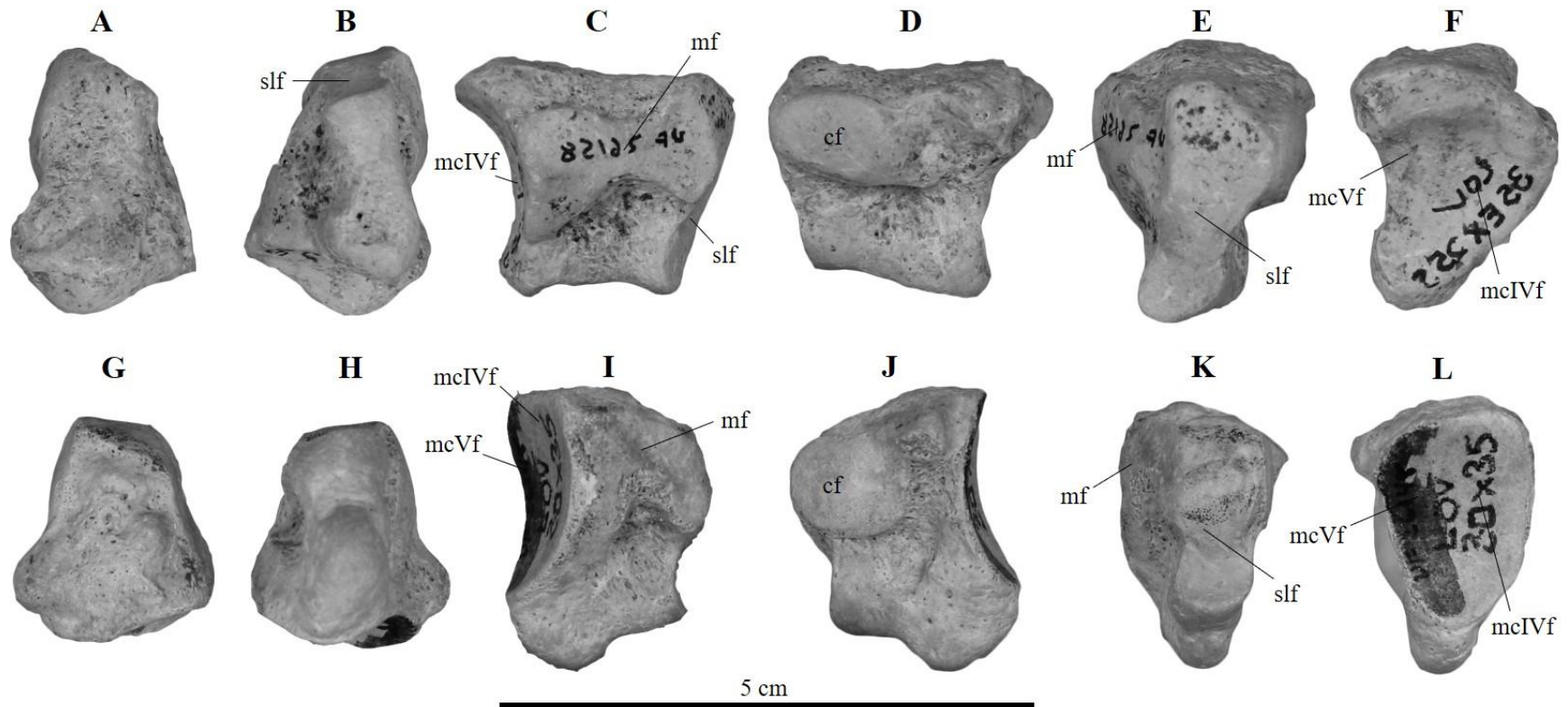


Figure 8. Unciform comparison views between both taxa. A-F *Nimravides galiani* UF 26158 left side inverted to right side: dorsal (A), palmar (B), medial (C), lateral (D), proximal (E), distal (F) views. G-L *Barbourofelis loveorum* UF 36148 right: dorsal (G), palmar (H), medial (I), lateral (J), proximal (K), distal (L) views. Abbreviations: cf, cuneiform facet; mcIVf, metacarpal IV facet; mcVf, metacarpal V facet; mf, magnum facet; slf, scapholunar facet.

Remarks—The unciform is slightly larger proximodistally in *N. galiani*, however is shorter dorsopalmarly compared to *B. loveorum*. In dorsal view, the surface is convex in *B. loveorum* and concave in *N. galiani*. On the proximal surface, the scapholunar facet is mediolaterally thinner in *N. galiani*, whereas *B. loveorum* has more pronounced concave-convex dorsopalmar curves. In lateral view, the cuneiform articulation is larger in *B. loveorum*, however the ridge palmar of it is proximodistally shorter. On the medial surface, the cuneiform articulation is similar in both taxa, however the groove just palmer to it is more proximodistally wide in *N. galiani*, and deeper in *B. loveorum*. In *B. loveorum*, the palmar end of the lateral and medial surfaces greatly extends palmarly, and only very slightly in *N. galiani*. In distal view, the articulation for the MC V is mediolaterally constricted along the lateral border of *N. galiani*, whereas in *B. loveorum* the lateral border is straight.

*Magnum. N. galiani*: one right, UF 26155, two left, UF 26154, UF 26156.

The magnum of *N. galiani* (Fig. 9) is semicircular, in medial and lateral views, along the proximal surface, and mediolaterally flattened towards the proximal end. On the dorsal surface there is a medial projection of the distal border that is dorsally convex. Proximal to the medial projection, a proximally concave curve begins and continues onto the proximal surface. In proximal view, this smooth curve articulates to the scapholunar and runs diagonally, dorsolaterally to palmarmedially. In lateral view, the unciform facet is on the dorsodistal ridge, dorsopalmarly, with no clear separation between the scapholunar and unciform facets. The distal edge of the lateral surface is concave. In medial view, the scapholunar facet curves into view on the dorsal region. On the dorsal medial projection there are two small articular surfaces. Near the palmar border is a round and slightly grooved facet for the MC III. Proximal to the MC III facet, and separated by a clear ridge, is a small and grooved facet for the trapezoid. There's no clear

articulation for the MC II on this medial projection. Proximopalmar to this projection is a rough and round facet for the trapezoid, continuing from the smoother facet from the medial projection. Palmar to the trapezoid facet is a large, round concave groove for the articulation of the MC II. In distal view, the largest facet of the magnum is present for the articulation of the MC III, continuing from the facet on the medial projection. The MC III facet is concave and dorsopalmarly elongated. At the center of the groove, the medial border is constricted, forming a facet with an hourglass-shape. In palmar view, the surface is rough, and the proximomedial edge is greatly palmarly extended.

*B. loveorum*: one right, UF 26139.

The magnum of *B. loveorum* (Fig. 9) is semicircular, in medial and lateral views, along the proximal surface, and mediolaterally flattened towards the proximal end. On the dorsal surface there is a medial projection of the distal border that is dorsally convex. Proximal to the medial projection, a proximally concave curve begins and continues onto the proximal surface. In proximal view, this smooth curve articulates to the scapholunar and runs diagonally, dorsolaterally to palmarmedially. In lateral view, the unciform facet is on the dorsodistal ridge, dorsopalmarly, with no clear separation between the scapholunar and unciform facets. The distal edge of the lateral surface is concave. In medial view, the scapholunar facet curves into view on the dorsal region. On the dorsal medial projection there are two small articular surfaces. Near the palmar border is a round and slightly grooved facet for the MC III. Proximal to the MC III facet, and separated by a clear ridge, is a small and grooved facet for the trapezoid. There is no clear articulation for the MC II on this medial projection. Proximopalmar to this projection is a rough and round facet for the trapezoid, continuing from the smoother facet from the medial projection. Palmar to the trapezoid facet is a larger, round concave groove for the articulation of the MC II.

In distal view, the largest facet of the magnum is present for the articulation of the MC III, continuing from the facet on the medial projection. The MC III facet is concave and dorsopalmarly elongated. At the center of the groove, the medial border is constricted, forming a facet with an hourglass-shape. In palmar view, the surface is rough, and the proximomedial edge is palmarly extended.

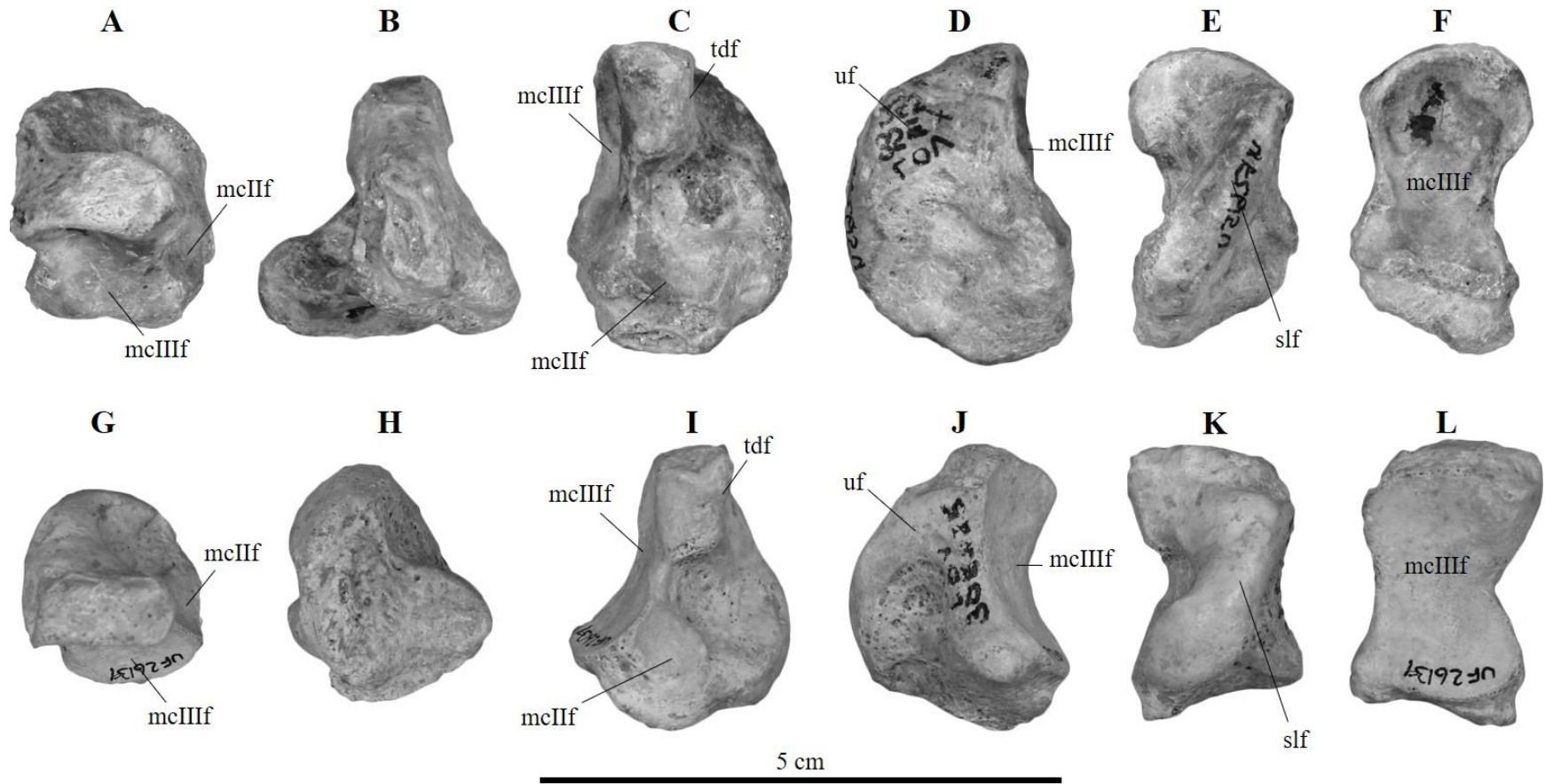


Figure 9. Magnum comparison views between both taxa. A-F *Nimravides galiani* UF 26154 left side inverted to right side: dorsal (A), palmar (B), medial (C), lateral (D), proximal (E), distal (F) views. G-L *Barbouroufelis loveorum* UF 26139 right: dorsal (G), palmar (H), medial (I), lateral (J), proximal (K), distal (L) views. Abbreviations: mcIIIf, metacarpal II facet; mcIIIIf, metacarpal III facet; slf, scapholunar facet; tdf, trapezoid facet; uf, unciform facet.

Remarks—The magnum of both taxa are mostly similar in size and shape. On the dorsal surface, the medial projection is larger in *B. loveorum* and less convex than in *N. galiani*. In lateral view, the scapholunar projection is pronounced more dorsally in *N. galiani*. On the dorsomedial projection, in medial view, both taxa appear to have no articulation for the MC II. In *N. galiani*, the facets for the MC III and trapezoid, on the medial projection, are more pronounced than that of *B. loveorum*. Additionally, the facet for the MC II, palmar to the projection, is larger in *N. galiani*. In palmar view, the roughened surface is more palmarly extended in *N. galiani*.

*Trapezoid. N. galiani*: one left, UF 37116.

The trapezoid of *N. galiani* (Fig. 10) is mostly triangular in proximal and distal views, tapering out to a point, palmarly, and is proximodistally thin. In dorsal view, the surface is rough and bends convex in the proximal direction, in the lateral half, and concave in the medial half. In proximal view, the majority of the surface is smooth and articulates with the scapholunar. Beginning at the dorsomedial border, the surface is convex, then turns concave approximately a third of the way, palmarly. In lateral view, the facet for the magnum is proximodistally thin, but wider at the palmar end. On the medial surface, the articulation for the trapezium is smooth and dorsopalmarly elongated. Proximodistally wider at the palmar region, the trapezium facet becomes thinnest at the center, then continues into the MC II facet on the distal surface. In distal view, the majority of the MC II facet is smooth, with a convex curve turning concave, mediolaterally.

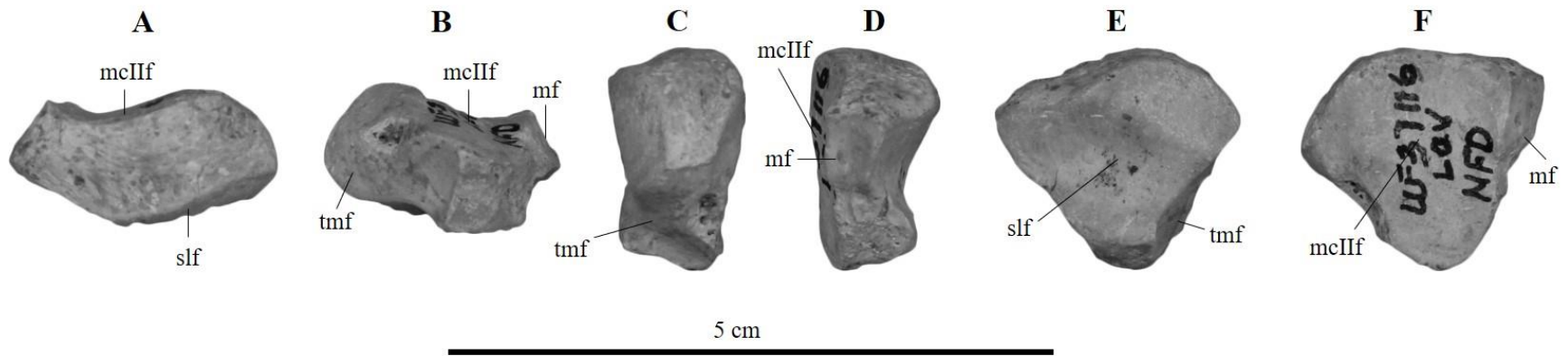


Figure 10. Trapezoid views for *Nimravides galiani* A-F UF 37116 left: dorsal (A), palmar (B), medial (C), lateral (D), proximal (E), distal (F) views. Abbreviations: mcIIif, metacarpal II facet; mf, magnum facet; tmf, trapezium facet; slf, scapholunar facet.

Remarks—The trapezoid for *B. loveorum* is unavailable to describe and discuss. As such, direct morphological descriptions were unable to be made, and only the trapezoid articulations found on the scapholunar, trapezium, and MC II surfaces can be identified and discussed.

### *Metacarpals*

*Metacarpal I. N. galiani*: one right, UF 25327.

The first metacarpal (MC I) of *N. galiani* (Fig. 11) is very robust, more than half as wide, mediolaterally, as it is long, proximodistally. In dorsal view, the MC I is cylindrical, with a mediolaterally wider proximal end, and a distally extended distolateral head. From the head, a smooth ridge runs proximally towards the proximolateral end. On the proximomedial side, the trapezium facet is smooth and elliptical, nearly mediolaterally. In proximal view, the trapezium facet continues and rounds off, taking up a third of the proximal surface of MC I. A thin dorsopalmar ridge separates the trapezium facet from the lateral side of the proximal face. In palmar view, closer to the distal border, there is a large elliptical keel protruding palmarly between the medial and lateral head extensions. This protrusion, and the palmar side of the head, is smooth for the articulation of the proximal phalanx.

*B. loveorum*: one right, UF 25326.

The first metacarpal (MC 1) of *B. loveorum* (Fig. 11) is very slender, with a mediolaterally and dorsopalmarly constricted shaft and enlarged proximal and distal ends. In dorsal view, the MC I is straight with concave medial and lateral sides and a distally extended distolateral head. On the proximomedial side, the trapezium facet is smooth and elliptical, proximodistally. In proximal view the trapezium facet continues and squares off, taking up the majority of the proximal surface. A well-pronounced dorsopalmar ridge separates the trapezium facet from the lateral side of the distally stretched proximal face. In palmar view, closer to the

distal border, there is a well-defined elliptical keel protruding palmarly between the medial and lateral head extensions. This protrusion, and the palmar side of the head, is smooth for the articulation of the phalanx.

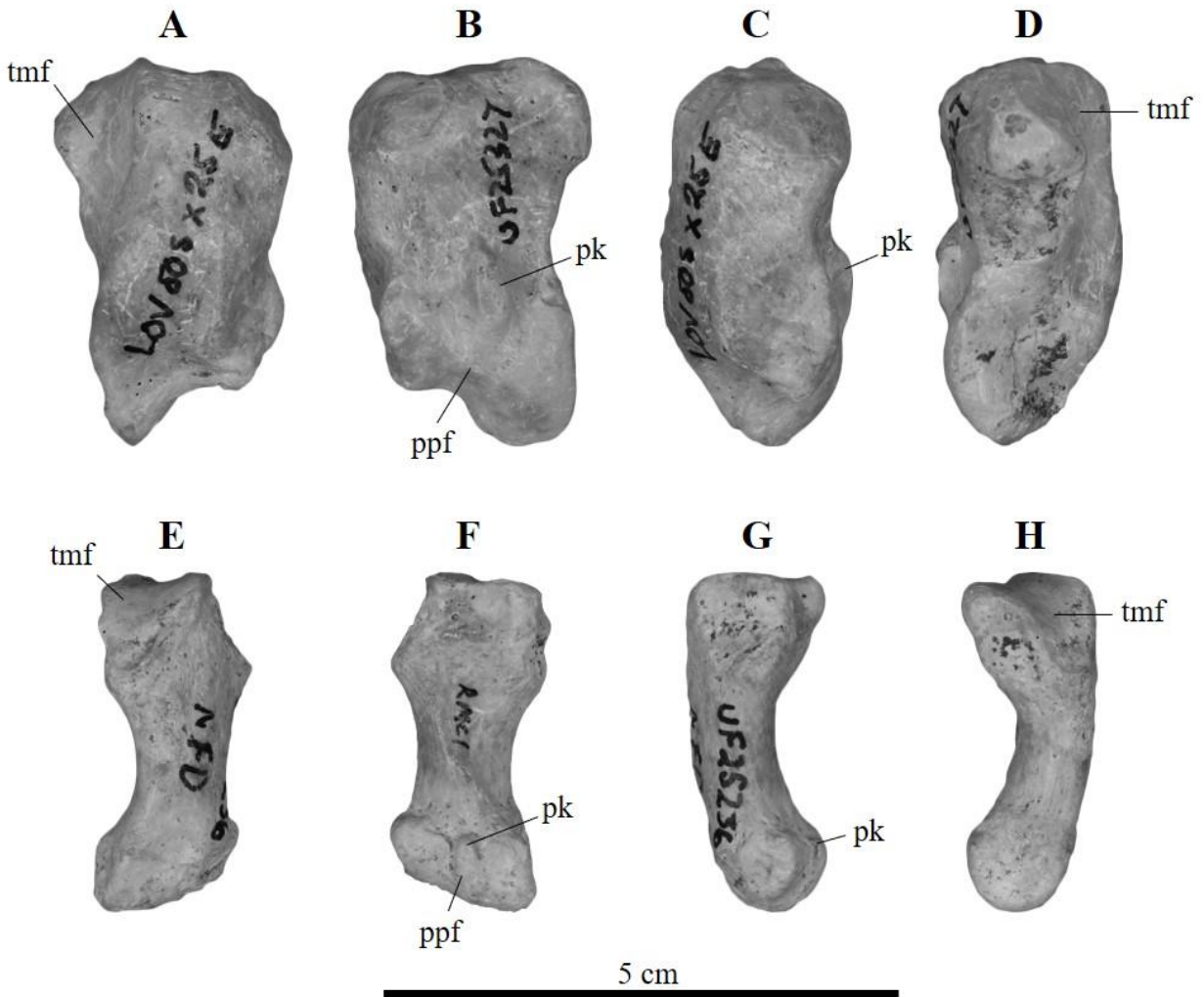


Figure 11. Metacarpal I comparison views between both taxa. A-D *Nimravides galiani* UF 25327 right: dorsal (A), palmar (B), medial (C), lateral (D) views. E-H *Barbourofelis loveorum* UF 25236 right: dorsal (E), palmar (F), medial (G), lateral (H) views. Abbreviations: pk, palmar keel; ppf, proximal phalanx facet; tmf, trapezium facet.

Remarks—MC I differs greatly between *N. galiani* and *B. loveorum*. On the distal surface, *N. galiani* has a stouter MC I with a diagonal ridge which is absent in *B. loveorum*. The large trapezium facet is deep and placed mediolaterally in *N. galiani*, whereas in *B. loveorum*, the trapezium facet is gently grooved and oriented proximodistal. In proximal view, the continuation of the trapezium facet is more than half of the surface in *B. loveorum*, but about a third in *N. galiani*, as *N. galiani* has a large and bulbous proximolateral end. In palmar view, the articulation for the phalanx in *N. galiani* has a larger central protrusion than in *B. loveorum*.

*Metacarpal II. N. galiani: one right, UF 25334.*

The second metacarpal (MC II) of *N. galiani* (Fig. 12) is cylindrical and elongated with an enlarged distal head and proximal base. The diaphysis is straight in dorsal view, and has a slight convex curve. On the dorsal surface, near the proximal base, is a deep oblique groove running from the medial side distally to the lateral side, continuing onto the palmar surface. In lateral view, on the proximal border, there are two articular surfaces for the trapezium, separated by an area of no articulation. The dorsal trapezium facet is the larger of the two and both are circular. Distal to the dorsal facet is a round and enlarged tubercle. In between the trapezium facets is a rough scar which elongates distally to the tubercle. In proximal view, the triangular surface is grooved for the articulation of the trapezoid. Palmar to the trapezoid facet is a round and smaller articulation surface for the magnum, bending into the lateral surface. In lateral view, a proximodistally elongated groove, near the dorsal-proximal ridge, is for the articulation of the MC III. Palmar to the MC III facet are rough ridges extending to the oblique groove originating from the dorsal surface.

*B. loveorum: two right, UF 37848, UF 25249.*

The second metacarpal (MC II) of *B. loveorum* (Fig. 12) is cylindrical and proximodistally compressed, with an enlarged distal head and proximal base. The diaphysis is straight in dorsal view, and is flat. On the dorsal surface, near the proximal base, is a shallow, circular groove. In lateral view, on the proximal border, there is an articular surface for the trapezium, and it does not appear that there is a second trapezium facet. The dorsal trapezium facet is large and circular. Distal to the facet is a round tubercle. Palmar to the tubercle and facet is a rough scar and ridge which elongates distally to the tubercle. In proximal view, the triangular surface is grooved for the articulation of the trapezoid. Palmar to the trapezoid facet is a round and smaller articulation surface for the magnum, bending into the lateral surface. In lateral view, a proximodistally elongated groove, near the dorsal-proximal ridge, is for the articulation of the MC III. Palmar and dorsodistal to the MC III facet are rough ridges extending more than half the length of the diaphysis.

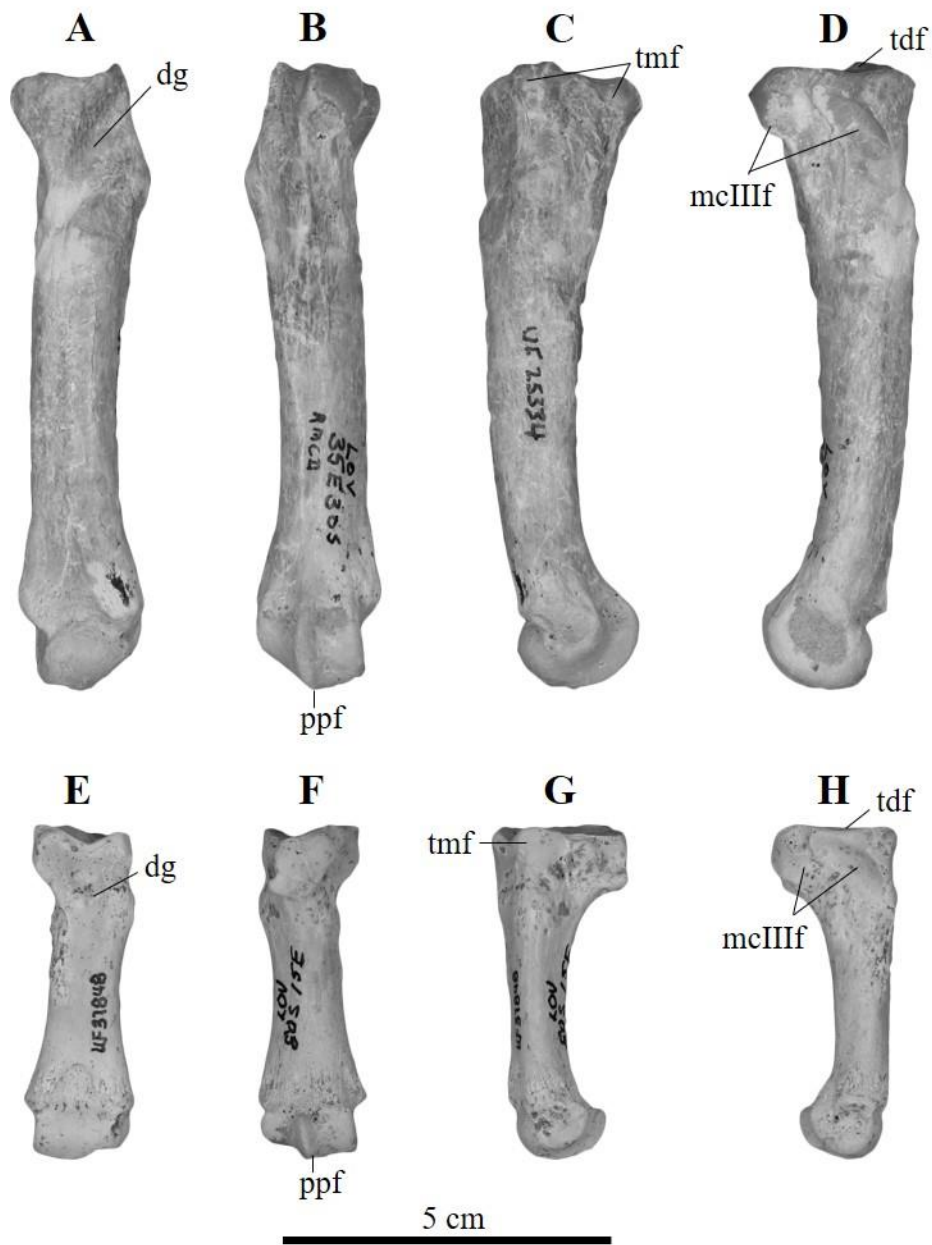


Figure 12. Metacarpal II comparison views between both taxa. A-D *Nimravides galiani* UF 25334 right: dorsal (A), palmar (B), medial (C), lateral (D) views. E-H *Barbourofelis loveorum* UF 37848 right: dorsal (E), palmar (F), medial (G), lateral (H) views. Abbreviations: dg, dorsal groove; mcIII f, metacarpal III facet; ppf, proximal phalanx facet; tdf, trapezoid facet; tmf, trapezium facet.

Remarks—MC II of *B. loveorum* is much smaller than that of *N. galiani*, approximately at half the proximodistal length. The diaphysis is flat in *B. loveorum*, yet convexly curved in *N. galiani*. Additionally, *B. loveorum* has a less defined dorsoproximal groove. In lateral view, on the proximal border, there are two articular surfaces for the trapezium in *N. galiani*, separated by an area of no articulation, whereas *B. loveorum* has one apparent dorsal facet. The lateral tubercle is larger and more defined in *N. galiani*. On the lateral surface, *B. loveorum* has more pronounced muscle scars, expanding further distal than *N. galiani*. The distal articulation with the proximal phalanx differs in shape, with *N. galiani* being more ball-shaped and *B. loveorum* being more flat.

*Metacarpal III. N. galiani*: one right, UF 25348, one left, UF 25352.

The third metacarpal (MC III) of *N. galiani* (Fig. 13) is the longest out of the other metacarpals. MC III is similar to the MC II in that it is proximodistally elongated, straight, and cylindrical. In dorsal view there is a small, smooth, and rounded groove near the medial side of the proximal end. On the proximal surface, two facets are present. The proximal face is triangular with a deep notch on the center of the medial border. Running dorsopalmarly through the center of the base is a deep groove. On the lateral side of the surface, including the groove, is the articulation for the magnum and takes up the majority of the proximal end. Dorsomedial to the magnum articulation is an elliptical facet for the MC II, going onto the medial surface. In medial view, a short and rough scar is palmar to the MC II facet. On the lateral surface there is a rough scar extending approximately a third of the distal width of the diaphysis, distal to the articulation for the MC IV.

*B. loveorum*: two left, UF 25269, UF 25267.

The third metacarpal (MC III) of *B. loveorum* (Fig. 13) is the second longest of the other metacarpals, of which the MC IV is proximodistally longer. MC III is similar to MC II in that it is proximodistally shortened, straight with a flat dorsal surface, and cylindrical. In dorsal view there is a small, rough, and deep groove near the medial side of the proximal end. On the proximal surface, two facets are present. The proximal face is triangular with a deep notch on the center of the medial border. Running dorsopalmarly through the center of the base is a deep groove. On the lateral side of the surface, including the groove, is the articulation for the magnum and takes up the majority of the proximal end. Dorsomedial to the magnum articulation is an elliptical facet for the MC II, going onto the medial surface. In medial view, a short and rough scar is palmar to the MC II facet. On the lateral surface there is a rough scar extending half the distal width of the diaphysis, distal to the articulation for the MC IV.

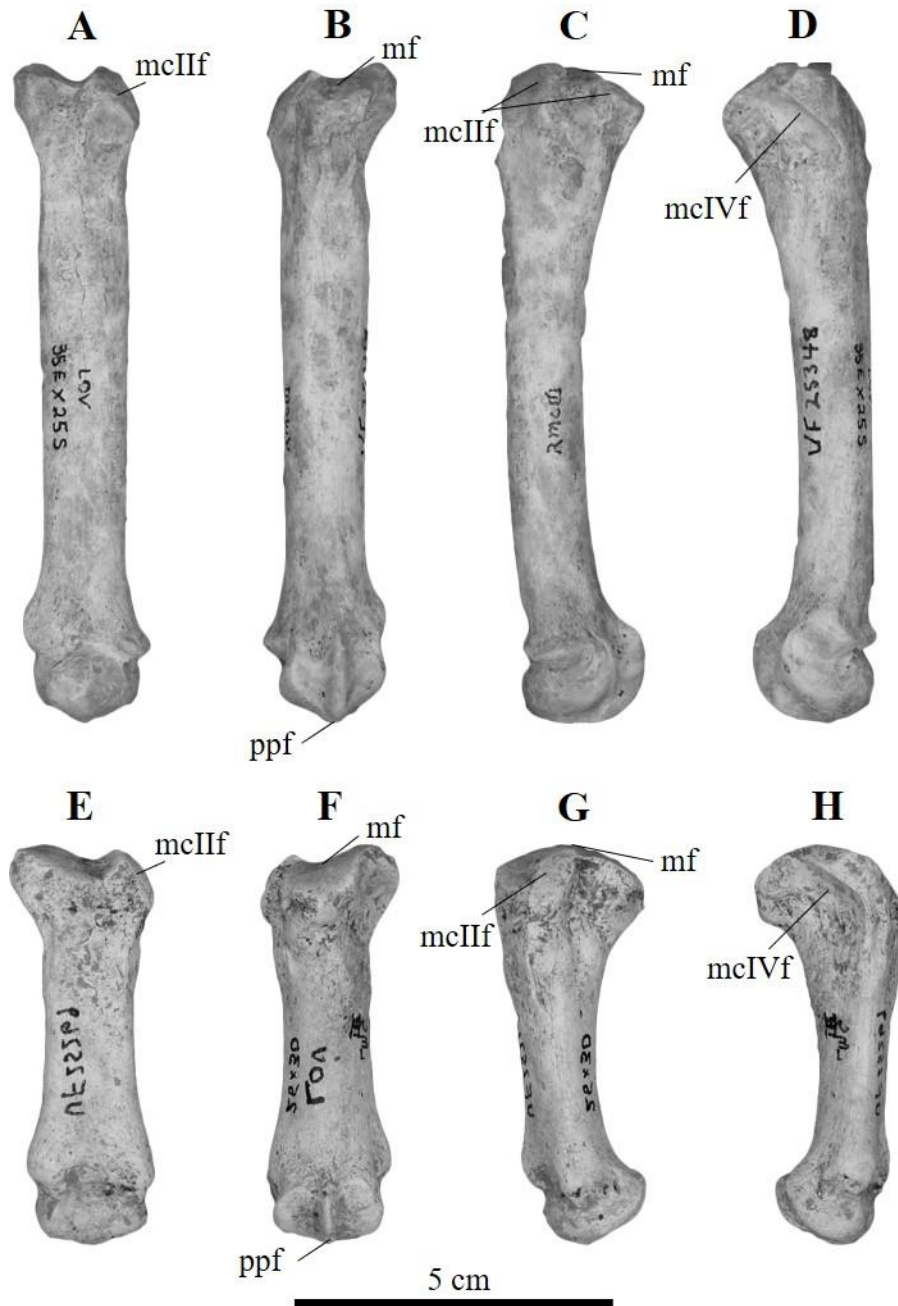


Figure 13. Metacarpal III comparison views between both taxa. A-D *Nimravides galiani* UF 25348 right: dorsal (A), palmar (B), medial (C), lateral (D) views. E-H *Barbourofelis loveorum* UF 25269 left side inverted to right side: dorsal (E), palmar (F), medial (G), lateral (H) views. Abbreviations: mcIIIf, metacarpal II facet; mcIVf, metacarpal IV facet; ppf, proximal phalanx facet.

Remarks—MC III is relatively longer and less condensed in *N. galiani*. On the dorsal surface, *N. galiani* has a noticeable shallow proximal groove, whereas *B. loveorum* has a deep and rough groove. The articulation for the magnum in *B. loveorum* is much larger than that of *N. galiani*. The distal articulation with the proximal phalanx differs in shape, with *N. galiani* being more ball-shaped and *B. loveorum* being more flat.

*Metacarpal IV. N. galiani*: one left, UF 25354.

The fourth metacarpal (MC IV) of *N. galiani* (Fig. 14) is nearly as long as MC III. MC IV is similar to the other metacarpals in that it is proximodistally elongated, straight, and cylindrical. On the dorsal surface, the proximal end of the diaphysis is scarred, and the medial side extends proximally. In medial view, the proximal region has rough and short scars palmar to the facet for MC III. On the proximal surface, the articulation for the MC III and unciform is dorsopalmarly split, of which the convex unciform facet takes up the majority of the proximal face and is extended proximally. In lateral view, the articulation for the MC V is deeply grooved and very large. On the palmar surface is a proximodistal elongated rough and elliptical scar, distally extended more than half the diaphysis length.

*B. loveorum*: one right, UF 25274, one left, UF 25283.

The fourth metacarpal (MC IV) of *B. loveorum* (Fig. 14) is the longest of the metacarpals. MC IV is similar to the other metacarpals in that it is proximodistally shortened, straight with a flat dorsal surface, and cylindrical. On the dorsal surface, the proximal end of the diaphysis is scarred, and the medial side extends proximally. In medial view, the proximal region has rough and short scars palmar to the facet for MC III. On the proximal surface, the articulation for the MC III and unciform is dorsopalmarly split, of which the convex unciform facet takes up the majority of the proximal face and is extended proximally. In lateral view, the articulation for the

MC V is deeply grooved and oriented more palmarly. On the palmar surface is a proximodistal elongated and elliptical scar, distally extended more than half the diaphysis length.

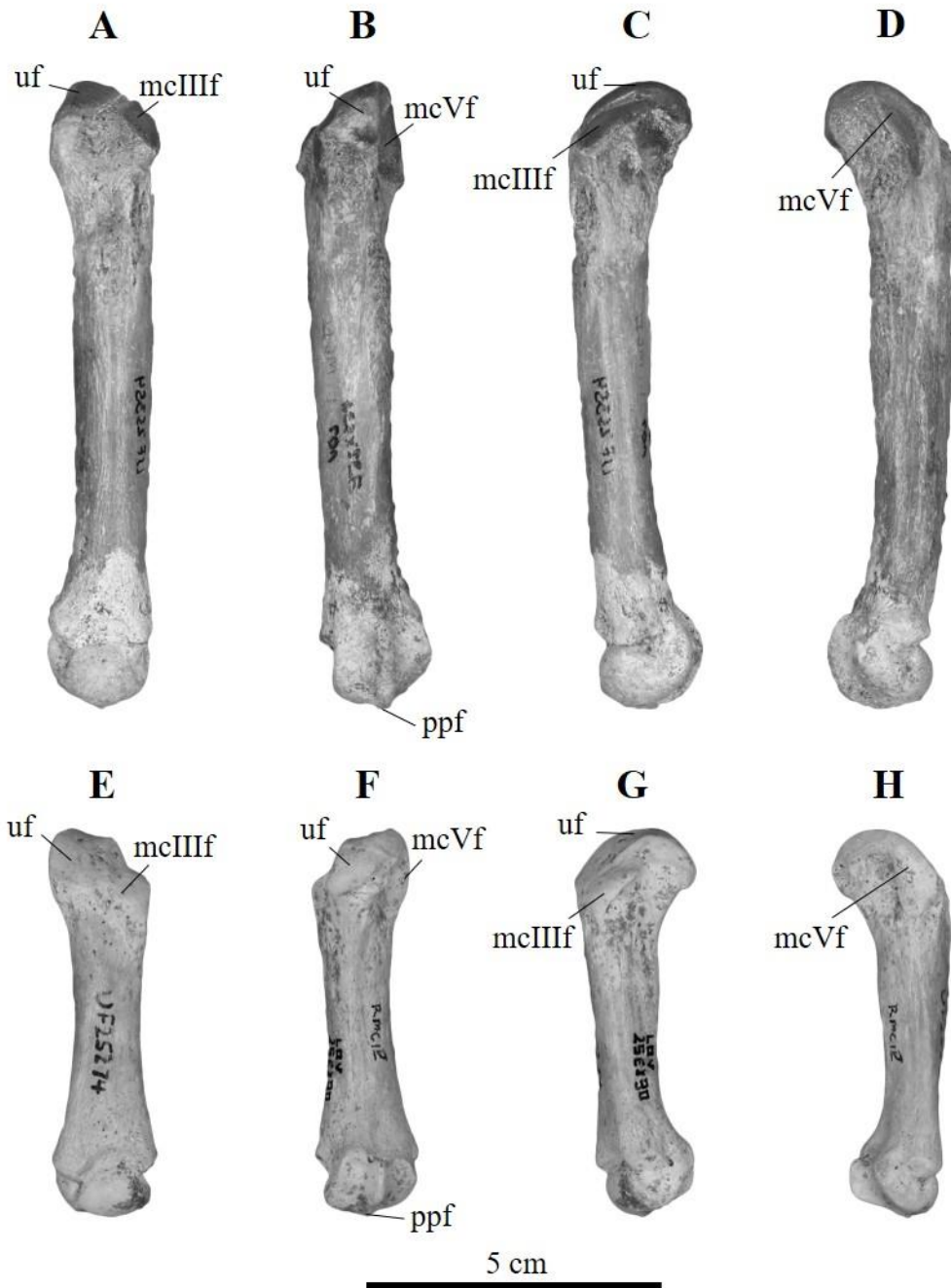


Figure 14. Metacarpal IV comparison views between both taxa. A-D *Nimravides galiani* UF 25354 left side inverted to right side: dorsal (A), palmar (B), medial (C), lateral (D) views. E-H *Barbourofelis loveorum* UF 25274 right: dorsal (E), palmar (F), medial (G), lateral (H) views. Abbreviations: mcIII f, metacarpal III facet; mcV f, metacarpal V facet; ppf, proximal phalanx facet; uf, unciform facet.

Remarks—MC IV of both taxa are very similar. In *B. loveorum*, the MC IV is proximodistal shortened, whereas the diaphysis for *N. galiani* is elongated. On the lateral side, the articular groove for the MC V is much larger and defined in *N. galiani*, which was much less prominent in *B. loveorum*, and more palmarly inset. In palmar view, the elliptical scar is more defined in *N. galiani* and less present in *B. loveorum*. The distal articulation with the proximal phalanx differs in shape, with *N. galiani* being more ball-shaped and *B. loveorum* being more flat.

*Metacarpal V. N. galiani*: two right: UF 25360, UF 25361.

The fifth metacarpal (MC V) of *N. galiani* (Fig. 15) is the second shortest metacarpal, larger only to the first. MC V is similar to the other metacarpals in that it is proximodistally elongated and cylindrical. On the dorsal surface, the diaphysis is laterally concave, and the proximal face extends proximally. In proximal view, the articulation for the unciform is half-moon shaped and convex, with the lateral border being convex and the medial border being concave. Medial to the unciform facet, the articulation for MC IV is distally placed on the medial surface. On the medial side, the MC IV facet is dorsopalmarly oriented, with the distal ridge protruding medially. In lateral view, distal to the proximal end, a large and well-developed tubercle is protruding laterally with a small groove in its center.

*B. loveorum*: two left, UF 25285, UF 25294.

Metacarpal V (MC V) of *B. loveorum* (Fig. 15) is thin and not stout. MC V is similar to the other metacarpals in that it is proximodistally shortened and cylindrical, however the dorsal surface is not flat and is instead dorsally-oriented convex. On the dorsal surface, the diaphysis is laterally concave, and the proximal face extends proximally. In proximal view, the articulation for the unciform is half-moon shaped and convex, with the lateral border being convex and the

medial border being concave. Medial to the unciform facet, the articulation for MC IV is distally placed on the medial surface. On the medial side, the MC IV facet is dorsopalmarly oriented, with the distal ridge protruding medially. In lateral view, distal to the proximal end, a large and well-developed tubercle is greatly protruding laterally with a large grooved out center. On the palmar surface, on the proximomedial side, there is a large tear-shaped tubercle on the diaphysis.

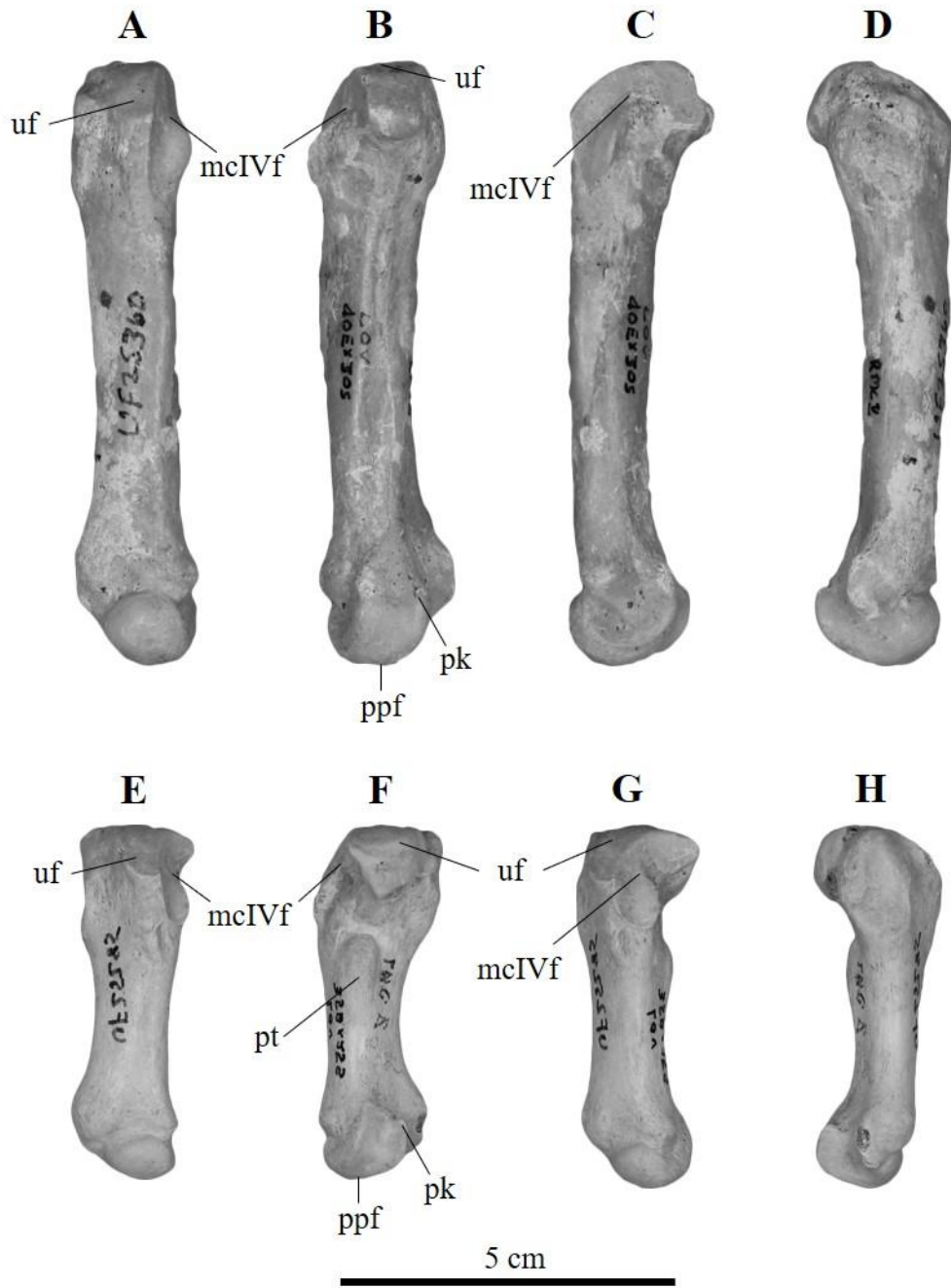


Figure 15. Metacarpal V comparison views between both taxa. A-D *Nimravidés galiani* UF 25360 right: dorsal (A), palmar (B), medial (C), lateral (D) views. E-H *Barbouroufelis loveorum* UF 25285 left side inverted to right side: dorsal (E), palmar (F), medial (G), lateral (H) views. Abbreviations: mcIVf, metacarpal IV facet; pk, palmar keel; ppf, proximal phalanx facet; pt, palmar tubercle; uf, unciform facet.

Remarks—MC V of both taxa are very similar. In *B. loveorum*, the MC V is proximodistal shortened, whereas the diaphysis for *N. galiani* is elongated. On the medial surface, *N. galiani* has a more medial pronounced projection close to the proximal base. In lateral view, *B. loveorum* has a relatively larger proximal tubercle than *N. galiani*, and the center of the tubercle is grooved out. Additionally, *B. loveorum* has another tubercle, located on the palmar-proximal region of the diaphysis, a feature not seen in *N. galiani*.

*Phalanx: MC I Proximal. N. galiani:* one left, UF 37144.

The proximal phalanx of the MC I in *N. galiani* (Fig. 16) is robust and oval in shape, with the anteroposterior length being longer than the mediolateral length. On the proximal articular surface, in dorsal view, are two facets, a lateral and medial facet, both of which articulate to the distal end of the MC I. This faceted region is the widest part of the phalanx, mediolaterally. The lateral facet is larger in circumference than the medial facet and is concave distally, whereas the medial facet is flat. At the proximal end, the facets are separated by a deep groove, making room for the MC Is distopalmar ridge. On the palmar surface, between the proximal and distal regions is a mediolateral groove, concave dorsally.

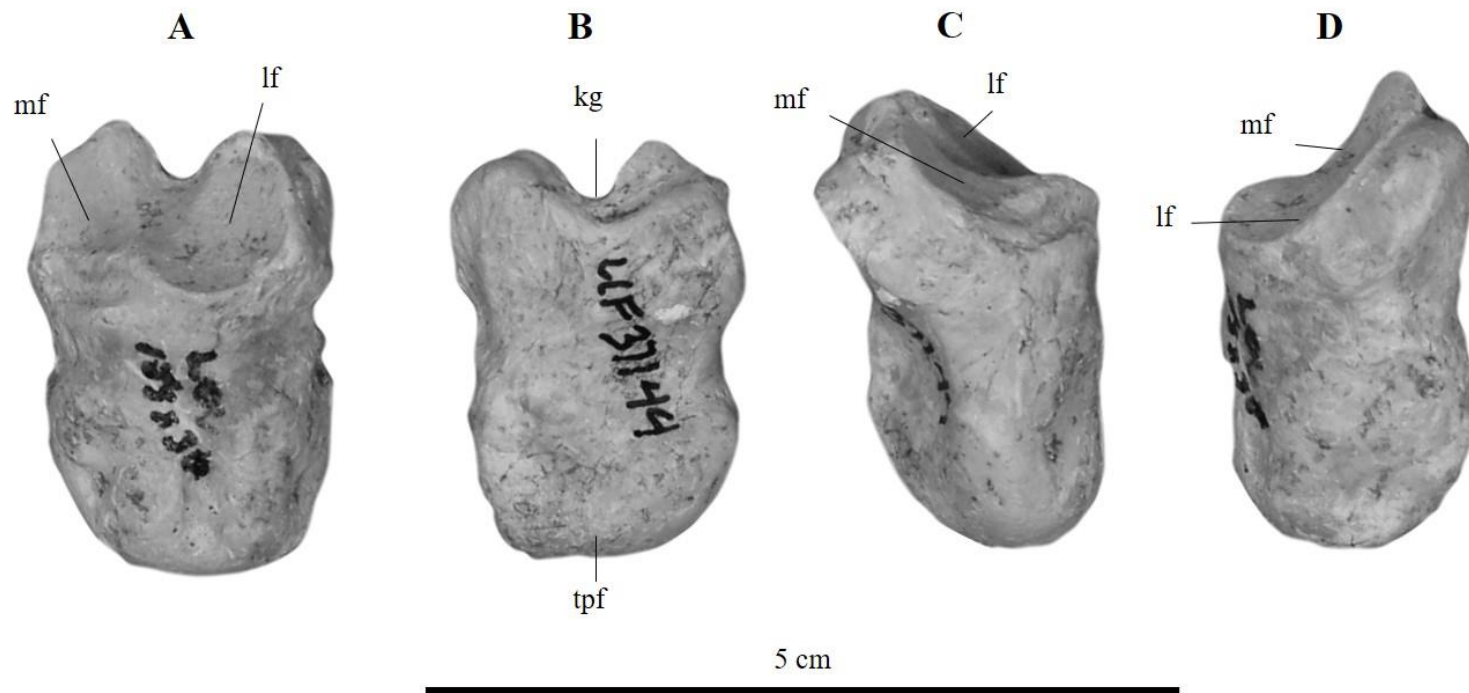


Figure 16. Proximal Phalanx of MC I views for *Nimravides galiani* A-D UF 37144 left: dorsal (A), palmar (B), medial (C), lateral (D) views. Abbreviations: kg, keel groove; lf, lateral facet; mf, medial facet; tpf, terminal phalanx facet.

Remarks – The proximal phalanx of the first digit for *B. loveorum* is unavailable to describe and discuss. As such, direct morphological descriptions were unable to be made, and only the phalanx articulations found on the MC I surface can be identified and discussed. The facet for the phalanx on MC I of *B. loveorum*, on the palmar surface, has a small ridge slightly elongated palmarly, whereas in *N. galiani* this larger and more developed ridge sits in a deep and tight groove between the lateral and medial facets.

### *Hindlimb*

*Innominate. N. galiani*: three partial right: UF 37158, UF 25680, UF 37154, one left, UF 37154.

The pelvis of *N. galiani* (Fig. 17) is partially preserved in a few specimens; however, all are missing at least the dorsoanterior end of the ilium, the ventroposterior ramus of the ischium, and the dorsoposterior ramus of the pubis. As such, the obturator foramen is not completely displayed by these pelvis boundaries. In the middle of the lateral surface is the acetabulum, a round and spherical depression. On the anterior border of the acetabular fossa is a deep groove extending anteroposteriorly on the ilium. In the posterior region of the acetabular fossa is a deep groove cutting through the acetabular border and traveling posteriorly into the ischium. The ilium is slightly constrained dorsoventrally in the posterior region and has a wider ilium wing that remains a consistent width. On the dorsal region of the ilium wing is a wide and shallow depression. The greater ischium notch is shallow. At the ventrolateral border of the ilium is a shallow tuberosity, anterior to the acetabulum border. On the dorsal border, just posterior to the acetabulum, is a small and well-defined knob, forming the ischium spine. Continuing posteriorly from this spine is the tuberosity of the ischium at the dorsoposterior end. Between the ischium

spine and tuberosity is a flattened lesser sciatic notch. From the ventral border of the acetabulum to the ischium tuberosity is a laterally projected and straight ridge. Ventral to the acetabulum is the pubis. The pubis is constricted anteroposteriorly in the center and the dorsal and ventral ends are wider. On the medial surface of the pelvis, a thick semi-circle, concave posteriorly, on the ilium where the sacrum articulates. In the center of the anterior border on the sacral facet is a small cavity. The remainder of the ventral surface is smooth throughout the rest of the pelvis.

*B. loveorum*: two partial, one right, UF 25689, one left, UF 36998.

The pelvis of *B. loveorum* (Fig. 17) is mostly incomplete in all specimens, missing at least the dorsoanterior end of the ilium, the majority of the ischium, and the ramus of the pubis. As such, the obturator foramen is not displayed by these pelvis boundaries. In the middle of the lateral surface is the acetabulum, a round and spherical depression. On the anterior border of the acetabular fossa is a deep groove extending anteroposteriorly on the ilium. In the posterior region of the acetabular fossa is a deep groove cutting through the acetabular border and traveling posteriorly into the ischium. The ilium is constrained dorsoventrally in the posterior region and has a slightly wider ilium wing that remains a consistent width. There is no marked depression on the ilium wing's dorsal region. Mediolaterally, the wing is thick and robust. The greater ischium notch is shallow. At the ventrolateral border of the ilium is a large tuberosity, anterior to the acetabulum border. On the dorsal border, just posterior to the acetabulum, is a small and well-defined knob, forming the ischium spine. Ventral to the acetabulum is the pubis. The pubis is constricted anteroposteriorly in the center and the dorsal and ventral ends are wider. On the medial surface of the pelvis, a thick semi-circle, concave posteriorly, on the ilium where the sacrum articulates. In the center of the anterior border on the sacral facet is a large cavity. The remainder of the ventral surface is smooth throughout the rest of the pelvis.



Figure 17. Pelvis comparison views between both taxa. A-B *Nimravidetes galiani* UF 37158 right: lateral (A), medial (B) views. C-F *Barbourofelis loveorum* UF 25389, UF 36998 left side inverted to right side: lateral (C, E), medial (D, F) views. Abbreviations: a, acetabulum; ag, anterior groove; I, ilium; Is, Ischium; pg, posterior groove; sf, sacrum facet.

Remarks—The pelvis of *N. galiani* and *B. loveorum* are both incomplete, of which *N. galiani* is missing only the outermost ends of the ilium and pubis and the ramus for both the pubis and ischium, whereas *B. loveorum* is also missing the majority of the ischium. As such, the boundaries for the obturator foramen are not complete in both taxa. On the lateral surface, the acetabulum is spherical and deeply depressed in both taxa, however *B. loveorum* has a larger circumference than *N. galiani*. On the anterior border of the acetabulum, *N. galiani* has a deeper groove projecting into the ilium, however the groove is dorsoventrally wider in *B. loveorum*. Outlining this groove, on the ventral region, is a small and undeveloped tuberosity in *N. galiani*, yet much larger and well-developed in *B. loveorum*. The ridge outlining the dorsal region of this groove is more pronounced in *N. galiani*. In both taxa, the ilium is constrained dorsoventrally towards the posterior end, and becomes wider towards the anterior end at a constant width. On the dorsolateral region of the ilium wing, *N. galiani* has a wide and shallow depression, not present in *B. loveorum*, of which the wing is mediolaterally thick and robust. The greater ischium notch on the dorsal border of the ilium is shallow in both taxa. From the posterior region of the acetabulum to the anterior region of the ischium is a deep groove cutting through the acetabular border in both taxa. On the dorsal border of the ischium, just posterior to the acetabulum, is a small and well-defined knob, forming the ischium spine. Continuing from the spine to the ischium's dorsoposterior end is the ischium tuberosity in *N. galiani*, but not preserved in *B. loveorum*. The pubis is relatively the same in both taxa, with a constricted center anteroposteriorly, and widened dorsal and ventral ends. On the ventral surface of the ilium, *N. galiani* has a well-defined semi-circle facet for the sacrum with a small cavity in the anterior center of this facet, whereas *B. loveorum* has a large cavity in this region.

*Femora. N. galiiani*: one right, UF 37064, two partial left, UF 25483, UF 25490.

The femur of *N. galiiani* (Fig. 18) is slender with an elongated and straight shaft. In all views the diaphysis is circular. At the proximal epiphysis, the spherical femoral head is projected medially and supported by a short and well-developed neck. On the head's medioposterior surface is a round depression ligament scar. Lateral to the head is a well-developed greater trochanter at approximately the same proximal height as the femoral head. In posterior view, between the femoral head and greater trochanter is a deep trochanteric fossa engulfed by the ridges of the greater trochanter. On the posterior ridge of the greater trochanter, the intertrochanteric line extends distally towards the shaft and ends by a small posteriorly projected knob, the lesser trochanter. Distal to the greater tuberosity, in lateral view, the gluteal tuberosity is not observed.

On the distal epiphysis, in anterior view, the smooth patellar articular surface is mediolaterally constrained and posteriorly concave. The center of the proximal border is level with the shaft. In posterior view there are two condyles, the medial and lateral condyles, separated by a deep and mediolaterally wide intercondyloid fossa, posteroventrally. Of the two condyles, the lateral condyle is mediolaterally wider and laterally inclined, whereas the narrower medial condyle is nearly vertical. In ventral view, both condyles have approximately the same posterior height. Both the medial and lateral epicondyles do not project past their respective condyles in posterior view.

*B. loveorum*: one right, UF 27259, one left, UF 27258.

The femur of *B. loveorum* (Fig. 18) is robust with an elongated and anteriorly-bowed shaft. In posterior view the diaphysis is flattened. At the proximal epiphysis, the spherical femoral head is projected anteromedially and supported by a long and well-developed neck. On

the head's medioposterior surface is a round depression ligament scar, continuing as a short groove to the posterior side. Lateral to the head is a well-developed great trochanter, of which the femoral head surpasses proximally. In posterior view, between the femoral head and greater trochanter is a deep trochanteric fossa engulfed by the ridges of the greater trochanter. On the posterior ridge of the greater trochanter, the intertrochanteric line extends distally towards the shaft and ending proximal to a large posteromedially projected knob, the lesser trochanter. From the neck another ridge continues distally to the lesser trochanter. Distal to the greater tuberosity, in lateral view, is a rough and anteroposteriorly wide gluteal tuberosity which continues as a distal ridge to the end of the shaft.

On the distal epiphysis, in anterior view, the smooth patellar articular surface is mediolaterally wide and posteriorly concave. The center of the proximal border is level with the shaft. In posterior view there are two condyles, the medial and lateral condyles, separated by a deep and mediolaterally constrained intercondyloid fossa, posteroventrally. Of the two condyles, the medial condyle is slightly mediolaterally wider and vertically oriented, whereas the lateral condyle is laterally inclined. In ventral view, the medial condyle is more proximally extended than the lateral condyle. Both the medial and lateral epicondyles do not project past their respective condyles in posterior view.

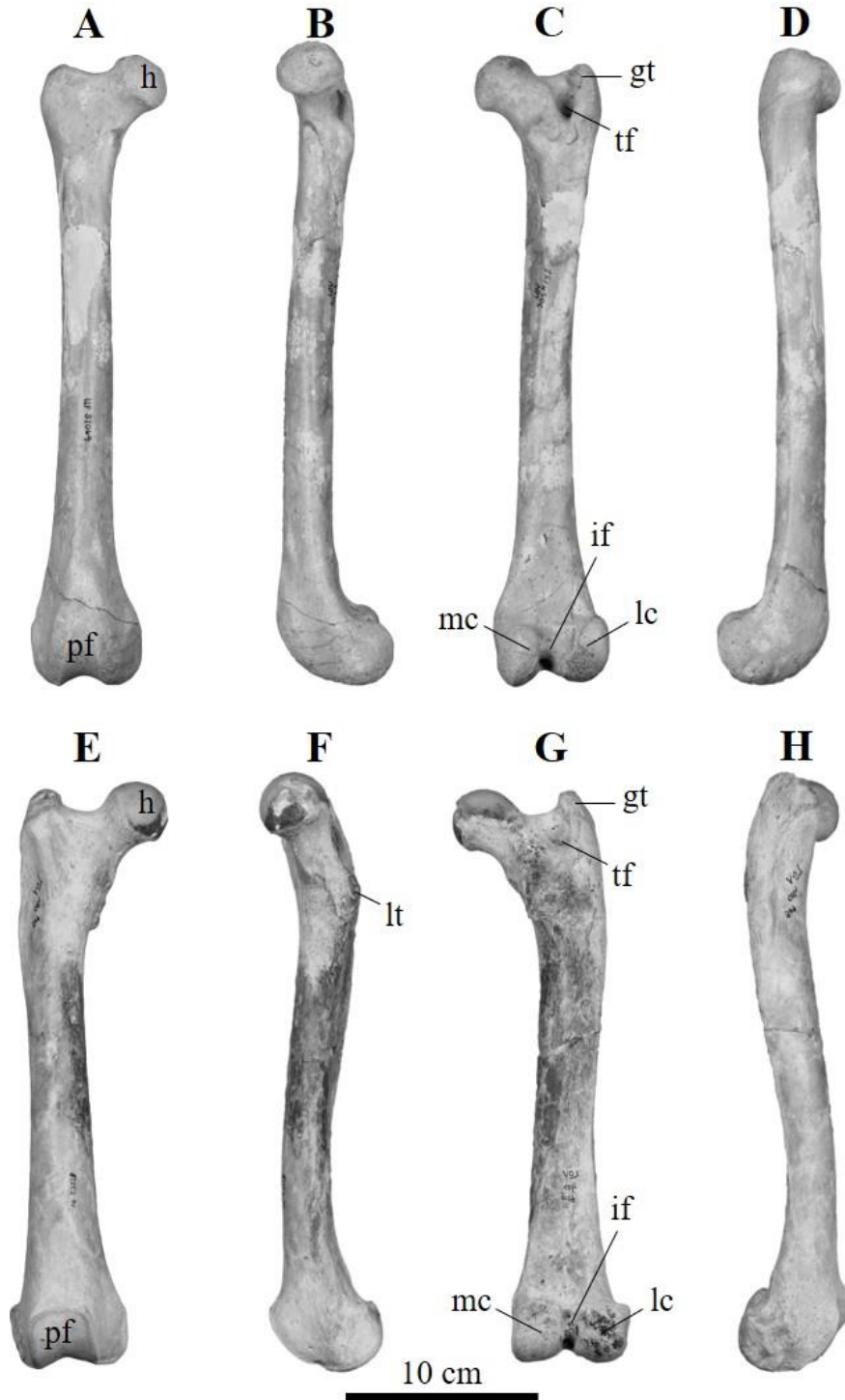


Figure 18. Femur comparison views between both taxa. A-D *Nimravidex galiani* UF 37064 right: anterior (A), medial (B), posterior (C), lateral (D) views. E-H *Barbourofelis loveorum* UF 27258 left side inverted to right side: anterior (E), medial (F), posterior (G), lateral (H) views. Abbreviations: gt, greater trochanter; h, femoral head; if, intercondyloid fossa; lc, lateral condyle; lt, lesser trochanter; mc, medial condyle; pf, patellar facet; tf, trochanteric fossa.

Remarks—The femora of *N. galiani* and *B. loveorum* show many differences in robustness and trochanter size. The diaphysis in *N. galiani* is straight and circular, whereas in *B. loveorum* the shaft is flattened on the posterior side and there is an anterior-oriented curve from the proximal to distal ends. On the proximal epiphysis, the femoral head is more anteriorly projected in *B. loveorum* with a longer neck. Additionally, the ligament depression on the medial surface of the head is posterodistally elongated in *B. loveorum* and is only a round depression in *N. galiani*. Between the femoral head and the greater trochanter, the proximal ridge of the trochanteric fossa is distally deeper in *B. loveorum* and the fossa is mediolaterally wider than in *N. galiani*. The proximal height of the greater trochanter is approximately the same height as the head in *N. galiani*, but is proximally shorter than the head in *B. loveorum*. The intertrochanteric line in *N. galiani* continues distally to the distal end of the lesser trochanter, whereas in *B. loveorum* this ridge continues distally to the proximal end of the lesser trochanter. This lesser trochanter is reduced to a small, round posterior projection in *N. galiani*, unlike in *B. loveorum* of which it is enlarged and projects medioposteriorly. On the lateral surface, distal to the greater trochanter, a rough gluteal tuberosity is present in *B. loveorum*, continuing distally into the distal end of the diaphysis. On the distal epiphysis, the patellar surface on the anterior surface is mediolaterally wider in *B. loveorum*. In posterior view, the intercondyloid fossa is mediolaterally wide in *N. galiani* and narrow in *B. loveorum*. The lateral condyle is mediolateral wider than the medial condyle in *N. galiani*, whereas the medial condyle is slightly wider than the lateral condyle in *B. loveorum*. In ventral view, both condyles project posteriorly at nearly the same height in *N. galiani*, however in *B. loveorum* the medial condyle is more posteriorly projected.

*Tibiae. N. galiani*: two right, UF 37079, UF 25553, one left, UF 25552.

The tibia of *N. galiani* (Fig. 19) is elongated with enlarged proximal and distal epiphyses. The diaphysis is straight and has a consistent mediolateral width. In medial and lateral views, the proximal epiphysis is anteriorly convex. In anterior and proximal views, the proximal epiphysis is triangular shaped. On the dorsal surface are two femoral facets, the medial and lateral condyles, separated by a proximally projected and small spine. The lateral condyle is mediolaterally wider and the posterior border projects further posteriorly than the medial condyle. On the lateral condyle is a proximally raised border and the condyle is mediolaterally flat and anteroposteriorly convex, whereas the medial condyle is nearly flat. In lateral view, the proximal epiphysis is anteroposteriorly wider than the medial side. Anterior to these condyles, in anterior view, is an anteriorly-convex slope leading to a mediolaterally thick tibia crest. In anterior and posterior views, the lateral condyle is more proximally oriented than the medial condyle. On the ventral surface of the lateral condyle, on the posterolateral side, is a small and round peroneal articular surface. In posterior view, the spine separating the condyles creates a proximodistal wide and shallow gap. On the anterior surface, the tibial crest is orientated towards the lateral side and the ridge continues distally towards the medial end of the diaphysis, distal to the midshaft. In posterior view, distal to the lateral condyle, two well-developed parallel ridges, the soleal line, travel mediodistally down the shaft and combine into one ridge proximal to the midshaft. This combined ridge continues distally towards the distal epiphysis.

The distal epiphysis is mediolaterally wide in anterior and posterior views, and is approximately the same width anteroposteriorly as the distal diaphysis in medial and lateral views. On the distal epiphysis, the medial malleolus is more distally elongated than the lateral side. In medial view, there are two well-defined parallel grooves running proximodistally on the

surface. In anterior view there is a deep proximally-oriented groove outlined by the medial and lateral facet borders. In lateral view, proximal to the ventral articular surface is a round facet for the distal end of the fibula. On the ventral surface are two primary grooves, a lateral and medial groove, for articulation with the astragalus. Both grooves are parallel to the other and are anteroposteriorly-oriented and medially inclined. Each groove is proximally concave, and the articular borders are well-developed.

*B. loveorum*: one right, UF 25526, two left, UF 36974, UF 25521.

The tibia of *B. loveorum* (Fig. 19) is elongated with enlarged proximal and distal epiphyses. The diaphysis is straight and the midshaft is slightly mediolaterally thinner than the proximal and distal ends of the shaft. In medial and lateral views, the proximal epiphysis is anteriorly convex. In anterior and proximal views, the proximal epiphysis is triangular shaped. On the dorsal surface are two femoral facets, the medial and lateral condyles, separated by a proximally projected and well-defined spine. The lateral and medial condyles are nearly similar in mediolateral width and both projects posteriorly at the same distance on the posterior border in dorsal view. On the lateral condyle is a proximally raised border and the condyle is mediolaterally concave and anteroposteriorly convex, whereas the medial condyle is nearly flat. In lateral view, the proximal epiphysis is anteroposteriorly wider than the medial side. Anterior to these condyles, in anterior view, is a posteriorly-concave slope leading to a mediolaterally thick tibia crest. In anterior and posterior views, the lateral condyle is more proximally oriented than the medial condyle. On the ventral surface of the lateral condyle, on the posterolateral side, is a large and round peroneal articular surface. In posterior view, the spine separating the condyles creates a proximodistal narrow and shallow gap. On the anterior surface, the tibial crest is orientated towards the lateral side and the ridge continues distally towards the medial end of

the diaphysis and continues into the distal epiphysis. In posterior view, distal to the lateral condyle, two underdeveloped parallel ridges travel mediolaterally down the shaft and combine into one ridge just proximal to the distal epiphysis.

The distal epiphysis is mediolaterally wide in anterior and posterior views, and is approximately the same width anteroposteriorly as the distal diaphysis in medial and lateral views. On the distal epiphysis, the medial malleolus is more distally elongated than the lateral side. In posterior view, close to the medial border, there is a wide well-developed groove running proximodistally on the surface with a slight ridge going down the center, possibly indicating the presence of two parallel ridges. In anterior view there is a shallow proximally-oriented groove outlined by the medial and lateral facet borders. In lateral view, proximal to the ventral articular surface is a round facet for the distal end of the fibula with a high ridge on its posterior border. On the ventral surface are two primary grooves, a lateral and medial groove, for articulation with the astragalus. Both grooves are parallel to the other and are anteroposteriorly-oriented and medially inclined. Each groove is proximally concave, and the posterior articular border is well-developed.

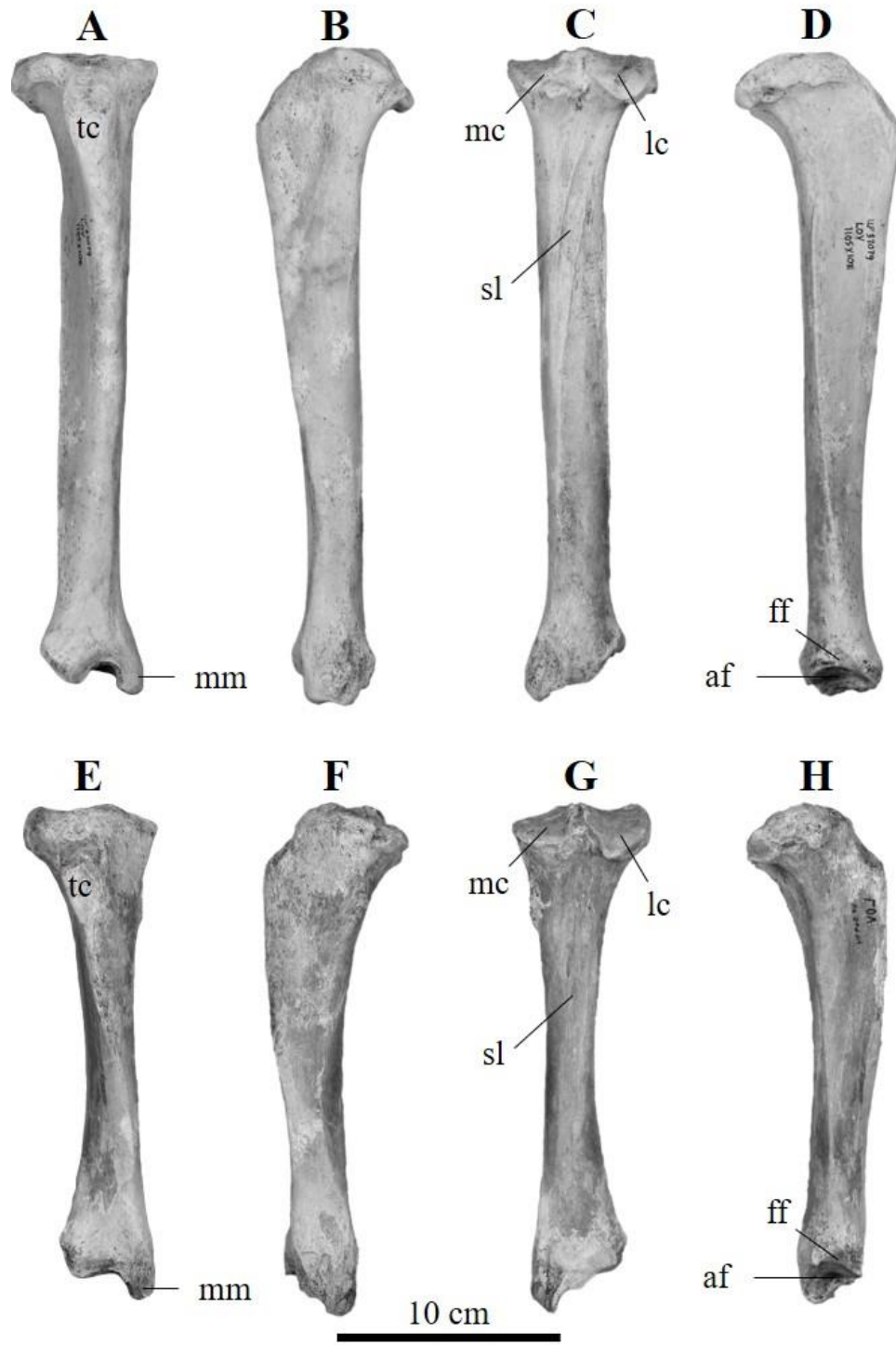


Figure 19. Tibia comparison views between both taxa. A-D *Nimravides galiani* UF 37079 right: anterior (A), medial (B), posterior (C), lateral (D) views. E-H *Barbourofelis loveorum* UF 36974 left side inverted to right side: anterior (E), medial (F), posterior (G), lateral (H) views. Abbreviations: af, astragalus facet; ff, fibula facet; lc, lateral condylar; mc, medial condyle; mm, medial malleolus; sl, soleal line.

Remarks—The tibiae of *N. galiani* and *B. loveorum* are different in overall shape and robustness. Both are elongated, with *N. galiani* being longer in size and maintaining a consistent mediolateral width of the diaphysis in anterior view, whereas *B. loveorum* has a mediolaterally thinner midshaft than the proximal and distal ends of the diaphysis. The crest of the tibia extends further distally down the shaft in *B. loveorum*, continuing onto the distal diaphysis, unlike in *N. galiani* of which the crest ends just distal to the midshaft. On the posterior surface of the diaphysis, both taxa have parallel ridges, the soleal line, beginning from the proximolateral region and traveling mediodistally to the medial region. In *N. galiani* these ridges are well-defined, however they are not well-developed in *B. loveorum*. On the dorsal surface the spine separating the lateral and medial condyles is more proximally elongated in *B. loveorum*. The lateral condyle is mediolaterally wider than the medial condyle in *N. galiani*, whereas the condyles are similar in width in *B. loveorum*. In *B. loveorum*, the condyles project at the same distance posteriorly in dorsal view, yet in *N. galiani* the lateral condyle projects slightly further than the medial condyle. Both the medial and lateral condyles are mediolateral flat in *N. galiani* with an anteroposteriorly convex lateral condyle. This differs from *B. loveorum* in that the lateral condyle is mediolaterally concave and anteroposteriorly convex. On the anterior surface, anterior to the condyles, *N. galiani* has an anteriorly convex slope leading to the tibial crest, whereas this slope in *B. loveorum* is posteriorly concave. Ventrolateral to the lateral condyle is the proximal articular surface for the fibula, a small facet in *N. galiani* and larger in *B. loveorum*. In posterior view, the gap separating the condyles is mediolaterally wider in *N. galiani*. On the distal epiphysis, the medial malleolus of *N. galiani* has two well-defined and parallel grooves running proximodistally in medial view, whereas the grooves are not well separated in *B. loveorum* and are located more posteriorly. In anterior view, *N. galiani* has a deep proximally-oriented groove

outlined by the medial malleolus and the lateral region, which is much shallower in *B. loveorum*. In lateral view, distal to the ventral articular surface, is a small, round facet for the distal articulation to the fibula in both taxa; however, this facet in *B. loveorum* has a high ridge on its posterior border. On the ventral articular surface for the astragalus is a medial and lateral groove, both of which are more proximally concave and well-defined in *N. galiani*. Additionally, the borders of this facet are well-developed in *N. galiani*, yet only the posterior border is well-developed in *B. loveorum*.

*Fibulae. N. galiani*: two partial left: UF 490608, UF 490607.

The only fibulae of *N. galiani* (Fig. 20) are two disarticulated ends, proximal and distal, with the majority of the diaphysis missing on both. The proximal end is mediolaterally compressed and anteroposteriorly wider than its distal shaft. In lateral and posterolateral views, at the proximal most regions, there are two round articular surfaces for the proximal end of the tibia, of which the lateral facet is the larger of the two. Separating these facets is a deep groove. On the posterior surface there are two bulky ridges corresponding to the location of the anterior facets. Distal to these ridges, the diaphysis begins, is concave, and anteroposteriorly wide. On the posterior surface there is a mediolaterally thin ridge travelling distally onto the shaft. The distal end is bulbous in all views and larger than the shaft. In medial view, on the anterior border, are two facets. The more proximal facet articulates with the distal end of the tibia and is round and smaller than the more distal facet. Distal to this is a larger facet for articulation with the lateral side of the astragalus. The astragular facet is greatly convex, creating a small ventral ridge which locks into the astragalus. On the lateral side there is a distolateral protrusion forming the lateral malleolus. In lateral view of the lateral malleolus, the anterior border protrudes posterolaterally

and is inclined proximally. Between this protrusion and the rest of the lateral malleolus is a shallow groove.

*B. loveorum*: one partial right: UF 466164.

The only fibula of *B. loveorum* (Fig. 20) is a distal end with the majority of the diaphysis missing. As such, the diaphysis and proximal epiphysis cannot be described. The distal epiphysis is bulbous in all views and larger than the shaft proximal to it. In medial view, on the anterior border, are two facets. The more proximal facet articulates with the distal end of the tibia and is round and smaller than the more distal facet. Distal to this is a larger facet for articulation with the lateral side of the astragalus. The astragular facet is greatly convex, creating a small ventral ridge which locks into the astragalus. On the lateral side there is a distolateral protrusion forming the lateral malleolus that does not extend distally past the lateral surface. In lateral view of the lateral malleolus, the anterior border protrudes posterolaterally and is inclined distally. Between this protrusion and the rest of the lateral malleolus is a shallow groove.

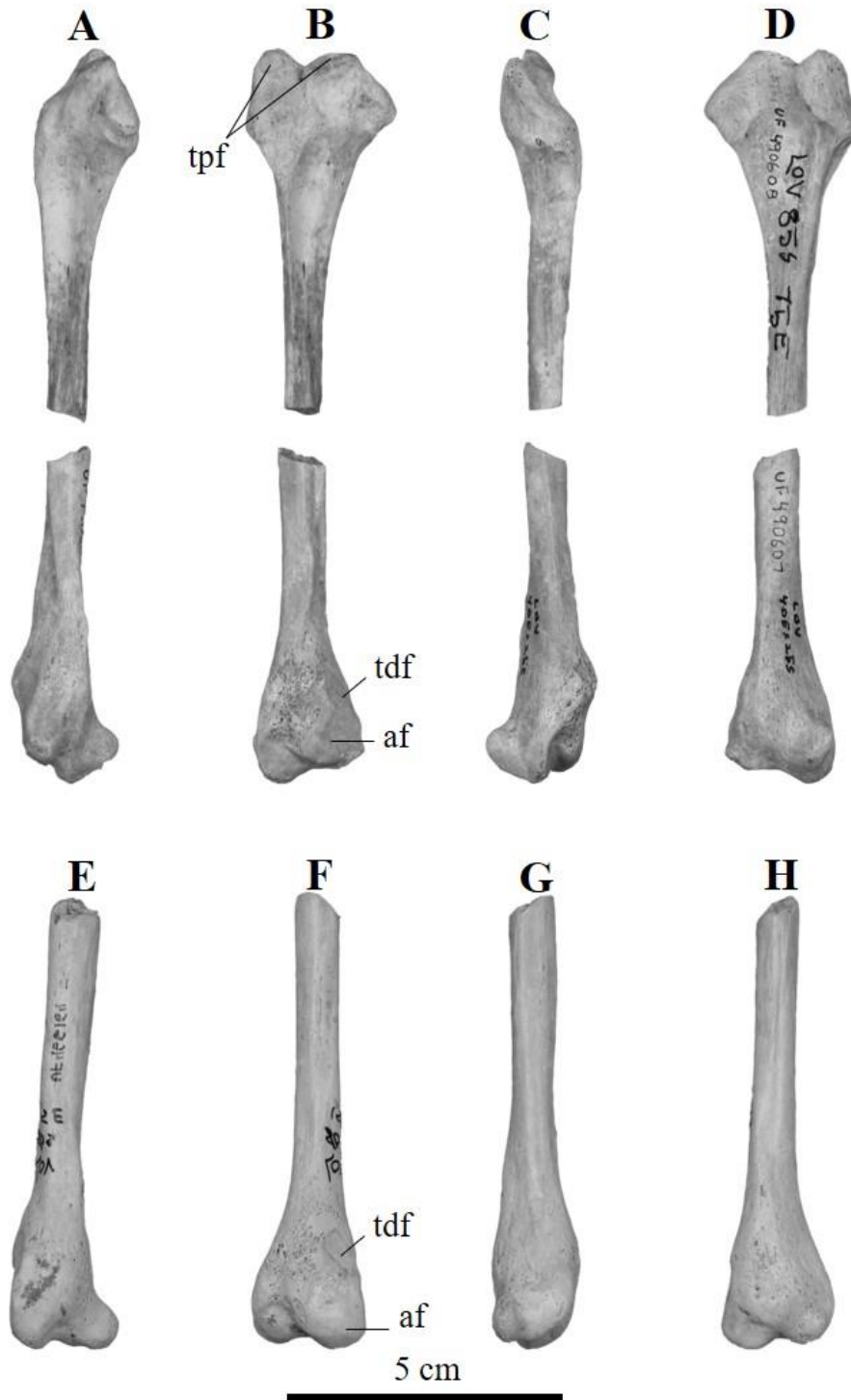


Figure 20. Fibula comparison views between both taxa. A-D *Nimravidex galiani* UF 490608 proximal left, UF 490608 distal left: anterior (A), medial (B), posterior (C), lateral (D) views. E-H *Barbourofelis loveorum* UF 466164 right side inverted to left side: anterior (E), medial (F), posterior (G), lateral (H) views. Abbreviations: af, astragalus facet; tdf, tibia distal facet; tpf, tibia proximal facets.

Remarks—The proximal ends cannot be compared between *N. galiani* and *B. loveorum* as there is not one preserved for the later. Overall, *B. loveorum* has a larger distal end than *N. galiani*. In medial view, the facet for the astragalus is larger in *B. loveorum*, however *N. galiani* has a sharper ventral groove. On the lateral surface, the lateral malleolus is larger in *B. loveorum* and the lateral projection is more distolaterally pronounced, whereas in *N. galiani* it is inclined more proximally. The groove running through the lateral malleolus is wider and shallower in *N. galiani*. The distal most end of the lateral malleolus extends distally further than the lateral side of the distal end in *N. galiani*, whereas in *B. loveorum* it is at the same height.

### *Tarsals*

*Astragalus. N. galiani*: one right, UF 25197, two left, UF 37098, UF 37097.

The astragalus of *N. galiani* (Fig. 21) has a rectangular body with a neck and head protruding from the distomedial region, in dorsal view. On the dorsal surface of the body there is a wide trochlea with a deep groove running proximodistal down its center, dividing the parallel lateral and medial ridges, for articulation with the tibia. This groove is oriented closer to the medial ridge than the lateral ridge. As such, the medial ridge is narrower than the lateral ridge. In proximal view the lateral ridge connects to the medial ridge via a medioplantar diagonal border. Dorsal to this junction is a round astragular foreman, however the foreman is fused shut in some specimens. The joined ridges point-out plantar to the medial ridge. In plantar view, two calcaneus facets, the lateral ectal facet and medial sustentacular facet, are separated by a deep and narrow sulcus tali running parallel with the facets, proximodistally. The ectal facet is rectangular, larger than the sustentacular facet, and concave, whereas the sustentacular facet is oval and convex. Additionally, the ectal facet occupies the majority of the plantar surface of the body and the medial facet is located over the neck's plantar surface, joining with the head's

navicular articular surface. In lateral view the fibula articulation is triangular and concave. On the distal surface a long and thick neck is projected distomedially and leads to a convex head. In distal view, the head is mediolaterally elliptical and wider than that of its neck.

*B. loveorum*: three left, UF 466158, UF 25228, UF 25226.

The astragalus of *B. loveorum* (Fig. 21) has a rectangular body with a neck and head protruding from the distomedial region, in dorsal view. On the dorsal surface of the body there is a wide trochlea with a shallow groove running proximodistal down its center, dividing the parallel lateral and medial ridges, for articulation with the tibia. This groove is oriented closer to the medial ridge than the lateral ridge. As such, the medial ridge is narrower than the lateral ridge. In proximal view the lateral ridge connects to the medial ridge via a mediopltantar diagonal border. Dorsal to this junction is a round and complete astragalus foreman. The joined ridges point-out proximal to the medial ridge. In plantar view, two calcaneus facets, the lateral ectal facet and medial sustentacular facet, are separated by a deep and wide sulcus tali running parallel with the facets, proximodistally. The ectal facet is elliptical, larger than the sustentacular facet, and concave, whereas the sustentacular facet is oval and convex. Additionally, the ectal facet occupies the majority of the plantar surface of the body and the sustentacular facet is located over the neck's plantar surface, joining with the head's navicular articular surface. In lateral view the fibula articulation is triangular and concave. On the distal surface a short and thick neck is projected distomedially and leads to a convex head. In distal view, the head is mediolaterally round and wider than that of its neck.

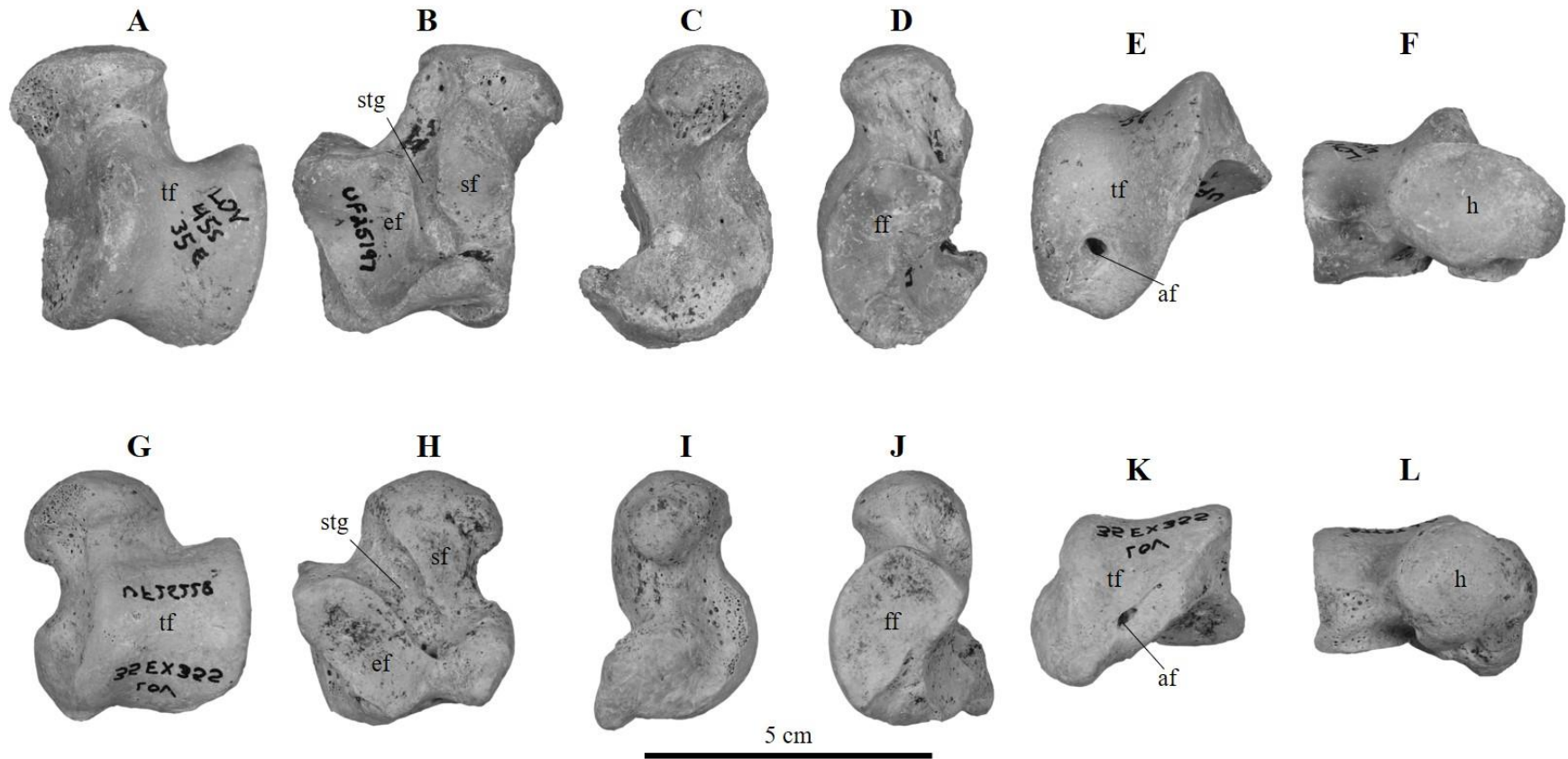


Figure 21. Astragalus comparison views between both taxa. A-F *Nimravides galiani* UF 25197 right: dorsal (A), plantar (B), medial (C), lateral (D), proximal (E), distal (F) views. G-L *Barbourofelis loveorum* UF 25228 left side inverted to right side: dorsal (G), plantar (H), medial (I), lateral (J), proximal (K), distal (L) views. Abbreviations: af, astragular foramen; ef, ectal facet; ff, fibula facet; h, astragular head; sf, sustentacular facet; stg, sulcus tali groove; tf, tibia facet.

Remarks—The astragali of *N. galiani* and *B. loveorum* are different in overall shape and size. In *N. galiani* the trochlear groove is deeper than that in *B. loveorum*, and the astragular foramen is closer to the medial ridge in proximal view. Additionally, not all astragali from *N. galiani* have an open foramen. The joining of the lateral ridge to the medial ridge forms a point that extends proximally in *B. loveorum* and plantarly in *N. galiani*. In plantar view, the sulcus tali separating the sustentacular and ectal facets is mediolaterally wider in *B. loveorum*. The sustentacular facet in *N. galiani* is more concave and rectangular than in *B. loveorum*, whereas the former has a more elliptical facet. On the distal surface, *N. galiani* has a longer neck than that of *B. loveorum*, however both are robust. In *B. loveorum*, the head's articular surface is round, whereas it is mediolaterally elliptical in *N. galiani*.

*Calcaneus. N. galiani*: one right, UF 37089, two left, UF 25136, UF 25167.

The calcaneus of *N. galiani* (Fig. 22) is robust and proximodistally elongated. In medial and lateral views, the calcaneus is dorsoplantarly wider in its midsection. In proximal view there is a proximodistally oriented groove in the center of the posterior surface. On the dorsal surface the tuber calcaneus is proximodistally the same length as the astragali articular distal region. The tuber calcaneus is proximally extended on its medial side. Distal from this tubercle, on the distal half of the dorsal surface, is the articular area for the astragalus with two facets, sustentacular and ectal, separated by a shallow groove. The ectal facet is dorsally convex and proximodistally elongated, whereas the medial facet is smaller and plantarly concave. The proximal border of the sustentacular facet is dorsomedially extended by a robust sustentaculum and the facet is facing distally. The distal border of the sustentacular facet is elongated distally, ending at the distal end of the calcaneus. In medial view there is a deep proximodistal groove plantar to the sustentaculum, wrapping dorsally towards the lateral facet. On the lateral surface the peroneal

tubercle is laterally extended near the distal border. This tubercle is well-developed and has a deep proximodistal groove through its center. Plantar to the peroneal tubercle is a dorsoplantarly wide groove extending proximally to the proximal end. In distal view the articular surface for the cuboid is nearly round with a concave medioplantar border.

*B. loveorum*: three right, UF 25194, UF 25189, UF 466155, two left, UF 466151, UF 466152.

The calcaneus of *B. loveorum* (Fig. 22) is robust and proximodistally short. In medial and lateral views, the calcaneus is dorsoplantarly wider in its midsection. In proximal view the proximal surface is rough with no distinct groove. On the dorsal surface the tuber calcaneus is proximodistally shorter than the astragali articular distal region. The tuber calcaneus is not proximally extended on either lateral or medial sides. Distal from this tubercle, on the distal half of the dorsal surface, is the articular area for the astragalus with two facets, the sustentacular and ectal facets, separated by a deep groove. The ectal facet is dorsally convex and proximodistally elongated, whereas the sustentacular facet is smaller and plantarly concave. The proximal border of the sustentacular facet is dorsomedially extended by a weak sustentaculum and the facet is facing laterodistally. The distal border of the sustentacular facet is elongated laterodistally, ending at the distal end of the calcaneus. In medial view there is no clear separation between the sustentaculum and the plantar region of the calcaneus. On the lateral surface the peroneal tubercle is laterally extended near the distal border. This tubercle is well-developed and has a slight proximodistal groove through its center. In distal view the articular surface for the cuboid is nearly round with a concave medioplantar border.

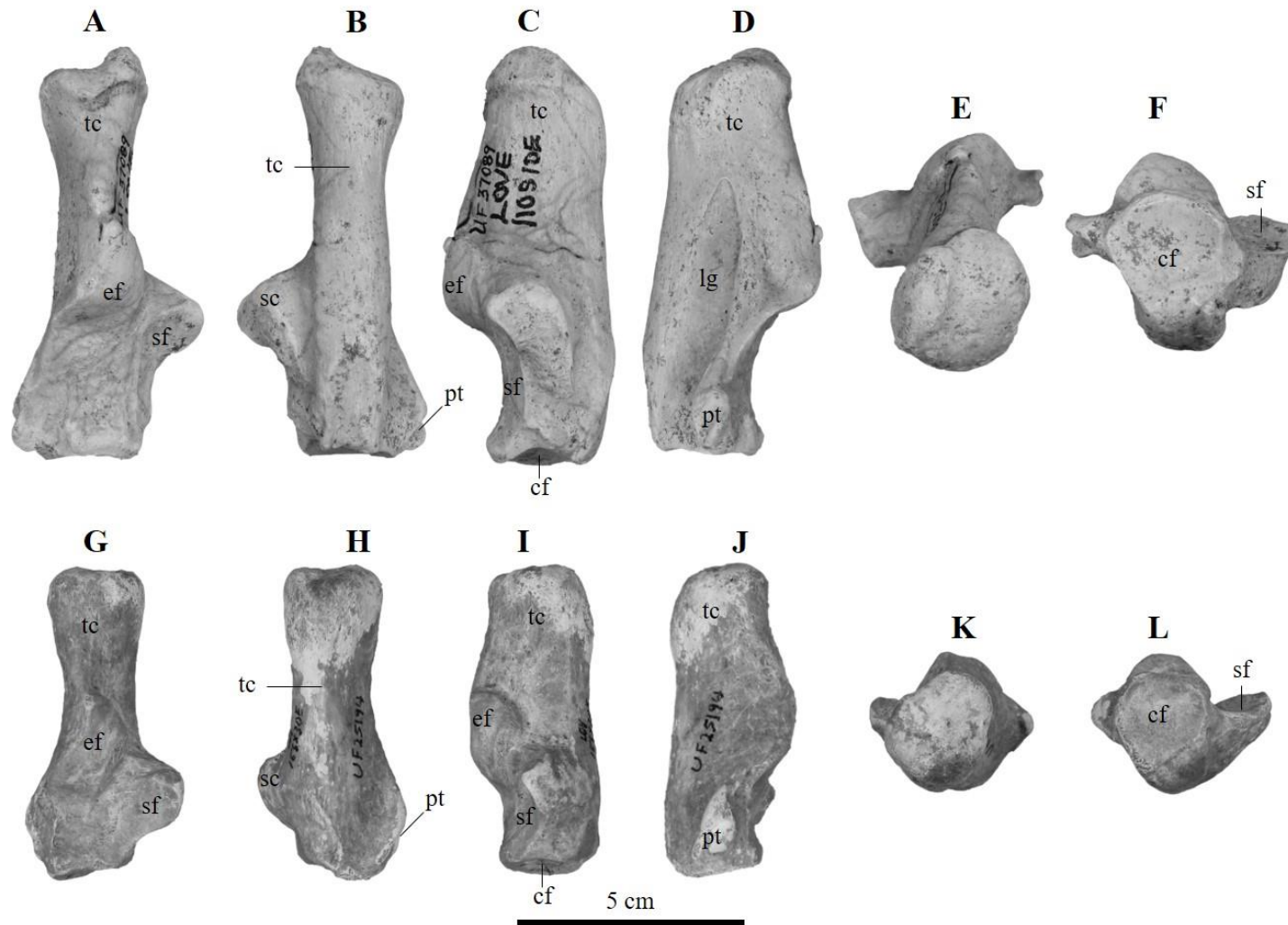


Figure 22. Calcaneus comparison views between both taxa. A-F *Nimravides galiani* UF 37089 right: dorsal (A), plantar (B), medial (C), lateral (D), proximal (E), distal (F) views. G-L *Barbourofelis loveorum* UF 25194 right: dorsal (G), plantar (H), medial (I), lateral (J), proximal (K), distal (L) views. Abbreviations: ct, cuboid facet; ef, ectal facet; lg, lateral groove; pt, peroneal tubercle; sc, sustentaculum; sf, sustentacular facet; tc, tuber calcaneus.

Remarks—The calcanei in *N. galiani* and *B. loveorum* differ in robustness and shape, with *N. galiani* having a more robust calcaneus than the slender one in *B. loveorum*. In proximal view, on the proximal surface, *N. galiani* has a proximodistally oriented groove and the medial region is proximally extended, both of which are not present in *B. loveorum*. The tuber calcaneus is proximodistally shorter than the astragali articular half of the calcaneus in *N. galiani*, whereas they are the same length in *B. loveorum*. Between the sustentacular and ectal astragali facets is a groove, deeper and more pronounced in *B. loveorum*. The sustentaculum is more robust in *N. galiani* and extends the sustentacular facet more dorsomedially. In *B. loveorum*, the sustentacular facet is oriented more anterolaterally than in *N. galiani* and is more closed. Additionally, the medial facet is elongated to the cuboid articular border in both taxa; laterodistally oriented in *B. loveorum* and distally oriented in *N. galiani*. In medial view, *N. galiani* has a well-defined separation between the sustentaculum and the calcaneus body in the form of a deep proximodistal groove, not present in *B. loveorum*. The sustentaculum of *B. loveorum* is closer to the distal end than that of *N. galiani*. In lateral view the peroneal tubercle in *N. galiani* is more developed and has a defined proximodistal groove, unlike in *B. loveorum* of which the tubercle is more knob-like. Plantar to this is a wide groove from the distal end on the lateral surface towards the proximal end. In *N. galiani* this groove is deep with well-defined borders and is longer than the groove in *B. loveorum*, for which the groove is nearly non-existent. On the distal surface, *N. galiani* has a deeper proximally-oriented concave facet for the cuboid.

*Cuboid. N. galiani*: one right, UF 25661, one left, UF 25664.

The cuboid in *N. galiani* (Fig. 23) is approximately cubed-shaped and robust. Overall, the cuboid is longer proximodistally than it is mediolaterally or dorsoplantarly. In proximal view, the calcaneus facet is proximally convex and mediolaterally rectangular. On the ventral end of the

articular surface the border is dorsally concave. In medial view are three articular surfaces. On the proximodistal and proximoplantar borders of the medial surface are small, round facets for articulation with the navicular. Distal to these is a dorsoplantarly elongated facet for articulation with the ectocuneiform. This facet is wider in its dorsal half and is distally inclined in its ventral half. The dorsal surface is grooved and ridged throughout. On the lateral surface, a deep peroneal groove travels distoplantarly and continues onto the distal end along the plantar border. The outermost ridge from the peroneal groove is extended laterally and projects distally. In distal view, the articulation for the MT IV and V are present, with the facet for the MT IV being much larger and concave than the facet for the MT V. The MT V facet is convex and oriented distolaterally.

*B. loveorum*: one right, UF 25668.

The cuboid in *B. loveorum* (Fig. 23) is approximately cubed-shaped and robust. Overall, the cuboid is longer proximodistally than it is mediolaterally or dorsoplantarly. In proximal view, the calcaneus facet is proximally convex and mediolaterally rectangular. On the ventral end of the articular surface the border is dorsally concave. In medial view are three articular surfaces, all of which are not well preserved. On the proximodistal and proximoplantar borders of the medial surface are small, round facets for articulation with the navicular. Distal to these is a dorsoplantarly elongated facet for articulation with the ectocuneiform. This facet is wider in its dorsal half and is distally inclined in its ventral half. The dorsal surface is grooved and ridged throughout. On the lateral surface, a deep peroneal groove travels distoplantarly and continues onto the distal end along the plantar border. The outermost ridge from the peroneal groove is extended laterally and projects distally. In distal view, the articulation for the MT IV and V are

present, with the facet for the MT IV being much larger and concave than the facet for the MT V. The MT V facet is broken off from its border with the facet for the MT IV.

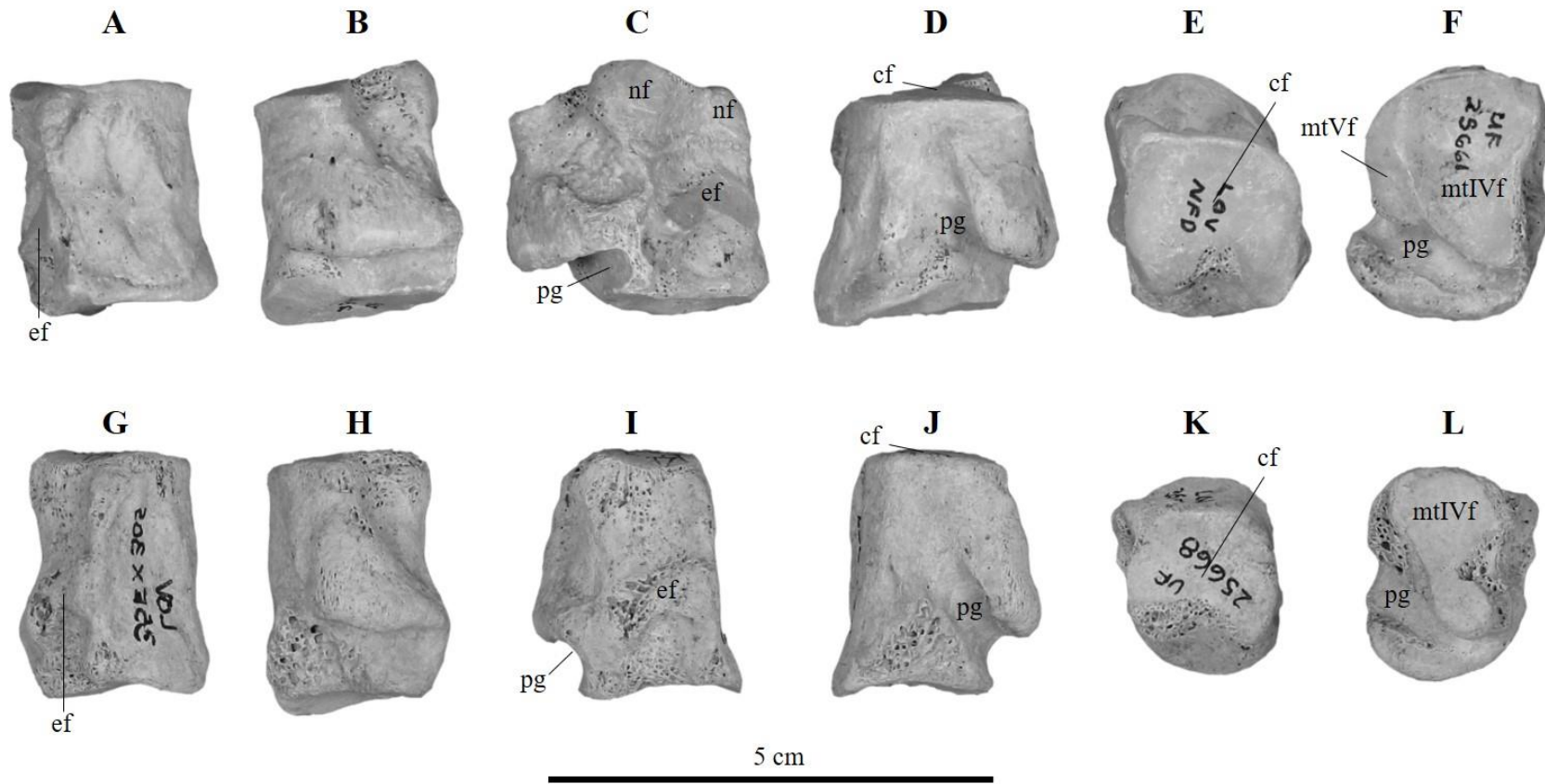


Figure 23. Cuboid comparison views between both taxa. A-F *Nimravidex galiani* UF 25661 right: dorsal (A), plantar (B), medial (C), lateral (D), proximal (E), distal (F) views. G-L *Barbourofelis loveorum* UF 25668 right: dorsal (G), plantar (H), medial (I), lateral (J), proximal (K), distal (L) views. Abbreviations: cf, calcaneus facet; ef, ectocuneiform facet; mtIVf, MTIV facet; mtVf, MTV facet; nf, navicular facet; pg, peroneal groove.

Remarks—There is little difference between the cuboids of *N. galiani* and *B. loveorum*. In overall size, *B. loveorum* is proximodistally longer than that of *N. galiani*, but is thinner mediolaterally and dorsoplantarly. The peroneal groove is more closed in *N. galiani* by the peroneal ridge and cuboid body, whereas it is more open in *B. loveorum*. However, the peroneal ridge in *N. galiani* is more robust and extends further laterally and distally.

*Navicular. N. galiani*: one right, UF 69825.

The navicular of *N. galiani* (Fig. 24) is oval and dorsoplantarly longer than it is mediolaterally. Proximodistally the navicular is thin. The majority of the proximal surface articulates with the distal head of the astragalus and is concave. On the medioplantar surface there is a large tubercle extending proximally, further making the proximal facet concave. Lateral to this is a large knob extending plantarly. In distal view, the navicular is convex with three articular surfaces, one for each of the three cuneiforms. The ectocuneiform facet is at the dorsolateral end of the distal surface, is the larger of the three facets, and is round. Connecting to the ectocuneiform facet's medial border is the smaller mesocuneiform facet. Plantar to this facet is the endocuneiform facet, which is smaller than the mesocuneiform facet and greatly distally projected. Both the meso and endocuneiform facets take up the majority of the medial side of the distal end and are connected. On the lateral surface the cuboid facet is not well preserved.

*B. loveorum*: one left, UF 90310.

The navicular of *B. loveorum* (Fig. 24) is oval and dorsoplantarly longer than it is mediolaterally. Proximodistally the navicular is thin. The majority of the proximal surface articulates with the distal head of the astragalus and is concave. On the medioplantar surface there is a large tubercle extending proximally, further making the proximal facet concave. Lateral to this is a large knob extending distoplantarly. Both these tubercles are very robust. In

distal view, the navicular is convex with three articular surfaces, one for each of the three cuneiforms. The ectocuneiform facet is at the dorsolateral end of the distal surface, continuing onto the lateral surface. It is the larger of the three facets and is round. Connecting to the ectocuneiform facet's medial border is the smaller mesocuneiform facet. Plantar to this facet is the endocuneiform facet, which is larger than the mesocuneiform facet but smaller than the ectocuneiform facet. Both the meso and endocuneiform facets take up the majority of the medial side of the distal end. The endocuneiform facet is separated from the other two distal facets by grooves, and it is extended onto the distal end of the medial tubercle. On the lateral surface is a dorsoplantarly elongated articular surface for the cuboid.

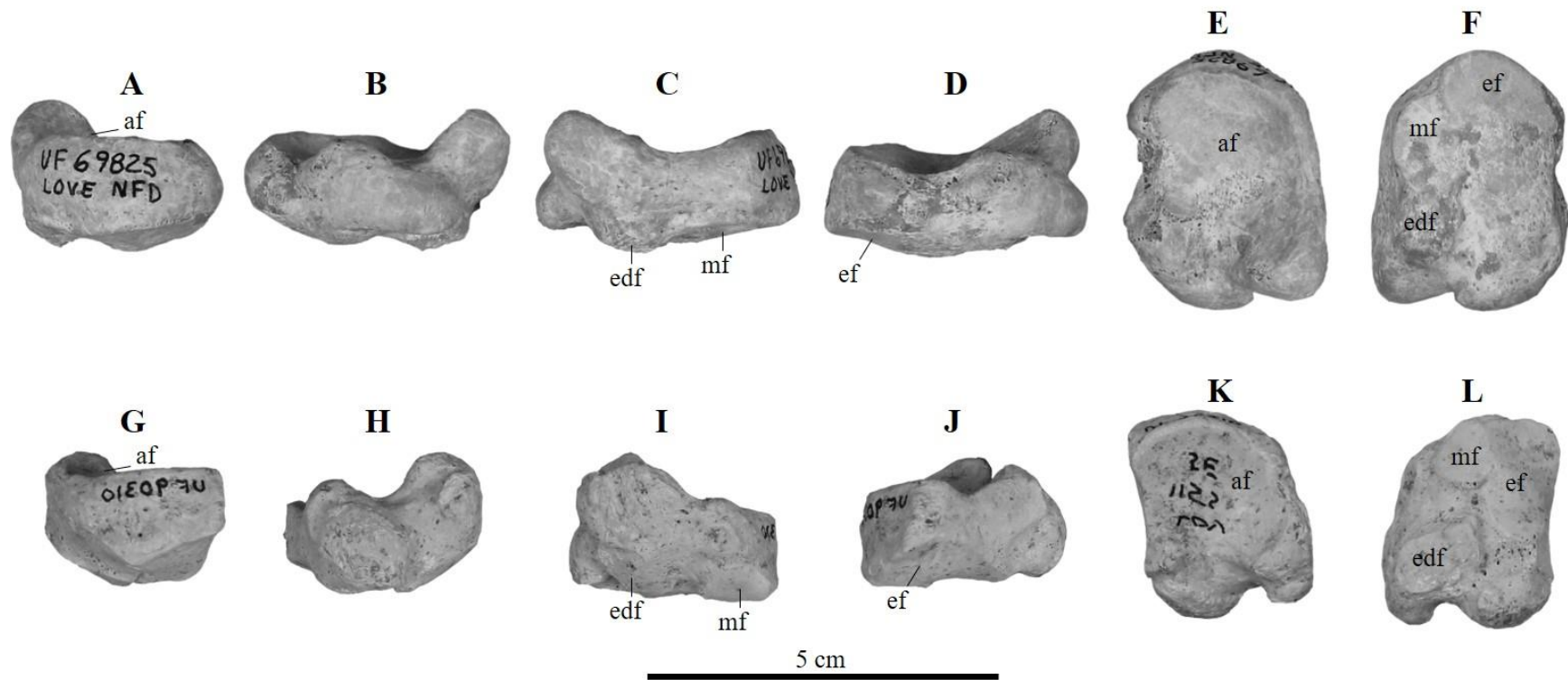


Figure 24. Navicular comparison views between both taxa. A-F *Nimravides galiani* UF 69825 right: dorsal (A), plantar (B), medial (C), lateral (D), proximal (E), distal (F) views. G-L *Barbourofelis loveorum* UF 90310 left side inverted to right side: dorsal (G), plantar (H), medial (I), lateral (J), proximal (K), distal (L) views. Abbreviations: af, astragalus facet; edf, endocuneiform facet; ef, ectocuneiform facet; mf, mesocuneiform facet.

Remarks—The naviculars of *N. galiani* and *B. loveorum* are both oval shaped with a concave proximal surface and convex distal end. In proximal view, the medial tubercle is projected more proximally in *B. loveorum*, slightly closing the articular area, whereas the facet is more open in *N. galiani*. Regardless, the proximal ends of both taxa are deeply concave. Lateral to this tubercle, the lateral knob is extended more distally in *B. loveorum*. Both the tubercle and knob in *B. loveorum* are proximodistally thicker than that of *N. galiani*. On the distal surface, the ectocuneiform facet of *B. loveorum* continues onto the lateral surface, whereas in *N. galiani* it stops at the dorsolateral border, and is the largest of the three facets in both taxa. The mesocuneiform facet is the second largest distal facet in *N. galiani*, whereas it is the third smallest in *B. loveorum*. Palmar to the mesocuneiform facet is the endocuneiform facet. In *N. galiani*, this facet is connected to the mesocuneiform facet by its dorsal border and it is greatly distally projected. In *B. loveorum*, the endocuneiform facet is separated by the other two distal facets by grooves and it is elongated onto the distal end of the medial tubercle.

*Ectocuneiform. N. galiani*: one right, UF 25672.

The ectocuneiform of *N. galiani* (Fig. 25) is triangular in proximal and distal views, and is rectangular in dorsal view. From the dorsal end to the plantar end, the ectocuneiform is elongated on the proximal region, with the plantar end forming a plantarly projected tubercle. On the proximal surface there is an elliptical and large articular area for the navicular, of which the medial border is straighter than that of the remaining articular border. This facet is slightly concave, with the plantar border extending proximally. Planter to this facet is a thick and dorsoplantarly short neck leading to an enlarged head that points distally. The medial surface of the head is more elongated than the rest of the head. In distal view, the articular surface for the MT III is large and 'T'-shaped, ending just dorsal to the beginning of the neck, and is slightly

concave. On the dorsal border, this facet is mediolaterally wider than the plantar border and the medial end is dorsoplantarly taller than the lateral end. On the medial side are two small and round articular surfaces, both for the MT II. In lateral view, the articulation surface with the cuboid is present via a dorsoplantarly elongated, and proximodistally thin, facet.

*B. loveorum*: one left, UF 25670.

The ectocuneiform of *B. loveorum* (Fig. 25) is triangular in proximal and distal views, and is rectangular in dorsal view. From the dorsal end to the plantar end, the ectocuneiform is elongated on the proximal region, with the plantar end forming a plantarly projected tubercle. On the proximal surface there is an elliptical and large articular area for the navicular, of which the medial border is straight than that of the remaining articular border. This facet is slightly concave, with the plantar border extending proximally. Planter to this facet is a thick and dorsoplantarly short neck leading to an enlarged head. The medial surface of the head is more elongated than the rest of the head. In distal view, the articular surface for the MT III is large and 'T'-shaped, ending just dorsal to the beginning of the neck, and slightly concave. On the dorsal border, this facet is mediolaterally wider than the plantar border and the medial end is dorsoplantarly taller than the lateral end. On the medial side are two large and elliptical articular surfaces, both for the MT II. In lateral view, the articulation surface with the cuboid is present via a dorsoplantarly elongated, and proximodistally thin, facet.

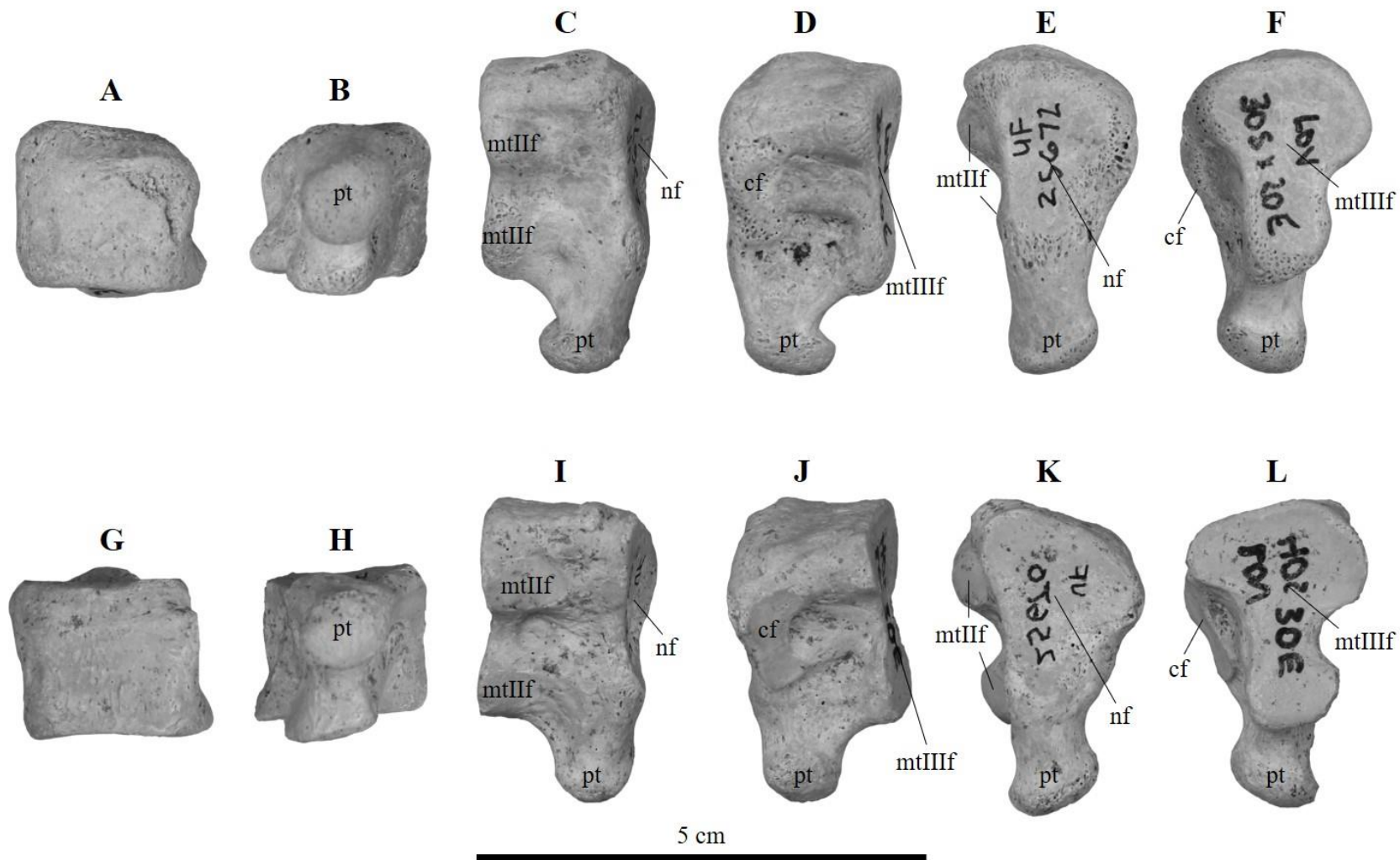


Figure 25. Pisiform comparison views between both taxa. A-F *Nimravidés galiani* UF 25672 right: dorsal (A), plantar (B), medial (C), lateral (D), proximal (E), distal (F) views. G-L *Barbourofelis loveorum* UF 25670 left side inverted to right side: dorsal (G), plantar (H), medial (I), lateral (J), proximal (K), distal (L) views. Abbreviations: cf, cuboid facet; pt, plantar tubercle; mtIIIf, MTII facet; mtIIIIf, MTIII facet; nf, navicular facet.

Remarks—The ectocuneiform of *N. galiani* and *B. loveorum* have few differences. Overall, the shape and proportions are very similar between both taxa. Plantar to the main body, *B. loveorum* has a longer neck than *N. galiani* does. The distal region of the head points distally in *N. galiani*, whereas in *B. loveorum* the head does not point in any direction. However, the ectocuneiform heads of both taxa are elongated medially. On the medial surface *B. loveorum* has larger facets for the MT II, proximodistally. Additionally, the facet for the cuboid on the lateral side is proximodistally wider in *B. loveorum*, whereas in *N. galiani* it is thin and not well preserved.

#### *Metatarsals*

*Metatarsal II. N. galiani*: one right, UF 25371, one left, UF 25368.

The second metatarsal (MT II) of *N. galiani* (Fig. 26) is proximodistally elongate and nearly straight. On the proximal surface is a subtriangular facet for the articulation with the mesocuneiform, and is mediolaterally concave. In lateral view there are four articular surfaces, two for the ectocuneiform and two for the MT III. On the dorsoproximal border is a small round and concave facet for the ectocuneiform. Along its distal border is a smaller facet for the MT III. This relationship is repeated distally on the proximoplantar border of the lateral surface, however the facet for the MT III is now elliptical. Distal to these facets, on the metatarsal shaft is a shallow dorsoplantar groove, with the dorsal end more proximal than the plantar end. The diaphysis is mediolaterally compressed in its proximal half. At the distal epiphysis is the articular region for the proximal phalanx, of which there is a well-developed distoplantar ridge running dorsoplantarly down the center of the epiphysis in distal view.

*B. loveorum*: one right, UF 25302, one left, UF 25313.

The second metatarsal (MT II) of *B. loveorum* (Fig. 26) is proximodistally shortened and nearly straight. On the proximal surface is a subtriangular facet for the articulation with the mesocuneiform, and is mediolaterally concave on its dorsal end. In lateral view there are four articular surfaces, two for the ectocuneiform and two for the MT III. On the dorsoproximal border is a small round and concave facet for the ectocuneiform. Along its distal border is a smaller facet for the MT III. This relationship is repeated distally on the proximoplantar border of the lateral surface; however, these facets are much smaller than the dorsal ones and the plantar facets are separated from each other by a pronounced convex ridge. The diaphysis is mediolaterally compressed in its proximal half. At the distal epiphysis is the articular region for the proximal phalanx, of which there is a well-developed distoplantar ridge running dorsoplantarly down the center of the epiphysis in distal view.

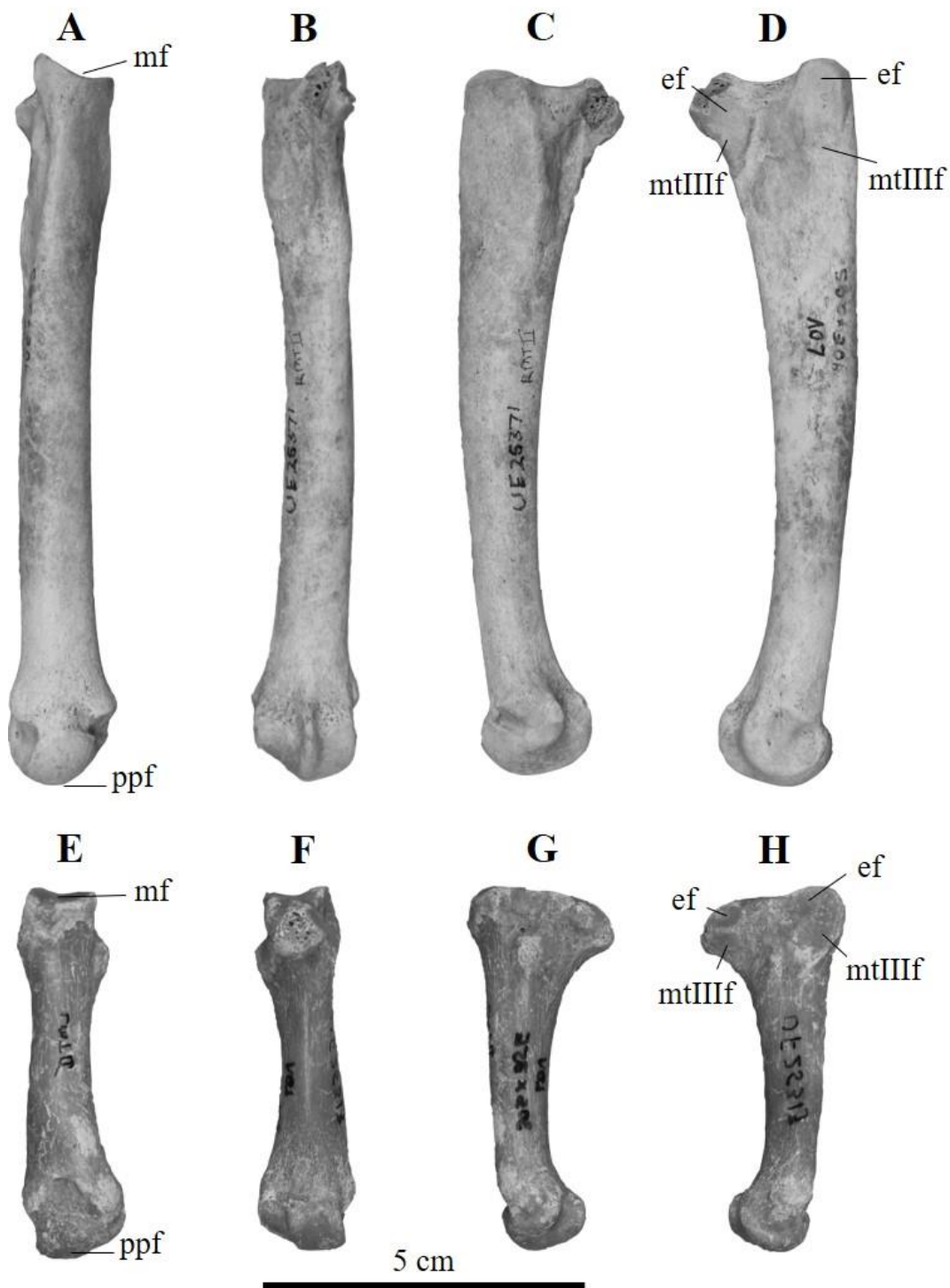


Figure 26. Metatarsal II comparison views between both taxa. A-D *Nimravides galiani* UF 25371 right: dorsal (A), plantar (B), medial (C), lateral (D) views. E-H *Barbourofelis loveorum* UF 25313 left side inverted to right side: dorsal (E), plantar (F), medial (G), lateral (H) views. Abbreviations: ef, ectocuneiform facet; mf, mesocuneiform facet; mtIII f, MT III facet; ppf, proximal phalanx facet.

Remarks—MT II of *N. galiani* and *B. loveorum* differ in proximodistal length, with the metatarsal in *B. loveorum* being approximately half that of *N. galiani*. In lateral view, the proximoplantar facets for the MT III and ectocuneiform are separated by a very pronounced ridge in *B. loveorum*, ensuring that the ectocuneiform facet faces proximolaterally and the MT III facet faces distolaterally. Whereas in *N. galiani* both facets face laterally. Distal to these facets, on the diaphysis, *N. galiani* has a shallow dorsoplantar groove that is not present in *B. loveorum*.

*Metatarsal III. N. galiani*: two right, UF 25372, UF 25352.

The third metatarsal (MT III) of *N. galiani* (Fig. 27) is proximodistally elongate and straight, with the diaphysis maintaining the same thickness from proximal end to the distal end. On the proximal surface is a large ‘T’-shaped facet for the articulation with the ectocuneiform, with the dorsal region being mediolaterally long. In medial view there are two small facets for the articulation with the MT II. Both are on the proximal border and are convex, however the dorsal facet is separated by the plantar facet by a deep groove. On the lateral surface are two facets for the MT IV, both just distal to the proximal border. The dorsal-most facet is concave, facing distolaterally, whereas the plantar-most facet is nearly flat and facing dorsolaterally. Distal to these facets are elliptical muscle scars. On the distal surface is the articular region for the proximal phalanx, of which there is a less pronounced central ridge on the distal head than that of the MT II.

*B. loveorum*: two right, UF 25320, UF 25319.

The third metatarsal (MT III) of *B. loveorum* (Fig. 27) is proximodistally shortened and straight, with the diaphysis having a mediolaterally compressed midshaft. On the proximal surface is a large convex ‘T’-shaped facet for the articulation with the ectocuneiform, with the dorsal region being mediolaterally long. In medial view there are two small facets for the

articulation with the MT II. Both are on the proximal border and are convex, however the dorsal facet is separated by the plantar facet by a shallow groove. On the lateral surface are two facets for the MT IV, both just distal to the proximal border. The dorsal-most facet is concave, facing distolaterally, and continues onto the proximal surface, whereas the plantar-most facet is nearly flat, facing dorsolaterally, and is very small. Distal to these facets are elliptical muscle scars. On the distal surface is the articular region for the proximal phalanx with a well-developed central ridge.

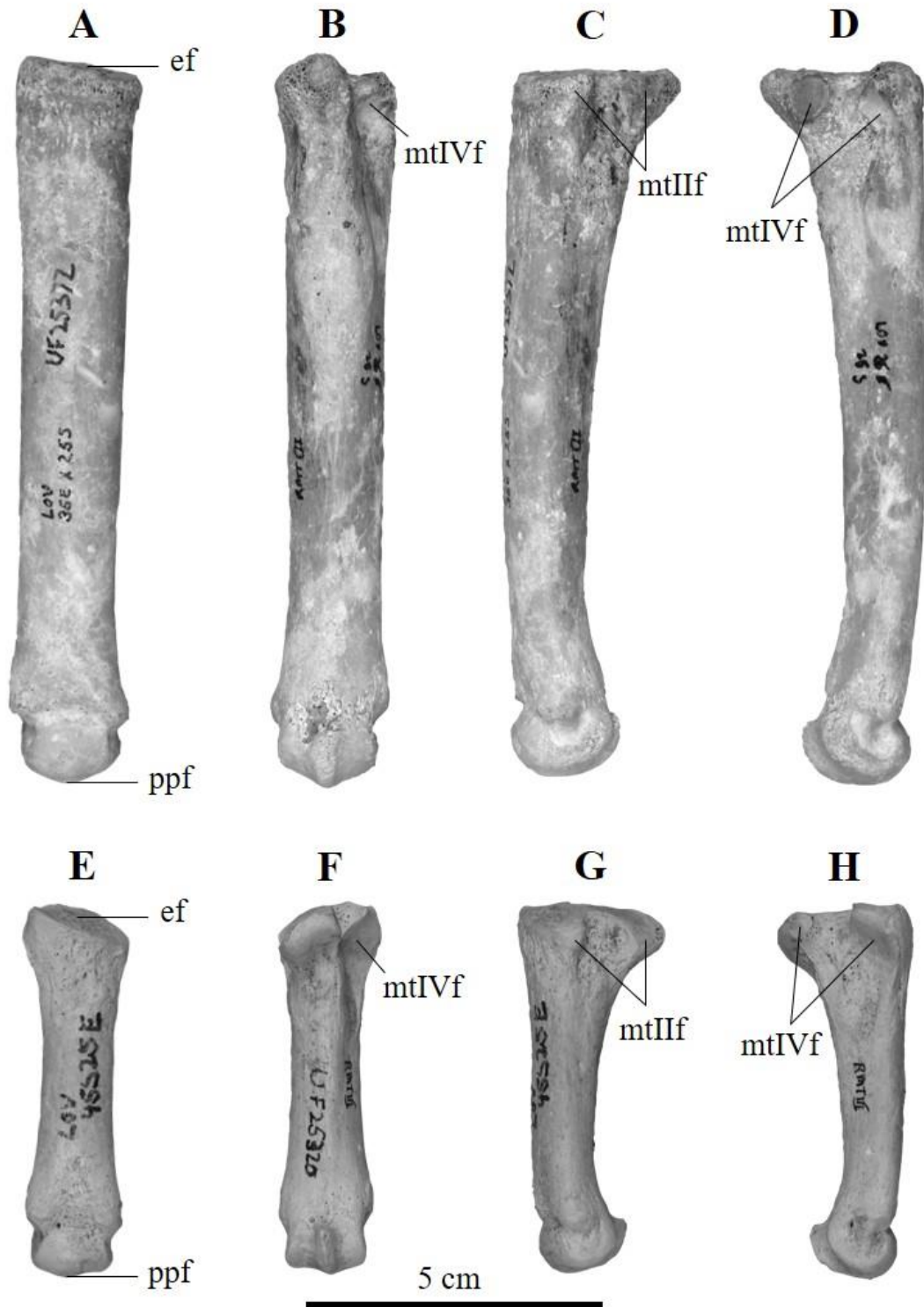


Figure 27. Metatarsal III comparison views between both taxa. A-D *Nimravides galiani* UF 25372 right: dorsal (A), plantar (B), medial (C), lateral (D) views. E-H *Barbourofelis loveorum* UF 25320 right: dorsal (E), plantar (F), medial (G), lateral (H) views. Abbreviations: ef, ectocuneiform facet; mtIIIf, MT II facet; mtIIIIf, MT III facet; ppf, proximal phalanx facet.

Remarks—MT III of *N. galiani* and *B. loveorum* differ in proximodistal length, with *B. loveorum* being less than half the length than in *N. galiani*. The diaphysis of *B. loveorum* is mediolaterally compressed mid-shaft, whereas the diaphysis maintains the same width in *N. galiani*. On the proximal surface, the ectocuneiform facet is convex in *B. loveorum* and flat in *N. galiani*. In medial view the two facets for the MT II are separated by a dorsoplantarly wide, yet shallow groove in *B. loveorum*, differing from the narrow and deep groove in *N. galiani*. On the lateral surface, *B. loveorum* has a much larger dorsoproximal facet for the MT IV than that of *N. galiani*, and this facet continues onto the proximal surface, unlike in *N. galiani*. Additionally, the proximoplantar facet is very reduced in *B. loveorum*, whereas both lateral facets in *N. galiani* are similar in size. On the distal surface, *B. loveorum* has a better developed central ridge than that of *N. galiani*.

*Metatarsal IV. N. galiani*: two left, UF 37112, UF 25354.

The fourth metatarsal (MT IV) of *N. galiani* (Fig. 28) is proximodistally elongated and mediolaterally thinner than the robust MT III. In medial and lateral views, the diaphysis is concave on the plantar side and convex on the dorsal region. On the proximal half of the dorsal surface there is a large dorsal ridge. In proximal view, the articular surface for the cuboid takes up the majority of the proximal side. This facet is rectangular, convex, and dorsoplantarly elongated. On the medial surface there are two facets for the MT III. Distal to the proximal border, near the dorsal region, is a round and convex articular knob, projecting medially and facing dorsoproximally. Plantar to this articular surface is a smaller convex articular knob, and is more proximally aligned, facing medially. On the lateral surface is a deep, round groove surrounded by a facet for the MT V. On the distal surface, the central ridge on the distal head is not pronounced.

*B. loveorum*: one right, UF 275518, one left, UF 25321.

The fourth metatarsal (MT IV) of *B. loveorum* (Fig. 28) is proximodistally shortened and is more robust and longer than MT II, III, and V. In medial and lateral views, the distal head is plantarly offset from the rest of the diaphysis. In proximal view, the articular surface for the cuboid takes up the majority of the proximal side. This facet is rectangular, strongly convex, and dorsoplantarly elongated. On the medial surface there are two facets for the MT III. Distal to the proximal border, near the dorsal region, is a round and concave articular facet, projecting medially and facing dorsoproximally. Plantar to this articular surface is a smaller concave facet, and is more proximally aligned, facing medially. On the lateral surface is a deep, round groove surrounded by a facet for the MT V. On the distal surface, the central ridge on the distal head is well-developed.

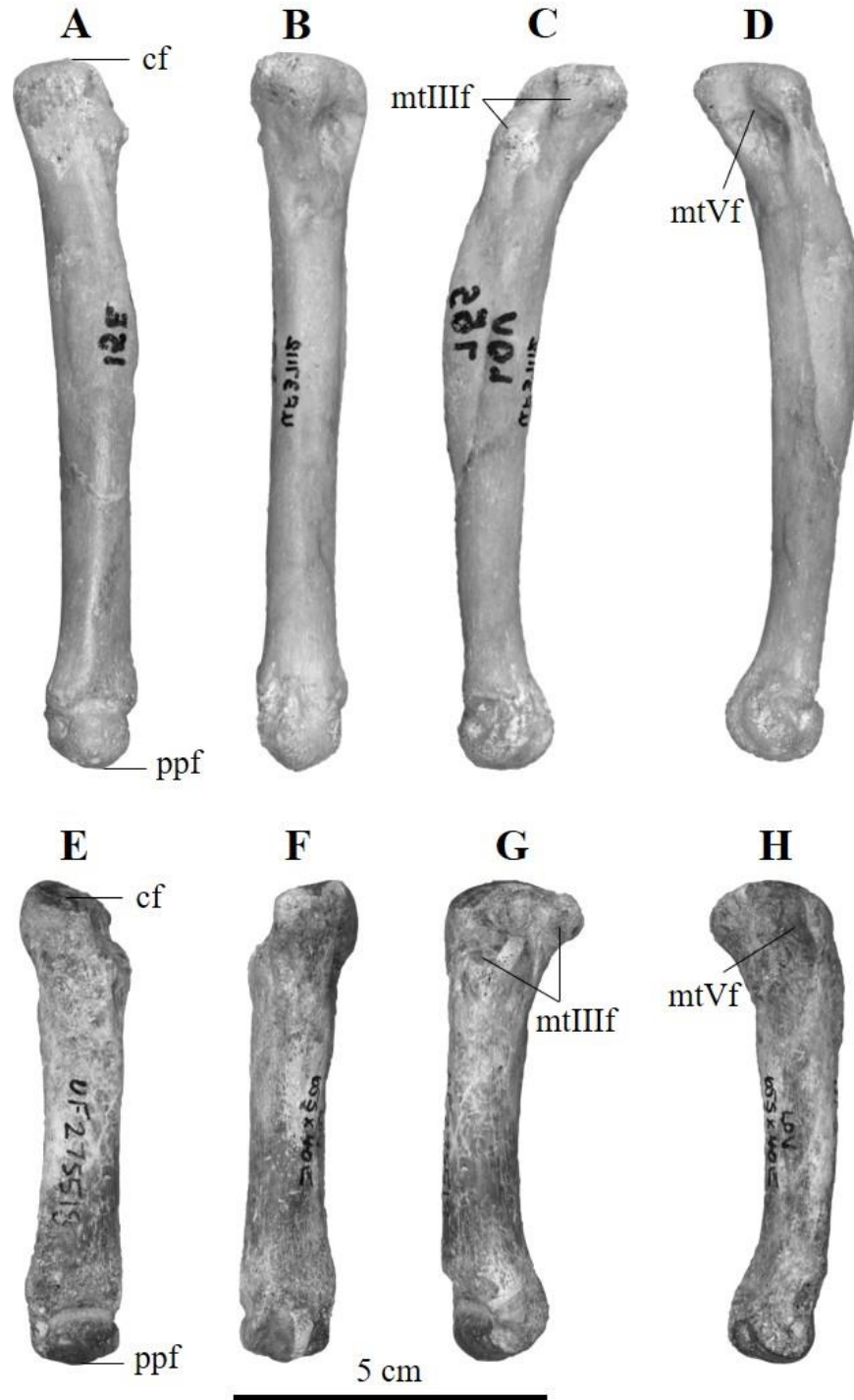


Figure 28. Metatarsal IV comparison views between both taxa. A-D *Nimravides galiani* UF 37112 left side inverted to right side: dorsal (A), plantar (B), medial (C), lateral (D) views. E-H *Barbourofelis loveorum* UF 275518 right: dorsal (E), plantar (F), medial (G), lateral (H) views. Abbreviations: cf, cuboid facet; mtIII f, MT III facet; mtV f, MT V facet; ppf, proximal phalanx facet.

Remarks—MT IV of *N. galiani* and *B. loveorum* differ in proximodistal length, with *B. loveorum* being approximately 75% that of *N. galiani*. In *B. loveorum* this is the longest of all the metatarsals, however in *N. galiani* it is the same length as the MT II and V. On the proximal surface, the facet for the cuboid articulation is much more convex in *B. loveorum* and is longer dorsoplantarly. On the medial surface, the dorsal articular region for the MT III is a convex knob in *N. galiani*, whereas in *B. loveorum* it is a concave facet. Both are projected medially, but it is more elongated in *N. galiani*. Additionally, this facet in *B. loveorum* is placed closer to the proximal end than in *N. galiani*. On the distal surface, *B. loveorum* has a more well-developed and pronounced central ridge on the distal head.

*Metatarsal V. N. galiani*: two right, UF 25397, UF 25361.

The fifth metatarsal (MT V) of *N. galiani* (Fig. 29) is proximodistally elongate and much more slender than MT II-IV. The diaphysis is straight and maintains a consistent width from proximal to distal ends. On the proximal epiphysis the plantar region is proximally elongated whereas the dorsal region begins distally on the shaft, making the articular surfaces diagonal from the dorsodistal area to the proximoplantar point. There are two facets on the proximal end, both facing medioproximally. The proximal most facet is for the articulation with the cuboid and is roughly elliptical and convex. Distal to the cuboid facet is an articular surface for the MT IV, which is mediolaterally elliptical with a compressed midsection, proximodistally. The lateral part of this facet is round and concave, whereas the medial part is much smaller. Lateral to the MT IV facets is a nonarticular knob pointing lateroproximally. On the distal surface, the head has a well-defined central ridge.

*B. loveorum*: one left, UF 25325.

The fifth metatarsal (MT V) of *B. loveorum* (Fig. 29) is proximodistally short and slightly more slender than MT II-IV. The diaphysis is mediolaterally curved, with the lateral side being concave. Between the epiphyses, the midshaft of the diaphysis is mediolaterally compressed. On the proximal epiphysis the plantar region is plantarly elongate. There are two facets on the proximal end. The proximal most facet is for the articulation with the cuboid and is dorsoplantarly elliptical and flat. Distal to the cuboid facet, continuing onto the medial surface, is an articular surface for the MT IV, which is dorsoplantarly elliptical, and compressed plantarly. The dorsal part of this facet is slightly concave. Lateral to the MT IV facets, and on the lateral surface, is a nonarticular knob pointing lateroproximally and close to the dorsal surface. On the distal surface, the head has a well-defined central ridge.

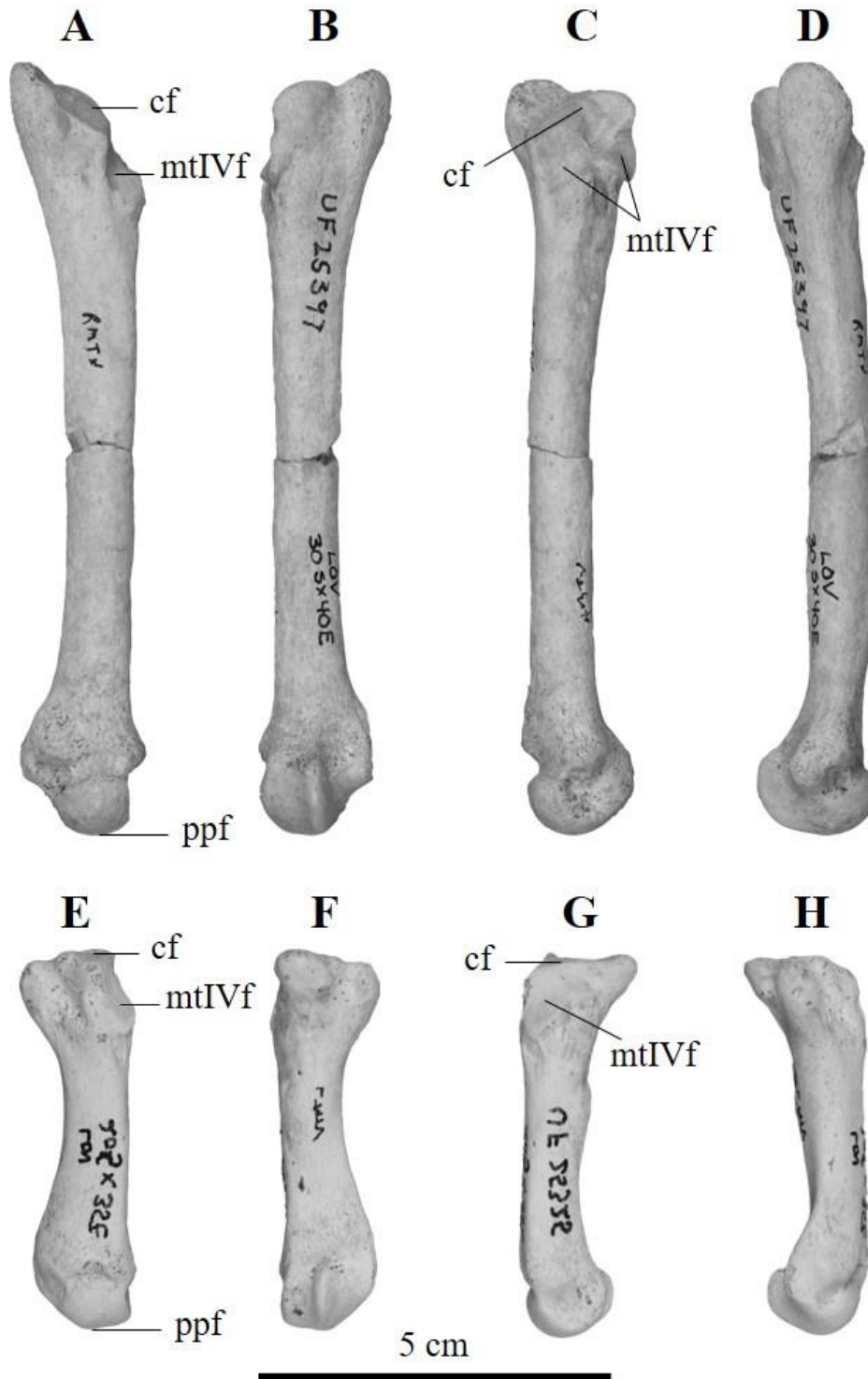


Figure 29. Metatarsal V comparison views between both taxa. A-D *Nimravides galiani* UF 25397 left side inverted to right side: dorsal (A), plantar (B), medial (C), lateral (D) views. E-H *Barbourofelis loveorum* UF 25325 right: dorsal (E), plantar (F), medial (G), lateral (H) views. Abbreviations: cf, cuboid facet; mtIVf, MT IV facet; ppf, proximal phalanx facet.

Remarks—MT V of *N. galiani* and *B. loveorum* differ in proximodistal length, with *B. loveorum* being less than half the length as that of *N. galiani*. In *B. loveorum* the diaphysis is curved, with the lateral side being concave and the dorsal surface being flat, whereas in *N. galiani* MT V is straight and round. The proximal surface is very different between the two taxa. In *N. galiani* the cuboid and MT IV facets are facing medioproximally and are separated by ridges. However, in *B. loveorum* the facets are differently oriented, with the cuboid facet dorsoplantarly flat and the MT IV facet is on the medial surface. On the lateral surface, *B. loveorum* has a laterally projected knob with grooves on its dorsal and plantar borders, and is close to the dorsal area. In *N. galiani*, this lateral tubercle is lateroproximally elongated and is closer to the plantar region.

### *Vertebrae*

#### *Atlas. N. galiani: UF 25593*

The single atlas of *N. galiani* (Fig. 30) is mostly intact, missing both transverse processes lateral to the transverse foramina. In dorsal view, the dorsal arch is convex and mediolaterally wider than it is anteroposteriorly. On the anterior surface are two facets for the occipital condyles on the skull. Both occipital condyle facets are round and deeply concave, facing anteromedially. The opening for the neural canal is large and round, taking up most of the atlas's body size. In lateral view, near the dorsal surface, is the atlantal foramen, a small and round opening facing posterolaterally and opening into the neural canal, dorsal to the anterior facets. Near the ventral surface, ventral to the transverse processes, there is a larger transverse foramen that separates into two smaller canals: a very small anterior foramen leading into the neural canal posterior to the atlantal foramen, and a larger posterior foreman leading to the posterior side of the atlas, on

the medial-most part of the transverse process. In posterior view, there are two posterior facets that articulate with the axis. These facets are triangular and slightly concave, facing posteromedially. The posterior opening for the neural canal is large and round.

*B. loveorum*: UF 36990

The single atlas of *B. loveorum* (Fig. 30) is mostly complete, missing the posterior most end of the transverse processes. In dorsal view, the dorsal arch is strongly convex and approximately the same width mediolaterally and anteroposteriorly. On the anterior surface are two facets for the occipital condyles on the skull. Both occipital condyle facets are round and deeply concave, facing anteromedially. The opening for the neural canal is small and round. In lateral view, near the dorsal surface, is the atlantal foramen, a large and round opening facing laterally and opening into the neural canal, dorsal to the anterior facets. Near the ventral surface, ventral to the transverse processes, there is a larger transverse foramen that separates into two smaller canals: an anterior foramen leading dorsally towards the atlantal foramen, and a smaller posterior foramen leading to the posterior side of the atlas, on the medial-most part of the transverse process. In dorsal view, the atlantal foramen is connected to the transverse foramen via the alar foramen; a deep, oval groove on the lateral surface. There is a clear lack of alar notches between the atlas body and transverse wings on the anterior side. Instead, the border of the transverse process is connected to the anterior facets. In posterior view, there are two posterior facets that articulate with the axis. In posterior view, there are two posterior facets that articulate with the axis. These facets are round and slightly concave, facing posteromedially. In lateral view, the transverse processes are mediolaterally narrow and their dorsal surfaces are concave and ridged. The posterior opening for the neural canal is roughly the same size as the anterior opening and is round.

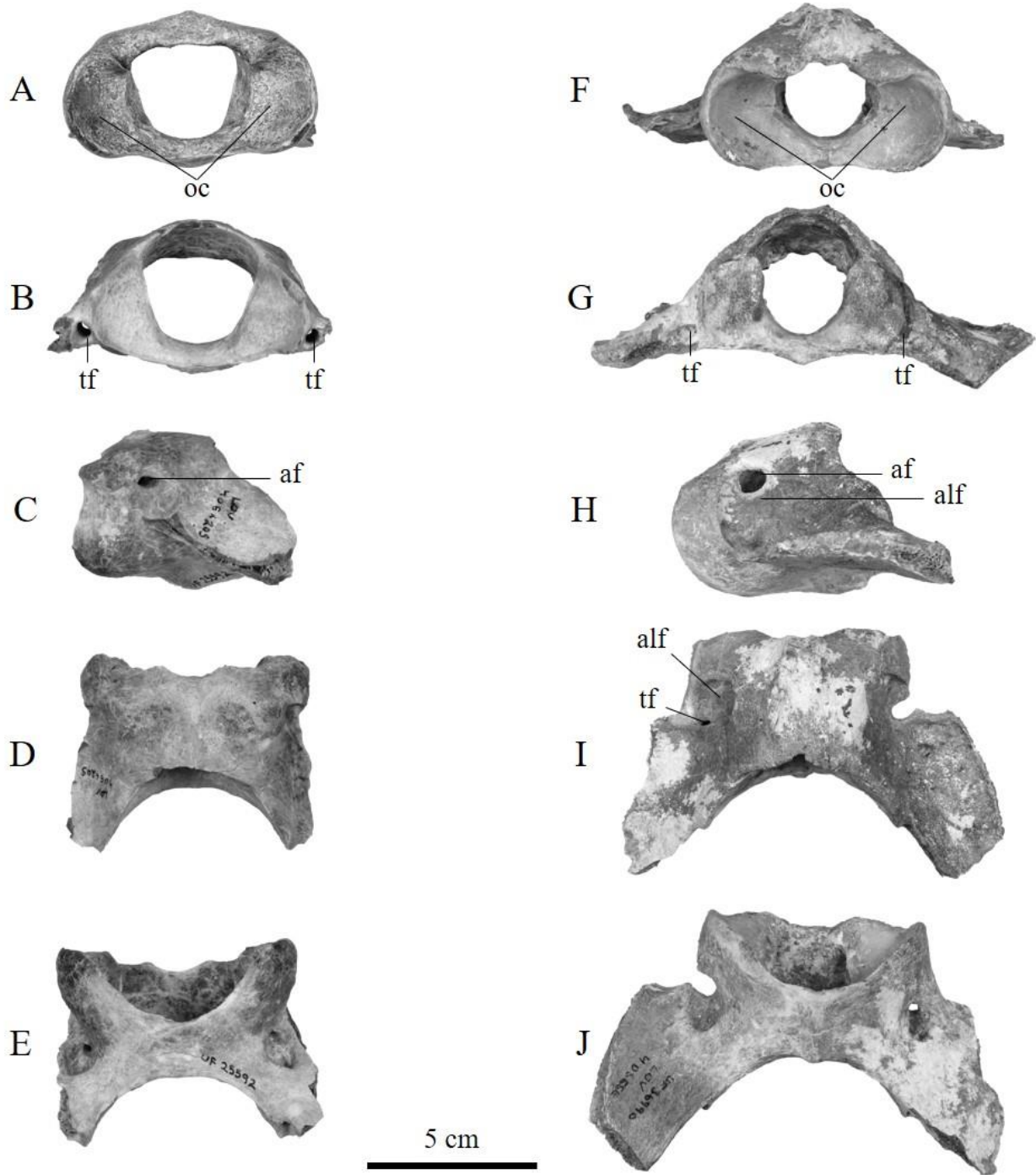


Figure 30. Atlas comparison views between both taxa. A-E *Nimravides galiani* UF 25593: anterior (A), posterior (B), lateral (C), dorsal (D), ventral (E) views. F-J *Barbourofelis loveorum* UF 36990: anterior (F), posterior (G), lateral (H), dorsal (I), ventral (J) views. Abbreviations: af, atlantal foramen; alf, alar foramen; oc, occipital condyles; tf, transverse foramen.

Remarks—The atlas of *N. galiani* and *B. loveorum* are similar in shape with some slight variations. On the dorsal surface, *B. loveorum* has a more convex and anteroposteriorly wider neural arch than in *N. galiani*. On the anterior surface, the anterior facets are larger and more concave in *B. loveorum*, and these facets are mediolaterally closer together due to the smaller neural canal *B. loveorum* has compared to *N. galiani*. In lateral view, *B. loveorum* has a larger atlantal foramen than *N. galiani*, that connects to the transverse foramen dorsal to the transverse process via a deep groove, unlike in *N. galiani* of which these two foramina are not connected. In ventral view, the transverse foramen separates into two smaller foramina in both taxa. In *N. galiani*, the anterior most foramen travels medially into the neural canal, not observed in *B. loveorum*, of which there is no additional foramen in the neural canal and the anterior most foramen travels dorsally onto the dorsal side of the transverse process towards the atlantal foramen. This is due to *B. loveorum* having reduced or missing alar notches as the anterior border of the transverse process connects close to the anterior facets. The second part of the transverse foramen is larger in both taxa and opens on the posterior surface of the atlas. On the posterior surface, *B. loveorum* has rounder and larger posterior facets, whereas in *N. galiani* these facets are more triangular and more closed, facing the other more medially than posteriorly.

*Axis. N. galiani:* UF 490611

The most complete axis of *N. galiani* (Fig. 31) is missing the neural spine and the posterior zygapophyses. As such, the neural canal is only preserved by the body of the axis. On the anterior surface is a conical shaped dens (odontoid process) projecting anteriorly from the center of the centrum. In lateral view, the dens is hooked with a convex dorsal surface. Lateral to the dens are the anterior zygapophyses, which are convex and triangular. On the lateral surface is a small transverse foramen facing anteroventrally, and continues posteriorly onto the posterior

surface. The transverse processes extend posterolaterally past the posterior surface of the centrum and are heavily worn. In posterior view the centrum is slightly concave mediolaterally elliptical, with the dorsal region anteriorly inclined. On the ventral surface there is a keel running anteroposteriorly down the center of the centrum, and on either side, there are two deep grooves parallel to the keel.

*B. loveorum*: UF 36485

The most complete axis of *B. loveorum* (Fig. 31) is missing the anterior-most part of the neural spine. On the anterior surface is a conical-shaped dens (odontoid process) projecting anteriorly from the center of the centrum. In lateral view, the dens is nearly straight. Lateral to the dens are the anterior zygapophyses, which are convex and round. On the lateral surface is a small transverse foramen facing anteroventrally, and continues posteriorly onto the posterior surface. The transverse processes extend posterolaterally past the posterior surface of the centrum. In posterior view the centrum is slightly concave mediolaterally elliptical, with the dorsal region anteriorly inclined. Dorsal to the centrum is a dorsally extended spine. The posterior region of the spine greatly projects posteriorly past the centrum. Dorsoventrally, this spine is very thin, with the ventral border curving anteriorly past the posterior zygapophyses dorsal to the spine. These zygapophyses are round and flat, facing ventrolaterally. On the ventral surface there is a keel running anteroposteriorly down the center of the centrum, and on either side, there are two deep grooves parallel to the keel.

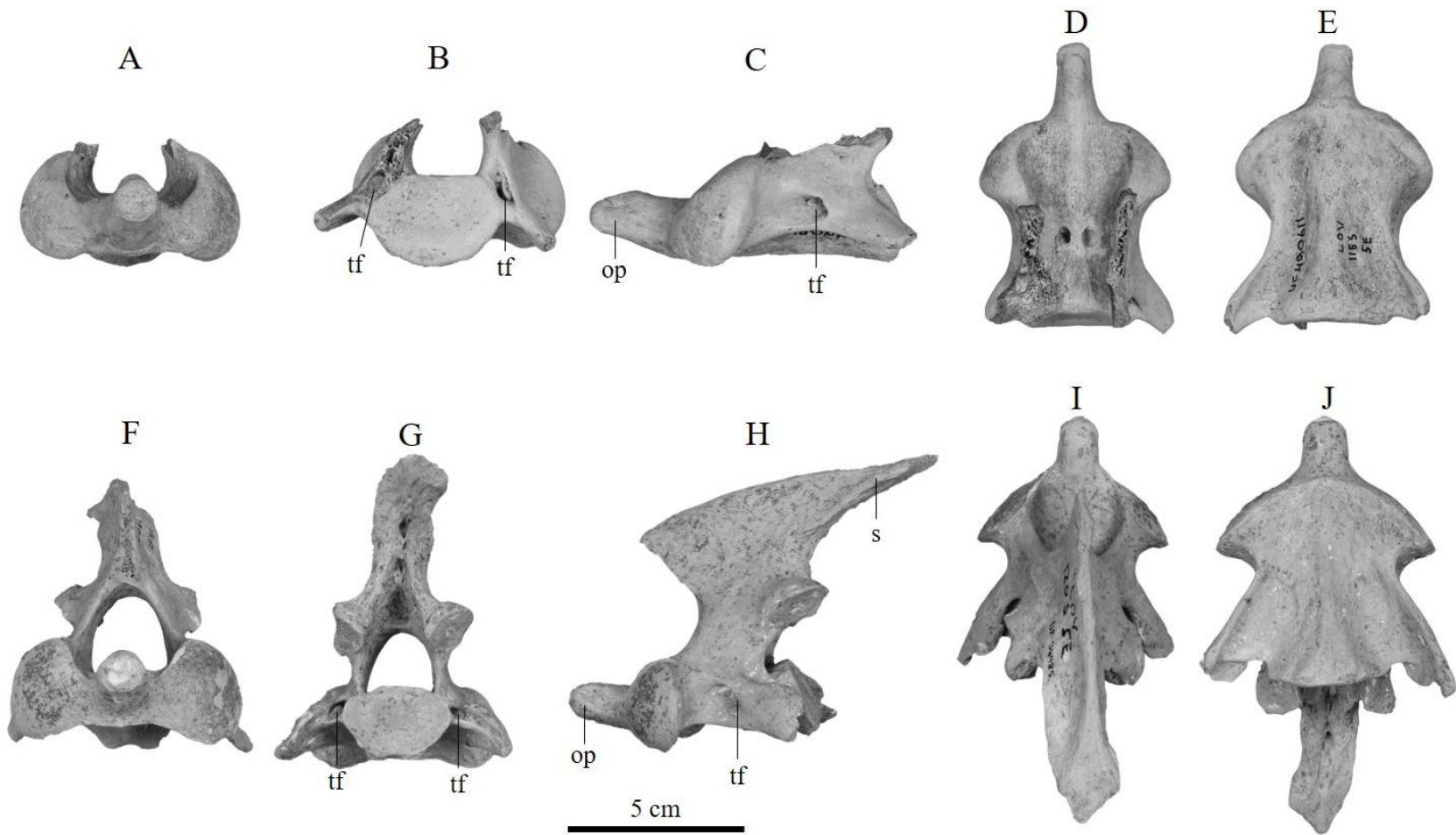


Figure 31. Axis comparison views between both taxa. A-E *Nimravidex galiani* UF 490611: anterior (A), posterior (B), lateral (C), dorsal (D), ventral (E) views. F-J *Barbourofelis loveorum* UF 36485: anterior (F), posterior (G), lateral (H), dorsal (I), ventral (J) views. Abbreviations: op, odontoid process; s, spine; tf, transverse process.

Remarks—The axis of *N. galiani* and *B. loveorum* vary in structure, however the shape is relatively the overall same. In anterior view, *N. galiani* has a more anteriorly elongated dens and there is a small dorsal process present, giving the dens a convex shape, unlike in *B. loveorum* of which this process is not present. Dorsal to the dens are the anterior zygapophyses which are triangular and more convex in *N. galiani*, yet rounded in *B. loveorum*. On the lateral surface, *B. loveorum* has a mediolaterally wider transverse foramen and a more laterally projected transverse process. The neural spine is missing in *N. galiani*, but is present in *B. loveorum* and has some interesting characteristics. The posterior extension of the spine greatly surpasses that of the centrum and there is a wide, concave groove separating the ventral border of the spine from the dorsal border of the posterior zygapophyses. On the ventral surface of the centrum, both taxa have a pronounced keel surrounded by two concave depressions. These depressions are mediolaterally wider in *B. loveorum* and more concave.

*Cervical Vertebrae 3. N. galiani: UF 490612*

The third cervical (C3) of *N. galiani* (Fig. 32) is missing the spinous process and transverse process in the one available specimen. In anterior view, the centrum is mediolaterally elliptical and concave. Lateral to the centrum are the transverse foramina which are small and mediolaterally compressed. Dorsal to the centrum is a rectangular neural canal. On the dorsal surface, along the anterior border, are the anterior zygapophyses, round and flat, facing dorsomedially. These facets are extended anteriorly past that of the centrum. On the posterior border of the dorsal surface are two pronounced ridges, located on the dorsal side of the posterior zygapophyses and running parallel to the spinous process. In posterior view, the centrum is convex. The posterior zygapophyses are round and flat, facing ventrolaterally and inclined posteriorly. On the dorsal surface there is an anteroposterior keel along the shaft of the centrum.

The centrum is anteroposteriorly longer than it is wide, and the dorsal region of the anterior and posterior ends are inclined anteriorly, whereas the ventral region ends are inclined posteriorly.

*B. loveorum*: UF 466169

The third cervical (C3) of *B. loveorum* (Fig. 32) is missing the spinous process and transverse process in the one available specimen. In anterior view, the centrum is mediolaterally elliptical and concave. Lateral to the centrum are the transverse foramina which are small and mediolaterally wide. Dorsal to the centrum is a rectangular neural canal. On the dorsal surface, along the anterior border, are the anterior zygapophyses, round and flat, facing dorsomedially. These facets are extended anteriorly past that of the centrum. On the posterior border of the dorsal surface are two pronounced ridges, located on the dorsal side of the posterior zygapophyses and running parallel to the spinous process. In posterior view, the centrum is convex. The posterior zygapophyses are round and flat, facing ventrolaterally and inclined posteriorly. On the dorsal surface there is an anteroposterior keel along the shaft of the centrum. The centrum is anteroposteriorly longer than it is wide, and the dorsal region of the anterior and posterior ends are inclined anteriorly, whereas the ventral region ends are inclined posteriorly.

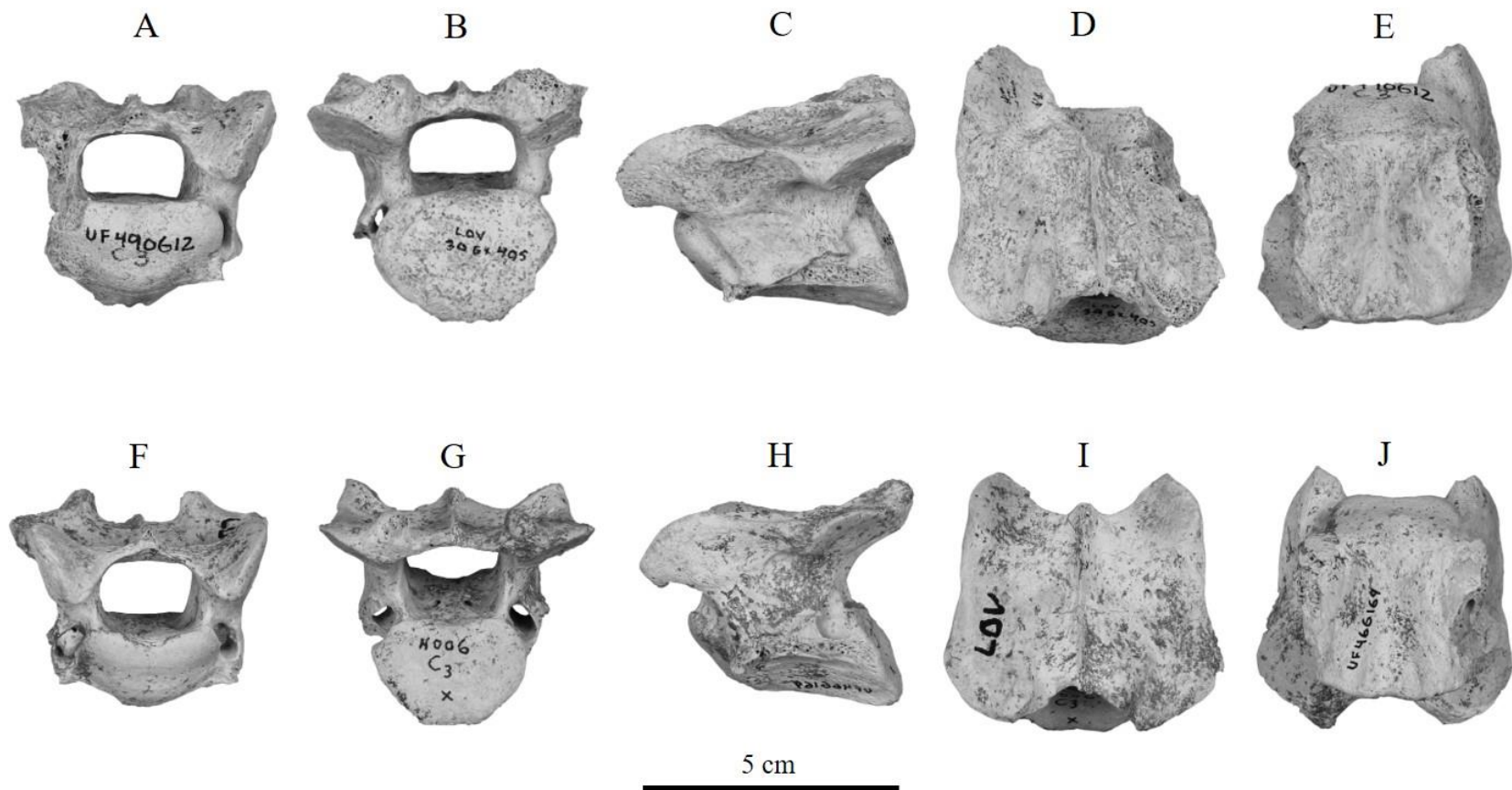


Figure 32. C3 comparison views between both taxa. A-E *Nimravides galiani* UF 490612: anterior (A), posterior (B), lateral (C), dorsal (D), ventral (E) views. F-J *Barbourofelis loveorum* UF 466169: anterior (F), posterior (G), lateral (H), dorsal (I), ventral (J) views.

Remarks—The C3 of *N. galiani* and *B. loveorum* are nearly identical with few differences. In anterior and posterior views, the transverse foramina are mediolaterally compressed in *N. galiani*, whereas in *B. loveorum* they are more open and rounder. Both the anterior and posterior zygapophyses of *N. galiani* are larger than that of *B. loveorum*. On the dorsal surface, *B. loveorum* has more pronounced processes dorsal to the posterior zygapophyses.

*Cervical Vertebrae 4. N. galiani: UF 490613*

The fourth cervical (C4) of *N. galiani* (Fig. 33) is very similar to its C3. In dorsal view, the lamina is anteroposteriorly smaller than that of the third cervical and there are two sets of parallel ridges and grooves. The broken region for the spinous process is located closer to the anterior border. In lateral view, there is a deep depression between the zygapophyses. Ventral to these facets, the transverse process extends laterally. The transverse foramina are more open than the foramina in the third cervical, but they are still compressed. On the ventral surface the transverse processes are clearly separated from the majority of the centrum's lateral sides.

*B. loveorum: UF 466173*

The fourth cervical (C4) of *B. loveorum* (Fig. 33) is very similar to its C3. In dorsal view, the lamina is anteroposteriorly smaller than that of the third cervical and there are two deep depressions on either side of the spine. The spine is dorsally short, projecting from the posterior side on the dorsal surface, and is posteriorly inclined. In lateral view the transverse process extends posterolaterally. On the ventral surface the transverse processes are attached to the centrum's lateral surface from anterior to posterior ends.

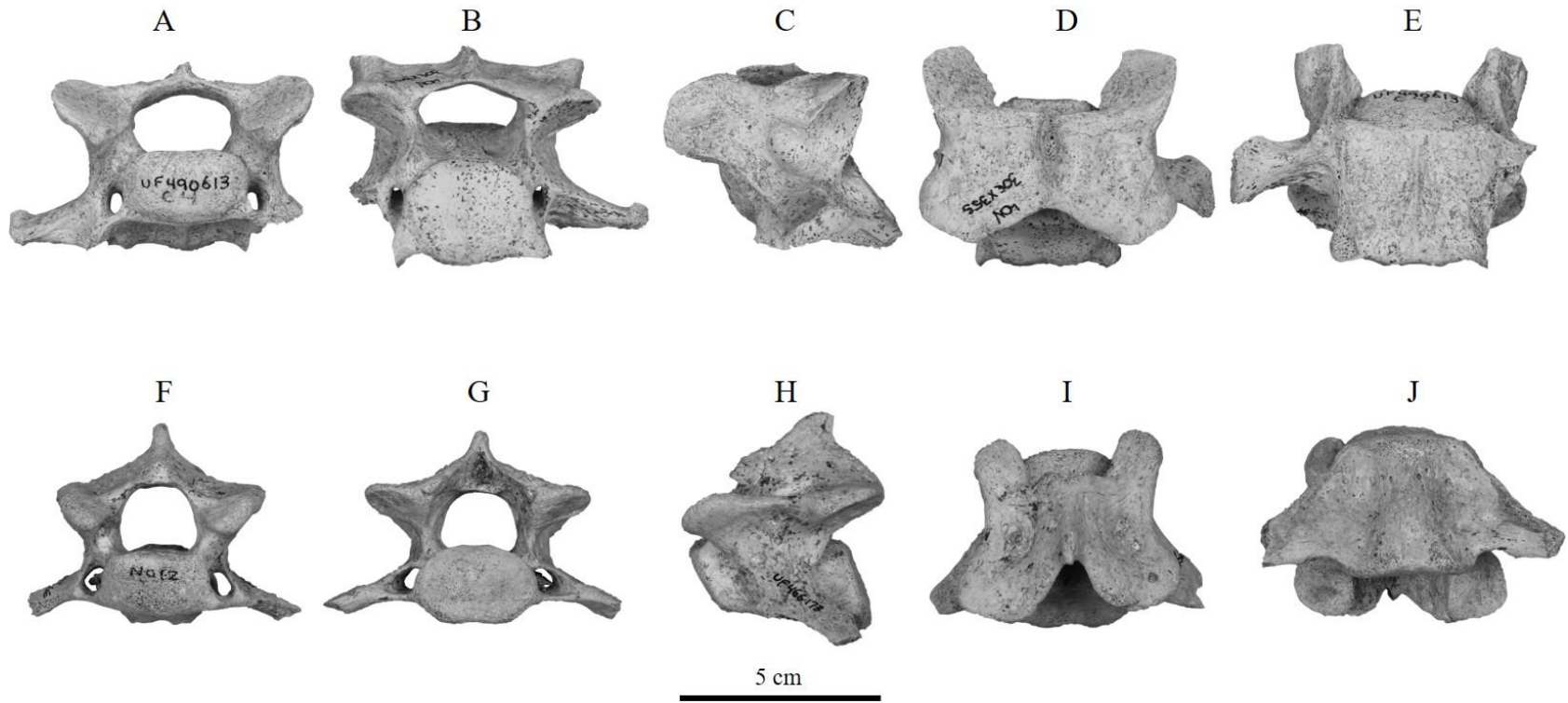


Figure 33. C4 comparison views between both taxa. A-E *Nimravides galiani* UF 490613: anterior (A), posterior (B), lateral (C), dorsal (D), ventral (E) views. F-J *Barbourofelis loveorum* UF 466173: anterior (F), posterior (G), lateral (H), dorsal (I), ventral (J) views.

Remarks—C4 of *N. galiani* and *B. loveorum* are very similar to the other and to their third cervical vertebrae. On the dorsal surface the spinous process is posteriorly placed in *B. loveorum*, whereas it is anteriorly located in *N. galiani*. On either side of the spine, *N. galiani* has parallel sets of ridges and grooves running anteroposteriorly, however *B. loveorum* has two deep depressions instead. On the lateral surface, the transverse process of *N. galiani* projects laterally, whereas in *B. loveorum* it is elongated posterolaterally. Dorsal to the transverse process there is a deep depression on the lateral side in *N. galiani* that is not present in *B. loveorum*. On the ventral surface, the transverse process of *B. loveorum* is connected to the whole lateral side of the centrum's body, unlike in *N. galiani*.

*Cervical Vertebrae 5. N. galiani*: UF 490615

The one specimen for the fifth cervical (C5) of *N. galiani* (Fig. 34) is similar to its C3 and C4. Following the trend of the previous cervical vertebrae, the dorsal lamina surface is more anteroposteriorly compressed. In the center of the lamina, the spine is dorsally elongated, but is broken close to the dorsal surface. The transverse foramina are no longer compressed.

*B. loveorum*: UF 490621

The one specimen for the fifth cervical (C5) of *B. loveorum* (Fig. 34) is similar to its C3 and C4. Following the trend of the previous cervical vertebrae, the dorsal lamina surface is more anteroposteriorly compressed. In the center of the lamina, the spine is dorsally elongated and inclined anteriorly. The transverse process is more laterally elongated than in previous cervical vertebrae.

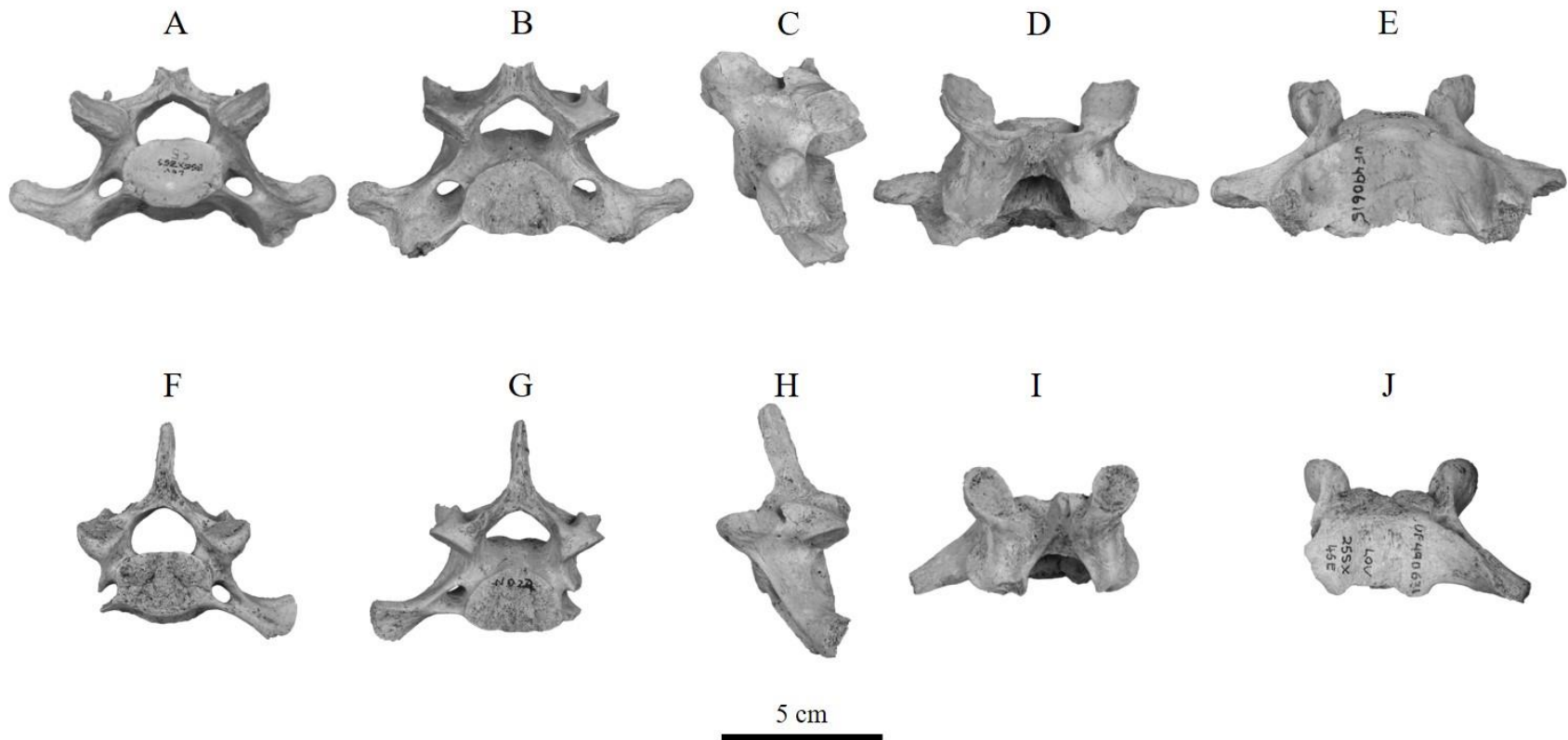


Figure 34. C5 comparison views between both taxa. A-E *Nimravides galiani* UF 490615: anterior (A), posterior (B), lateral (C), dorsal (D), ventral (E) views. F-J *Barbourofelis loveorum* UF 490621: anterior (F), posterior (G), lateral (H), dorsal (I), ventral (J) views.

Remarks—The fifth cervical vertebrae of *Nimravides galiani* and *Barbourofelis loveorum* are similar to each other and to the previously described cervical vertebrae. Overall, *N. galiani* has a larger fifth cervical than *B. loveorum*. The transverse foramina in *N. galiani* are larger than the foramina in *B. loveorum*.

*Cervical Vertebrae 6. N. galiani: UF 490617*

The sixth cervical (C6) of *N. galiani* (Fig. 35) is missing the spinous process, lamina, and posterior zygapophyses. Although similar to the previously described cervical vertebrae, C6 differs in that the anterior and posterior ends of the centrum are smaller in circumference. Additionally, the transverse process is much shorter and projecting dorsolaterally.

*B. loveorum: UF 490622*

The sixth cervical (C6) of *B. loveorum* (Fig. 35) is missing the spinous process and transverse processes. Although similar to the previously described cervical vertebrae, C6 differs in that the zygapophyses are more robust.

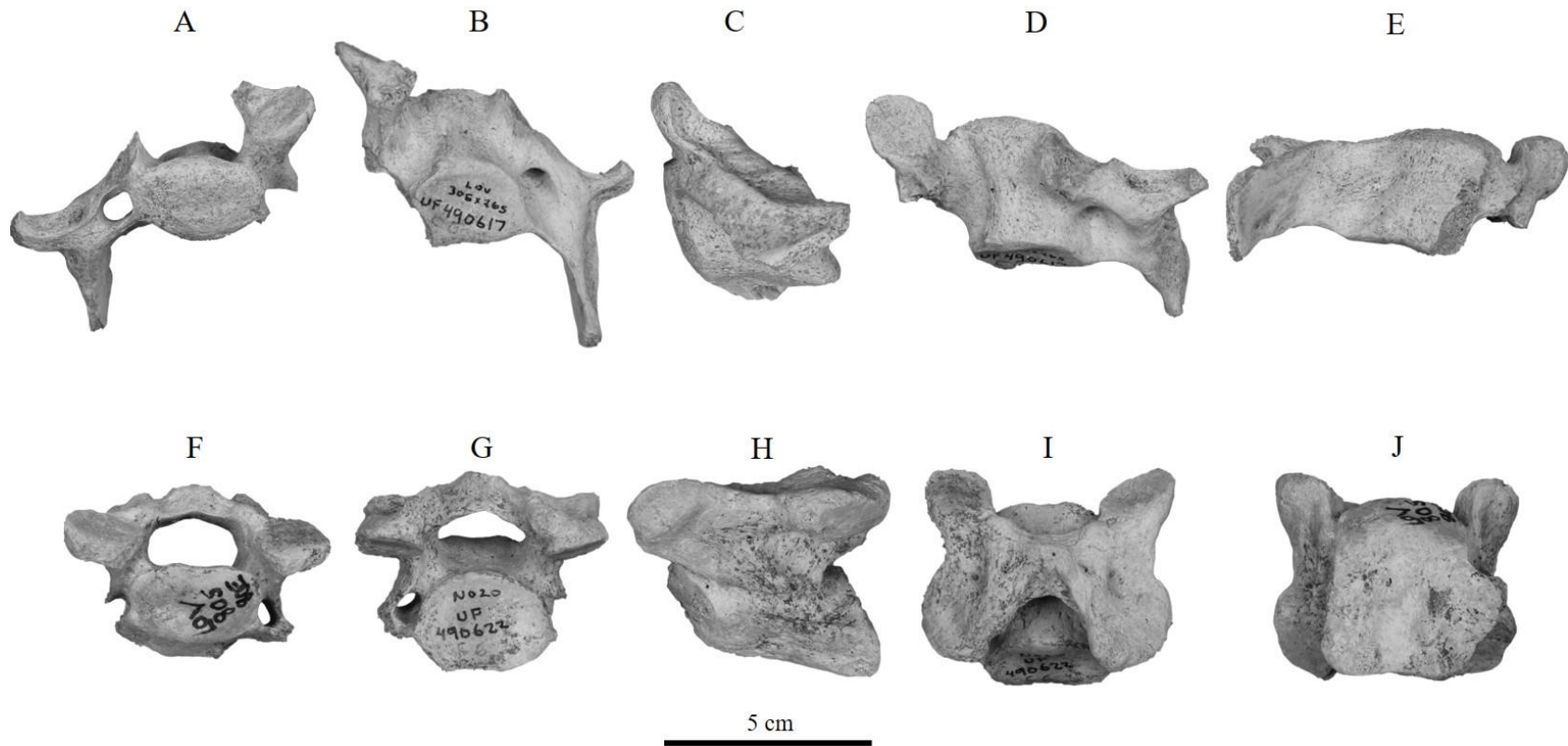


Figure 35. C6 comparison views between both taxa. A-E *Nimravides galiani* UF 490617: anterior (A), posterior (B), lateral (C), dorsal (D), ventral (E) views. F-J *Barbourofelis loveorum* UF 490622: anterior (F), posterior (G), lateral (H), dorsal (I), ventral (J) views.

Remarks—C6 of *N. galiani* and *B. loveorum* are almost no different than their previously described cervical vertebrae. In *N. galiani*, the centrum circumference is smaller than that of *B. loveorum* and previous cervical vertebrae. In *B. loveorum*, the zygapophyses are more robust than in *N. galiani*.

*Cervical Vertebrae 7. N. galiani*: UF 490619

The seventh cervical vertebra (C7) of *N. galiani* (Fig. 36) is missing the spinous process, lamina, posterior zygapophyses. This vertebra is similar to the third to sixth cervical vertebrae. On the dorsal surface, dorsal to the posterior zygapophyses is the presence of a broken anteroposterior ridge, which was more apparent in the fifth cervical.

*B. loveorum*: UF 490623

The seventh cervical vertebra (C7) of *B. loveorum* (Fig. 36) is missing the spinous process. This vertebra is similar to the third to sixth cervical vertebrae. On the dorsal surface, dorsal to the posterior zygapophyses is a sharp anteroposterior ridge, also observed in the fifth cervical. The posterior end of the centrum is larger than that of the other centrum ends.

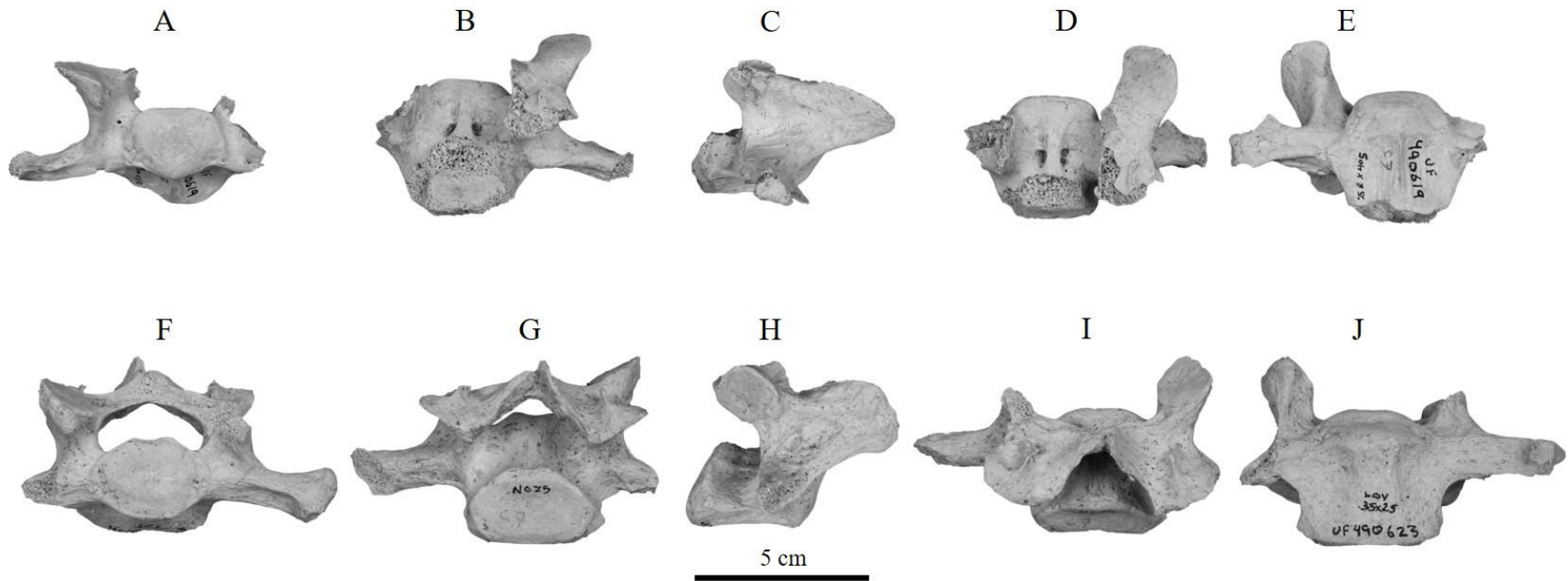


Figure 36. C7 comparison views between both taxa. A-E *Nimravides galiani* UF 490619: anterior (A), posterior (B), lateral (C), dorsal (D), ventral (E) views. F-J *Barbourofelis loveorum* UF 490623: anterior (F), posterior (G), lateral (H), dorsal (I), ventral (J) views.

Remarks—C7 of *N. galiani* and *B. loveorum* are similar to the other and to the previously described cervical vertebrae. Both taxa have a posterior dorsal ridge on the lamina surface, dorsal over both posterior zygapophyses. In *N. galiani*, the anterior zygapophyses has a larger surface area than in *B. loveorum*. The transverse processes in *B. loveorum* are more robust than in *N. galiani*.

*Sacra. N. galiani*: UF 26137; UF 21138; UF 37156; UF 37157

The sacrum of *N. galiani* (Fig. 37) comprises of three fused vertebrae in mature adults. It is triangular in shape, with a wider anterior end that tapers out posteriorly. The sacrum is much more anteroposteriorly elongate than it is wide mediolaterally. Each centrum of the three vertebrae have approximately the same length, antero-posteriorly. In all specimens, the first dorsal spines are broken at their base, whereas the second and third dorsal spines are broken either midway or the dorsal ends are highly worn. On the second and third dorsal spines, the spines are mediolaterally thick and robust. Additionally, the third spine is mediolaterally stretched and is inclined vertically with a bulbous dorsal end. The dorsal foramina are elliptical and small. On the anterior end of the dorsal surface, the anterior zygapophyses are oval shaped and are open, facing dorsomedially. There is no separation between this articular surface and the lateral transverse process of the first sacral vertebra. On the lateral surface, the transverse process of the first vertebra is anteroposteriorly extended slightly past the first vertebra, and ventrally elongated. The fused anterior processes between each vertebra are broken from each specimen.

On the anterior surface, the centrum is oval, mediolaterally, and large. The wings of the transverse process extend laterally and dorsoventrally. Dorsal to the anterior centrum, the neural arch is mediolaterally wide, but smaller in width than the centrum. On the posterior surface, the centrum is mediolaterally oval and smaller than that of the first vertebra centrum. Dorsal to the

posterior centrum, the neural arch is approximately the same width as the centrum. Posterior to the third neural spine, and dorsal to the neural arch, are large and well-developed, elliptical posterior zygapophyses. On the ventral surface, the centrans protrude ventrally and are convex. In between each fused vertebra are small and oval dorsal foramen, with the anterior most set being larger.

*B. loveorum*: UF 25605; UF 466166

The sacrum of *B. loveorum* (Fig. 37) comprises of three to four fused vertebrae in mature adults, of which the anterior most caudal vertebra is fused to the posterior sacral vertebra in the latter. Primary descriptions will be of the three fused vertebrae sacrum. It is triangular in shape, with a wider anterior end that tapers posteriorly. However, the sacrum is compressed anteroposteriorly and is overall as wide mediolaterally as it is long. Each centrum of the three vertebrae are progressively shorter from the first vertebra to the third. When compared between specimens, all three dorsal spines have been preserved. On all three dorsal spines, the spines are mediolaterally thin and fragile. Additionally, spines two and three are anteroposteriorly stretched and inclined posteriorly, with the dorsal ends being a thick, bulbous region. Alternatively, the first spine tapers out, dorsally, and is more vertically inclined. The dorsal foramina are round and small. On the anterior end of the dorsal surface, the anterior zygapophyses are round and slightly closed, facing more medially than dorsally. Lateral to this articular surface is a deep gouge separating the anterior zygapophyses from the lateral transverse process of the first sacral vertebra. On the lateral surface, the transverse process of the first vertebra is very large anteroposteriorly and ventrally when compared to the overall size of the sacrum. This process is anteroposteriorly wider than the first two vertebrae. The fused articular processes between each vertebra are well-developed, more so between the first and second vertebrae.

On the anterior surface, the centrum is oval, mediolaterally, and small. The wings of the transverse process extend laterally and dorsoventrally. Dorsal to the anterior centrum, the neural arch is mediolaterally wide, and near the same width as the centrum. On the posterior surface, the centrum is mediolaterally oval and greatly smaller than that of the first vertebra centrum. Dorsal to the posterior centrum, the neural arch is the same width or larger than the centrum. Posterior to the third neural spine, and dorsal to the neural arch, are highly reduced and elliptical posterior zygapophyses. On the ventral surface, the centroms do not protrude ventrally and are instead flat, less so with the third centrum which has a slight ventral keel. In between each fused vertebra are small and round dorsal foramen, all of which are approximately the same size.

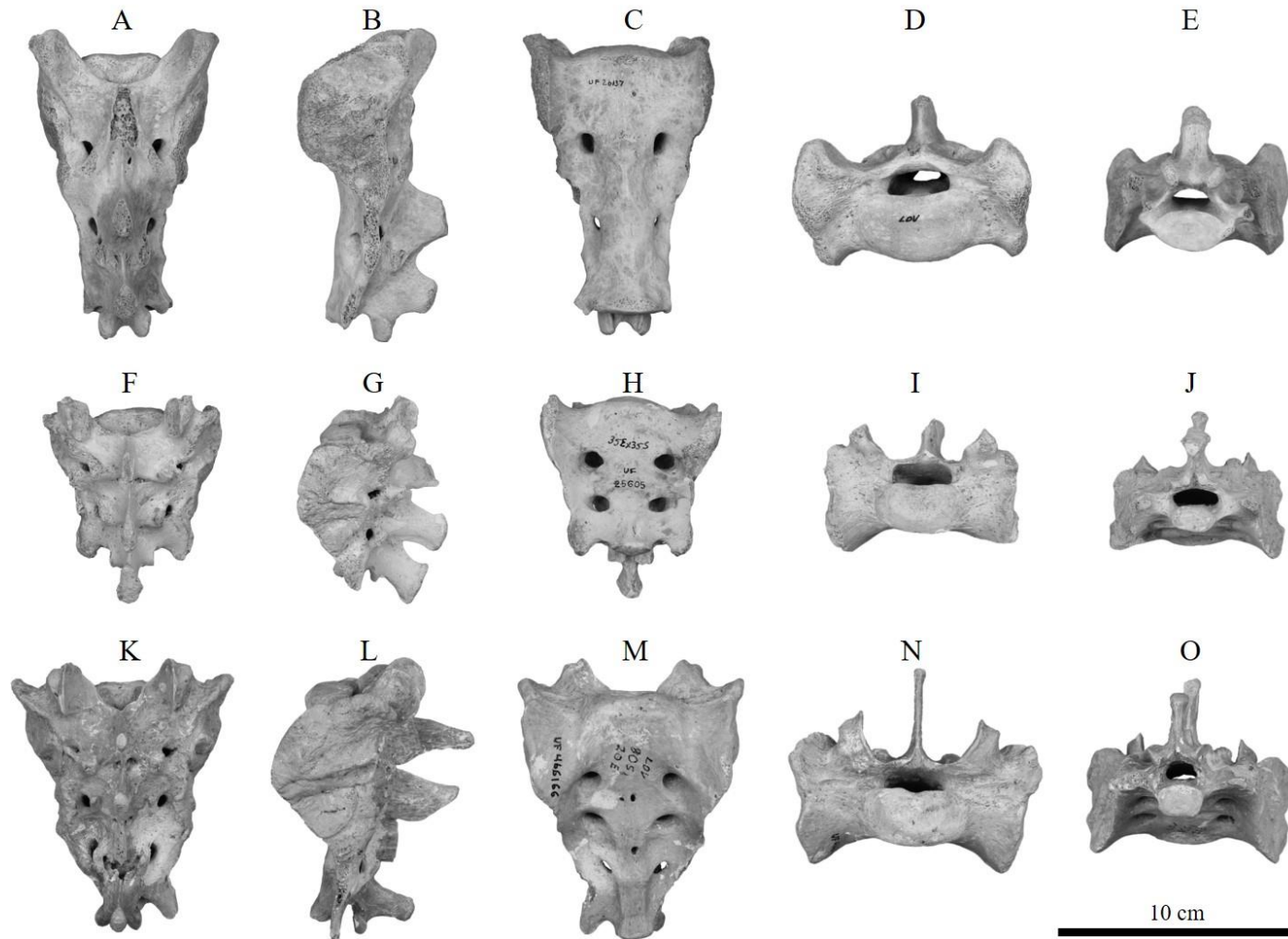


Figure 37. Sacrum comparison views between both taxa. A-E *Nimravides galiani* UF 26137: dorsal (A), lateral (B), ventral (C), posterior (D), anterior (E) views. F-J *Barbourofelis loveorum* with three fused sacral vertebra UF 25605, K-O with four fused sacral vertebra UF 466166: dorsal (F, K), lateral (G, L), ventral (H, M), posterior (I, N), anterior (J, O) views.

Remarks—The sacrum of both *N. galiani* and *B. loveorum* is pyramidal in shape with three fused sacral vertebrae, however *B. loveorum* may have three to four fused vertebrae. The anterior end is mediolaterally wider than the posterior end. In *N. galiani*, the sacrum is anteroposteriorly elongated due to the long centrums of similar size, whereas *B. loveorum* is anteroposteriorly compressed due to the short centrums which decrease in size posteriorly. On the dorsal surface, the remaining dorsal spines of *N. galiani* are mediolaterally thick and robust, yet thin and fragile in *B. loveorum*, and both taxa have bulbous dorsal ends. On the lateral sides of the spines are two sets of dorsal foramina, small and elliptical in *N. galiani* and more elliptical in *B. loveorum*. The anterior zygapophyses on the anterior surface are round and more open in *N. galiani*, facing dorsomedially, but are rounder and more closed in *B. loveorum*, facing more medially. There is a deep gouge separating the anterior zygapophyses and lateral transverse process of the first vertebrae (transverse wing) in *B. loveorum* and not present in *N. galiani*. On the lateral surface, the transverse wing of *B. loveorum* is more than double the anteroposterior width of the sacrum, however the transverse wing is approximately a third of this width in *N. galiani*. The neural canal above the anterior centrum is close in width to the centrum, mediolaterally, in *B. loveorum*, but small in width in *N. galiani*. On the posterior surface, the centrum circumference is smaller than the anterior centrum in both taxa, however it is much more pronounced in *B. loveorum*. The neural canal above the posterior centrum is mediolaterally wider than the centrum in *B. loveorum* and smaller in *N. galiani*. The posterior zygapophyses in *B. loveorum* are much smaller and reduced than in *N. galiani*, of which are larger and well-developed. On the ventral surface, *B. loveorum* has flat centrums that do not protrude ventrally, unlike *N. galiani*, however the third centrum has a slight keel. The ventral foramina are larger and round in *N. galiani*, whereas in *B. loveorum* they are small and round.

## Functional Morphology

### Forelimb

*Scapulae* described for *Nimravides galiani* and *Barbourofelis loveorum* are partial with intact distal ends for articulation with their respective humeri. As such, the scapular ‘fan’ is not available to infer paleoecology. The shape and outline of the scapular fan would be important for inferring functional morphology should it be preserved in other specimens. One of the main differences between these two taxa is the presence of a relatively large coracoid process in *N. galiani* that is highly reduced in *B. loveorum*. This protrusion is the origin for the *m. coracobrachialis*, which aids in stabilizing and weakly extending the glenohumeral joint (Barone 2010; Julik et al. 2012). A more enlarged coracoid process in *N. galiani* than in *B. loveorum* may imply that the *m. coracobrachialis* was much stronger than that of *B. loveorum*, aiding in adduction and forearm pronation (Barone 2010; Salesa et al. 2010), possibly to hold the limbs in tight when running or for wrestling down prey. Distal to the coracoid process is the supraglenoid tubercle, which is well-developed in both taxa, however in *B. loveorum* it is more pronounced. The attachment for the *m. biceps brachii* originates from this tubercle (Barone 2010; Salesa et al. 2010; Julik et al. 2012) and aids in forearm flexion and supination (Barone 2010; Salesa et al. 2010). This relationship may imply that *B. loveorum* was better able to have forearm supination and flexion, whereas *N. galiani* was better able to have forearm adduction and pronation.

*Humeri*. In *N. galiani*, the humerus is similar to that of extant large felids, as described by Carlon (2014), whereas in *B. loveorum* it is more similar to descriptions made by Merriam and Stock (1932) for *Smilodon fatalis*, as both have enlarged pectoral and deltoid ridges, as well as

being short and robust. The pectoral crest is the attachment for the *m. pectorales* (*profundus* and *superficialis*) which aid in forelimb adduction and body support on the forelimbs, retracting a limb back towards the body or bringing the body toward a fixed forelimb (Julik et al. 2012). On the medial surface, the deltoid ridge is the attachment area for the insertion of the *m. deltoideus* and aids in abducting and flexing the glenohumeral joint (Julik et al. 2012). Additionally, *B. loveorum* has a more developed lateral epicondyle than present in extant felids, which serves for the attachment of many extensor muscles for the forelimb and carpals (Julik et al. 2012). The largest of these is the *m. anconeus*, which aids in the extension of the elbow joint (Julik et al. 2012). In *N. galiani* the pectoral ridge, deltoid ridge, and lateral epicondyle are more reduced, possibly indicating reduced forelimb adduction, glenohumeral joint abduction and flexion, and elbow joint extension. On the lateral surface of the proximal epiphysis, attachment for insertion of the *m. infraspinatus* aids in glenohumeral joint stabilization and lateral torsion of the humerus (Julik et al. 2012), and is more prominent in *B. loveorum*. On the medial surface of the lesser tubercle, the subscapular groove serves for the insertion area for the *m. subscapularis* and aids in glenohumeral stabilization and adduction, and possibly flexion and/or extension of this joint (Julik et al 2012). In *N. galiani*, the subscapular groove has worn away. Between the lesser and greater tubercles lies the intertubercular groove, where the *m. biceps brachii* tendon travels through (Taylor 1974; Julik et al. 2012; Salesa et al. 2020), stabilizing the elbow joint when standing (Julik et al. 2012). A larger groove, as present in *B. loveorum*, may indicate a larger tendon and stronger muscle use (Taylor 1974). In viverrids, an enlarged groove was indicative of more arboreal locomotion, rather than terrestrial since this would create stronger extensor and flexor forearm muscles (Taylor 1974). As such, a larger *m. biceps brachii* in *B. loveorum* may have been beneficial for prey grappling, ambush predation, and possibly climbing. The humeral

head is rounded in both taxa; however, this is less pronounced in *N. galiani*, a common feature in more terrestrial carnivorans (Salesa et al. 2017). In *B. loveorum* the greater tubercle is highly pronounced, increasing the attachment area for the *m. supraspinatus* (Julik et al. 2012) and aiding in humeral extension and lateral rotation (Taylor 1974; Barone 2010). Since the greater tubercle is proximally expanded in *B. loveorum*, the moment arm of *m. supraspinatus* is lengthened and may produce less energy use during locomotion (Jolly 1967).

On the distal epiphysis, the medial epicondyle has many facets for the flexor and pronator muscles of the forearm and carpals (Taylor 1974; Salesa et al. 2008; Barone 2010; Julik et al. 2012). A higher degree of medial projection of the medial epicondyle is indicative of more robust limbs used for noncursor locomotion and ambush prey-capture hunting behavior for large prey within a closed habitat (Argot 2001; Argot 2004; Salesa et al. 2008). Additionally, this medial projection is indicative of increased supination and pronation abilities in the forearm, typical in closed habitat species (Taylor 1974; Samuels et al. 2013; Salesa et al. 2020). An enlarged medial projection of the medial epicondyle is more prominent in *B. loveorum*, of which there are deep grooves on the anterior face that would increase muscle area attachment. As such, *B. loveorum* may have displayed less cursor abilities and would have relied more on ambush predator style, whereas the less pronounced medial epicondyle in *N. galiani* may imply this taxon was more capable of cursor locomotion, possibly in a more open habitat. It should be noted that the medial epicondyle in *N. galiani* is medially projected at nearly the same length as *B. loveorum*, however there is a distinct lack of muscle scars. The lack of muscle scars on the medial epicondyle suggests that *N. galiani* was not a cursorial felid like *A. jubatus*, but instead may simply have been better adapted to running than *B. loveorum*. An enlarged medial epicondyle has previously been linked to large prey capture in felids (Meachen-Samuels and Van

Valkenburgh 2009), suggesting both taxa hunted relatively large prey to their body size. The shape of the olecranon fossa has been used to infer running ability in felids (Gonyea 1978), of which a narrow opening is indicative of more cursor ability due to the potential decrease in mediolateral movement of the elbow joint during locomotion (Gonyea 1978; Salesa et al. 2017). The presence of a thinner olecranon fossa in *N. galiani* (relative to *B. loveorum*) further supports terrestrial locomotion within this species, whereas the wide olecranon fossa present in *B. loveorum* implies less pendulum-like motion typically seen in cursor carnivorans (Gonyea 1978).

*Radii.* The radius of *B. loveorum* is very similar to that of *S. fatalis*, as depicted by Merriam and Stock (1932), with both being short and robust, whereas the long and slender radius of *N. galiani* is more similar to extant large felids. Slender long limbs may reduce energy use in terrestrial locomotion due to the increased stride length, allowing for long-distance traveling (Hildebrand 1985, Carrano 1996; Martin-Serra et al. 2014a). A more robust radius is indicative of less cursor locomotor ability and a stronger forelimb (Salesa et al. 2011), features that are present in *B. loveorum*. Both taxa have relatively round distal articular surfaces for the scapholunar, indicating high degrees of pronation and supination of the wrist, similar to extant felids, in order to grapple and subdue prey and/or climb up trees (Salesa et al. 2011). In *B. loveorum*, the styloid process is more enlarged than in *N. galiani*, possibly reducing mediolateral wrist mobility (Martin-Serra et al. 2014a). On the posterior surface, the bicipital tuberosity in *N. galiani* is large and well-developed, similar to extant pantherins, whereas it is much smaller and less-developed in *B. loveorum*. Insertion of the *m. biceps brachii* tendon occurs into the bicipital tuberosity, having originated from the scapula, and assists with extending the glenohumeral joint as well as flexing and stabilizing the elbow joint (Fisher et al. 2009; Julik et al. 2012). This may imply *B. loveorum* has less glenohumeral joint extension and elbow joint flexion than in *N.*

*galiani* and extant pantherins, reducing elbow joint stabilization when standing. A reduced *m. biceps brachii* has generally been observed in terrestrial and cursorial species by Taylor (1974), and is one of the main elbow joint flexors among felids (Barone 2010), which would indicate *B. loveorum* had high terrestrial capabilities. However, *B. loveorum* has an enlarged knob lateral to the bicipital tuberosity, previously described by Baskin (1980) as the attachment area for the lateral collateral ligament, that is not present in *N. galiani*. This ligament forms the *m. supinator*, along with the anular ligament, and is the primary muscle that supinates the forearm (Fisher et al. 2009; Julik et al. 2012). This implies *B. loveorum* had better supination potential than *N. galiani*. However, the insertion of the *m. brachioradialis* on the distomedial protrusion of the styloid process also helps in forearm supination (Julik et al. 2012), and the attachment site is larger in *N. galiani* which would also imply relatively good forearm supination.

*Ulnae*. There are many differences in the ulna between *B. loveorum* and *N. galiani*. The ulna of *B. loveorum* is very similar to *S. fatalis*, as depicted by Merriam and Stock (1932), with both being strikingly different from most felids due to the short and highly robust features. In *N. galiani*, the ulna is similar to that of felids due to the long and slender shaft and gentle curvature. The radial notch in *B. loveorum* is more laterally oriented, whereas in *N. galiani* it is more anteriorly oriented. An anterior orientation would restrict supination and increase pronation of the forearm of the elbow joint, as compared with a lateral orientation which would indicate a high degree of supination-pronation (Gonyea 1978a). With this in mind, pronation may have been more limited for *N. galiani*. On the olecranon process, the lateral and medial tuberosities serve as the attachment for the *m. triceps brachii* (Fisher et al. 2009; Julik et al. 2012), with forest felids generally having larger lateral tuberosities, allowing for a higher degree of distal limb deviation from the parasagittal plane (Gonyea 1978a). These tubercles serve for the

attachment of two main muscles from *m. triceps brachii*: *m. anconeus* attaches to the lateral tuberosity and *m. caput mediale* attaches to the medial tuberosity (Gonyea 1978a; Julik et al. 2012). In *B. loveorum*, the lateral tuberosity is primarily dominant and overtakes the highly reduced medial tuberosity, and is indicative that *B. loveorum* was similar to forest felids. In *N. galiani*, the medial tuberosity is more enlarged, a rare feature in extant felids (Salesa et al. 2010), and there is a clear separation between it and the lateral tuberosity. This may suggest *N. galiani* preferred more open habitats as taxa with greater running capabilities display this morphology (Gonyea 1978a). Extant felids displaying this morphology generally have reduced distal limb deviation from the parasagittal plane (Gonyea 1978a) during locomotion. A larger medial tuberosity is also present in *A. jubatus* which assists in cursor locomotion as it would restrict deviation from the parasagittal plane (Salesa et al. 2010).

On the medial surface of *B. loveorum* there is a highly pronounced ridge, of which is reduced to a distal knob in *N. galiani*. This ridge increases the surface area attachment for the *m. pronator quadratus* and aids in forearm and wrist pronation (Salesa et al. 2008; Julik et al. 2012), indicating *B. loveorum* had more pronation control than *N. galiani*. On the lateral surface of the diaphysis, *N. galiani* has an extended scar for the *m. digiti I longus*, similar to other felids, which would increase extension and abduction in digit I (Barone 2000; Salesa et al. 2011). However, this facet is highly reduced in *B. loveorum*. As such, *B. loveorum* may have relied more on forearm and wrist pronation to assist in hunting and climbing capabilities and less so on the abduction of digit I. Whereas *N. galiani* may have relied more on digit I abduction due to a decrease in pronation capability. Lateral to the trochlear notch is a well-excavated groove for the origin of the *m. extensor digiti I et II* (Barone 2000; Julik et al. 2012) in *B. loveorum* and a lesser developed groove in *N. galiani*, probably indicating extensor muscles acting on digits I and II in

*B. loveorum*, and less so in *N. galiani*. However, this marked groove may be a primitive condition within Felidae as it is present in felids that exhibit different locomotor behaviors (Salesa et al. 2017).

*Carpals.* Scapholunar articulation with the radius allows palmar flexion and medial abduction in most felids (Meachen-Samuels and Van Valkenburgh 2009). In *N. galiani*, the scapholunar articular surface with the radius allows for abduction-extension (wrist extension during abduction, drawing the palms towards one another medially), however regular extension is impacted by the proximally projected ridge on the anterior border of this surface. Similarly, *B. loveorum* has nearly the same articular surface, however with greater potential abduction-extension and a highly limited regular extension. The styloid process of the radius in *B. loveorum* has two articular surfaces, one angled proximally and the other anteriorly, indicating the radius was able to rock-back posteriorly on the scapholunar, allowing *B. loveorum* more flexion of the wrist than is present in *N. galiani*. Since *B. loveorum* would be unable to extend the wrist back dorsally, this may imply a digitigrade forelimb stance to some degree. The posterior tubercle in *B. loveorum* is more similar to *S. fatalis* than to pantherines, due to its proximal orientation (Salesa et al. 2010). The articulating surfaces on the distal end of the scapholunar in *B. loveorum* are very different from other felids and *N. galiani*. The articulation for the unciform is distally oriented, indicating that MC IV and V may be closer together, whereas in *N. galiani*, this articular surface is laterally oriented, indicating the metacarpals may be more spread apart.

On the pisiform, the posterior tubercle is elliptical, compressed proximodistally, in both taxa. This is a basal morphological feature present in less cursorial felids, including *S. fatalis*, *Panthera tigris*, *P. onca*, *P. concolor*, and *P. pardus*, whereas the cursorial felids, such as *A. jubatus*, *P. leo*, and *P. atrox* have round tubercles (Salesa et al. 2010). The pisiformis of *B.*

*loveorum* and *N. galiani* are of similar length, much alike the other carpals, and slightly shorter than extant pantherines. However, the pisiform in *N. galiani* is very robust, unlike pantherines and more similar to *S. fatalis* and other saber-toothed felids, where more strength is needed for non-cursorial prey capture (Merriam and Stock 1932; Salesa et al. 2010). The ulnar articular surface on the lateral side of the pisiform is slightly concave in *N. galiani*, implying more movement among this articulation could occur, whereas in *B. loveorum* this facet is highly concave which may have locked the ulnar styloid in place, limiting movement.

The unciform of *B. loveorum* is more similar to *S. fatalis*, whereas in *N. galiani* it is more similar to larger felids (Merriam and Stock 1932). On the lateral side, the articulation for the cuneiform in *B. loveorum* has a lateral protruding ridge, limiting the anterior movement of the cuneiform and pisiform more so than in *N. galiani*. Although similar to *S. fatalis*, the palmar tuberosity in *B. loveorum* is enlarged, providing more surface area for attachment of the *m. flexor carpi ulnaris*, implying *B. loveorum* had good flexion and abduction of the wrist (Fisher et al. 2009; Julik et al. 2012).

The magnum of both *B. loveorum* and *N. galiani* are highly similar to one another and to felids. As such, there does not appear to be any significant behavioral differences originating from the magnum between these two taxa. Similarly, the trapezoid has little variation among felids (Salesa et al. 2008). Only the trapezoid of *N. galiani* was used in this study as the trapezoid for *B. loveorum* was unavailable. The scapholunar articular surface on the proximal face of the trapezoid sits more dorsal on the scapholunar than that of the magnum. As such, MC II would sit dorsally higher than MC III, allowing for more cursorial capabilities (Salesa et al. 2010). *N. galiani* is more similar to *P. atrox* than *S. fatalis* when compared to Merriam and Stock (1932) diagrams.

*Metacarpals.* The robustness of MC I in *N. galiani* is similar to that of other sabertooth felids and is not present in extant felids, of whom have a mediolaterally thinner and proximodistally elongated MCI (Merriam and Stock 1932; Salesa et al. 2010). These differences greatly increase the abduction and flexion of the dewclaw, as well as having more powerful forelimbs to subdue prey (Salesa et al. 2010). Lateral movement of the proximal phalanx for MC I is restricted by the pronounced keel on the distal end of the palmar surface (Salesa et al. 2012). The slender MC I in *B. loveorum* is similar to extant felids; however, the shaft is more constricted, and the dorsal surface is flatter. A long and slender MC1 may be a basal state for feliforms as it is present in *Pseudaelurus* sp. (Rothwell 2001). Additionally, the medial side of the shaft is greatly concave. In MC II, the pronounced ridge on the dorsoproximal surface is a round scar for the *m. extensor carpi radialis longus*, which extends the carpals and flexes the elbow (Salesa et al. 2011; Julik et al. 2012). This feature is present in *N. galiani*, along with the groove for the radial artery, whereas both are absent in *B. loveorum*. In *N. galiani* this may have supported greater forces that were applied to the carpal and elbow joints when immobilizing prey (Salesa et al. 2011). On the proximodistal surface of MC III, the attachment for the *m. extensor carpi radialis brevis* is present in *N. galiani*, however the scar is smaller than that in other felids, and is not seen in *B. loveorum*. A larger muscle scar indicates higher mobility in carpal to manus extension and abduction, indicating *N. galiani* had more wrist control than *B. loveorum*. The facet between MC III and IV is large and well-defined in *N. galiani*, yet even larger in *B. loveorum*. This suggests *B. loveorum* had a more stable and controlled articulation, similar to terrestrial viverrids and most felids (Salesa et al. 2017). On MC V, the facet for *m. extensor carpi ulnaris*, on the lateral side of the proximal head, is actually a flexor of the carpals and assists

with forearm rotation (Salesa et al. 2017). In *B. loveorum*, this facet is more distally elongated than in *N. galiani*, suggesting a larger range of wrist flexion.

### *Hindlimb*

*Innominate*. Although the pelvic remains described from *N. galiani* and *B. loveorum* are partial elements, there are some differences between the two taxa. The pelvis is composed of two innominates (left and right), which are each composed of three bones: ilium, ischium, and pubis. (Reighard 1901). In *N. galiani*, most of the pelvis is preserved, with the pubis-ischium symphysis and the crest of the ilium having been worn away. In *B. loveorum*, the preservation is less than that of *N. galiani*, including only the acetabulum with the pubis and ischium projections in one specimen, and the ilium wing in another specimen. During locomotion, the pelvis is primarily used for hindlimb muscle origin, allowing for the movement of the hindlimbs to and from the body (Fisher 2009; Martin-Serra et al 2014c). On the lateral side of the iliac wing of *B. loveorum*, the surface area origin for the *m. gluteus medius* and *m. gluteus profundus* (Fisher et al. 2008) are not excavated out, as is present in *N. galiani*, *S. fatalis* (Merriam and Stock 1932), and extant felids. These two muscles aid in hip joint extension and abduction (Fisher et al. 2008), and may imply that *B. loveorum* had less hip joint control than that of *N. galiani*. However, the iliac wing is much more robust in *B. loveorum*, with the ventral surface being nearly three times the width as that in *N. galiani*, increasing the surface area for muscle attachment. This ventral surface is the origin area for *m. rectus femoris* (which continues onto the lateral surface, anterior to the acetabulum) and *m. tensor fasciae latae* (anterior to *m. rectus femoris*) (Fisher et al. 2008). *M. rectus femoris* aids in hip joint flexion and knee joint extension, whereas *m. tensor fasciae latae* weakly assists with hip joint abduction (Fisher et al. 2008). As such, the increased

robustness on the wing for these muscles may imply *B. loveorum* had better flexion of the hip joint and extension of the knee joint than that of *N. galiani*. Posterior to the acetabulum is a deep groove for the passage of the ligamentum teres, which would connect the head of the femur into the acetabulum (Reighard and Jennings 1901). In *B. loveorum* this groove is slightly wider than in *N. galiani*, implying a presence for a thicker ligament. Additionally, the acetabulum in *B. loveorum* is much larger than in *N. galiani*, and the opening is more open, suggesting more movement around the hip joint, whereas in *N. galiani* the acetabulum is more closed and better able to control hip joint rotation.

*Femora.* In *B. loveorum*, the femur is similar in shape and robustness to *S. fatalis*, however the shaft is more anteriorly bowed (Baskin 1980). The femur of *N. galiani* is slender, straight, and elongate, similar to *P. atrox* (Merriam and Stock 1932) and other large felids. A study by Carlon (2014) noted some major differences among felids that suggest either cursorial or ambush behaviors, including the height of the greater trochanter to that of the femoral head. A higher femoral head, such as in *B. loveorum*, suggests ambush behavior, whereas a lower femoral head, as seen in *N. galiani*, suggests a more cursorial behavior (Carlon 2014; Ercoli and Youlatos 2016; Salesa et al. 2020). Similarly, if the lesser trochanter is closer to the hip joint (proximally closer to the femoral head), the taxon is likely cursorial, whereas a relatively distal lesser trochanter implies ambush behavior. In *N. galiani*, the lesser trochanter is proximally closer to the femoral head than in *B. loveorum*, suggesting a higher capability for cursor locomotion, whereas *B. loveorum* would have higher capability for ambush behavior.

The greater trochanter is the insertion point for the *mm. gluteus superficialis*, *gluteus medius*, and *gluteus profundus*, all of which assists it hip joint abduction and extension (Fisher et al. 2008). In *B. loveorum*, the greater trochanter is greatly enlarged for these muscles, suggesting

an increase in muscle use, whereas in *N. galiani*, although worn, has a smaller greater trochanter. Such a configuration suggests that *B. loveorum* had more muscular control of hip joint abduction and extension than that of *N. galiani*. The lesser trochanter is slightly reduced in *N. galiani*, whereas it is greatly developed in *B. loveorum*, and is the insertion area for the *m. iliopsoas*, which assists in flexing the hip joint (Fisher et al. 2008). As such, *B. loveorum* may have had better flexion capability of the hip joint than *N. galiani*, with the latter resembling that of most felids. Additionally, the *m. quadratus femoris* insertion is greatly enlarged in *B. loveorum*, aiding in hip joint extension and lateral rotation (Fisher et al. 2008). The lateral ridge, *linea aspera*, on *B. loveorum*, which is not as developed in felids, serves as the origin for the *m. vastus lateralis*, which assists the *m. quadriceps femoris* in knee joint extension (Fisher et al. 2008), implying *B. loveorum* may have had more of a mechanical advantage on the knee joint than in *N. galiani* in extending the knee.

On the distal end, the trochlea is worn in *N. galiani*, however the boundaries are still apparent. Proximodistal height of the trochlea is long, similar to that of extant felids, and is less square shaped. However, in *B. loveorum* the trochlea is proximodistally short and square shaped, a condition observed in arboreal mustelids (Ercoli and Youlatos 2016), yet the trochlea is as deeply grooved as in felids. An elongated trochlea suggests a greater range of patella excursion for cursor locomotion (Argot 2003; Salesa et al. 2017). The robust femur of *B. loveorum* has been similarly compared with *Patriofelis* (an extinct creodont), the ursids *Ailuropoda melanoleuca* and *Ursus spelaeus*, *Hoplophoneus*, and *Smilodon* by Martin-Serra et al. (2014b), where they suggested robust limbs help resist axial and bending stresses, either through fossorial activity or weight bearing for hunting. Additionally, Martin-Serra et al. (2015) found that robust fore and hindlimbs are mostly associated with saber-toothed predators, whereas

longer and more slender postcranial limbs are more commonly found in non-saber-toothed felids. As such, the femur of *B. loveorum* is more similar to saber-toothed felids, and that of the machairodont *N. galiani* would be morphologically closer to the conical-toothed cats, such as the extant large felids.

*Tibiae.* In *B. loveorum*, the tibia is greatly compressed, proximodistally, and is much shorter than the femur. Many morphological features are similar to *S. fatalis*, as depicted by Merriam and Stock (1932), such as the large and elongated tibial crest relative to tibial size, large fibular articular surfaces, flat distal diaphysis on the posterior surface, and a narrow gap between the femur facets. In felids these features are typically opposite, as the tibial crest is less elongated down the diaphysis, the fibular facets are smaller, the posterior surface of the distal diaphysis is convex, and the gap separating the femur facets is wide (Merriam and Stock 1932); characters displayed by *N. galiani*. Articular condyles for the femur in *B. loveorum* face more dorsal than that of *N. galiani* and other felids, suggesting the tibia is situated more vertically towards the ground; a feature that has been suggested to support a sub-plantigrade stance (Anyonge 1993; Anyonge 1996; Panciroli et al. 2017; Polly 2020). Similarly, the vertical positioning may increase the length of the hindlimb stance since the length of the metatarsals are greatly shortened. Mediolateral movement is restricted in *B. loveorum* by the dorsally raised intercondylar gap and the concave medial and lateral condyles. Additionally, an enlarged ridge distal to the medial condyle, on the medial surface, suggests a large attachment area for the medial collateral ligament. This ligament resists lateral movement of the tibia from the knee joint (Fisher et al. 2008). In *N. galiani*, the position and shape of the proximal condyles are similar to most felids, suggesting the knee is more bent and the tibia is less vertical to the ground. Enlarged fibular facets relative to tibial size have been observed by Davis (1964) in ursids, a condition

present in *B. loveorum*. The large fibular facets may suggest *B. loveorum* was distributing its body weight and stance on the fibula more than that of *N. galiani*, further suggesting that *B. loveorum* was less cursorial, as a more modified fibula (either a very thin fibula or a fused fibula to the tibia) suggests more of a cursor locomotion (Walmsley 1918; Carleton 1941). As such, the tibia of *B. loveorum* exhibits more basal carnivoran traits than that of *N. galiani*, which appears to exhibit characteristics typically associated with taxa adapted for running.

*Fibulae.* There are few studies on fibula morphology, and even less so on the behavioral inferences based on its morphology. This may suggest that the fibula is not a good indicator for paleoecological deductions among felids. The proximal epiphysis of *N. galiani* is similar to extant felids; however, the two facets for the tibia are reduced relative to its size. Muscle attachment facets do not greatly differ in relative size and shape than that of large extant felids. The proximal epiphysis leads to a slender shaft. The distal epiphysis of *N. galiani* comes from a continuation of a slender diaphysis, whereas in *B. loveorum* the diaphysis is slightly more robust. Additionally, the distal end in *B. loveorum* is more robust than that of *N. galiani*, and similar to *S. fatalis*, as depicted by Merriam and Stock (1932). The thicker shaft may suggest that more weight is placed on the fibula in *B. loveorum*. On the medial surface, the facet for the astragalus is larger and convex in *B. loveorum*, but flat in *N. galiani*, possibly indicating more ankle mobility in *B. loveorum*.

*Tarsals.* Astragular articulation with the tibia allows for anteroposterior rotation during locomotion and is the primary region where ankle flexion and extension occurs (Carrano 1996; Panciroli et al. 2017). In *B. loveorum*, the astragalus suggests a more plantigrade stance. Articulation with the calcaneus is loose in *B. loveorum*, allowing for an increase in rocking and sliding between the astragalus and calcaneus, as described by Baskin (1980), and the dorsal

condyles for tibial articulation are asymmetrical with a shallow groove, a feature described for sub plantigrade mammals by Carrano (1996) that permits mediolateral joint movement. Digitigrade mammals, however, lack this mediolateral excursion and the dorsal groove is much deeper (Carrano 1996), as seen in *N. galiani*. Additionally, a tightly locked astragalus articulation with the calcaneus is an indicator for either cursorial or terrestrial locomotion, and a looser joint often suggests a more scansorial locomotion (Panciroli et al. 2017). As such, the astragalus may indicate *N. galiani* was more terrestrial than *B. loveorum*. Tibioastragali flexion is more pronounced in *N. galiani*, and reduced in *B. loveorum*. As the astragalus fully rotates plantarly, the astragalar head is more able to plantarflex in *N. galiani*, as there is no ridge on the proximal surface of the astragalus that would prohibit further flexion, whereas in *B. loveorum* a ridge is present on the proximal surface. This difference may suggest *N. galiani* was more digitigrade than *B. loveorum*. Additionally, the astragalar head is mediolaterally parallel to the dorsal condyles in plantigrade mammals, whereas in digitigrade forms the head mediolateral axis is perpendicular (Carrano 1996), features exhibited by *B. loveorum* and *N. galiani*, respectively. Overall, the astragalar morphology in *B. loveorum* is similar to that described by Merriam and Stock (1932) for *S. fatalis* due to their relatively small size, shallow grooved trochlea, and short neck compared to other felids, whereas *N. galiani* closely resembles terrestrial pantherines, such as *P. atrox* described by Merriam and Stock (1932), by having a long neck, albeit thinner, and a deeply grooved trochlea.

The calcaneus of *B. loveorum* resembles that described for *S. fatalis* by Merriam and Stock (1932) and for *Homotherium* by Madurell-Malapeira et al. (2014), because of its proximodistally short length, with a short neck. Additionally, the astragalus facets are close to the distal end, and the sustentacular facets are combined into a singular concave facet, unlike in

*N. galiani* and large felids, where the sustentacular facets remain separated. This squat morphology in *Homotherium* was interpreted as bear-like by Madurell-Malapeira et al. (2014), and as a strong indication for being semiplantigrade. In contrast, the calcaneum of *N. galiani* is more similar to pantherines, such as that described for *P. atrox* by Merriam and Stock (1932), albeit smaller in size; where the neck is relatively long and the astragular facets are further away from the distal end. This morphology has been described in *Machairodus aphanistus* by Madurell-Malapeira et al. (2014) and indicates a digitigrade stance. A relatively shorter calcaneal neck, as seen in *B. loveorum*, has been interpreted by Carrano (1996) for sub plantigrade mammals to acquire faster speed of the metatarsals since less muscular force is available. In other words, calcaneal length acts as an *in-lever* for locomotion, whereas the metatarsals act as the *out-lever*, so a shorter neck would greatly allow rapid motion of the metatarsals (Carrano 1996; Polly 2010). A longer calcaneal heel, as seen in *N. galiani*, implies that more muscular force was applied to each foot stroke (Carrano 1996; Polly 2010).

In *N. galiani*, the proximal end of the calcaneus, known as the tuber calcanei, has a deep groove with an elongated medial surface, and is a distal attachment area for multiple muscles associated with plantarflexing the ankle joint: *m. biceps femoris*, *m. abductor cruris caudalis*, *m. gastrocnemius*, *m. soleus*, and *m. flexor digitorum superficialis* (Fisher et al. 2008). These muscles imply *N. galiani* had good plantarflexion control of the ankle joint; a digitigrade character since digitigrade mammals have a near constant hindfoot plantarflexion (Carrano 1996). In *B. loveorum*, the tuber calcanei is nearly flat with almost no noticeable groove for these muscles; implying that *B. loveorum* had weaker muscles associated with plantarflexion, and as a result may have had a plantigrade stance. On the lateral surface of the calcaneus in *N. galiani* is a wide and deep groove for the origin of the *m. quadratus plantae* (Fisher et al. 2008; Salesa et al.

2011). This muscle joins with the *mm. flexor digitorum lateralis* and *medialis* and assists with metatarsophalangeal flexion, as well as flexing the phalangeal joints for each digit (Fisher et al. 2008). In *B. loveorum* there is no observable groove present. This may suggest *B. loveorum* had less metatarsophalangeal and phalangeal joint flexion control, whereas *N. galiani* may have had better flexion control of these joints. However, in most extant felids, the *m. quadratus plantae* groove is reduced (Vollmerhaus and Roos 2001). Yet, in early felids and machairodonts the *m. quadratus plantae* groove is well developed, taking up the majority of the lateral surface of the calcaneus (Salesa et al. 2012). A large groove is related to climbing ability and an increase in lateral movement (Salesa et al. 2012). The presence of a deep groove in *N. galiani* may be a retained basal character that aids in flexion, but still suggests cursor adaptability.

The cuboid for both *B. loveorum* and *N. galiani* has few differences. On the plantar surface, the tuberosity for the peroneal groove is more distally placed in *N. galiani*, and projects further outward, similar to that described for *S. fatalis* by Merriam and Stock (1932). Passing through the peroneal groove is the tendon of *m. peroneus longus* (Merriam and Stock 1932, Fisher et al. 2008, Salesa et al. 2008), which assists in pes eversion (turning the pes outward, laterally) (Fisher et al. 2008). Although the peroneal groove tuberosity is more developed in *N. galiani*, the passageway for the tendon is smaller and more constricted than that of *B. loveorum*, possibly implying *B. loveorum* had a larger *m. peroneus longus* and a better capability to evert the pes. In *N. galiani*, the facets for MT IV and V are separated by a sharp ridge, with the facet for MT V facing laterally away from the MT IV facet. This may imply MT V was slightly distally spread apart from MT IV, similar to extant felids. In *B. loveorum* the facet for MT V has worn away, however Baskin (1980) described the surface as very small. Yet, the facet on MC V for the cuboid in *B. loveorum* faces more proximally than that of *N. galiani*, suggesting MC V

was farther spread from MC IV than in *N. galiani*. An increase in metatarsal spread further suggests a sub plantigrade stance in *B. loveorum*.

The navicular of *N. galiani* has some key differences from that of *B. loveorum*. On the distal surface, the ridge separating the articular surfaces for the ectocuneiform and mesocuneiform is less pronounced in *N. galiani* than in *B. loveorum*. Additionally, these surfaces are nearly facing the same direction in *N. galiani*, whereas in *B. loveorum* they are facing away from each other, with the ectocuneiform facet facing distolaterally and the mesocuneiform facet facing distomedially. In *B. loveorum* this configuration may indicate that the ectocuneiform and mesocuneiform would be pointed outwards laterally and medially, respectively, suggesting that MT II and III are spread apart from one another. An increase of metatarsal surface area would indicate a more plantigrade foot posture than what is seen in most felids (Carrano 1997). In *N. galiani*, these facets are not diverging, implying MT II and III are not mediolaterally spread apart. The endocuneiform facet is separated by grooves in *B. loveorum*, unlike that of *N. galiani* and other felids. This facet is larger than the mesocuneiform facet, and elongated plantomedially-dorsolaterally. As such, this may indicate that the endocuneiform was large and offered additional plantar support. On the proximal surface, the facet for the astragular head is more concave in *B. loveorum*, possibly allowing for an increase in astragalus-navicular rotation, whereas in *N. galiani* such rotation would be restricted.

The ectocuneiform of *B. loveorum* and *N. galiani* are very similar in size and shape to one another and to other felids. However, in *N. galiani* the plantar projection is hooked, whereas there is no hook present in *B. loveorum*. On the distal region of the plantar projection there is a groove for the passage of the *m. peroneus longus* tendon, as noted by Merriam and Stock (1932) for *S. fatalis*. However, in *S. fatalis* this feature greatly varies among individuals, with some

exhibiting a truncated and/or poorly-developed plantar projection (Merriam and Stock 1932; Shaw and Tejada-Flores 1985) and might not have a functional implication.

*Metatarsals.* Metatarsals of *B. loveorum* are noticeably shorter than those of *N. galiani*, however the proportion of the proximal and distal ends, as well as the shaft thickness, are similar. The stocky metatarsals of *B. loveorum* are similar to descriptions by Merriam and Stock (1932) of *S. fatalis*, whereas *N. galiani* shows more similarities with large felids. Carrano (1996) suggested that shortened metatarsals may indicate a more plantigrade stance, with more muscular force applied to each step, while relying on a shorter stride. Though short, metatarsals in *B. loveorum* show odd proportions, when compared to felids, with shortest to longest being MT V-II-III-IV, whereas the longer metatarsals in *N. galiani*, increases in length from MT V-II-IV-III. The dorsal region of the head in MT II-V is flat in *B. loveorum*, yet convex in *N. galiani* and other felids, however, the significance of this feature is unclear.

On the proximal end of MT II in *B. loveorum*, the facet for the mesocuneiform is smaller than in *N. galiani*, taking up approximately half of the surface. In *B. loveorum* the MT II articulation with the ectocuneiform in the plantar region is highly angled away from the plantar articulation with MT III, suggesting that MT II had a high capability to medially extend outward, possibly to increase stance stability. Similar flexibility is not indicated in *N. galiani*, since the ectocuneiform facets lock MT II in place. Additionally, the two facets for MT III are very small in *B. loveorum*, further suggesting a limited amount of contact between MT II and III.

On MT III, the facet for the ectocuneiform is the dominant feature on the proximal end in both taxa. However, in *B. loveorum* the plantar portion of the ectocuneiform facet slopes laterally at a large degree, suggesting MT III could extend medially away from MT IV, rocking on the articular surface with the ectocuneiform. On the lateral surface, near the proximal end, are the

two facets for articulation with MT IV. In *N. galiani* these facets are of similar size and shape, and functionally resemble those described for *P. atrox* by Merriam and Stock (1932). In *B. loveorum*, the dorsal facet is enlarged and continues onto the proximal surface and merges with the small cuboid facet. However, the plantar facet is very small and is adjacent to the proximal border. When articulated with MT IV, the MT III of *B. loveorum* is distally spread away from MT IV. Additionally, dorsoplantar movement is restricted, similar to *N. galiani*, but mediolateral movement can occur. In *N. galiani*, the MT III is the longest compared to the other metatarsals, a trait shared by both extinct (Merriam and Stock 1932) and extant felids.

MT IV of *B. loveorum* is the longest and the most robust when compared to the other metatarsals, unlike that of modern and extinct felids (Merriam and Stock 1932). Facets for MT III are more convex in *N. galiani*, whereas in *B. loveorum* they are nearly flat. When articulated, this the convex facets in *N. galiani* would limit movement of the MT IV, whereas in *B. loveorum* this would allow for sliding on the facet and increased movement. Additionally, in *B. loveorum*, the dorsal facet on MT III, for articulation with MT IV, is located more dorsally than in *N. galiani* and other felids; placing MT III and IV at equal dorsal height in the proximal region. However, in *N. galiani*, the MT IV is more plantar adjacent to the MT III. In *N. galiani*, the cuboid facet of MT IV is similar in shape to felids described by Merriam and Stock (1932), ensuring that the cuboid sits on most of the proximal surface. However, in *B. loveorum*, this facet is only present in the dorsal region of the proximal end, making the cuboid articulate at an angle to the proximodistal length of MT IV. The unique configuration in *B. loveorum* provides further evidence of a sub plantigrade posture, where most of the ankle joint flexion is located in the tarsometatarsal joint instead of the metatarsophalangeal joint observed in most felids (Carrano 1996), including *N. galiani*. The facet for MT V in *N. galiani* is similar to *P. atrox*, as described

by Merriam and Stock (1932), however more proximally placed. In *B. loveorum*, the facet is dorsally placed, allowing MT V to have a similar proximal height to MT IV.

MT V in *B. loveorum* is dissimilar to that of felids. The proximal facet for articulation with MT IV is nearly flat, possibly allowing for more lateral movement. When articulated with MT IV, MT V is laterally spread apart in the distal region. The spread between MT IV and MT V further suggest a sub plantigrade stance in *B. loveorum*. The cuboid articulation in *B. loveorum* on MT V takes up the majority of the proximal end and is nearly dorsopalmarly vertical. In *N. galiani* this surface is greatly slanted proximodistally, which likely allows MT V to close-off the peroneal groove on the distal surface of the cuboid. Such closure does not appear to be the case for *B. loveorum*, as the plantar-most extension of the proximal end of MT V serves as the location of the facet for the cuboid. Significance of these differences is unclear, but it could allow unrestricted plantar flexion for MT V in *B. loveorum* before hitting the tendon passing through the groove.

## *Vertebrae*

*Cervical.* The axis and atlas for *B. loveorum* and *N. galiani* are the only cervical vertebra identified with a level of certainty due to their highly independent features, whereas the identification of the C3-7 vertebra in this study are less certain. In *B. loveorum* the atlas is very distinct from that of felids, but shares similar characteristics with the nimravid *Hoplophoneus* (Scott and Jepsen 1936) and ursids, such as the lack of alar notches (Baskin 1980). Instead, an alar foramen is present, which would better guide the vertebralis artery from the lateral atlantal foramen to the transverse foramen, as described by Davis (1964). Additionally, *B. loveorum* is comparable to *S. fatalis*, as the latter also has posteriorly elongated transverse processes discussed by Merriam and Stock (1932) and Baskin (2005). This posterior extension suggests the presence of a longer *m. obliquus capiti anterior*, between the atlas and the mastoid, and *m. obliquus capiti posterior*, between the atlas and axis. Such a configuration could allow the skull to have an increase in atlas-mastoid depression and extension; motions needed to enact the canine shear-bite (Antón 2004; Salesa et al. 2005; Antón 2020). In *N. galiani*, the atlas is not well-preserved; however, there are still many similarities to felids discussed by Merriam and Stock (1932) and Baskin (1980), such as the presence of alar notches and unconnected atlantal and transverse foramina. This suggests the kill bite of *N. galiani* would have used their sabers to assist in slicing their prey's neck, but less neck strength would have been necessary. Alternatively, *B. loveorum* would have had more muscle capability to subdue prey, using their larger sabers to execute the canine shear-bite as their robust forearms held the animal down.

Similar to the atlas, the axis of *B. loveorum* is unlike felids, as the spinous process is elongated posteriorly past the postzygapophyses. The *m. obliquus capiti posterior* originates from the transverse wings of the atlas and attaches to the spinous process of the axis. Hence, an

elongated spinous process of the axis could indicate a larger muscle, increasing neck muscle strength and extension (Davis 1964; Antón 2004; Salesa et al. 2005; Antón 2020). Furthermore, the spinous process is the attachment for the *m. multifidus* and *m. rectus capitis*, providing neck and head extension, as well as neck rotation. Consequently, an elongated spine would greatly increase the action of these muscles (Davis 1964; Antón 2020). On the ventral surface of the axis in *B. loveorum*, the large keel is surrounded by deep muscle attachments for the *m. longus capitis*, of which moderately increase flexion of the neck in extant felids (Antón 2020). These features suggest *B. loveorum* had a very powerful neck, capable of enacting the canine shear-bite and/or dragging prey. Previous studies have suggested that the lengthening of neck muscles also lengthens the lever arm, thus increasing neck strength (Antón and Galobart 1999; Salesa et al. 2005; Antón 2020). In *N. galiani* the dorsal spinous process is broken and worn away, so inferences cannot be made. However, the ventral keel in *N. galiani* is less pronounced, suggesting a slight decrease in neck flexion.

Cervicals 3-7 of *N. galiani* have little variation and are very similar to those of felids. The transverse processes preserved on C5-C7 are relatively short and felid-like. In *B. loveorum*, the transverse processes preserved on C4, C5, and C7 are robust and laterally elongated, similar to *S. fatalis* as depicted by Merriam and Stock (1932). At the tips of the transverse processes are attachments for the *m. longissimus*, *m. scalenii*, and *m. serratus*, all of which increase neck strength (Antón 2020), suggesting *B. loveorum* was able to strongly hold its head in many positions, possibly to help with the canine shear-bite. An increase in neck muscle strength would also increase neck stability when enacting the kill-bite. Additionally, the increased muscle strength would have been beneficial for *B. loveorum* to assist in dragging and hiding prey away from larger carnivorans.

*Sacrum.* In *B. loveorum*, the sacrum differs from that of felids by being mediolaterally longer than anteroposteriorly, and the sacral wings for articulation with the pelvis take up approximately 80% of the lateral surface, whereas in felids, such as *N. galiani*, the sacral wings are approximately 50% of the lateral surface in the two most complete specimens. A similar (stronger) pelvis attachment area was described for *S. fatalis* (Merriam and Stock 1932), whereas that of *N. galiani* resembles that described for *P. atrox* and extant felids by Merriam and Stock (1932). Sacral vertebral count in all felids is three (Reighard and Jennings 1901), however many of the preserved sacra of *B. loveorum* have up to four fused vertebrae, with the first caudal vertebrae fusing to the third sacral vertebrae. A similar condition has been described by Well and Camens (2018) for *Thylacoleo carnifex* (marsupial ‘lion’). Prezygapophyses in *B. loveorum* are more angled towards each other than is seen in *N. galiani*, and similar to that described for *S. fatalis* by Merriam and Stock (1932) and Christiansen and Adolfssen (2007), possibly limiting movement between the lumbar and sacral vertebrae. A more locked-in lumbosacral region in *B. loveorum* indicates a different running style than that of felids, which have a very flexible lumbosacral region. In *N. galiani*, the prezygapophyses are more open, similar to most felids discussed by Christiansen and Adolfssen (2007), and may allow for more lumbar-sacral movement than in *B. loveorum*. Separating the lateral sacral wing from the dorsal prezygapophyses is a deep and wide groove in *B. loveorum*, which is not present in *N. galiani*. This groove is also present on *S. fatalis* (Baskin 1980) and some extant felids, such as *Caracal caracal* (caracal) and *Leopardus serval* (serval), and suggests a capability to increase lumbar-sacral lateral movements (Salesa et al. 2017); whereas the lack of a groove is a character seen in *P. atrox* and other extant felids (Merriam and Stock 1932), similar to *N. galiani*. Postzygapophyses of the last sacral vertebra of *B. loveorum* are smaller in size to all other felids.

The extremely small postzygapophyses, centrum, and sacrum size are strong indicators that *B. loveorum* had a short tail (Baskin 1980; Russo 2015) of unknown caudal count. In *N. galiani*, these characters are much larger, implying a moderately sized tail was present, but possibly shorter than that of *P. onca* (jaguar) (Baskin 1980).

CHAPTER 3. PREDICTING PALEOECOLOGICAL BEHAVIORS FOR *NIMRAVIDES*  
*GALIANI* AND *BARBOUROFELIS LOVEORUM*

Ecomorphological studies using postcrania are commonly applied to extant mammalian groups to infer locomotor and hunting behaviors of extinct taxa, as well as past ecology and guild structures (e.g., Van Valkenburgh 1985, 1987; Anyonge 1996; Meloro 2011; Walmsley et al. 2012; Samuels et al. 2013; Martin-Serra et al. 2014a; Martin-Serra et al. 2014b). Gross morphology can be used to infer locomotion and hunting behavior when compared to extant taxa, as seen for the arboreal forager *Simocyon batalleri* (Salesa et al. 2008) and the terrestrial ambush predator *Leptofelis vallesiensis* (Salesa et al. 2017). Relationships between form and function are generally used to infer broad paleoecological behaviors by combining multiple carnivoran groups together in analyses, usually a combination of felids, ursids, and canids; however, representatives of more carnivoran families are occasionally used (Van Valkenburgh 1985; Van Valkenburgh 1987; Samuels et al. 2013). Past studies on these broadly applied carnivoran behaviors are then used to infer the ecological structure of extinct taxa. In other words, extant taxa within each family are classified within very generalized locomotor and/or hunting behavioral groups. Due to this possibility, the ecological roles of extinct taxa may be misclassified. This is especially true for members of Felidae; taxa are usually generalized as cursor/noncursor, or further split between arboreal, scansorial, and terrestrial, with the latter placing most felids in terrestrial (Van Valkenburgh 1985; Van Valkenburgh 1987; Mattern and McLennan 2000; Walmsley et al. 2012; Meloro et al. 2013; Martin-Serra et al. 2014). Similarly, felids are often classified as pursuit or ambush predators, undersimplifying pouncing behavior and pursuit distance (Van Valkenburgh 1985; Figueirido et al. 2015). Extinct felid-like

carnivorans, such as taxa within Nimravidae and Barbourfelidae, are often included in locomotor and hunting behavioral analyses to infer the paleoecological behaviors and structures among carnivoran groups (Van Valkenburgh 1985; Anyonge 1996; Samuels et al. 2013), but the broad classifications used on extant taxa may be misclassifying such taxa into incorrect paleoecological structures. Clearly, locomotor and hunting behavior need to be further examined within Felidae, and other previously considered felid-like taxa, before being used in ecomorphological studies combining multiple carnivoran families.

### *Traditional Locomotor Classifications*

Classifications of felid locomotor behaviors are inconsistent throughout past research studies because the felid body plan, one capable of climbing, is not well sub-classified for locomotion due to slight postcranial differences between species (e.g., Anyonge 1996; Mattern and McLennan 2000; Day and Jayne 2007; Meloro 2011; Meloro et al. 2013; Martin-Serra et al. 2014c). As a result, many studies including taxa from other carnivoran families may be biased, and results may place felids to be more similar to each other than the ecomorphs assigned to include non-felid taxa, such as bears or hyenas. To negate such an outcome, locomotor behaviors should be defined on how species respond to other predators and potential dangers, as well as how they catch their prey, instead of broad classifications. Most felids, including the most arboreal cats, will hunt on the ground, then move their prey to safety before consumption (Sunquist and Sunquist 2002). Here, felid locomotor behavioral groups are further examined, highlighting how classifications have shifted from one to another among past studies. Different locomotor behaviors are assigned by determining which felid taxa are more arboreal, scansorial, or cursorial when compared to other felids. It should be noted that these groups are not natural

separations, but are instead points along a continuous scale, where overlap can (and will) occur (Van Valkenburgh 1985).

**Arboreal**—All felids have the capability to climb; however, only a few species rely on this locomotion to flee from other predators and to consume their prey (Sunquist and Sunquist 2002; Day and Jayne 2006). Arboreal species typically spend a large portion of their time climbing in trees for shelter and/or stalking prey (Van Valkenburgh 1985; Van Valkenburgh 1987; Samuels et al. 2013). In past studies, the felids classified as arboreal have remained fairly consistent and include the margay (*Leopardus wiedii*), ocelot (*L. pardalis*), clouded leopard (*Neofelis nebulosa*), and marbled cat (*Pardofelis marmorata*) (Gonyea 1976a; Gonyea 1976b; Van Valkenburgh 1985; Mattern and McLennan 2000; Day and Jayne 2006; Meachen-Samuels and Van Valkenburgh 2009; Kitchener et al. 2010; Samuels et al. 2013). The margay and marbled cats are the best representatives of arboreal locomotion; exhibiting specializations specific to an arboreal lifestyle (being able to descend trees headfirst due to 180° of rotation of their tarsals (Sunquist and Sunquist 2002; Kitchener et al. 2010). Similarly, the clouded leopard has been observed hanging from branches with their hind feet to hunt in tree canopies (Sunquist and Sunquist 2002).

**Scansorial**—Felids in this category occasionally climb trees to flee, but may also run and hide on the ground if there are any available burrows, rock crevasses, or brush nearby (Van Valkenburgh 1985; Van Valkenburgh 1987; Samuels et al. 2013). In past studies, felids that are placed in the scansorial locomotor group include the cheetah (*Acinonyx jubatus*), lion (*Panthera leo*), tiger (*P. tigris*), and Canada lynx (*Lynx canadensis*), as other locomotor groups are typically omitted (Van Valkenburgh 1985; Van Valkenburgh 1987). Past studies of scansorial felids commonly include the bobcat (*L. rufus*), cougar (*Puma concolor*), and snow leopard (*Panthera*

*uncia*) (Iwaniuk et al. 1999; Meachen-Samuels and Van Valkenburgh 2009; Samuels et al. 2013). Additionally, Gonyea (1976a) includes the jaguar (*P. onca*) and Mattern and McLennan (2000) include both the caracal (*Caracal caracal*) and serval (*C. serval*) within this category. The African wildcat (*Felis silvestris libyca*) has also been placed within the scansorial group in past research (Van Valkenburgh 1985). Felids are often classified as scansorial because it is assumed that all cats have the capability to climb; however, this classification should be determined by how often a species has to climb to survive.

**Cursorial**—Among all of the classifications for felid locomotion, cursorial behavior has consistently been left out in previous studies, except for the *A. jubatus*, as cursorial locomotion often is describing a species that runs consistently and efficiently to hunt prey (Anyonge 1996; Carrano 1999; Day and Jayne 2006; Kitchener et al. 2010; Samuels et al. 2013). Yet, some studies do not include cursorial as a locomotor category, but instead classify *A. jubatus* as a terrestrial cat alongside *P. leo* and many other felids (Gonyea 1976b; Meachen-Samuels and Van Valkenburgh 2009; Carlon 2014). Similarly, Christiansen and Adolfssen (2007) claim that no felid, including *A. jubatus*, is cursorial since all felids rely on stealth and ambush hunting strategies when compared to other carnivorans. However, within Felidae, *A. jubatus* is anatomically adapted to run at fast speeds over short distances, rarely relying on climbing, to hunt and/or flee (Sunquist and Sunquist 2002; Krausman and Morales 2005).

Cursorial behavior has often been linked to open habitats (Figueirido et al. 2015), and the felids in these environments will not have tree access to flee from danger and must chase their prey over relatively long distances (Gonyea 1976a; Mattern and McLennan 2000; Christiansen and Adolfssen 2007). Both *A. jubatus* and *P. leo* rely on cursorial strategies, with *A. jubatus* displaying slightly more cursorial behavior (Sunquist and Sunquist 2002; Krausman and Morales

2005). *P. leo* pursues its prey at a fast speed and is behaviorally similar to *A. jubatus*, except *P. leo* stalks prey at longer distances before the eventual chase and relies on pack hunting, similar to canids (Gonyea 1976a; Sunquist and Sunquist 2002; Haas et al. 2005).

**Generalist**—In past studies, often classified as terrestrial behavior, the generalist category includes *A. jubatus*, *P. leo*, *P. tigris*, *P. uncia*, *C. serval*, jungle cat (*Felis chaus*), *L. canadensis*, and manul (*Otocolobus manul*) (Gonyea 1976a; Mattern and McLennan 2000; Meachen-Samuels and Van Valkenburgh 2009). Generalist felids rarely climb; however, this classification differs among past studies. In addition to a lack of climbing, Samuels et al. (2013) includes the lack of swimming, and the ability to dig within a study combining multiple carnivoran families. Similarly, Van Valkenburgh (1985; 1987) includes modifying burrows through digging in this category, but defines most felids as scansorial. In this study, generalist felids are well adapted to different locomotor behaviors and are relatively unspecialized; *L. rufus* is able to climb and run, similar to scansorial felids, however when fleeing, *L. rufus* typically runs instead of climbs (Larivière and Walton 1997; Sunquist and Sunquist 2002). Alternatively, *O. manul* is neither good at running or climbing, but instead stays near rock crevasses for retreat (Sunquist and Sunquist 2002).

#### *Traditional Hunting Behavior Classifications*

Like most carnivorans, felids are opportunistic hunters, including the more specialized taxa, such as the fishing cat (*Prionailurus viverrinus*), who primarily hunts fish and waterfowl (Sunquist and Sunquist 2002), and *A. jubatus*, which quickly chases down its prey (Sunquist and Sunquist 2002; Krausman and Morales 2005). When presented with an easy chance to catch prey, any felid will do so. For example, felids that hunt large prey will still consume rodents and

birds when easily obtainable; however, felids that consume small prey typically do not hunt large prey (Sunquist and Sunquist 2002). Additionally, all felids stalk their prey before initializing their main attack, getting as close as they can to minimize spent energy, like most carnivorans (Sunquist and Sunquist 2002; Christiansen and Adolfssen 2007). Although these behaviors are consistent throughout Felidae, the main mode of attack differs among species. Even so, past research tends to classify all felids, except *A. jubatus*, as ambush predators, and not further separating differences between ambush, pursuit, and pounce-pursuit behaviors (Van Valkenburgh 1985; Anyonge 1996; Figueirido et al. 2015). In each of those studies, members of Felidae are used in analyses of multiple carnivoran families to infer predator guild structures, which generalizes felids. Here, felid hunting behavior groups are further examined. Similar to locomotor categories, these groups are not natural separations, but are instead points along a continuous scale, where overlap can (and will) occur (Van Valkenburgh 1985).

**Ambush**—Most felids, except for *A. jubatus*, have been described as ambush predators due to their stalking behavior and short distance pursuit of prey when compared to other carnivorans (e.g., Canidae, Hyaenidae, Ursidae) (Van Valkenburgh 1985; Anyonge 1996; Figueirido et al. 2015). Ambush behavior is often connected to a closed habitat (Figueirido et al. 2015), which would help in disguising the predator from its prey by hiding in trees, bushes, and rock crevasses, and smaller felids (Gonyea 1976a; Mattern and McLennan 2000). Although all felids stalk their prey, not all should be considered as ambush predators when describing hunting behavior within Felidae.

**Pursuit**—*A. jubatus* is considered the only pursuit felid (Anyonge 1996; Figueirido et al. 2015), except by Christiansen and Adolfssen (2007), who consider any stalking behavior as an ambush characteristic. Similar to ambush predators, pursuit predators are often connected to

habitat, in this case an open habitat (Gonyea 1976a; Mattern and McLennan 2000). African savannas are open and sparse with vegetation and the *A. jubatus* is highly adapted to this environment, as well as other similarly open environments (Sunquist and Sunquist 2002; Krausman and Morales 2005). However, *A. jubatus* is an extreme case of a pursuit felid, as other felids are only adapted for chasing prey at a relatively short distance.

**Pounce-Pursuit**—Predators within this category are not well defined, especially within Felidae. Van Valkenburgh (1985) classifies this behavior as a constant search for prey that ends in a pounce or chase, such as observed in foxes. Additionally, prey grappling is not used as it is for ambush predators (Van Valkenburgh 1985). Pounce-pursuit hunting was classified as pounce hunting by Schwab (2019), where Felidae, Canidae, Hyaenidae, and Viverridae are classified into ambush, pursuit, pounce, and occasional hunting styles. However, unlike in previous studies, Schwab (2019) does not assign felids a general classification, but instead includes ambush, pounce, and pursuit hunting behaviors. Pounce-pursuit predators are commonly in mixed habitats that can be very close to open habitat or closed habitat (Gonyea 1976a; Mattern and McLennan 2000; Sunquist and Sunquist 2002; Figueirido et al. 2015).

### *Materials and Methods*

**Anatomical Abbreviations**—**DPCL**, deltopectoral crest length of humerus; **FD**, femur anteroposterior diameter; **FEB**, femur epicondylar breadth; **FGT**, femur greater trochanter height; **FL**, femur length; **HD**, humerus mediolateral diameter; **HEB**, humerus epicondylar breadth; **HL**, humerus length; **HMAD**, sum of the humerus mediolateral and anteroposterior diameters; **MT3L**, metatarsal III length; **OL**, ulna olecranon length; **RL**, radius length; **TD**, tibia

mediolateral diameter; **TL**, tibia length; **TSL**, tibia tuberosity length; **UL**, ulna length; **UD**, ulna mediolateral diameter.

**Institutional Abbreviations**—**AMNH**, American Museum of Natural History; **ETVP**, East Tennessee Vertebrate Paleontology; **LACM** and **LACMHC**, Natural History Museum of Los Angeles County; **NAU QSP**, Northern Arizona University, Quaternary Sciences Program; **UCLA**, University of California, Los Angeles; **UF**, Florida Museum of Natural History, University of Florida, Gainesville, Florida; **USNM**, Smithsonian National Museum of Natural History.

Data was obtained from Schubert et al. (2013) and included measurements on the humerus, radius, ulna, femur, tibia, and third metatarsal from 12 extant felids (*Acinonyx jubatus*, *Caracal serval*, *Felis silvestris*, *Leopardus wiedii*, *Lynx canadensis*, *L. rufus*, *Neofelis nebulosa*, *Otocolobus manul*, *Pardofelis marmorata*, *Panthera leo*, *P. uncia*, *Puma concolor*) and four extinct taxa (*Dinictis* sp., *Hoplophoneus* sp., *Panthera atrox*, and *Smilodon fatalis*) (Van Valkenburgh 1985; Van Valkenburgh 1987; Samuels et al. 2013). Measurements of additional extant felids (*Felis chaus*, *Panthera leo*, *P. onca*, and *P. tigris*) and extinct taxa (*Barbourofelis loveorum* and *Nimravides galiani*) was added to this dataset (Appendix A). Following Van Valkenburgh (1985), Meachen-Samuels and Van Valkenburgh (2009), and Samuels et al. (2013), 15 ratios from 17 postcranial linear measurements (Fig. 38) were used as training data for a Stepwise Discriminant Function Analysis (DFA) of locomotor categories and hunting behavior. Through these measurements, 15 morphological indices (ratios) were used to best represent differences in limb proportions due to different locomotor behaviors (Table 1). Since hunting behavior and locomotion are not independent of one another, these same measurements and indices were used to infer hunting behavior as they have been traditionally used in past studies

(Van Valkenburgh 1985; Van Valkenburgh 1987; Meachen-Samuels and Van Valkenburgh 2009).

Table 1. Morphological Indices and Definitions. Measurements Used to Create These Indices Are Shown in Figure 38. Measurements and Indices follow Van Valkenburgh (1987) and Samuels et al. (2013).

Indices	Definition
Shoulder moment (SMI)	Length of deltopectoral crest divided by length of humerus ( <b>DPCL/HL</b> )
Brachial index (BI)	Length of radius divided by length of humerus ( <b>RL/HL</b> )
Humeral diameter robustness (HRDI)	Humeral diameter divided by humerus length ( <b>[HMLD+HAPL]/HL</b> )
Humeral robustness (HRI)	Humeral mediolateral width divided by humerus length ( <b>HMLD/HL</b> )
Humeral epicondylar (HEI)	Humeral epicondylar width divided by humerus length ( <b>HEB/HL</b> )
Ulnar robustness (URI)	Ulnar mediolateral diameter divided by ulna length ( <b>UD/UL</b> )
Olecranon length (OLI)	Length of olecranon process divided by ulnar length ( <b>OL/UL</b> )
Crural index (CI)	Tibia length divided by femure length ( <b>TL/FL</b> )
Femoral robustness (FRI)	Femoral anteroposterior width divided by femur length ( <b>FD/FL</b> )
Gluteal index (GI)	Greater trochanter length divided by femure length ( <b>FGT/FL</b> )
Femoral epicondylar (FEI)	Femoral epicondylar width divided by femur length ( <b>FEB/FL</b> )
Tibial robustness (TRI)	Tibial mediolateral width divided by tibia length ( <b>TD/TL</b> )
Tibial spine index (TSI)	Tibial tuberosity length divided by tibia length ( <b>TSL/TL</b> )
Pes length index (PES)	Third metatarsal length divided by femur length ( <b>MT3L/FL</b> )
Intermembral index (IM)	Humerus and radius length divided by femur and tibia length ( <b>[HL+RL]/[FL+TL]</b> )

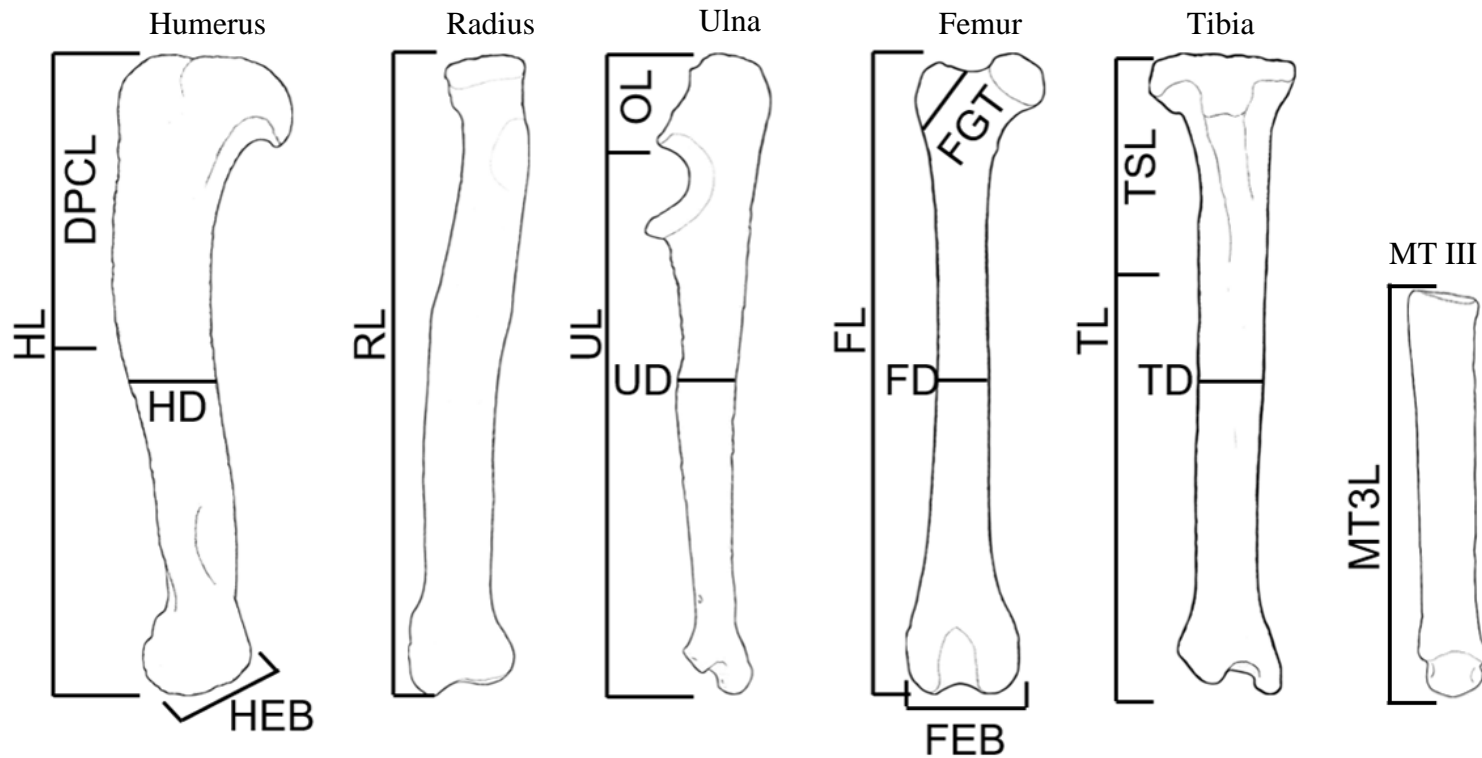


Figure 38. Measurements used for analyses in mm. Limb elements of *Nimravides galiani* showing the 17 measurements used in the analysis, not scaled to size. Measurement abbreviations: (HL) humerus length, (HD) humerus mediolateral diameter, HMLD, and humerus anteroposterior diameter, HAPD, (HEB) humerus epicondylar breadth, (DPCL) deltopectoral crest length of humerus, (RL) radius length, (UL) ulna length, (UD) ulna mediolateral diameter, (OL) ulnar olecranon length, (FL) femur length, (FD) femur anteroposterior diameter, (FEB) femur epicondylar breadth, (FGT) femur greater trochanter height, (TL) tibia length, (TD) tibia mediolateral diameter, (TSL) tibia tuberosity length, (MT3L) MT III length.

Among the extant Felidae, taxa were assigned to locomotion categories based on literature and observed behaviors (Table 2; Appendix B) for each taxon. Six extinct feliforms (the felids *Panthera atrox*, *Smilodon fatalis*, and *Nimravides galiani*, the nimravids *Dinictis* sp. and *Hoplophoneus* sp., and the barbourofelid *Barbourofelis loveorum*) were included as unknowns for a stepwise Discriminant function analysis to infer their behaviors based on the training set. The phylogenetic tree of the taxa used in this study (Antón 2013; Polly et al. 2020; Hassaninet et al. 2021) (Fig. 39) illustrates the assigned locomotor behaviors among the extant felids. Wilks  $\lambda$  scores were used to determine if extant taxa can be separated by locomotion through postcranial morphology.

Table 2. Locomotor Descriptions Used in This Study Based on Hunting and Evading Behaviors. See Appendix B for a Complete List of Species Assigned Behavior and Associated Citations.

Locomotion	Classification
Arboreal	Climbs to hunt and evade.
Scansorial	Occasional climbing to evade. Powerful jumpers.
Cursorial	Runs to chase prey and evade.
Generalists	Rare climbing. Ambush/pounces prey.

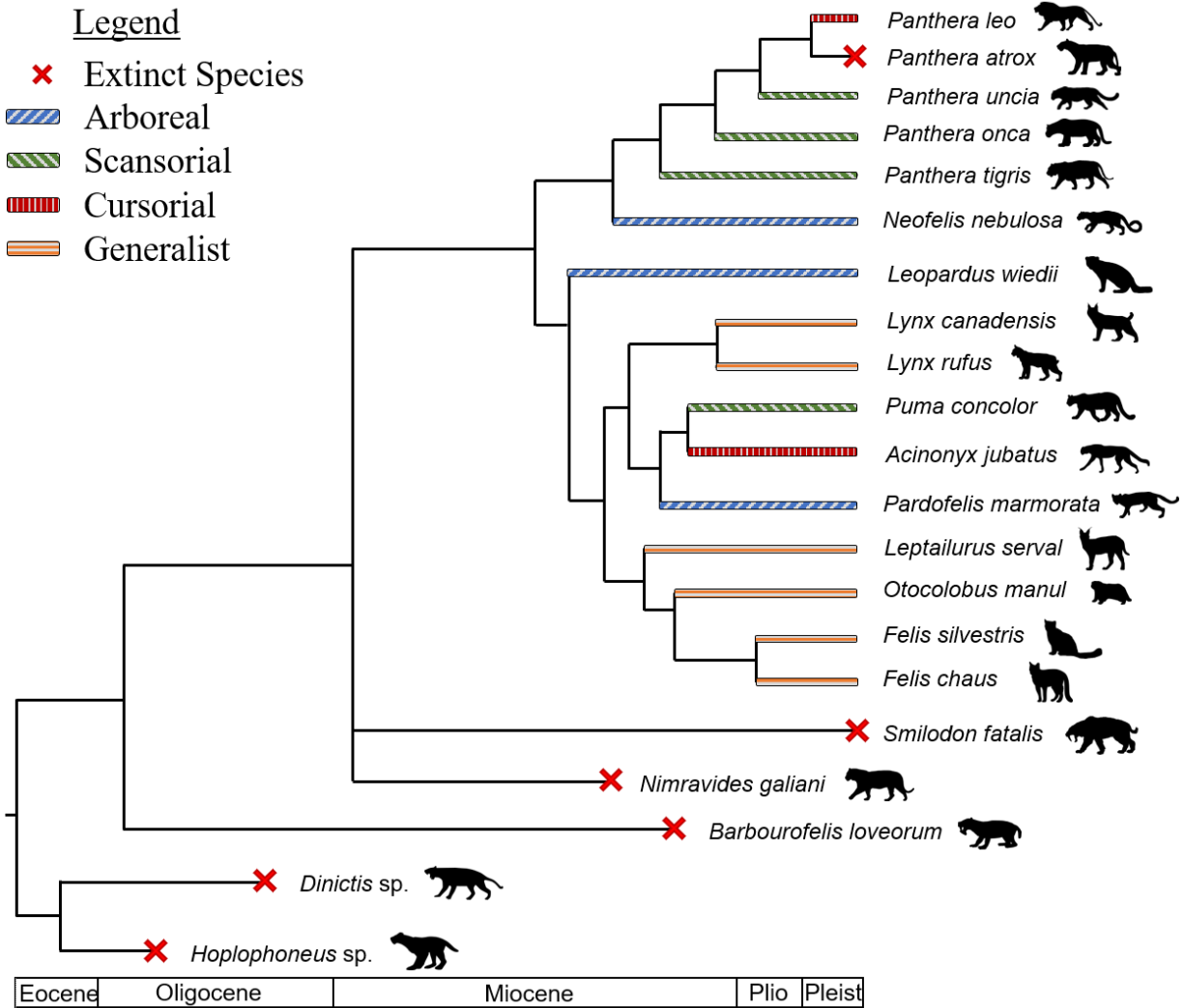


Figure 39. Felid locomotion and phylogenetic tree of taxa used in analysis (tree modified from Anton 2013; Piras et al. 2018; Polly et al. 2020; Hassaninet et al. 2021). Locomotion classifications for extant felids (used here) are represented on specific branches and extinct taxa are represented by the red X. Taxa silhouettes from phylopic.org.

Similarly, the 15 extant taxa were assigned to hunting behavior categories based on literature and observed behaviors (Table 3; Appendix C). The six extinct taxa were designated as unknowns for a stepwise Discriminant function analysis to infer their behaviors based on the training set. The phylogenetic tree of the taxa used in this study (Fig. 40) illustrates the assigned hunting behavior among the extant felids. Wilks  $\lambda$  scores were used to determine if extant taxa can be separated by hunting behavior through postcranial morphology.

Table 3. Hunting Behavior Descriptions Based on Prey Acquisition. See Appendix C for a Complete List of Species Assigned Behavior and Associated Citations.

Hunting Behavior	Classification
Ambush	Prey not pursued if initial pounce fails.
Pounce-Pursuit	Prey pursued for short distances if initial pounce fails.
Pursuit	Prey are pursued for long distances.

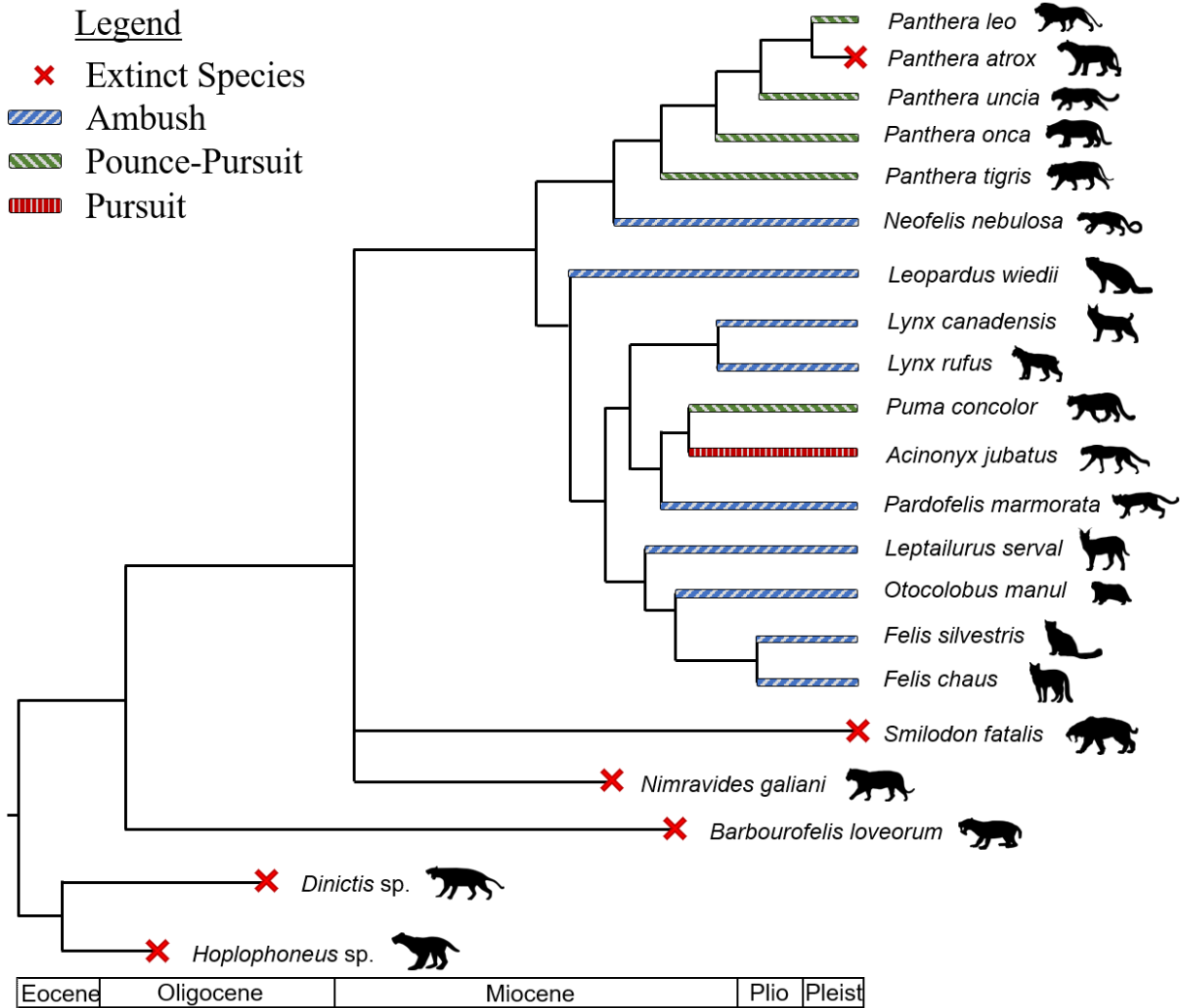


Figure 40. Felid hunting behavior and phylogenetic tree of taxa used in analysis (tree modified from Antón 2013; Piras et al. 2018; Polly et al. 2020; Hassaninet et al. 2021). Hunting categories for extant felids are represented on specific branches and extinct taxa are represented by the red X.

## Results

### *Locomotion*

Five of the 15 indices used in the analyses were retained (passed significance test) by the stepwise discriminant function to separate the locomotor groups (Table 4): Wilks  $\lambda$  was 0.031 for the analysis as a whole and was significant ( $p < 0.05$ ). This analysis gave three discriminant functions that account for 100% of the variance. Classification results indicated 92.3% of the extant species were correctly classified and 88.5% were correctly classified when cross-validated (leave one out analysis).

Each of the discriminant functions for the locomotor analysis are further broken down in Table 4. DF1 primarily separates arboreal and generalist groups from each other, as well as the extinct feliforms, *B. loveorum*, *S. fatalis*, *Dinictis* sp., and *Hoplophoneus* sp. (Fig. 41). Arboreal and scansorial felids have negative DF1 scores, whereas generalist and cursorial felids have positive scores. DF2 primarily separates the cursorial and scansorial locomotor groups, as well as *N. galiani*, *B. loveorum*, *S. fatalis*, and *P. atrox*, from the arboreal and generalist groups. Arboreal and generalist felids have a negative DF2 score, whereas scansorial felids have mostly positive scores, and all cursorial felids have positive scores. DF3 did not clearly separate any locomotor group from the others and is less significant. Prediction probabilities for the extinct taxa are shown in Table 5.

Table 4. Locomotor Prediction Discriminant Function Structure Matrix for the Five Significant Indices, Eigenvalues, Percent Variance Explained, and Wilks'  $\lambda$

Index	DF 1	DF 2	DF 3
BI	0.857	0.069	0.070
HRI	-0.531	0.477	0.577
FRI	-0.383	0.622	-0.052
TRI	-0.291	0.764	0.291
PES	0.692	-0.242	0.267
Eigenvalues	3.818	2.570	0.887
% variance explained	52.5	35.3	12.2
Wilks' $\lambda$	0.031	0.148	0.530
X <sup>2</sup>	158.327	86.782	28.886
Canonical correlation	0.890	0.848	0.686

Table 5. Prediction Probabilities for Extinct Taxa Locomotion

Taxonomic Name	Highest Prediction %	Second Highest Prediction %
<i>Nimravides galiani</i>	Scansorial (99.9)	Cursorial (0.1)
<i>Barbourofelis loveorum</i>	Scansorial (83.0)	Cursorial (17.0)
<i>Panthera atrox</i>	Cursorial (95.8)	Scansorial (4.2)
<i>Smilodon fatalis</i>	Scansorial (97.2)	Cursorial (2.8)
<i>Dinictis</i> sp.	Scansorial (57.2)	Arboreal (42.7)
<i>Hoplophoneus</i> sp.	Arboreal (90.7)	Cursorial (9.1)

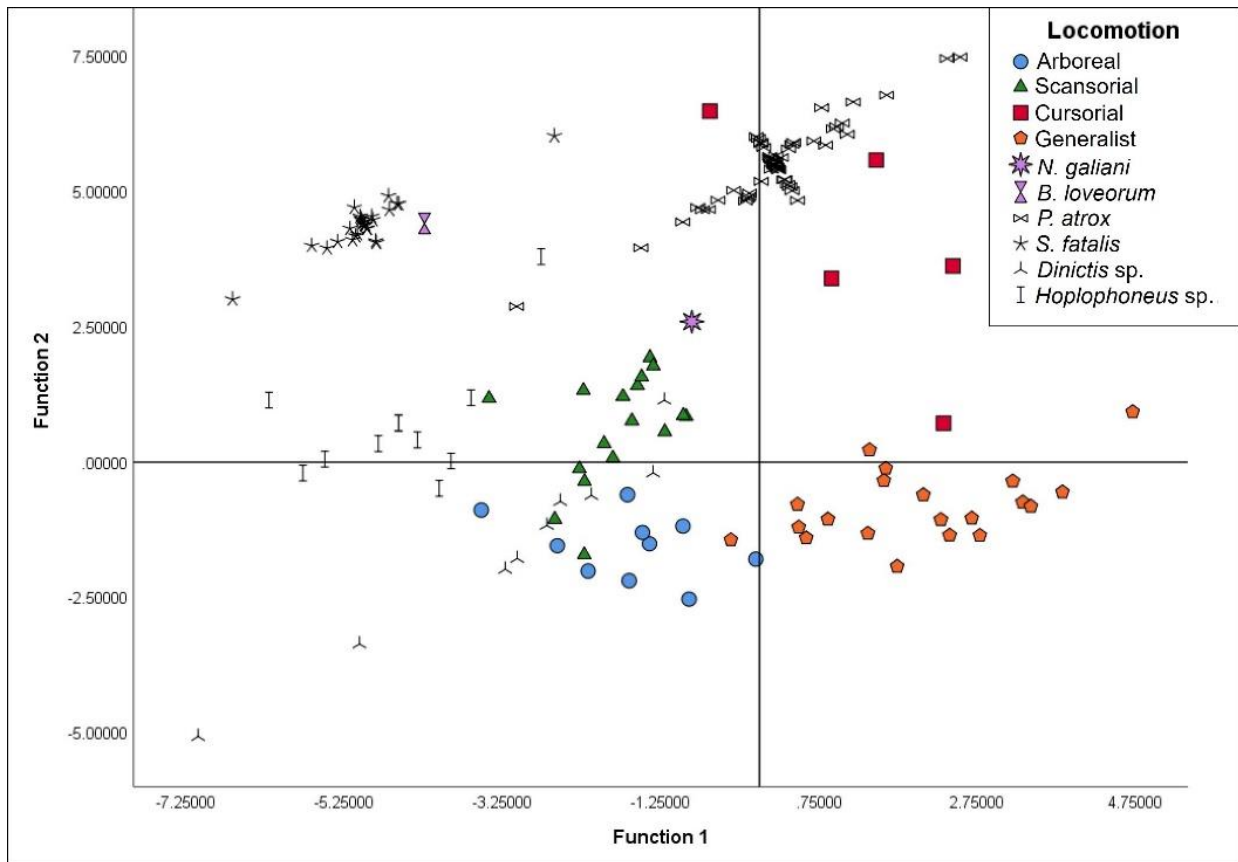


Figure 41. Locomotion DFA Stepwise plot analysis of 15 extant felids (Appendix B) and 6 extinct taxa illustrating their locomotor classifications and predictions, respectively. Note that *Nimravides galiani* plots between Scansorial and Cursorial felids. *Barbourofelis loveorum* and *Smilodon fatalis* plot near each other, but away from others. *Panthera atrox* plots within Cursorial alongside *Panthera leo*. *Dinictis* sp. and *Hoplophoneus* sp. overlap each other and are widespread.

The five indices chosen by the stepwise analysis can be used to determine the measurements and postcrania that are the most important in differentiating locomotor types (Fig. 42). Arboreal and scansorial felids are characterized by having shorter radii (low BI), compared to cursorial and generalist felids, however the radius of all felids is relatively shorter than their humerus. The midshaft thickness of the tibia and humerus is thinner, when compared to their respective lengths, in arboreal and (especially) generalist felids (low TRI and HRI) than in the scansorial and cursorial felids. Generalist felids have thinner midshaft femur thickness when compared to humerus length (low FRI), whereas the other locomotor groups have similar FRI means. Generalist and cursorial felids also have elongated digits (high PES), with the former having longer digits.

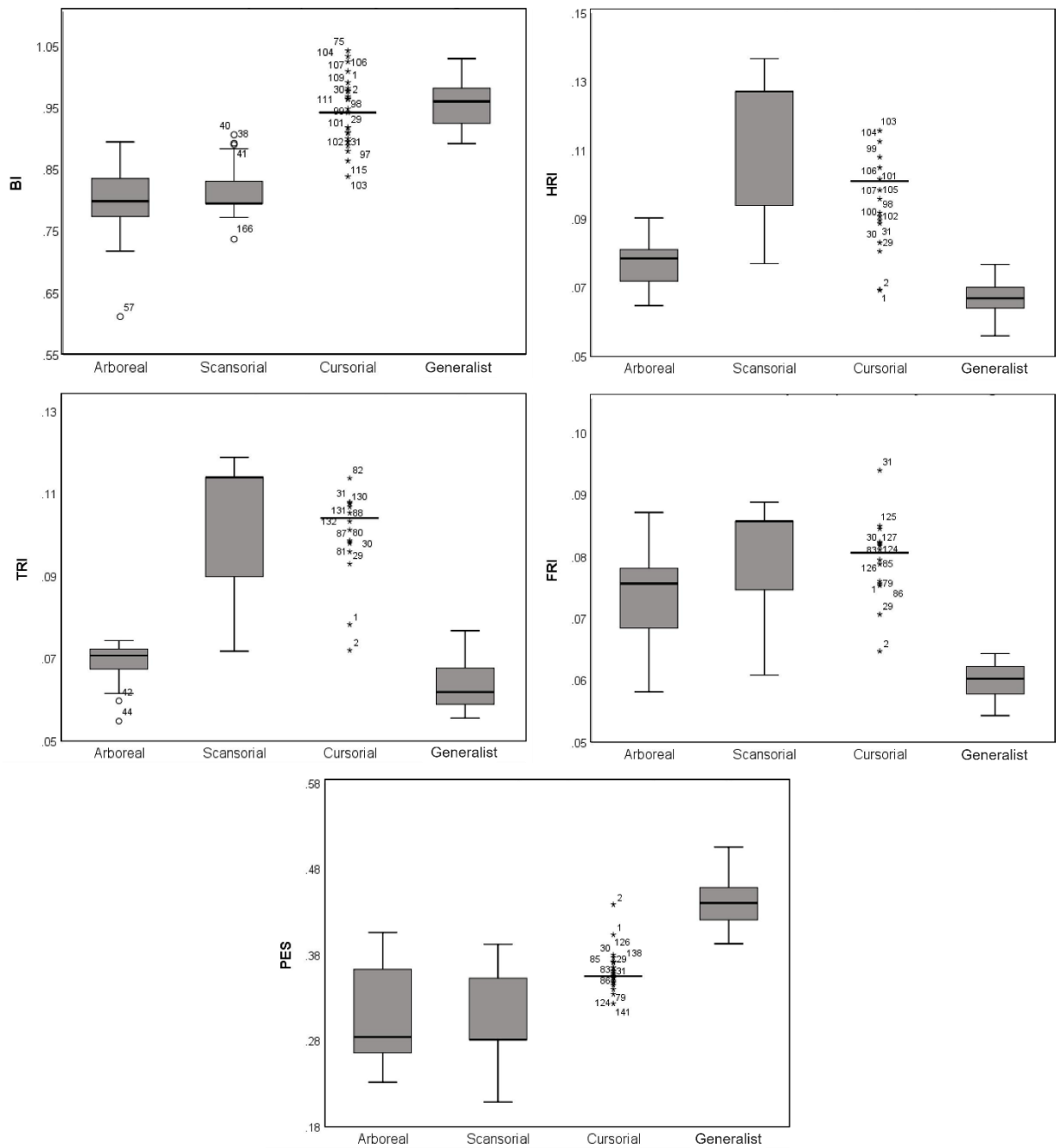


Figure 42. Boxplots of the locomotor morphological indices used in the stepwise DF analysis (Table 4) for each locomotor group. Outliers are represented by open circles.

### *Hunting Behavior*

Of the 15 indices used in the stepwise discriminant analysis, five statistically (Wilks  $\lambda = 0.071$ ;  $p < 0.05$ ) separated the hunting behavior categories (Table 6). This analysis gave two discriminant functions accounting for 100% of the variance. Additionally, the discriminant analysis was determined to accurately separate felids into hunting behavior groups by the classification output, which indicated 98.1% of the extant species were correctly classified and 96.2% were correctly classified with cross-validated (leave one out analysis).

Each of the discriminant functions for the hunting behavior analysis are described in detail in Table 6. DF1 primarily separates the ambush and pursuit predators from the pounce-pursuit hunters, as well as *B. loveorum* and *S. fatalis*. (Fig. 43). Ambush and pursuit felids have negative DF1 scores, whereas pounce-pursuit felids, and all six extinct taxa, have positive scores. DF2 primarily separates the pursuit felids from the ambush and pounce-pursuit predators. Additionally, *S. fatalis* and *B. loveorum* are separated from *P. atrox*, *N. galiani*, *Dinictis* sp., and *Hoplophoneus* sp. Pursuit felids have a positive DF2 score, whereas ambush and pounce pursuit felids have a mixture of positive and negative scores.

Table 6. Hunting Behavior Prediction Discriminant Function Structure Matrix for the Five Significant Indices, Eigenvalues, Percent Variance Explained, and Wilks'  $\lambda$

Index	DF 1	DF 2
HEI	0.795	-0.001
HRDI	0.729	0.445
TSI	0.356	0.437
URI	0.763	-0.084
OLI	0.390	0.097
Eigenvalues	5.224	1.259
% variance explained	80.6	19.4
Wilks' $\lambda$	0.071	0.443
X <sup>2</sup>	118.949	36.672
Canonical correlation	0.916	0.747

Table 7. Prediction Probabilities for Extinct Taxa Hunting Behavior

Taxonomic Name	Highest Prediction %	Second Highest Prediction %
<i>Nimravides galiani</i>	Pounce-pursuit (100.0)	—————
<i>Barbourofelis loveorum</i>	Pounce-pursuit (100.0)	—————
<i>Panthera atrox</i>	Pounce-pursuit (99.0)	Ambush (1.0)
<i>Smilodon fatalis</i>	Scansorial (97.2)	Cursorial (2.8)
<i>Dinictis</i> sp.	Pounce-pursuit (85.0)	Pursuit (11.5)
<i>Hoplophoneus</i> sp.	Pounce-pursuit (100.0)	—————

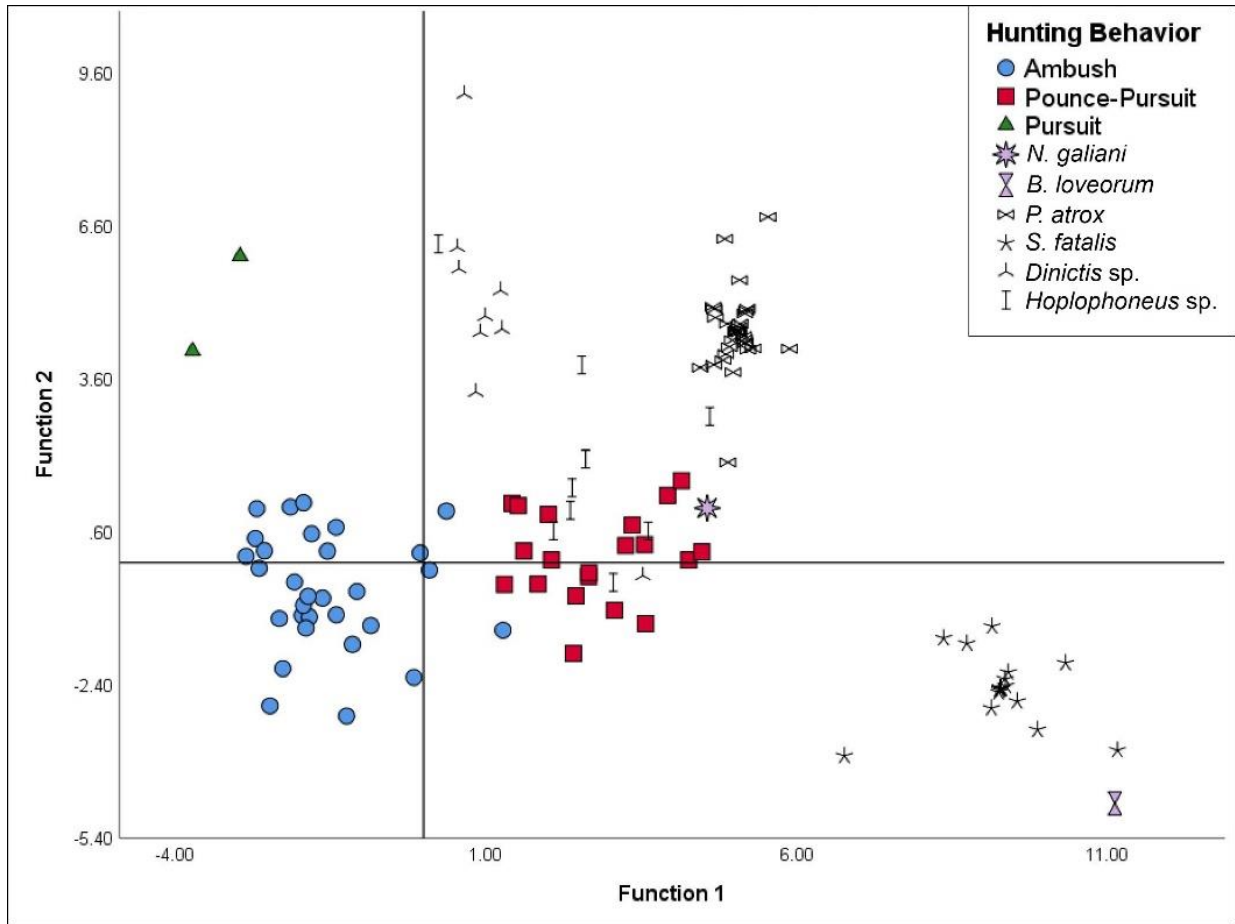


Figure 43. Hunting behavior DFA Stepwise plot analysis of 15 extant felids (Appendix C) and 6 extinct felid-like taxa illustrating their hunting classifications and predictions, respectively. Note that *Nimravides galiani* plots within pounce-pursuit felids. *Barbourofelis loveorum* and *Smilodon fatalis* plot near each other, but away from others. *Panthera atrox* plots away from all groups, but closest to pounce-pursuit. *Dinictis* sp. and *Hoplophoneus* sp. overlap each other and are widespread.

Similar to the locomotion analysis, the five indices chosen by the stepwise analysis can be used to determine the measurements and postcrania that are the most important in differentiating hunting behavior types (Fig. 44). Ambush and pursuit predators have shorter distal epicondylar breadth of the humerus when compared to humerus length (low HEI), whereas pounce-pursuit felids have wider breadths to humeri length. Additionally, in ambush and pursuit predators, the humeri midshaft diameter is constrained and the humeri is elongated (low HRDI) when compared to pounce-pursuit felids. The tibial spine of ambush felids is anteroposteriorly shorter when compared to overall tibia length (low TSI), whereas pounce-pursuit and pursuit predators have similar lengths. Pursuit felids have thin ulnar midshaft thickness and long ulnar length, followed by ambush felids (low URI). Similarly, ambush and pursuit hunters have a shorter olecranon when compared to ulnar length (low OLI).

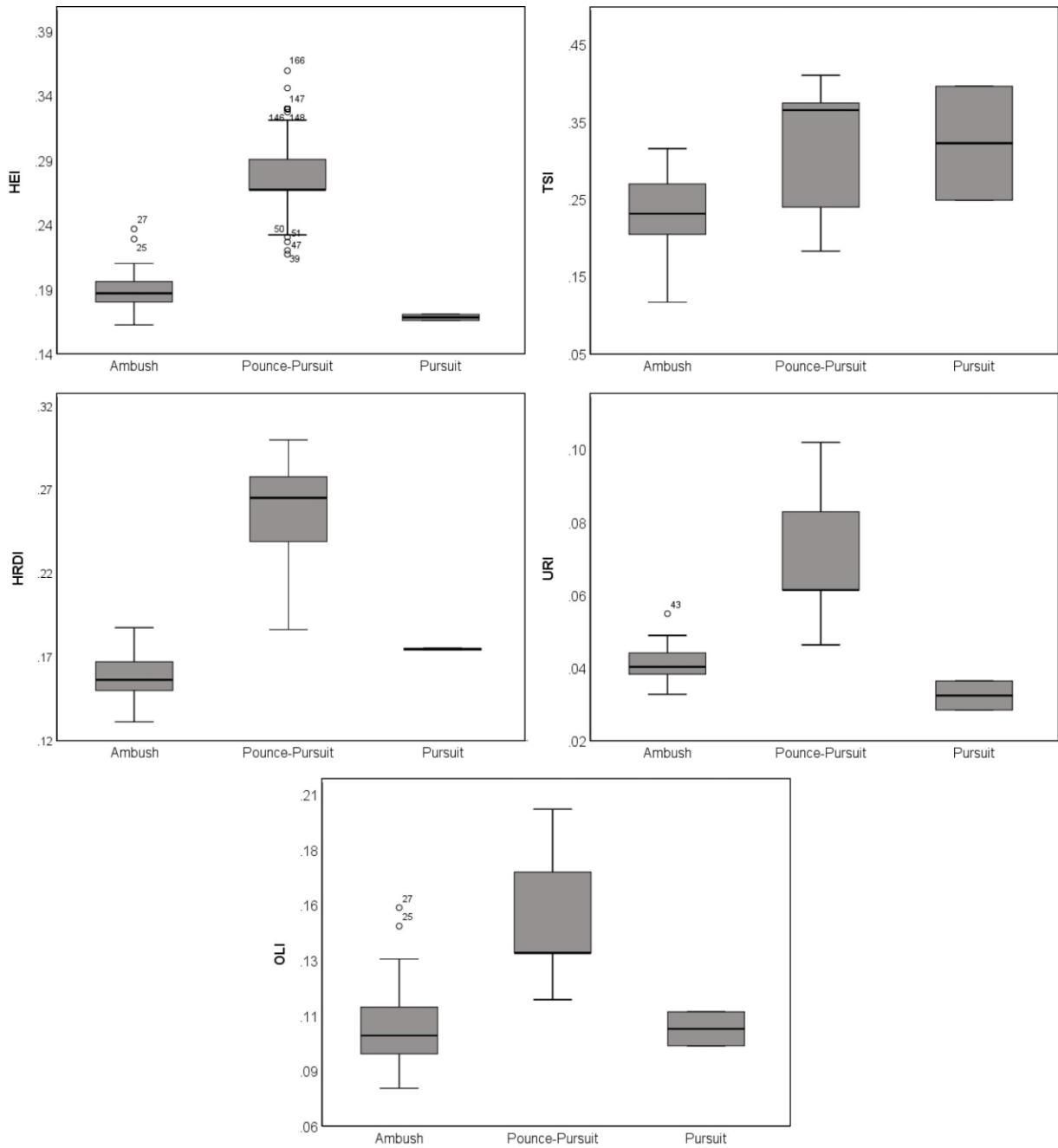


Figure 44. Boxplots of the hunting behavior morphological indices used in the stepwise DF analysis (Table 6) for each hunting behavior group. Outliers are represented by open circles.

## Prediction Discussion

Many researchers have studied felid locomotor and hunting behavior; however, only a few have attempted classifications within Felidae to infer behavior of select extinct feliforms. Results presented here strongly suggest that felids can be classified as having more than two locomotion behaviors and/or a single hunting style. Wilks's lambda in both discriminant analyses indicate that these newly assigned groups are significantly separated (Tables 4, 6). Observed overlap between each group is most likely because these separations are on a continuous scale. For locomotion there are some species that fall between arboreal and scansorial, as well as between arboreal and generalist (Fig. 41). For hunting style, some species fall between ambush and pounce-pursuit (Fig. 43).

The extinct taxa investigated here were predicted to be either arboreal, scansorial, or cursorial, with no taxa being placed within the generalist group (Table 5). *N. galiani*, *B. loveorum*, and *S. fatalis* were placed as scansorial feliforms; however, they are greatly separated by DF1 (Fig. 41). Additionally, both *B. loveorum* and *S. fatalis* are placed far away from all other taxa, but remain close to each other, possibly indicating that the locomotor categories used do not accurately reflect what these two taxa were really doing. Past research indicates that both these two feliforms are more bear-like in their postcranial morphology, so ambulatory locomotion behavior may be taking place (Anyonge 1996). The two nimravids, *Dinictis* sp. and *Hoplophoneus* sp., overlap between the arboreal and scansorial groups, not truly placed within either, agreeing with previous studies (Samuels et al. 2013). The highest prediction for *Dinictis* sp. was 57.2% for scansorial, then 42.7% for arboreal, whereas the highest prediction for

*Hoplophoneus* sp. was 90.7% for arboreal (Table 5). Only one of the extinct felids, *P. atrox*, was placed within the cursorial group, overlapping with *P. leo* (Fig. 41).

Ambush and pursuit felids have small humeral epicondylar breadths, shorter ulnar olecranon processes, and less robust humeri and ulnar limbs. Additionally, ambush felids have shorter tibial spines than the other felids. Pounce-pursuit felids have more robust limbs, greater humeral epicondylar breadth, and longer olecranon processes. As pounce-pursuit predators rely more heavily on muscle strength to grapple with their prey (including both large and small prey) than ambush predators (which primarily hunt small prey), the limbs would need to be larger for more muscle attachment. Cursorial felids also grapple with large prey; however, the two felids classified as cursorial, *A. jubatus* and *P. leo*, rely on different methods to take their prey down. *A. jubatus* relies on tripping their prey using their dew claw, whereas *P. leo* relies on socialized pack hunting, similar to canids (Sunquist and Sunquist 2002). Still, both taxa chase down their prey for greater distances than any other felid.

Extinct taxa used in this analysis all fell within the pounce-pursuit category, except for *Hoplophoneus* sp., which was predicted to be a pursuit predator, with great differences between DF1 and DF2 scores (Tables 5, 7; Fig. 43). Similar to the locomotion discriminant analysis, both *B. loveorum* and *S. fatalis* plot together, yet far from all other taxa, separated by DF1 (Fig. 43). Once again, this could be that the analysis did not have the ecomorph that accurately matched what these two taxa were really doing. *P. atrox*, although near the pounce-pursuit felids, is slightly separated from this group by DF2, whereas *N. galiani* falls between the pounce-pursuit felids and *P. atrox*. Both nimravids, *Dinictis* sp. and *Hoplophoneus* sp., are greatly dispersed by the DF1 and DF2 scores and do not plot within a specified group or with their own taxa (Fig. 43).

It is possible that the linear measurements in Figure 38, although good for locomotor separation, are not the best tools to use for hunting behavior analyses. Past research strays away from linear morphometrics to infer hunting style, instead favoring geometric analyses (Figueirido et al. 2015). Regardless, felids can be separated into at least four different locomotor groups and extinct felid locomotion can be inferred. Although the analysis for hunting behavior indicates that felids can be separated into at least three different groups, extinct feliforms were not well placed (Fig. 43). Future research should further define feliform locomotion with additional species not used here, and including ambulatory behavior for *B. loveorum* and *S. fatalis*. Geometric morphometrics, including 2D and 3D landmarks, could be used for hunting style to determine if these categories can be better applied to extinct taxa.

## CHAPTER 4. DISCUSSION

### *Paleoecology*

Mammologists have long recognized that extant felids have varying degrees of locomotor and prey capture, often related to their preferred habitat (for summary, see Sunquist and Sunquist 2002 and references therein). Many of these felids are sympatric, providing observable examples of resource competition and niche partitioning. The geology and fossils found at the Love Bone Bed strongly suggests the presence of multiple environments immediately surrounding the paleo channel during the late Miocene (Webb et al. 1981). West to the paleo channel lied the coast, as sea level was much higher than present by approximately 20 meters (Fig. 1) (Williams et al. 1977; Webb et al. 1981). The higher banks of this stream (and to the east) was a closed deciduous forest, intermixed with open grassland and savanna habitats (Webb et al. 1981). Fossils of forest dwelling taxa are proportionately more abundant at the Love site than the grassland adapted forms, suggesting that the late Miocene C3/C4 transition was in its early stages in this region (Webb et al. 1981; Feranec and MacFadden 2006). Additionally, fossil material of *Barbourofelis loveorum* is approximately three times more abundant than that of *Nimravides galiani*, indicating the habitat preference for the two species was the closed forest and the open habitat, respectively (Webb et al. 1981). Although both taxa existed in the same region over a short amount of depositional time (Webb et al. 1981), interactions between the two may have been minimal, further insinuating differences in terrestrial locomotion and hunting style based on habitat preference alone.

Felids use their forelimbs to subdue prey through supination and pronation of the elbow and wrist joints (Sunquist and Sunquist 2002; Kitchner et al. 2010; Meachen-Samuels and Van Valkenburgh 2009). In *N. galiani*, supination and pronation capability were more similar to that of pantherine felids, and not machairodonts, for the wrist and elbow joints. The more constrained forearm joints in *N. galiani*, as well as the relatively straight and slender limbs, suggest a more cursorial locomotion when compared to *B. loveorum*. Although the forearm morphology in *N. galiani* is predominantly felid in function, the highly robust MC I, and associated proximal phalanx, is distinctly similar to machairodonts as it would increase dew claw flexion and abduction, spreading this digit away from the other digits and bending the dew claw towards the manus. Additionally, MC I in *N. galiani* had good extension and abduction capability, similar to felids. However, these MC I morphologies are reduced in *B. loveorum* relative to *N. galiani*, as the MC I is relatively small and slender, closer to that of extant felids. Combined, these morphologies suggest that *N. galiani* may have relied more on dew claw use, possibly to assist in grappling with larger prey or to trip running prey in a similar style of *Acinonyx jubatus*; whereas *B. loveorum* would have relied more on forearm strength to wrestle prey down. Additionally, the more locked-in joints in *N. galiani* strongly suggests a reliance on running ability, with the forearms moving within a parasagittal plane. As such, *B. loveorum* may have quickly grabbed its prey when ambush hunting, whereas *N. galiani* may have snagged its prey when pounce-pursuit hunting.

Compared to *N. galiani* and extant felids, *B. loveorum* had a less constrained forearm movement, with many indicators supporting a possible retention for supination and pronation abilities. Specifically, the glenohumeral joint in *B. loveorum* suggests an increase in flexion, abduction, and lateral rotation, features that are present, but less pronounced in felids. As such,

*B. loveorum* may have been better able to swing their forearms forward anteriorly and laterally away from their body. The carpals of *B. loveorum* suggests an increase in flexion and combined abduction-extension capability; bending the wrist palmarly downward and mediodorsally, respectively. This increase in mobility suggests that *B. loveorum* may have relied on grappling and subduing prey, possibly as an ambush predator, rather than chasing down and “catching”, or snagging, prey. Additionally, such forearm morphology/capability may have been beneficial for climbing. Although the body size of *B. loveorum* has been estimated by Meachen-Samuels (2012) to be approximately 70 kg (~154 lbs), close to the size of *Puma concolor* (mountain lion), size alone is not a good proxy for locomotor behavior, as *A. jubatus* and *Panthera pardus* (leopard) are also near this size; a runner and climber respectively (Sunquist and Sunquist 2002; Krausman 2005).

The metacarpals of *N. galiani* are nearly as long as those in larger felids and suggest a digitigrade stance; whereas in *B. loveorum* they are considerably shorter and suggest a semi plantigrade stance, similar to nimravids as described by Bryant (1991). Elongate metacarpals indicate greater stride length, more cursorial locomotion, and a digitigrade stance; whereas shorter metacarpals may suggest opposite behaviors, such as shorter stride length, less cursorial locomotion, and a more plantigrade stance (Ginsburg 1961; Wang 1993). Salesa et al. (2017) suggests that shortened metacarpals would reduce the weight of the limbs when moving around, thus conserving energy. Unlike the metacarpals in nimravids, barbourofelids have proximal overlap among them, with MC II overlapping MC III and similarly with MC III overlapping MC IV (Bryant 1991). As such, *B. loveorum* would have been more similar to felids in this regard. Short metacarpals suggest a smaller manus, limiting prey size for *B. loveorum* relative to *N. galiani*. In sum, the metacarpals imply that *N. galiani* may have been better at chasing down

larger prey through snagging; whereas *B. loveorum* may have had different hunting and locomotor behaviors not observed in extant felids as observed in its overall forearm mobility.

Felids use their hindlimbs for locomotor propulsion when traversing terrain (Carrano 1996; Dev et al. 2020); relying on the flexion and extension of joints throughout the limb, within the ankle, and between the metatarsals and associated phalanges (Carrano 1996; Panciroli et al. 2017; Polly 2020). *B. loveorum* has less constrained hindlimbs than that of *N. galiani*, which implies that *N. galiani* relied on more parasagittal movement for running ability (cursorial adaptations), whereas *B. loveorum* was less specialized for running. The hip joint between the femur and acetabulum of *B. loveorum* also suggests increased flexion, extension, abduction, and lateral rotation than in *N. galiani* and most other felids. Increased ability for such movements in *B. loveorum* indicates the femur could move further, and with more stability, posteriorly and anteriorly, and could be compensation for shorter limbs. Additionally, the limb could be placed further under the body when standing, and the limb had better capability to rotate outward, laterally. In *N. galiani*, hindlimb movement was more restrained, but not more so than that of felids. The tibia of *B. loveorum* is very short, similar to the distal elements of the forelimb. A shortened tibia decreases the overall length of the limb and reduces cursor adaptability. Although *B. loveorum* had more movement capability than *N. galiani* and extant felids, the knee joint had reduced mediolateral movement and acted mostly like a hinge joint. Additionally, plantarflexion capability at the ankle and metatarsophalangeal joints was reduced in *B. loveorum* relative to *N. galiani*. Movement of the hindfoot towards the ground may suggest more of a digitigrade stance in *N. galiani* as the foot would already be in that flexed position, whereas a more plantigrade stance in *B. loveorum* may show less plantarflexion ability. The ankle joint of *B. loveorum* strongly suggest a sub plantigrade stance, similar to *S. fatalis* and ursids. A more plantigrade

stance would imply a less cursorial locomotion and possibly more of an ambush hunting style. In *N. galiani*, the ankle joint is predominantly digitigrade.

Metatarsals of *B. loveorum* also suggest a sub plantigrade stance as each metatarsal is greatly shortened. Additionally, the facets ensure each metatarsal is spread apart, possibly to increase surface area during locomotion. Furthermore, MT II and MT III could extend medially, and MT V laterally, all of which would continue to increase surface area during locomotion and prey capture grabbing. In most felids, such as *N. galiani*, metatarsals are instead tightly grouped together and lengthened to increase the functional length of the limb (stride length) (Pancioli et al. 2017; Polly 2020). Since *N. galiani* was an open-grassland felid, adaptations to running would have been beneficial for chasing down fast running prey. As *B. loveorum* was a closed-forest predator, high running capability and stride length would not have been as important as sure footing and rapid directional changes.

Cervical vertebrae in felids are often used to determine canine killing mechanisms, such as the downward stabbing motions or shear-bite described for *Homotherium latidens* (Antón and Galobart 1999), extant larger felids (Antón et al. 2004), and *Machairodus aphanistus* (Antón et al. 2020). *B. loveorum* shares an interesting morphology on the atlas that is only present in ursids and the nimravid, *Hoplophoneus*: the lack of an alar notch and presence of an alar foramen that combines the transverse and atlantal foramina on the dorsal surface of the transverse process. Functional significance of the alar foramen is not understood or well documented (Davis 1964; Baskin 1980); however, it may provide additional vertebral robustness and protection of the artery passing through when *B. loveorum* is delivering the kill bite. As an ambush predator, *B. loveorum* would likely quickly grab its prey and wrestle it down. The prey might still have a lot of momentum to try and get away, so additional neck muscle strength may have been beneficial

when bringing down a struggling animal. Similar to *Smilodon* and other machairodonts, *B. loveorum* had increased neck flexion and extension capability and an increased angle of rotation when trying to enact the shear-bite. Cervicals in *N. galiani* show no noticeable differences to that of large felids, implying *N. galiani* may have been killing prey using the strangulation method typical of extant felids (Seidensticker and McDougal 1993; Sunquist and Sunquist 2002).

The sacrum of *B. loveorum* indicates a small or reduced tail. A short tail would impact balancing while climbing, whereas a longer tail is used for stabilization in either running or navigating a three-dimensional landscape on the ground or in the canopy (Hickman 1979; Walker et al. 1998). Since *B. loveorum* had a short tail, balancing when climbing and running on terrain to obtain prey would have been impacted. As such, this further suggests *B. loveorum* was neither cursorial or arboreal, and instead may have ambushed and wrestled prey down. The sacrum of *N. galiani* suggests a moderately sized tail which would've been helpful for running and quickly changing direction when chasing prey on the ground.

Based on the differences described here, *N. galiani* and *B. loveorum* appear to be functionally very different from one another, with *N. galiani* having more similarities to most large extant felids, whereas *B. loveorum* is more similar to *Smilodon fatalis* and ursids. These morphological differences suggest a dissimilarity in locomotion and prey capture between the two taxa and provides fresh insights to the paleoecological structure of Florida during the late Miocene. Interestingly, the results of the Discriminant Function Analyses diverge with the morphological inferences of locomotion and prey capture in *N. galiani* and *B. loveorum*. Analyses predicted scansorial locomotion for both extinct taxa; *N. galiani* at 99% and *B. loveorum* at 83%. My analysis was based on morphological indices that favor limb length and width ratios (Table 3; Table 4), instead of muscle attachment surface area, articular surface

dimensions, and surface curvatures, so results may reflect an inability of the former to differentiate between taxa belonging to a morphologically derived lineage. Additionally, as *B. loveorum* is not a felid, the locomotor and hunting behavior classifications used to describe felid ecology would not accurately describe the paleoecology for *B. loveorum*. However, it is important to note that although the statistical analyses used here cannot accurately infer the paleoecology of *B. loveorum*, it does indicate that *B. loveorum* is not truly ‘cat-like’ in its morphology.

Although the forearm morphology in *B. loveorum* might greatly assist in prey grappling, these features would also be beneficial to climbing, so it is not implausible to predict *B. loveorum* was scansorial. However, many studies (Anyonge 1993; Anyonge 1996; Martin-Serra et al. 2014b; Panciroli et al 2017; Polly 2020), including this research, have drawn morphological similarities between barbourofelids, *Smilodon* spp., and ursids; suggesting that *B. loveorum* exhibited ambulatory locomotion, a category not used in my statistical analysis. Since discriminant function analyses force unknowns into one of the specified categories, scansorial locomotion might have been the second-best choice (when ambulatory was not an option) for *B. loveorum*. Additionally, Figure 43 further implies a missing locomotor category as both *S. fatalis* and *B. loveorum* are separated from all other locomotor groups, yet remain together. As the same measurements were used to also predict hunting behavior, it is not surprising that *S. fatalis* and *B. loveorum* clustered together again and away from all other taxa (Fig. 45). If anything, these statistical analyses showed that there are more morphological similarities between *B. loveorum* and *S. fatalis*, than between the former and *N. galiani*.

Terrestrial fauna recovered at the Love site strongly suggests the presence of a large closed-deciduous forest, with interspersed open-plains surrounding the paleochannel (Webb et al.

1981). Webb et al. (1981) specified that the forest inhabitants included species of *Tapirus* (tapirs), *Prosthennops* (peccaries), *Aepycamelus* (giraffe-camel), various ungulates, and *B. loveorum*; all of which were unusually abundant compared to other late Miocene sites (Fig. 1). Many of these taxa would have been easy prey for *B. loveorum*, as it hid in the ground cover to quickly ambush prey and pin them to the ground. Morphology of the cervical vertebra of *B. loveorum* suggest an increase in tugging ability, similar to ursids, indicating an ability to drag prey away from sight of larger predators, such as *N. galiani* and the hyaenoid canid *Aelurodon*; perhaps onto low-hanging tree branches. However, balancing ability when climbing would have been negatively impacted by their highly reduced tail. Although probably an ambush hunter, *B. loveorum* may have also been opportunistic while walking around the forest floor as an ambulatory predator, attacking prey that came within reach. Additionally, *B. loveorum* may have relied on scavenging behavior, similar to *Gulo gulo* (wolverine). *G. gulo* is a large, bear-like opportunistic predator that possess large shearing carnassials and is known to follow canids and felids to obtain their kills (Pasitschniak-Arts and Larivière 1995). It is possible *B. loveorum* shared these similar behavioral traits with that of *G. gulo*, although still differed in dental morphology.

Conversely, in the open-grassland habitat, faunal inhabitants included an abundance of Equidae (horses), such as *Pliohippus*, *Neohipparion*, and *Astrohippus*, species of *Aphelops* (a hornless rhino), *Procamelus* (a small camelid), *Aelurodon* (a borophagine canid), and *Nimravides galiani* (Webb et al. 1981). As a large felid (approximately 120 kg, or 264 lbs) (Anyonge 1993; Meachen-Samuels 2012), *N. galiani* may have hunted some of these larger herbivores. Such prey might have given *N. galiani* a chase if the initial hunting pounce was unsuccessful. Similar to the extant pounce-pursuit felids used in this study, *N. galiani* may have

stalked towards its prey, hidden in the surrounding grasses, pounced, pursued prey over a short distance, and eventually snagged and pulled the prey to the ground.

Differences in locomotion and hunting behavior, as well as prey preference, between *B. loveorum* and *N. galiani* suggest they were not directly competing over resources. Some overlap may have occurred between the closed forest and open habitat boundaries, however, probably not enough to have ecologically affected either species. Instead, it is much more likely *N. galiani* competed with other open-habitat carnivorans, such as the canid *Aelurodon*, as both had cursor adaptations to the open-habitat they shared. Due to this plausible competition, it may have been possible that *N. galiani* would seek shelter in the trees along the forest boundaries when fleeing from canid packs, or to hide captured prey when under stress. However, this was not the case between *N. galiani* and *B. loveorum*, of whom were most likely niche partitioning during the late Miocene of Florida.

### *Conclusion*

- Though both are large cat and “cat-like” carnivorans, the data presented here (differences in locomotion and hunting behavior, as well as habitat preference) suggest that *B. loveorum* and *N. galiani* did not directly compete for similar resources, but instead partitioned the ecosystem by occupying separate niches.
- *N. galiani* most likely stayed within the open habitat surrounded by the closed deciduous forests and would pounce-pursuit prey for short distances until snagging its prey, possibly using the forest edge as cover to pounce at unsuspecting prey.

- *B. loveorum* most likely stayed within the closed deciduous forest and would ambush prey from the thick groundcover, grappling the prey to the ground with their strong forearms. Additionally, *B. loveorum* may have relied on the saber-toothed canine shear-bite to kill prey quickly. It is possible prey may have been carried and hid on tree branches away from larger predators.
- Morphological analyses suggest *N. galiani* was scansorial with an increase in cursor capabilities, pursuing prey on the open grassland regions for short distances, and rarely climbing in the surrounding forests.
- Morphological analyses suggest *B. loveorum* was an ambulatory predator (not truly classified in any locomotor category analyzed here), walking and trotting around the forest floor similar to extant ursids, wolverines, and badgers.

### *Future Work*

Because the sample size used in this study was small, additional specimens could clarify the results, or at least add statistical significance. Additional statistical methods could also include landmark analyses. Results of these analyses may not only confirm or refute the conclusions reached in this study, but may also provide insight to the phylogenetic relationships between barbourofelids and felids. The morphological similarities between *Barbourofelis loveorum*, *Smilodon fatalis*, and ursids, warrant further analyses, perhaps including these additional taxa in the statistical analyses might provide a better understanding of the locomotion and prey capture behavior of *B. loveorum*. Isotopic research would be a beneficial addition to this research in order to study the dietary differences or similarities between *Nimravides galiani*

and *B. loveorum*. Additional research covering possible pack structure dynamics as well as preferred temporal activity for both taxa would be highly beneficial in determining the paleoecological structure at the Love Bone Bed.

## REFERENCES

- Antón M, Galobart A. 1999. Neck function and predatory behaviour in the scimitar toothed cat *Homotherium latidens* (Owen). *J. Vertebr. Paleontol.* 19:771-784.
- Antón M, Salesa MJ, Pastor JF, Sánchez IM, Fraile S, Morales J. 2004. Implications of the mastoid anatomy of larger extant felids for the evolution and predatory behaviour of sabretoothed cats (Mammalia, Carnivora, Felidae). *Zool. J. Linn. Soc.* 140:207-221.
- Antón M. 2013. Sabertooth. Indiana: Indiana University Press.
- Antón M, Salesa MJ, Siliceo G. 2013. Machairodont adaptations and affinities of the Holarctic Late Miocene homotherin *Machairodus* (Mammalia, Carnivore, Felidae): The case of *Machairodus catocopsis* Cope, 1887. *J. Vert. Paleo.* 33(5):1202-1213.
- Antón M, Siliceo G, Pastor JF, Morales J, Salesa M. 2020. The early evolution of the sabretoothed felid killing bite: the significance of the cervical morphology of *Machairodus aphanistus* (Carnivora: Felidae: Machairodontinae). *Zool. J. Linn. Soc.* 188:319-342.
- Anyonge W. 1993. Body mass in large extant and extinct carnivores. *J. Zool.* 231(2):339-350.
- Anyonge W. 1996. Locomotor behaviour in Plio-Pleistocene sabre-tooth cats: a biomechanical analysis. *J. Zool. Lond.* 238:395-413.
- Argot C. 2001. Functional-adaptive anatomy of the forelimb in the Didelphidae, and the paleobiology of the Paleocene marsupials *Mayulestes ferox* and *Pucadelphys andinus*. *J. Morphol.* 247:51-79.

- Argot C. 2003. Functional Adaptations of the Postcranial Skeleton of two Miocene borhyaenoids (Mammalia, Metatheria), *Borhyaena* and *Prothylacinus*, from South America. *Paleontology*. 46:1213-1267.
- Argot C. 2004. Evolution of the South American mammalian predators (Borhyaenoids, Mammalia, Metatheria): anatomical and paleobiological implications. *Zool. J. Linn. Soc.* 140:487-521.
- Baron R. 2010. Anatomie comparée des mammifères domestiques tome second arthrologie et myologie. Quatrième édition. Éditions Vigot Frères, Paris, 1021 p.
- Barrett PZ. 2016. Taxonomic and systematic revisions to the North American Nimravidae (Mammalia, Carnivora). *PeerJ*. 4: e1658.
- Baskin JA. 1980. Carnivora from the late Clarendonian Love Bone Bed, Alachua County, Florida. University of Florida Dissertation. 1-229.
- Baskin JA. 1981. *Barbourofelis* (Nimravidae) and *Nimravides* (Felidae), with a description of two new species from the late Miocene of Florida. *J Morphol.* 62(1):122-139.
- Baskin JA. 2005. Carnivora from the late Miocene Love Bone Bed of Florida. *Bull. Fla. Mus. Nat. Hist.* 45(4):413–434.
- Bertram JEA, Biewener AA. 1990. Differential scaling of the long bones in the terrestrial carnivora and other mammals. *J Morphol.* 204(2):157–169.
- Bramble DM. 1985. Functional vertebrate morphology. Cambridge MA: Harvard University Press.

- Carleton A. 1941. A comparative study of the inferior tibio-fibular joint. *J. Anat.* 53(3):326-331.
- Carlson B. 2014. Functional limb morphology of extinct carnivores *Smilodon fatalis*, *Panthera atrox*, and *Canis dirus* based on comparisons with four extant felids and one extant canid. Dissertation Northern Illinois University, Department of Biological Sciences. 1-241.
- Carrano MT. 1997. Morphological indicators of foot posture in mammals: a statistical and biomechanical analysis. *Zool. J. Linn. Soc.* 121:77-104.
- Carrano MT. 1999. What, if anything, is a cursor? Categories versus continua for determining locomotor habitat in mammals and dinosaurs. *Proc. Zool. Soc. Lond.* 247:29-42.
- Christiansen P, Harris JM. 2005. Body Size of *Smilodon* (Mammalia: Felidae). *J. Morphol.* 266: 369-384.
- Christiansen P, Adolfssen JS. Osteology and ecology of *Megantereon cultridens* SE311 (Mammalia; Felidae; Machairodontinae), a sabrecat from the Late Pliocene – Early Pleistocene of Senéze, France. *Zool. J. Linn. Soc.-Lond.* 151: 833-884
- Christiansen P. 2012. Phylogeny of the sabertoothed felids (Carnivora: Felidae: Machairodontinae). *Cladistics.* 29:543-559.
- David DD. 1964. The Giant Panda: A morphological study of evolutionary mechanisms. In Ross LA, Williams PM, Nash EG, editors. Chicago: Chicago Natural History Museum.
- Day LM, Jayne BC. 2007. Interspecific scaling of the morphology and posture of the limbs during the locomotion of cats (Felidae). *J. Exp. Biol.* 210:642-654.

- Dev B, Tran L, Jacob S, Granatosky MC. 2020. Feline Locomotion. In Vonk J, Shackelford TK, editors. Encyclopedia of Animal Cognition and Behavior. New York: Springer International Publishing. 1-8.
- Di Bitetti MS, De Angelo CD, Di Blanco YE, Paviolo A. 2010. Niche partitioning and species coexistence in a Neotropical felid assemblage. *Acta Oecologica*. 36(4):403-412.
- Domingo S, Domingo L, Badgley C, Sanisidro O, Morales J. 2012. Resource partitioning among top predators in a Miocene food web. *Proc R Soc Lond [Biol]*. 280(1750):1-9.
- Feranec RS, MacFadden BJ. 2006. Isotopic discrimination of resource partitioning among ungulates in C<sub>3</sub>-dominated communities from the Miocene of Florida and California. *Oecologia*. 32(2):191-205.
- Figueirido B, Martín-Serra A, Tseng ZJ, Janis CM. 2015. Habitat changes and changing predatory habits in North American fossil canids. *Nat. Commun.* 6:1-11.
- Fisher RE, Adrian B, Elrod C, Hicks M. 2008. The phylogeny of the red panda (*Ailurus fulgens*): evidence from the hindlimb. *J. Anat.* 213:607-628.
- Fisher RE, Adrian B, Barton M, Holmgren J, Tang SY. 2009 The phylogeny of the red panda (*Ailurus fulgens*): evidence from the forelimb. *J. Anat.* 215:611-635.
- Flower WH. 1885. An introduction to the osteology of the Mammalia. London: MacMillan and Co.
- Friscia A, Goswami A. 2010. Carnivoran evolution: new views on phylogeny, form and function. Cambridge: Cambridge University Press.

- Ginsburg L. 1961. Plantigrady and digitigrady in the fissiped carnivorans. *Mamm*, 25(1):1-21.
- Gonyea WJ. 1976a. Behavioral implications of saber-toothed felid morphology. *Paleobiology*. 2:332-342.
- Gonyea WJ. 1976b. Adaptive differences in the body proportions of large felids. *Acta Anat*. 96:81-96.
- Gonyea WJ. 1978. Functional implications of felid forelimb anatomy. *Acta Anat*. 102:111-121.
- Haas SK, Hayssen V, Krausman P. 2005. *Panthera leo*. *Mamm. Species*. 762:1-11.
- Hemmer H. 1972. *Uncia uncia*. *Mamm. Species*. 20:1-5.
- Hickman GC. 1979. The mammalian tail: a review of functions. *Mamm. Rev*. 9(4):143-157.
- Hildebrand M. 1985. Walking and running. In: Hildebrand M, Bramble DM, Liem KF, Wake DB, editors. *Functional Vertebrate Morphology*. Cambridge, MA: Harvard University Press. pp 38-57.
- Iwaniuk AN, Pellis SM, Whishaw IQ. 1999. The relationship between forelimb morphology and behaviour in North American carnivores (Carnivora). *Can. J. Zool*. 77: 1064-1074.
- Johnson WE, Eizirik E, Pecon-Slattery J, Murphy WJ, Antunes A, Teeling E, O'Brian SJ. 2006. The late Miocene radiation of modern Felidae: A genetic assessment. *Sci*. 311:73-76.
- Jolly CJ. 1967. The evolution of the baboons. In: Vagbog H, editor. *The Baboon in Medical Research*. Vol. II. Austin (TX). University of Texas Press. p. 23-50.

- Julik E, Zack S, Adrian B, Maredia S, Parsa A, Poole M, Starbuck A, Fisher, RE. 2012. Functional anatomy of the forelimb muscles of the Ocelot (*Leopardus pardalis*). *J. Mamm. Evol.* 19:277-304.
- Krausman P, Morales S. 2005. *Acinonyx jubatus*. *Mamm. Species.* 771:1-6.
- Kitchener AC, Van Valkenburgh B, Yamaguchi N. 2010. Felid form and function. In: Macdonald DW, Loveridge AJ, editors. *Biology and conservation of wild felids*. New York (NY). Oxford University Press. p. 83-106.
- Madurell-Malapeira J, Robles JM, Casanovas-Vilar I, Abella J, Obradó P, Alba DM. 2014. The scimitar-toothed cat *Machairodus aphanistus* (Carnivora: Felidae) in the Vallès-Penedès Basin (NE Iberian Peninsula). *C. R. Palevol.* 13:569-585.
- Martin L. 1980. Functional morphology and the evolution of cats. *TNAS.* 8:141-154.
- Martin L. 1998. Felidae. In: Janis CM, Gunnell GF, Jacobs LL, Scott KM, Uhen MD, editors. *Evolution of Tertiary mammals of North America*. Cambridge: Cambridge Univ. Press. 1:236-242.
- Martin L. 1998. Nimravidae. In: Janis CM, Gunnell GF, Jacobs LL, Scott KM, Uhen MD, editors. *Evolution of Tertiary mammals of North America*. Cambridge: Cambridge Univ. Press. 1:228-235.
- Martín-Serra A, Figueirido B, Palmqvist P. 2014a. A three-dimensional analysis of morphological evolution and locomotor performance of the carnivoran forelimb. *Plos One.* 9(1):1-20.

- Martín-Serra A, Figueirido B, Palmqvist P. 2014b. A three-dimensional analysis of morphological evolution and locomotor performance of the carnivoran hindlimb. *BMC Evol. Biol.* 14(129):1-13.
- Martín-Serra A, Figueirido B, Pérez-Claros JA, Palmqvist P. 2014c. Patterns of morphological integration in the appendicular skeleton of mammalian carnivores. *Evolution.* 69(2):321-340.
- Mattern MY, McLennan DA. 2000. Phylogeny and speciation of felids. *Cladistics.* 16:232-253.
- Mazák V. 1981. *Panthera tigris*. *Mamm. Species.* 152:1-8.
- Meachen-Samuels JA, Van Valkenburgh B. 2009. Forelimb Indicators of Prey-Size Preference in the Felidae. *J Morphol.* 70: 729-744.
- Meachen-Samuels JA. 2012. Morphological convergence of the prey-killing arsenal of sabertooth predators. *Paleobiology.* 38(1):1-14.
- Meloro C. 2011. Locomotor adaptations in Plio-Pleistocene large carnivores from the Italian peninsula: Palaeoecological implications. *Curr. Zool.* 57:269-283.
- Meloro C, Elton S, Louys J, Bishop LC, Ditchfield P. 2013. Cats in the forest: Predicting habitat adaptations from humerus morphometry in extant and fossil Felidae (Carnivora). *Paleobiology.* 39(3):323-344.
- Merriam JC, Stock C. 1932. *Felidae of Rancho La Brea*. Washington: Carnegie Institution of Washington.

- Morlo M, Peigné S, Nagel D. 2004. A new species of *Prosansanosmilus*: Implications for the systematic relationships of the family Barbourfelidae new rank (Carnivora, Mammalia). *Zool J Linn Soc-Lond.* 140(1):43-61.
- O'Brian SJ, Johnson WE. 2007. Evolution of cats. *Sci. Am.* 297:68-75.
- Oliveira TG. 1998. *Leopardus wiedii*. *Mamm. Species.* 579:1-6.
- Paijmans JLA, Barnett R, Gilbert MTP, Zepeda-Mendoza ML, Reumer JWF, De Vos J, Zazula G, Nagel D, Baryshnikov GF, Leonard JA, Rohland N, Westbury MV, Barlow A, Hofreiter M. 2017. Evolutionary history of saber-toothed cats based on ancient mitogenomics. *Curr. Biol.* 27:1-7.
- Panciroli E, Janis C, Stockdale M, Martin-Serra A. 2017. Correlates between calcaneal morphology and locomotion in extant and extinct carnivorous mammals. *J. Morphol.* 278:1333-1353.
- Pasitschniak-Arts M, Larivière S. 1995. *Gulo gulo*. *Mamm. Species.* 499:1-10.
- Piras P, Silvestro D, Carotenuto F, Castiglione S, Kotsakis A, Maiorino L, Melchionna M, Mondanaro A, Sansalone G, Serio C, Vero VA, Raia P. 2018. Evolution of the sabertooth mandible: A deadly ecomorphological specialization. *Palaeogeogr. Palaeoclimatol. Palaeoecol.* 496:1-9.
- Polly DP. 2010. Tiptoeing through the trophics: Geographic variation in carnivoran locomotor ecomorphology in relation to environment. In: Goswami A, Friscia A, eds. *Carnivoran*

Evolution: New views on Phylogeny, Form, and Function. Cambridge (UK). Cambridge University Press. p. 374-410.

Polly DP. 2020. Ecometrics and Neogene faunal turnover: the roles of cats and hindlimb morphology in the assembly of carnivoran communities in the New World. *Geodiversitas*. 42(17):257-304.

Randau M, Goswami A, Hutchinson JR, Cuff AR, Pierce SE. 2016. Cryptic complexity in felid vertebral evolution: shape differentiation and allometry of the axial skeleton. *Zool. J. Linn. Soc-Lond*. 178(1):1-20.

Reighard J, Jennings HS. 1901. *Anatomy of the cat*. Henry Holt, New York.

Rothwell T. 2001. A partial skeleton of *Pseudaelurus* (Carnivora: Felidae) from the Nambé Member of the Tesuque Formation, Española Basin, New Mexico. *Am. Mus. Novit*. 3342:1-31.

Rothwell T. 2003. Phylogenetic Systematics of North American *Pseudaelurus* (Carnivora: Felidae). *Am. Mus. Novit*. 3403:1-64.

Russo GA. 2015. Postsacral Vertebral Morphology in Relation to Tail Length Among Primates and Other Mammals. *Anat. Rec*. 298:354-375.

Russo GA. 2016. Comparative sacral morphology and the reconstructed tail lengths of five extinct primates: *Proconsul heseloni*, *Epipliopithecus vindobonensis*, *Archaeolemur edwardsi*, *Megaladapis grandidieri*, and *Palaeopropithecus kelyus*. *J. Hum. Evol*. 90:135-162.

- Salesa MJ, Antón M, Peigné S, Morales J. 2008. Functional anatomy and biomechanics of the postcranial skeleton of *Simocyon batalleri* (Viret, 1929) (Carnivora, Ailuridae) from the Late Miocene of Spain. *Zool. J. Linn. Soc.* 152:593-621.
- Salesa MJ, Antón M, Turner A, Morales J. 2010. Functional anatomy of the forelimb in *Promegantereon ogygia* (Felidae, Machairodontinae, Smilodontini) from the Late Miocene of Spain and the origins of the sabre-toothed felid. *J. Anat.* 216:381-396.
- Salesa MJ, Antón M, Morales J, Peigné S. 2011. Functional anatomy of the postcranial skeleton of *Styriofelis lorteti* (Carnivora, Felidae, Felinae) from the Middle Miocene (MN 6) locality of Sansan (Gers, France). *Estud. Geol.* 67(2):223-243.
- Salesa MJ, Pesquero MD, Siliceo G, Antón M, Alcalá L, Morales J. 2012. A Rich Community of Felidae (Mammalia, Carnivora) from the Late Miocene (Turolian, MN 13) Site of Las Casiones (Villalba Baja, Teruel, Spain). *J. Vertebr. Paleontol.* 32(3):658-676.
- Salesa MJ, Siliceo G, Antón M, Peigné S, Morales J. 2017. Functional and systematic implications of the postcranial anatomy of a late Miocene feline (Carnivora, Felidae) from Batallones-1 (Madrid, Spain). *J. Mamm. Evol.* 26:101-131.
- Samuels JX, Meachen JA, Sakai SA. (2013), Postcranial morphology and the locomotor habits of living and extinct carnivorans. *J. Morphol.* 274:121-146.
- Schwab JA, Kriwet J, Weber GW, Pfaff C. 2019. Carnivoran hunting style and phylogeny reflected in bony labyrinth morphometry. *Sci. Rep.* 9(70):1-9.

- Scott WB, Jepsen GL. 1936. The mammalian fauna of the White River Oligocene part I-  
Insectivora and Carnivora. Proc. Am. Philos. Soc. 28:1-153.
- Seidensticker J, McDougal C. 1993. Tiger predatory behavior, ecology and conservation. Symp.  
Zool. Soc. Lond. 65:105-125.
- Seymour KL. 1989. *Panthera onca*. Mamm. Species. 340:1-9.
- Shaw CA, Tejada-Flores AE. 1985. Biomechanical implications of the variation in *Smilodon*  
ectocuneiforms from Rancho La Brea. Contrib. sci. 359:1-8.
- Sunquist M, Sunquist F. 2002. Wild Cats of the World. Chicago: University of Chicago Press.
- Tedford RH, Albright LB III, Barnosky A, Ferrusquia-Villafranca I, Hunt RM Jr, Storer J,  
Swisher CC III, Voorhies MR, Webb SD, Whistler D. 2004. Mammalian biochronology of  
the Arikareean through Hemphillian interval (Late Oligocene through early Pliocene epochs),  
North America. In: Woodburne MO, ed. Late Cretaceous and Cenozoic Mammals of North  
America; Biostratigraphy and Geochronology. New York: Columbia University Press. 169-  
231.
- Tseng, Z.J., Takeuchi, G.T. and Wang, X., 2010. Discovery of the upper dentition of  
*Barbourofelis whitfordi* (Nimravidae, Carnivora) and an evaluation of the genus in  
California. Journal of Vertebrate Paleontology, 30(1), pp.244-254.
- Tumlison R. 1987. *Felis lynx*. Mamm. Species. 269:1-8.
- Taylor ME. 1974. The functional anatomy of the forelimb of some African Viverridae  
(Carnivora). J. Morphol. 143:307-336.

- Van Valkenburgh B. 1985. Locomotor diversity within past and present guilds of large predatory mammals. *Paleobiology*. 11(4):406-428.
- Van Valkenburgh B. 1987. Skeletal indicators of locomotor behavior in living and extinct carnivores. *J. Vertebr. Paleontol.* 7:162– 182.
- Vollmerhaus B, Roos H. 2001. Konstruktionsprinzipien an der Vorder- und Hinterpfote der Hauskatze (*Felis catus*). III. Mitteilung: Muskulatur. *Anat. Histol. Embryol.* 30:89-105.
- Walker C, Vierck Jr CJ, Ritz LA. 1998. Balance in the cat: role of the tail and effects of sacrocaudal transection. *Behav. Brain Res.* 91:41-47.
- Wang X. 1993. Transformation from plantigrady to digitigrady: Functional morphology of locomotion in *Hesperocyon* (Canidae: Carnivora). *Am. Mus. Novit.* 3069:1-23.
- Wang X, White SC, Guan J. 2020. A new genus and species of sabretooth, *Oriensmilus liupanensis* (Barbourofelinae, Nimravidae, Carnivora), from the middle Miocene of China suggests barbourofelines are nimravids, not felids. *J. Syst. Palaeontol.* 18(9):1-21.
- Walmsley T. 1918. The reduction of the mammalian fibula. *J. Anat.* 52:326-331.
- Walmsley A, Elton S, Louys J, Bishop LC, Meloro C. 2012. Humeral epiphyseal shape in the Felidae: The influence of phylogeny, allometry, and locomotion. *J. Morphol.* 273(12):1-15.
- Wesley-Hunt GD. 2005. The morphological diversification of carnivores in North America. *Paleobio.* 31(1):35-55.
- Williams KE, Nicol D, Randazzo AF. 1977. The Geology of the Western Part of Alachua County, Florida. Dept. Nat. Resources, Bur. Geology, Rept. Inv. No. 85:1-98.

Webb SD, MacFadden BJ, Baskin JA. 1981. Geology and paleontology of the Love Bone Bed from the late Miocene of Florida. *Am. J. Sci.* 281(5):513-544.

Wells RT, Camens AB. 2018. New skeletal material sheds light on the paleobiology of the Pleistocene marsupial carnivore, *Thylacoleo carnifex*. *Plos One.* 13(12):1-31.

Werdelin L, Yamaguchi N, Johnson WE, O'Brien SJ. 2010. Phylogeny and evolution of cats (Felidae). In: Macdonald DW, Loveridge AJ, editor. *Biology and Conservation of Wild Felids*. New York (NY). Oxford University Press. p. 59-82.

## APPENDICES

*Appendix A. Taxa used in the analyses and mean postcranial measurements. Data from Samuels et al. (2013) with taxa added in this study. † designates extinct taxa.*

<b>Species</b>	<b>N</b>	<b>Museum</b>	<b>HL</b>	<b>HD</b>	<b>DPCL</b>	<b>HEB</b>	<b>RL</b>	<b>UL</b>	<b>UD</b>	<b>OL</b>	<b>FL</b>	<b>FD</b>	<b>FGT</b>	<b>FEB</b>	<b>TL</b>	<b>TD</b>	<b>TSL</b>	<b>MT3L</b>
<i>Acinonyx jubatus</i>	2	LACM, UCLA	244.51	16.95	141.81	41.10	239.65	278.53	7.73	29.18	269.23	19.07	36.30	46.83	271.95	19.15	86.30	113.01
<i>Caracal serval</i>	1	LACM	169.70	10.81	77.47	29.31	172.60	196.06	6.46	16.80	191.59	10.41	31.40	27.59	197.95	14.21	40.55	88.74
<i>Felis chaus</i>	1	ETVP	150.87	9.82	63.91	25.74	146.59	168.40	4.68	15.14	168.32	9.47	19.76	26.08	173.11	11.50	53.64	77.49
<i>Felis silvestris</i>	2	LACM	114.26	7.21	54.46	19.44	114.64	132.24	3.97	11.77	128.60	7.94	18.27	19.97	135.21	7.33	33.24	63.59
<i>Leopardus wiedii</i>	3	USNM	108.16	7.39	34.37	21.60	92.93	110.04	3.93	13.55	121.35	7.74	19.91	19.18	119.11	7.01	25.10	46.92
<i>Lynx canadensis</i>	6	UCLA	165.71	10.50	72.36	30.29	162.88	186.73	6.32	16.85	202.88	11.87	27.03	27.11	207.77	11.09	39.22	92.36
<i>Lynx rufus</i>	9	LACM, UCLA	137.77	9.76	59.30	25.44	128.27	151.67	5.44	16.15	157.93	9.64	18.47	24.59	158.52	9.78	38.49	66.47
<i>Neofelis nebulosa</i>	3	USNM	146.71	11.24	69.41	33.10	117.27	143.66	5.96	21.31	164.88	10.99	29.41	29.38	155.63	9.95	43.38	56.64
<i>Otocolobus manul</i>	1	LACM	97.39	6.67	45.28	19.09	86.86	102.90	—	9.90	99.77	6.42	18.94	17.25	105.97	5.74	25.18	39.26
<i>Panthera leo</i>	3	ETVP, LACM	303.84	25.58	179.73	78.07	279.34	334.28	17.84	46.32	333.98	27.31	49.54	69.00	288.58	27.10	105.25	122.25
<i>Panthera onca</i>	1	ETVP	213.77	16.47	100.99	51.43	170.58	214.59	11.78	32.74	243.12	15.63	26.71	42.76	200.36	16.00	72.67	78.19
<i>Panthera tigris</i>	5	ETVP, NAU QSP	322.12	28.48	154.27	82.55	269.18	335.34	18.33	53.03	367.02	25.69	41.05	72.95	313.91	26.62	120.88	127.53
<i>Panthera uncia</i>	4	ETVP, LACM	209.42	18.17	138.51	50.40	184.07	227.87	11.53	30.20	232.69	17.59	46.11	45.55	231.87	16.52	65.69	89.66
<i>Pardofelis marmorata</i>	4	LACM	108.71	7.58	53.37	21.35	92.34	109.71	4.60	11.58	122.71	8.07	21.62	20.43	127.13	7.17	30.81	46.02

<b>Species</b>	<b>N</b>	<b>Museum</b>	<b>HL</b>	<b>HD</b>	<b>DPCL</b>	<b>HEB</b>	<b>RL</b>	<b>UL</b>	<b>UD</b>	<b>OL</b>	<b>FL</b>	<b>FD</b>	<b>FGT</b>	<b>FEB</b>	<b>TL</b>	<b>TD</b>	<b>TSL</b>	<b>MT3L</b>
<i>Puma concolor</i>	7	LACM, UCLA	220.32	19.00	96.82	51.24	183.47	221.96	11.22	28.06	259.40	18.93	37.29	45.27	237.62	17.67	68.91	98.06
<i>Nimravides galiani</i> †	6	UF	270.65	26.23	121.66	73.12	238.9	297.13	17.95	47.43	324.39	23.5	36.89	55.64	292.9	26.71	99.3	118.71
<i>Panthera atrox</i> †	70	LACMHC	352.96	35.65	220.17	94.32	332.56	399.63	22.55	55.34	415.72	33.54	70.54	86.63	356.08	35.29	133.42	147.71
<i>Smilodon fatalis</i> †	36	LACMHC	329.76	41.93	236.24	108.80	262.05	330.42	26.40	57.83	352.08	30.20	78.43	70.55	276.78	30.17	59.23	99.08
<i>Barbourofelis loveorum</i> †	7	UF	249.77	26.51	119.65	76.67	198.9	255.34	24.76	39.65	294.66	22.6	39.2	61.32	219.5	21.74	77.14	61.52
<i>Dinictis</i> sp. †	9	AMNH, LACM	182.50	14.48	113.03	45.32	142.20	174.94	—	26.98	195.40	14.80	60.60	35.44	186.10	12.24	58.42	—
<i>Hoplophoneus</i> sp. †	11	LACM, USNM	173.02	14.03	101.93	47.48	133.85	170.59	8.84	32.85	189.61	14.81	56.80	36.75	168.12	11.32	59.77	50.44

*Appendix B: Assigned locomotor groups for extant felids from literature.*

<b>Taxonomic Name</b>	<b>Common Name</b>	<b>Locomotion</b>	<b>Sources</b>
<i>Acinonyx jubatus</i>	Cheetah	Cursorial	8, 10
<i>Caracal serval</i>	Serval	Terrestrial	8
<i>Felis chaus</i>	Jungle Cat	Terrestrial	8
<i>Felis silvestris libyca</i>	African Wildcat	Terrestrial	8
<i>Leopardus wiedii</i>	Margay	Arboreal	7, 8
<i>Lynx canadensis</i>	Canada Lynx	Terrestrial	4, 8
<i>Lynx rufus</i>	Bobcat	Terrestrial	6, 8
<i>Neofelis nebulosa</i>	Clouded Leopard	Arboreal	8
<i>Otocolobus manul</i>	Manul	Terrestrial	8
<i>Panthera leo</i>	Lion	Cursorial	8, 9
<i>Panthera onca</i>	Jaguar	Scansorial	5, 8
<i>Panthera tigris</i>	Tiger	Scansorial	2, 8
<i>Panthera uncia</i>	Snow Leopard	Scansorial	1, 8
<i>Pardofelis marmorata</i>	Marbled Cat	Arboreal	8
<i>Puma concolor</i>	Cougar	Scansorial	3, 8

[1] Hemmer, 1972; [2] Mazák, 1981; [3] Currier, 1983; [4] Tumlison, 1987; [5] Seymour, 1989; [6] Larivière and Walton, 1997; [7] Oliveira, 1998; [8] Sunquist and Sunquist, 2002; [9] Haas et al., 2005; [10] Krausman and Morales, 2005.

*Appendix C: Assigned predatory groups for extant felids from literature.*

<b>Taxonomic Name</b>	<b>Common Name</b>	<b>Hunting Behavior</b>	<b>Prey Size</b>	<b>Sources</b>
<i>Acinonyx jubatus</i>	Cheetah	Pursuit	Large	9, 11, 12, 13
<i>Caracal serval</i>	Serval	Ambush	Mixed	9, 12
<i>Felis chaus</i>	Jungle Cat	Ambush	Small	9, 12
<i>Felis silvestris libyca</i>	African Wildcat	Ambush	Small	9, 12
<i>Leopardus wiedii</i>	Margay	Ambush	Small	8, 9, 12
<i>Lynx canadensis</i>	Canada Lynx	Ambush	Mixed	5, 9, 12
<i>Lynx rufus</i>	Bobcat	Ambush	Mixed	7, 9, 12
<i>Neofelis nebulosa</i>	Clouded Leopard	Ambush	Mixed	4, 9, 12
<i>Otocolobus manul</i>	Manul	Ambush	Small	9, 12
<i>Panthera leo</i>	Lion	Pounce-Pursuit	Large	9, 10, 12
<i>Panthera onca</i>	Jaguar	Pounce-Pursuit	Large	6, 9, 12
<i>Panthera tigris</i>	Tiger	Pounce-Pursuit	Large	2, 9, 12
<i>Panthera uncia</i>	Snow Leopard	Pounce-Pursuit	Large	1, 9, 12
<i>Pardofelis marmorata</i>	Marbled Cat	Ambush	Small	9, 12
<i>Puma concolor</i>	Cougar	Pounce-Pursuit	Large	3, 9, 12

[1] Hemmer, 1972; [2] Mazák, 1981; [3] Currier, 1983; [4] Van Valkenburgh, 1985; [5] Tumilson, 1987; [6] Seymour, 1989; [7] Larivière and Walton, 1997; [8] Oliveira, 1998; [9] Sunquist and Sunquist, 2002; [10] Haas et al., 2005; [11] Krausman and Morales, 2005; [12] Meachen-Samuels and Valkenburgh, 2009; [13] Figueirido et al., 2015.

VITA

CHRISTIANNE ORMSBY

- Education: M.S. Geosciences, East Tennessee State University, Johnson City, Tennessee, 2021
- B.S. Geological Sciences, San Diego State University, San Diego, California, 2019
- Sonora High School, Sonora, California
- Professional Experience: Graduate Research Assistant, East Tennessee State University, Department of Geosciences, 2020-2021
- Graduate Teaching Assistant, East Tennessee State University, Department of Geosciences, 2019-2020
- Publications: **Ormsby, C.**, Wallace, S., and Samuels, J. 2020. Inferred Locomotion of Select Feliforms: Implications for *Barbourofelis loveorum* (Barbourofelidae) and *Nimravides galiani* (Felidae, Machairodontinae) from the Late Miocene (Latest Clarendonian) of Florida. 80th Society of Vertebrate Paleontology Abstracts with Programs.
- Ormsby, C.** and Deméré, T. 2019. Morphology as a means for determining the paleoecology of a North American Oligocene Canid (Mammalia: Carnivora). Geological

Society of America Abstracts with Programs. Vol. 51, No.  
5.

**Ormsby, C.,** Gearty, W., and Payne, J.L. 2018. The effect of  
habitat on diversification rate in snakes. Geological Society  
of America Abstracts with Programs. Vol. 50, No. 6.

Honors and Awards:	Paleontology Department Scholarship (\$100)	Apr 2021
	GSA Graduate Student Research Grant (\$2800)	May 2020
	Outstanding Senior Thesis Presentation (\$100)	June 2019
	Awona Harrington Memorial Scholarship (\$4000)	May 2019
	Baylor Brooks Scholarship (\$3000)	May 2018
	Paleontological Society Student Ambassador (\$1000)	Nov 2018
	SURGE Travel Funds (\$300)	Nov 2018